ATOMIC WEAPONS ESTABLISHMENT

AWE Report No. O 2/95

P seismograms from explosions in the S Pacific recorded at four arrays

A Douglas
P D Marshall
J B Young
T Milbourne

Recommended for issue by: A Douglas, Group Leader, Seismic Detection Group

Approved for issue by: G J George, Manager, Systems Engineering Division

CONTENTS

SUMMARY

The report presents short period, broad band and deconvolved P seismograms from 108 known or presumed underground explosions that took place during the period 1975-1989 at Tuamotu in the S Pacific. The explosions were fired at two sites separated by 50 kms: Mururoa atoll (where the majority of the tests took place) and Fangataufa. The recordings used are short period seismograms at four arrays: Yellowknife, Canada (YKA); Eskdalemuir, Scotland (EKA); Warramunga, Australia (WRA); and Gauribidanur, India (GBA). The broad band and deconvolved seismograms are derived from the short period; the deconvolved seismograms being broad band seismograms corrected for attenuation. The nearest of the four arrays (WRA) is at a distance of about 80° and two of the arrays (EKA and GBA) lie in the PKP range. Most of the data is from YKA, WRA and GBA.

The detection thresholds for Tuamotu explosions reported in the Bulletin of the International Seismological Centre (ISC) is $\approx m_b 4.5$. The detection threshold for the arrays is below the ISC threshold and many of the presumed explosions are not reported in the Bulletins but are detected by the arrays.

As well as the seismograms the report lists estimates of various characteristics of the initial P pulse such as the long term level of the reduced displacement potential (ψ_∞), duration and rise time, and various measures of explosion size including conventional magnitude m_b and rms signal amplitudes in several time windows. The correlation of these observations with m_b^{ML} is investigated; m_b^{ML} being the maximum likelihood magnitude of the explosions derived from the amplitude and period observations given in the ISC bulletins. m_b^{ML} is taken to be the best estimate of explosion size.

The most striking features shown by the seismograms presented here is that whereas those for Mururoa explosions recorded at YKA and those from the Fangataufa explosions are relatively simple, the seismograms from Mururoa explosions recorded at WRA and GBA are complex. The complexity appears to be due to a reduction in the amplitude of the first arrival at WRA and GBA rather than an increase in the coda amplitude. It seems clear that near source effects are responsible for the reduction in the first arrival at WRA and GBA. For WRA seismograms for Mururoa explosions for example, the apparent pP (A_{pP}) is poorly developed whereas A_{pP} is identifiable on almost all YKA seismograms. On WRA seismograms for Fangataufa explosions A_{pP} is clearly seen. It may also be significant that at least 4 of the 5 explosions at Fangataufa appear to have been fired at a greater depth (A_{pP}-P time, 0.8s) than those at Mururoa (A_{pP}-P time, 0.4-0.6s). However, at this stage it is not possible to give a convincing explanation of the variations in complexity.

The main conclusions come from the analysis of the YKA and WRA observations. These are given below.

(i) The lines relating ψ_∞ and m_b^{ML} for YKA and WRA observations have slopes close to 1.0 implying that m_b^{ML} is a measure of amplitude at or below the corner frequency of the source pulse.

(ii) The predominant period of the initial arrival on the SP seismograms - particularly the unfiltered version - increases slowly with m_b^{ML} from about 0.8 to 1.0s presumably due to a decrease in the corner frequency of the source pulse with magnitude.

(iii) The measures of source size (logA_0, logA, logA/T and rms amplitudes) are highly correlated with m_b^{ML}. (A_0 is the ½ peak-to-peak amplitude as read from the seismogram and A the amplitude corrected for the gain at period T of a system with a gain of unity at 1 Hz). However, apart from logA, the slope of the lines relating observation to m_b^{ML} are usually significantly less than 1.0. The departure of the slope from 1.0 is due to the lack of a correction to A_0 and rms amplitudes to allow for changes in period with m_b^{ML} and over-correction for period when using logA/T to compute magnitude. With A allowance is made for departures in T from 1 Hz.

(iv) The variance of the rms observations against m_b^{ML} are similar to and often less than the variance of station magnitudes. This is particularly true for WRA where the seismograms are more complex than those for YKA. The results suggest that at least as a measure of the relative size of explosions, rms amplitudes might give estimates with smaller variance than conventional magnitudes.

1. INTRODUCTION

Since 1968 France has carried out nuclear tests in the Tuamotu Archipelago in the South Pacific at two sites separated by about 50 kms: Mururoa atoll (where the majority of the tests took place) and Fangataufa. The early tests were in the atmosphere but since 1975 all tests have been underground. In this report we present array recordings of the P waves from some of the underground explosions at Tuamotu. The arrays are at Yellowknife, Canada (YKA); Eskdalemuir, Scotland (EKA); Warramunga, Australia (WRA) and Gauribidanur, India (GBA).

The report is one of a series that present array seismograms recorded from explosions at the main test sites. The main purpose of the report is to provide a catalogue of the short period (SP) seismograms together with broad band (BB) and deconvolved seismograms derived from the SP; the deconvolved seismograms being BB seismograms corrected for attenuation. It is hoped that such seismograms will help in characterising the explosion source and in understanding how explosions generate seismic waves. The SP, BB and deconvolved seismograms and the measurements made on them are given in appendices. The main text describes the processing of the data and the principal characteristics of the seismograms and gives the results of some analyses of the measurements.

2. THE TUAMOTU TEST SITES

The Tuamotu test sites are remote from most of the world's seismological stations: there are few stations in the teleseismic zone at distances of less than 60°. Figure 1 is a map showing the position of the arrays relative to the test site. The detection thresholds for Tuamotu explosions reported in the Bulletin of the International Seismological Centre (ISC) is $\approx m_b 4.5$, where m_b is body wave magnitude. The detection threshold for the arrays is below the ISC threshold and many signals have been recorded from presumed explosions of low magnitude at the test sites that are not reported in the Bulletins.

The archipelago has little or no natural seismic activity so that any seismic disturbance in the area must be treated as a possible explosion. Positive identification of the disturbances as explosions is difficult using the ratio of m_b to surface wave magnitude, M_s - usually the most reliable identification criterion. The surface waves are only detected from the largest yield explosions. However, T phases recorded at the seismic station at Rarotonga from known explosions at Tuamotu have a characteristic form. The detection of such a T phase from a disturbance at Tuamotu can thus be used to identify the source as an explosion. In recent years France has announced many of the explosions.

Data are presented here from 108 known or presumed underground explosions at Tuamotu that occurred during the period 1975-1989. Douglas et al [1] give estimates of the relative locations of the 71 underground explosions reported by the ISC. The results presented by Douglas et al [1] (Figure 2) show that only three of the explosions took place at Fangataufa. Of the 37 known or presumed explosions not reported by the ISC there is no travel time data that can be used to determine whether the explosions were at Mururoa or Fangataufa. However, newspaper and other reports [2,3] state that two of the 37, which were the first two underground tests at Tuamotu (5 June and 26 November, 1975), were fired at Fangataufa. Inspections of the seismograms presented in this report support this view (see later). For the other presumed explosions not reported by the ISC what evidence there is suggests they were fired at Mururoa and this is assumed to be so in what follows. Table 1 lists the explosions by test site (Mururoa or Fangataufa) and shows the arrays which recorded each explosion. Also given for the explosions reported by the ISC are the bodywave magnitude (m_b) taken from the bulletin and the maximum-likelihood magnitude (m_b^{ML}) estimated by Douglas et al [1]. In this report m_b^{ML} is taken to be the best estimate of explosion size. The average distances, azimuths and backbearing of the arrays from Mururoa and Fangataufa are given in Tables 2 & 3 respectively. The nearest of the four arrays (WRA) is at a distance of about 80° and two of the arrays (EKA and GBA) lie in the PKP range. Most of the data comes from YKA, WRA and GBA.

The shallow geological structure of Mururoa is roughly that of a layer over a half space (Crusem [4]). The layer thickness varies from 1.9-2.4 kms and the P-wave speed in the layer from 3.3-3.8 km s^{-1}. The P-wave speed in the half space is 5.05-5.25 km s^{-1}. Evidence from refraction surveys in the area show the crust to be about 30 kms thick and the P_n wave speed to be 8.1 km s^{-1} (Talandier & Okal [5]). No information is available on the structure of Fangataufa but as it is an atoll it has presumably a similar structure to that of Mururoa.

3. DATA AND PROCESSING METHODS

The data used here are SP array recordings. Figure 3 shows the layout of the arrays. All the arrays have 19 or 20 vertical-component Willmore Mk II seismometers in two lines which are roughly at right angles. Recording at the arrays was initially on analogue tape but over the period 1976-1989 each array in turn has been converted to digital recording. The sampling rate of both the digitally recorded and digitised analogue data is 20 samples per second. The frequency response of the SP recording system of one array (YKA) is shown in Figure 4. The responses of the other arrays differ slightly from the response shown but these differences and variations in the system gain have been taken into account in the processing.

The main processing carried out is the derivation of BB and deconvolved seismograms. When SP array recordings are available the P signals for each seismometer channel are time shifted to correct for the travel time of the signal across the array and the channels are summed. The BB seismogram is obtained by multiplying the spectrum of the array sum by $a_2(\omega)/a_1(\omega)$ and transforming back to the time domain. $a_1(\omega)$ and $a_2(\omega)$ are the responses at frequency ω of the SP and BB instruments respectively. In addition to the instrument conversion each seismogram is filtered to attenuate noise outside the pass band of the instrument. The seismogram is also filtered using a single channel Wiener filter designed by making some simple assumptions about the signal, and using the noise preceding the signal as the noise model.

The deconvolved seismogram is obtained by dividing the spectrum of the BB seismogram by the spectrum of the attenuation operator of Carpenter [6] before transforming into the time domain. The amplitude spectrum of the operator has the form $\exp(-\omega t^*/2)$ and the phase spectrum is specified using the theory of Futterman [7]. t^* is the ratio of travel time to the specific quality factor Q. To carry out the deconvolution requires an estimate of t^*. Douglas et al [8] argue that t^* is around 0.35s for the Mururoa-YKA path and this value is also used for the paths to WRA and GBA. Figure 5 shows an example of the output (analysis sheet) from the analysis of each observed seismogram. The figure shows the array sum, the BB seismogram and the deconvolved seismogram for the explosion of 25 May 1988 recorded at YKA. Also shown are two filtered versions of the SP seismogram; one version being filtered in the 0.5-4 Hz band, the other in the 1.0-4.0 Hz band. The additional filtering is applied to improve the signal-to-noise ratio and so it is hoped reduce the errors in the observations; the predominant noise having frequencies below 1 Hz.

Appendices A and B show SP, BB and deconvolved seismograms for all the available recordings of the Tuamotu explosions at the four arrays. Observations from these seismograms are listed in Appendices C and D. The observations from the unfiltered and filtered SP seismograms are principally half peak-to-peak amplitude, period, and rms amplitudes. The amplitudes and periods are used to compute magnitudes. The rms amplitudes are used to investigate the relationship between such amplitudes and body wave magnitudes (see section 5). Appendices E & F show the analysis sheets for all the observed seismograms.

The observations from the unfiltered SP seismograms are A_0 & T; A_0 being half the range between the first negative deflection (for a system with a gain of unity at 1 Hz) and the succeeding positive deflection and T the corresponding period (see Figure 5). The position where A_0 (& T) is read is picked by the analyst. Amplitudes and periods of the signals are also measured on the two filtered versions of the SP seismograms together with measurements of the rms amplitudes in seven time windows (0-3s, 0-6s, 0-9s, 0-15s, 3-9s, 3-15s and 9-18s, where time zero is the onset of the signal). The rms amplitude of the noise preceding the signal is also measured. All the measurements on the filtered SP seismograms are made automatically without analyst intervention. The value of A_0 measured is half the maximum peak-to-peak amplitude within the first three seconds after the onset of the signal. Station magnitudes are computed from A_0, A & A/T; where A is $A_0/g(T)$ and g(T) is the gain of the recording system at period T. All the magnitudes are computed using the amplitude-distance curve of Lilwall [9] which covers the distance range 20-180°. This allows magnitudes to be computed for GBA and EKA which lie at PKP distances.

No measurements are made from the deconvolved seismograms for EKA and GBA. The EKA seismograms have too low a signal-to-noise ratio to give useful results and those from GBA show multiple arrivals, at least one of which appears to have been Hilbert transformed (which is not unexpected) on the path from source to receiver and this makes reliable measurements difficult to obtain. The measurements made from the deconvolved YKA and WRA seismograms are: the area under the initial positive pulse; the rise and fall times of the pulse; and the duration of the pulse. If an apparent surface reflection (A_{pP}) can be identified the A_{pP}-P time is also estimated; the time used being that between maximum positive deflection of the P pulse and maximum negative deflection of A_{pP}. The rise time is defined following Gladwin & Stacey [10] as $u_{max}/(du/dt_{max})$, where u_{max} is the maximum amplitude of the initial pulse and $(du/dt)_{max}$ is the maximum gradient of the leading edge of P. Fall-time is measured in a similar way on the trailing edge of the P pulse (see Figure 5). From the area (H) of the P pulse it is possible to estimate ψ_∞ and the seismic moment of the explosion. Thus ψ_∞ is given by

$$\psi_\infty = \{2KG(\Delta)\}^{-1} H$$

where $G(\Delta)$ corrects for loss of amplitude due to geometrical spreading on the path between test-site and station. The values for $G(\Delta)$ listed by Carpenter [11] are used here. K allows for loss of amplitude at discontinuities in the crust at source and at the receiver and for the effects of differences between the acoustic impedence at the source and receiver. The moment M_o is given by

$$M_o = 4\pi\rho\alpha^2\psi_\infty$$

where ρ and α are respectively the density and P wave speed in the firing medium. More details on the computation of ψ_∞ and M_o are given in Appendix C.

4. THE SEISMOGRAMS

Figure 6 shows the SP and deconvolved P seismograms for two explosions at Mururoa and two at Fangataufa as recorded at the three stations YKA, WRA and GBA. Most of the signals are too weak to be recorded above noise at EKA: a few signals are detected but these have very low signal-to-noise ratio and are considered later. At all stations other phases in addition to P are predicted to arrive within about 10s of signal onset. These phases and their relative arrival times are listed in Table 4 and the predicted times are indicated in Figure 6. (The travel times assumed throughout this report are as predicted by the IASPEI 1991 Seismological Tables, Kennett [12]).

Inspection of the seismograms shows clear variation with station and test site. The YKA seismograms for the two test sites though differing in detail are typical simple explosion seismograms. The core reflected phase PcP is expected to arrive just over two seconds after onset but none of the YKA seismograms in Figure 6 show clear evidence of any such arrival. A few YKA seismograms (see for example those of the explosions of 8 December 1981, 19 April 1983 and 31 October 1989, Appendix A) do show a prominent arrival within 4 seconds of the P onset which has about the right arrival time to be PcP. However, further evidence is required before the arrival can be accepted as being PcP. In particular it remains to be explained why the observed arrival is so clear on some YKA seismograms and absent on others.

The deconvolved YKA seismograms show P and an apparent pP (A_{pP}) with A_{pP}-P time for the Mururoa explosions of about 0.5s and for the Fangataufa explosions about 0.8s. This difference in the A_{pP}-P time between explosions at the two test sites produces an observable difference in the SP seismograms. For the Fangataufa explosions the P pulse is complete before the onset of A_{pP} and this results in an inflexion on the second positive deflection of the SP seismogram. For the Mururoa explosions the trailing edge of P and the leading edge of A_{pP} merge so that the pulses interfere constructively around 1 Hz and there is no inflexion. The effect of the difference on the way P and A_{pP} interfere is to enhance the maximum peak-to-peak amplitude of the SP seismograms for Mururoa explosions relative to those for the Fangataufa explosions. This shows up in the ratio of the first motion to peak-to-peak amplitude which is 0.15 or less for the Mururoa explosions whereas for the Fangataufa explosions the ratio is greater than 0.25.

Whereas the YKA seismograms of Mururoa and Fangataufa explosions are similar, with the main differences arising because of the differences in the A_{pP}-P time for the two test sites, the seismograms recorded at WRA from the two sites are strikingly different (Figure 6). Thus the Fangataufa seismograms usually show P & A_{pP} and have a coda that falls-off in roughly the same way as those for YKA but the WRA seismograms for Mururoa are significantly more complex than those of YKA and show no clear evidence of A_{pP}. Note that it is not that the absolute amplitude of the WRA coda is large that makes the WRA seismograms for Mururoa explosions complex - the YKA coda amplitudes are in fact larger than at WRA - but that the first arrival is small. This is illustrated in Figure 7 which shows a comparison of station magnitudes, coda rms and ψ_∞ for the two stations. Figure 7a shows the YKA and WRA magnitudes against m_b^{ML} and Figure 7b the YKA and WRA rms amplitudes for the 3-15s window against m_b^{ML}. (0.05 has been subtracted from the log of the WRA rms amplitudes to allow for differences in the distance correction factors for YKA and WRA).

From the Mururoa explosions it is clear that whereas the rms amplitude of the coda for the two stations differ by about a factor of 2 the YKA station magnitudes are almost one unit larger than those at WRA. For ψ_∞ (Figure 7c) the YKA estimates are only about 3 times larger than those for WRA.

The explosions of 30 November 1988 and 10 June 1989 shown in Figure 6 are known to have been fired at Fangataufa because the estimated epicentres fall close to the island. The two explosions of 1975 (5 June and 26 November) are also reported [2,3] to have been fired at Fangataufa. This is consistent for the 26 November 1975 explosion with the evidence that WRA seismograms of Mururoa and Fangataufa explosions are significantly different (Figure 6). (There is no WRA seismogram for the 5 June 1975 explosion). Thus the WRA seismograms for the 27 November 1975 explosion (Appendix B) is both simple and has a maximum amplitude that is only about a factor of 2 less than that at YKA which is typical of Fangataufa explosions. Had the explosion been fired at Mururoa the WRA seismogram would be expected to be complex and have an amplitude at least a factor of 4 less than that observed at YKA.

GBA lies very near the PKP focus. Travel time tables predict (Table 4) there will be a series of arrivals with very similar onset times. Inspection of the GBA seismograms from the Fangataufa explosions (Figure 6) shows that there are indeed several arrivals. Taking the first arrival to be PKP_{BC} + PKP_{AB} two of the later arrivals coincide roughly with the predicted times of PKP_{DF} and PKiKP. Further, the onset of the signal does not show the typical first motion of explosion seismograms: although first motion on the SP does appear to be positive it is of low amplitude and emergent. This is to be expected if PKP_{AB} predominates as the first arrival because this is a mini-max phase and should approximate to the Hilbert transform of the P phase. This produces an emergent onset.

The seismograms from the Mururoa explosions recorded at GBA (Figure 6) are more complex than those from the Fangataufa explosions. Following the first arrival, which is predicted to be PKP_{DF}, several arrivals are observed. One of these arrivals usually coincides roughly with the calculated time for PKiKP which is the only other phase predicted from travel time tables. Comparison of the seismograms with those from WRA suggests that in fact the prominence at GBA of many arrivals in the coda not predicted by tables is again due to the first arrival being weak rather than the coda arrivals being strong. This is supported by Figure 7 where YKA and GBA magnitudes and rms amplitudes (3-15s window) are plotted against m_b^{ML}. (0.21 has been subtracted from the log of the GBA rms amplitudes to allow for differences in the distance correction factor for YKA and GBA.) Thus the GBA magnitudes are one unit lower than at YKA whereas the rms amplitudes differ by a factor of only about 3. These differences in GBA and YKA magnitudes and rms amplitudes are similar to but somewhat larger than the differences for WRA and YKA. Similarity in the complexity of the GBA seismograms to the WRA seismograms is perhaps to be expected as the rays to the two stations take-off in similar directions, there being only 10° difference in the azimuths to the two stations.

As with the GBA recordings from the Fangataufa explosions the recordings from the Mururoa explosions have a relatively low amplitude, emergent first motion suggesting that the first arrival at Mururoa is a minimax phase. However, it is only arrivals from the PKP_{AB} branch that are expected to be mini-max phases and this branch is only predicted to exist for ranges of 144.55° and beyond, which is just slightly greater than the GBA-Mururoa distance but less than the GBA-Fangataufa distance. Thus if the first arrival at GBA from Mururoa explosions is PKP_{AB} and not PKP_{DF} the travel time tables for this distance range are incorrect. The observations of Tuamotu explosions at GBA provide important data to enable the tables to be corrected. However, detailed study is needed to disentangle the various PKP branches. Such a study is outside the scope of this report.

Figure 8 shows 7 of the clearest detections at EKA of Mururoa explosions - these are SP array beams. There seems to be no doubt that the signals are seen but the signal-to-noise is poor. Summing the signals (top trace) confirms the presence of the signals showing the typical explosion shape but with low predominant frequency suggesting that high frequencies have been lost from the signal either through scattering or anelastic attenuation.

5. ANALYSIS OF OBSERVATIONS

Figures 9-14 show the various measurements made from the YKA seismograms of the Mururoa explosions plotted against m_b^{ML}. Figures 15-20 and 21-25 show the results for WRA and GBA respectively.

The lines through the data are least squares lines estimated assuming that there is no error in m_b^{ML}. In general the YKA observations are less scattered than those for WRA and GBA presumably because the YKA seismograms have higher signal-to-noise ratios and are simpler than the corresponding WRA and GBA seismograms. (No graphs are shown of the measurements from the Fangataufa explosions as the number of explosions at that site is too small.)

The durations, rise times and fall times at YKA and WRA all increase with m_b^{ML} but the correlation coefficients are not all significant at the 5% level. Comparison of the rise times shows that although the results for WRA are more scattered than at YKA, on average there is little difference between the two stations. The durations of the pulses do appear to differ with station: the average duration for WRA is around 0.9s whereas that for YKA is around 0.6s. Further, the fall times at WRA are greater than those at YKA. These differences can be understood if the effect of A_{pP} is taken into account. At YKA A_{pP} is identifiable on almost all the seismograms whereas at WRA A_{pP} is usually absent. Also the measured A_{pP}-P time for YKA is very similar to the apparent pulse duration. Thus it appears that the P pulse of YKA is truncated by the arrival of A_{pP} so the apparent pulse duration is reduced relative to the pulses observed at WRA. The pulse observed at WRA is thus a better estimate of P than that at YKA. The interference of P & A_{pP} at YKA apparently produces a P pulse with a sharper trailing edge than the WRA pulse, ie the apparent fall time of the YKA P is shorter than the true fall time.

The least squares lines relating the estimates of source size to m_b^{ML} have slopes in the range 0.60-1.15. For ψ_∞ against m_b^{ML} the slope of the line relating the two variables is close to 1.0 (Figure 9a). This implies that m_b^{ML} is measuring the amplitude at a roughly constant period and that this period is at or below the corner frequency of the explosion source. As most of the observations contributing to m_b^{ML} probably come from very narrow band SP systems the suggestion that there is little variation in T with magnitude is plausible: that is m_b^{ML} is proportional to amplitude A, with T, being independent of magnitude, having no effect on the slope of the least squares line.

For the YKA SP observations T increases with m_b^{ML} (Figure 10a) consequently the station magnitude for YKA which depends on log(A/T) has a slope (0.86) that is significantly less than 1.0. This is confirmed if magnitude is computed using logA (Figure 11a) when the slope of the line (0.93) is now close to 1.0. Similar effects are seen for the WRA observations (Figure 16a) although the results are more scattered and in fact the slope of WRA station magnitude (Figure 16b) against m_b^{ML} is not significantly different from 1.0. For GBA on the other hand the slope of the least squares line relating station magnitude to m_b^{ML} (Figure 21b) is significantly less than 1.0 and T appears to be independent of m_b^{ML} (Figure 21a). At around m_b^{ML}4.5 the observed period of about 0.8s is similar to that observed at YKA and WRA but whereas at the latter two stations period increases to around 1.0 at m_b^{ML}6.0, the period for GBA remains constant at around 0.8s. It might be possible to account for the lack of variation in period at GBA by source effects. However, one significant difference between the GBA seismograms and those from YKA and WRA is that the main arrival on the GBA seismograms has probably been Hilbert transformed on propagation from source to receiver and it may be that the effect of this is to make the observed period appear more uniform. An investigation of the effect of Hilbert transformation on the measured period is being carried out and will be reported elsewhere.

Turning now to the station magnitudes measured on the band-pass filtered seismograms. On the unfiltered YKA and WRA seismograms the average period at around m_b^{ML}4.5 is 0.8s whereas that at m_b^{ML}6.0 is about 1.0 Hz. The effect of the additional filtering is to attenuate those signals with the largest predominant period and to make the observed period over the range m_b^{ML}4.5-6.0 more nearly constant. The result of this is that station magnitudes calculated from the filtered seismograms (Figures 10d & f and 16d & f) increase more slowly with m_b^{ML} than do the magnitudes estimated from the unfiltered seismograms. (The effect for the GBA seismograms where the period on the unfiltered versions is almost uniform is to produce apparently, a slight decrease in period with magnitude although the estimated slope of the period-magnitude lines are not significantly different from zero). The results for YKA and WRA suggest that the corner frequency varies from just above 1 Hz at m_b^{ML}4.5 to just below at m_b^{ML}6.0 and the effect of band pass filtering is to confine the measurements to a pass band above the corner.

For the explosions not reported in the ISC no estimate of m_b^{ML} is available. However, an estimate of m_b^{ML} can be obtained for these explosions if they have been recorded at YKA by using the relationship between the station and maximum likelihood magnitudes. Estimates of m_b^{ML} derived in this way, m_b^{ML} (YKA), are listed in Table 1. For the explosions at Mururoa the m_b^{ML} (YKA) estimates were obtained using the relation between

m_b^{ML} and the YKA m_b given in Figure 10b. For the Fangataufa explosion m_b^{ML} (YKA) is calculated by subtracting 0.04 from the YKA m_b; 0.04 being the average difference between m_b^{ML} and the station m_b for the three Fangataufa explosions recorded by YKA and reported in the ISC bulletins. The results suggest that the detection threshold for YKA for Mururoa explosions is below m_b^{ML}3.5.

The rms observations are all highly correlated with m_b^{ML}. The slopes of the least squares lines are similar to those relating station magnitudes measured on the filtered SP seismograms to m_b^{ML} but often the scatter of the observations about the least squares line is less for the rms observations than for the magnitudes. This is particularly true for WRA where the variance of magnitude observations is 2-3 times that of the rms observations.

6. DISCUSSION

All the deconvolved seismograms have been derived on the assumption that the value of t* (0.35s) suggested by Douglas et al [8] for the Mururoa-YKA path applies to the other paths studied. From the results presented here at least for paths to YKA and WRA there is no evidence that t* for paths to these two stations are widely different. The rise times on the deconvolved seismograms are similar for both stations for example. It seems unlikely then that the large differences in the station magnitudes of YKA and WRA for Mururoa explosions can be attributed to differences in anelastic attenuation on the paths to these stations. If the anelastic attenuation on the path to WRA were greater than on the path to YKA the region of high attenuation would have to be very localised; on the paths from Mururoa and Fangataufa to WRA, GBA and YKA the only paths that can cross the region are those from Mururoa to WRA and GBA.

Ignoring the amplitudes it would appear from inspection of the SP seismograms that if anything the WRA recordings of Tuamotu explosions show higher predominant frequencies than YKA recordings. This is particularly true for the Fangataufa explosions recorded at WRA and YKA (Figure 6).

The rms (3-15s) amplitudes and the station magnitudes of the Fangataufa explosions suggests that the differences in the WRA and YKA station magnitudes for Mururoa (and Fangataufa) explosions in the absence of near source effects is about a factor of 2. The ψ_∞ observations for WRA and YKA show that the total differences for the P pulse between the two paths is a factor of 3 which suggests that because of near source effects the P pulse radiated to WRA is about a factor of 1.5 smaller than that radiated to YKA. The large differences in WRA and YKA station magnitudes for Mururoa explosions (equivalent to a factor of about 6 in amplitude) can thus be roughly accounted for by a difference of a factor of 1.5 in the amplitude of the radiated P pulse, a factor of 2 for differences in path effects and a factor of 2 from the absence of A_{pP} at WRA. What the mechanisms are that result in the P pulse radiated to WRA having on average two thirds the amplitude of that radiated to YKA and the lack of A_{pP} is not clear and remains to be investigated.

7. CONCLUSIONS

The most striking features shown by the seismograms presented here is that whereas those for Mururoa explosions recorded at YKA and those from the Fangataufa explosions are relatively simple, the seismograms from Mururoa explosions recorded at WRA and GBA from Mururoa explosions are complex. The complexity appears to be due to a reduction in the amplitude of the first arrival at WRA and GBA rather than an increase in the coda amplitude. It seems clear that near source effects are responsible for the reduction in the first arrival at WRA and GBA. For WRA seismograms for Mururoa explosions for example A_{pP} is poorly developed whereas A_{pP} is identifiable on almost all YKA seismograms. On WRA seismograms for Fangataufa explosions A_{pP} is clearly seen. It may also be significant that at least 4 of the 5 explosions at Fangataufa appear to have been fired at a greater depth (A_{pP}-P time, 0.8s) than those at Mururoa (A_{pP}-P time, 0.4-0.6s). However, at this stage it is not possible to give a convincing explanation of the variations in complexity.

Numerous conclusions can be drawn from the analysis of the observations. The main conclusions from the analysis of the observations from the YKA and WRA seismograms are given below.

(i) The lines relating ψ_∞ and m_b^{ML} for YKA and WRA observations have slopes close to 1.0 implying that m_b^{ML} is a measure of amplitude at or below the corner frequency of the source pulse.

(ii) The predominant period of the initial arrival on the SP seismograms - particularly the unfiltered versions - increases slowly with m_b^{ML} from about 0.8 to 1.0s presumably due to a decrease in the corner frequency of the source pulse with magnitude;

(iii) The measures of source size ($\log A_0$, $\log A$, $\log A/T$ and rms amplitudes) are highly correlated with m_b^{ML}. However, apart from logA, the slope of the lines relating observation to m_b^{ML} are usually significantly less than 1.0. The departure of the slope from 1.0 is due to the lack of a correction to A_0 and rms amplitudes to allow for changes in period with m_b^{ML} and over-correction for period when using logA/T to compute magnitude. With A allowance is made for departures in T from 1 Hz.

(iv) The variance of the rms observations against m_b^{ML} are similar to and often less than the variance of station magnitudes. This is particularly true for WRA where the seismograms are more complex than those for YKA. The results suggest that at least as a measure of the relative size of explosions, rms amplitudes might give estimates with smaller variance than conventional magnitudes.

ACKNOWLEDGEMENTS

We thank the operators of the arrays for their conscientious work over many years, which has produced a large library of high quality recordings from which the seismograms presented here are taken.

<u>REFERENCES</u>

1. Douglas, A, Marshall, P D & Young J B. "Body wave magnitudes and locations of French explosions in the South Pacific". AWE Report O 11/93, HMSO, London (1993).

2. Ponchelet, H. "Polynésie: Bombes Nucleares sous les atolls". Le Figaro, 17 September 1975.

3. A S Burrows, R S Norris, W M Arkin & T B Cochran. "French Nuclear Testing, 1960-1988. Nuclear Weapons Data Center Working Paper NWD 89-1. Natural Resources Defense Council, Washington, USA (1989).

4. Crusem, R. "Simulation de signaux sismiques et etude de sources nucleaires souterraines par inversion de moments". Thesis. Ecole Centrale des Arts et Manufacturers, Paris, France (1986).

5. J Talandier & E A Okal. "Crustal structure of the Society and Tuamotu Islands, French Polynesia". Geophys. J R astr Soc, **88**, 499-528 (1987).

6. E W Carpenter. "Absorption of elastic waves - an operator for a constant Q mechanism". AWRE Report O 43/66, HMSO, London (1966).

7. W I Futterman. "Dispersive body waves". J Geophys Res, **67**, 5279-5291 (1961).

8. A Douglas, P D Marshall, J B Young. "Comment on "Teleseismic *P* wave attenuation and nuclear explosion source functions inferred from Yellowknife array data, by Kin-Yip Chun, Tianfei Zhu and Gordon F West". J Geophys Res, **98**, 9921-9925 (1993).

9. Lilwall, R C. "Empirical Amplitude-Distance/Depth curves for short-period P waves in the distance range 20-180°". AWRE Report No. O 30/86, HMSO, London (1987).

10. M T Gladwin, F D Stacey. "Anelastic degradation of acoustic pulse in rock". Phys Earth Planet Int, **8**, 332-336, (1974).

11. E W Carpenter. "A quantitative evaluation of seismic signals at teleseismic distances". Proc Roy Soc, A, 290, 396-407 (1966).

12. B L N Kennett (Ed). "IASPEI 1991 Seismological Tables". Research School of Earth Sciences, Australian National University, Canberra, Australia (1991).

Table 1
Mururoa Explosions

Date	YKA	EKA	WRA	GBA		m_b(ISC)	m_b^{ML}	m_b^{ML}(YKA)
760711	*	-	N	*	ISC	5.0	4.93	4.83
770219	*	-	N	N	ISC	5.2	5.02	4.90
770319	O	*	N	*	ISC	5.8	5.92	0.00
770706	*	-	*	*	ISC	5.2	4.81	4.81
771112	*	-	N	*		0.0	0.00	4.51
771124	N	-	N	*	ISC	6.0	5.86	0.00
771217	N	-	N	*		0.0	0.00	0.00
780227	*	-	-	-		0.0	0.00	3.48
780322	*	-	*	*	ISC	4.8	4.73	4.66
780719	*	-	*	-		0.0	0.00	4.20
780726	*	-	-	-		0.0	0.00	3.86
781102	*	-	N	*		0.0	0.00	4.38
781130	O	*	*	*	ISC	5.8	5.86	0.00
781217	*	-	N	*		0.0	0.00	4.65
781219	*	-	*	*	ISC	4.9	5.01	4.94
790301	*	-	*	*		0.0	0.00	4.64
790309	*	-	*	*		0.0	0.00	4.69
790324	*	-	*	*	ISC	4.9	4.93	4.90
790404	*	-	N	-	ISC	4.7	4.69	4.77
790618	*	-	*	*	ISC	4.7	4.71	4.66
790629	*	-	*	*	ISC	5.4	5.21	5.16
790725	O	*	*	*	ISC	6.0	6.11	0.00
790728	*	-	*	*	ISC	4.4	4.73	4.58
791122	*	-	*	-		0.0	0.00	4.40
800223	*	-	*	*		0.0	0.00	4.11
800303	*	-	*	*		0.0	0.00	4.22
800323	*	-	*	*	ISC	5.7	5.63	5.60
800401	*	-	*	*	ISC	5.1	5.05	5.11
800404	*	-	-	*	ISC	4.5	4.30	4.37
800616	*	-	*	N	ISC	5.4	5.30	5.32
800621	*	-	*	*		0.0	0.00	4.53
800706	*	-	*	-	ISC	4.6	4.54	4.51
800719	N	*	*	*	ISC	5.8	5.73	0.00
801203	N	-	*	*	ISC	5.6	5.58	0.00
810227	*	-	*	*		0.0	0.00	4.20
810306	*	-	*	*		0.0	0.00	4.31
810328	*	-	*	*	ISC	4.7	4.75	4.70
810410	*	-	*	*	ISC	4.8	4.76	4.78
810708	*	-	*	*	ISC	5.3	5.14	5.08
810711	*	-	N	-		0.0	0.00	3.86
810718	*	-	*	-		0.0	0.00	4.20
810803	*	-	*	-	ISC	5.3	5.09	5.12
811111	*	-	*	*	ISC	4.5	4.71	4.74
811205	*	-	*	*	ISC	4.6	4.68	4.58
811208	*	-	*	*	ISC	5.2	5.14	4.94
820220	*	-	-	-		0.0	0.00	3.58
820224	*	-	*	-		0.0	0.00	3.59
820320	*	-	*	*	ISC	4.9	4.96	4.96
820627	*	-	-	-		0.0	0.00	3.75
820701	*	-	*	*	ISC	5.1	5.08	5.11
820725	*	*	N	*	ISC	5.7	5.60	5.58
830419	*	*	*	*	ISC	5.6	5.70	5.63
830425	*	-	-	-		0.0	0.00	3.22
830525	N	*	*	*	ISC	5.9	5.87	0.00
830618	*	-	-	-		0.0	0.00	3.87
830628	*	-	*	*	ISC	5.4	5.32	5.36
830720	*	-	*	-		0.0	0.00	4.44
830804	*	-	*	*	ISC	5.3	5.13	5.06
831203	*	-	*	-		0.0	0.00	4.10
831207	*	-	*	*	ISC	5.0	4.89	4.85
840508	*	-	N	*		0.0	0.00	4.51
840512	*	*	*	*	ISC	5.7	5.57	5.61
840612	*	-	-	*		0.0	0.00	4.54
840616	*	-	*	*	ISC	5.3	5.28	5.28
841027	*	-	*	-	ISC	4.5	4.49	4.43
841102	*	*	*	*	ISC	5.6	5.64	5.49
841201	*	-	-	-		0.0	0.00	3.57
841206	*	-	*	*	ISC	5.6	5.56	5.57
850430	*	-	*	-	ISC	4.5	4.51	4.54
850508	*	-	*	*	ISC	5.6	5.64	5.57
850603	*	-	*	*	ISC	5.1	4.83	4.73
850607	*	-	*	-		0.0	0.00	4.43
851024	*	-	-	-		0.0	0.00	4.26
851026	*	-	*	*	ISC	5.3	5.30	5.31
851124	*	-	*	*	ISC	4.7	4.55	4.65
851126	O	-	*	*	ISC	5.9	5.76	0.00
860426	*	-	*	-	ISC	4.8	4.45	4.43
860506	*	-	*	-		0.0	0.00	4.46
860527	*	-	*	-		0.0	0.00	4.62
860530	*	*	*	*	ISC	5.6	5.58	5.60

861112	N	-	*	*	ISC	5.2	5.28	0.00
861206	*	-	*	*		0.0	0.00	4.68
861210	*	-	*	*	ISC	5.1	5.23	5.21
870505	*	-	*	*	ISC	4.8	4.55	4.46
870520	*	-	*	*	ISC	5.6	5.51	5.54
870606	*	-	*	*	ISC	4.7	4.40	4.61
870621	*	-	*	*	ISC	5.1	5.10	5.31
871023	*	*	*	*	ISC	5.5	5.54	5.64
871105	*	*	*	*	ISC	5.4	5.36	5.45
871119	O	*	*	*	ISC	5.8	5.74	0.00
871129	*	-	*	*		0.0	0.00	4.55
880511	*	-	*	*	ISC	5.4	5.27	5.41
880525	*	-	*	*	ISC	5.6	5.50	5.59
880616	*	-	*	*		0.0	0.00	4.41
880623	*	-	*	*	ISC	5.3	5.18	5.35
881105	*	-	*	*	ISC	5.5	5.30	5.35
881123	*	-	*	N	ISC	5.4	5.29	5.41
890511	*	-	N	*	ISC	5.5	5.16	5.21
890520	*	-	N	-		0.0	0.00	4.49
890603	*	-	*	*	ISC	5.2	5.16	5.36
891024	*	-	*	*	ISC	5.4	5.37	5.29
891031	*	-	*	*	ISC	5.2	5.30	5.16
891120	N	-	*	*	ISC	5.3	5.19	0.00

Fangataufa Explosions

Date	YKA	EKA	WRA	GBA		m_b(ISC)	m_b^{ML}	m_b^{ML}(YKA)
750605	*	-	N	-		0.0	0.00	4.51
751126	*	-	*	*		0.0	0.00	4.72
881130	*	-	*	*	ISC	5.5	5.58	5.62
890610	*	*	*	*	ISC	5.5	5.51	5.57
891127	*	*	N	*	ISC	5.6	5.59	5.48

* Signal detected.
\- Signal not detected or tape not processed.
N No tape available.
O Signal overloaded.

Table 2

Epicentral distances, azimuths and backbearings
of arrays from Mururoa*

Station	Distance (°)	Azimuth (°)	Backbearing (°)
YKA	86.24	11.0	202.5
EKA	133.14	33.1	297.3
WRA	79.91	252.5	109.6
GBA	144.49	262.8	108.5

*Angles measured from centre of Mururoa, taken to be: 21.835°S 138.91°W

Table 3

Epicentral distances, azimuths and backbearings
of arrays from Fangataufa*

Station	Distance (°)	Azimuth (°)	Backbearing (°)
YKA	86.6	11.0	202.3
EKA	133.38	33.4	296.8
WRA	79.95	252.6	110.0
GBA	144.60	262.2	109.2

*Angles measured from centre of Fangataufa, taken to be: 22.233S 138.74W

Fangataufa lies 0.43° (47.25 km) from Mururoa on a bearing of 158.3°. The bearing of Fangataufa from Mururoa is 338.3°

TABLE 4

Relative arrival times of P phases for the four arrays

		Time after onset(s)	
Station	Phase	Mururoa	Fangataufa
YKA	P	0.0	0.0
	PcP	2.37	2.19
EKA	PKP_{DF}	0.0	0.0
	PKiKP	1.48	1.52
WRA	P	0.0	0.0
	PcP	7.32	7.27
GBA	PKP_{BC}	Not predicted	0.0
	PKP_{AB}	Not predicted	0.0
	PKP_{DF}	0.0	1.61
	PKiKP	4.23	5.87

The times are as predicted by the IASPEI 1991 Seismological Tables (Kennett [12])

FIGURE CAPTIONS

Figure 1 Azimuthal-great circle projection of the earth centred on Tuamotu showing the positions of the four arrays.

Figure 2 Map showing Mururoa and Fangataufa and the estimated epicentres of the 71 underground explosions which were reported by the ISC.

(a) Epicentres of the 71 explosions estimated relative to that of 25 July 1979 which is restrained to the position 21.88°S 138.94°W.

(b) Epicentres of the three Fangataufa explosions estimated relative to that of the 30 November 1988 which is restrained to the centre of the island (22.233°S 138.74°W).

Figure 3 Plans of the arrays showing seismometer positions.

Figure 4 Relative amplitude response of short period and broad band systems.

Figure 5 Example of the output (analysis sheet) for an observed seismogram. The observed short period (array sum), the filtered short periods, the broad band and the deconvolved seismograms (for t*=0.35s) are shown at the top of the figure. The shaded area on the deconvolved seismogram is used to estimate ψ_∞. The insets at the bottom of the figure shows how the rise and fall times of the pulse and A_0 and T/2 on the unfiltered SP are measured. The table at the bottom of the figure give the observations made on the seismograms.

Figure 6 Short period and deconvolved seismograms for two Mururoa and two Fangataufa explosions as recorded at YKA, WRA and GBA.

Figure 7 Comparison of some WRA and GBA estimates of source size with those for YKA.

(a) YKA & WRA station m_b against m_b^{ML}.
(b) YKA & WRA rms (3-15s) amplitudes against m_b^{ML}.
(c) YKA & WRA ψ_∞ against m_b^{ML}.
(d) YKA & GBA station m_b against m_b^{ML}.
(e) YKA & GBA rms (3-15s) amplitudes against m_b^{ML}.

Figure 8 Observed EKA short period seismograms for the 7 Mururoa explosions with the largest signal-to-noise ratios at the station. The top trace is the sum of the 7 observed seismograms. For each seismogram the station m_b and m_b^{ML} are given.

Figure 9 Graphs of various observations taken from the YKA seismograms against maximum likelihood m_b. (a) ψ_∞; (b) Pulse duration; (c) Pulse rise time; (d) Pulse fall time. The lines are least squares estimates obtained assuming no errors in the abscissa. The equations of the lines are given at the top of each figure with 95% confidence limits on the slopes and intercepts. x and y stand for the abscissa and ordinate respectively of the graphs.

Figure 10 Graphs of various observations taken from the YKA seismograms against maximum-likelihood m_b. (a) Period; (b) Station m_b; (c) Period (0.5-4.0 Hz); (d) Station m_b (0.5-4.0 Hz); (e) Period (1.0-4.0 Hz); (f) Station m_b (1.0-4.0 Hz).

The lines are least squares estimates obtained assuming there are no errors in the abscissa. The equations of the lines are given at the top of each figure with the 95% confidence limits on the slope and intercepts. x and y stand for the abscissa and ordinate respectively of the graphs.

Figure 11 Graphs of various observations taken from the YKA seismograms against maximum likelihood m_b.

(a) Station m_b computed using logA rather than logA/T;

(b) Station m_b computed using $\log A_0$ where A_0 is the ½ peak-to-peak amplitude for a system with a gain of unity at 1 Hz;

(c) Station m_b (0.5-4.0 Hz) computed using logA (0.5-4.0 Hz) rather than logA/T (0.5-4.0 Hz);

(d) Station m_b (0.5-4.0 Hz) computed using $\log A_0$ (0.5-4.0 Hz) where A_0 (0.5-4.0 Hz) is the ½ peak-to-peak amplitude for a system with unit gain at 1 Hz;

(e) Station m_b (1.0-4.0 Hz) computed using logA (1.0-4.0 Hz) rather than logA/T (1.0-4.0 Hz);

(f) Station m_b (1.0-4.0 Hz) computed using $\log A_0$ (1.0-4.0 Hz) where A_0 (1.0-4.0 Hz) is the ½ peak-to-peak amplitude for a system with unit gain at 1 Hz.

The lines are least squares estimates obtained assuming there are no errors in the abscissa. The equations of the lines are given at the top of each figure with the 95% confidence limits on the slope and intercepts. x and y stand for the abscissa and ordinate respectively of the graphs.

Figure 12 Graphs of YKA rms amplitudes in the 0.5-4 Hz band and a number of time windows, against m_b^{ML} (squares). The time windows are: (a) 0-3s; (b) 0-6s; (c) 0-9s; (d) 0-15s; (e) 3-9s; (f) 3-15s. Time zero is the onset of the signal. The asterisks show the rms noise amplitude measured in a window before signal onset.

The lines are least squares estimates obtained assuming there are no errors in the abscissa. The equations of the lines are given at the top of each figure with the 95% confidence limits on the slope and intercepts. x and y stand for the abscissa and ordinate respectively of the graphs.

Figure 13 Graphs of YKA rms amplitudes in the 1.0-4 Hz band and a number of time windows, against m_b^{ML} (squares). The time windows are: (a) 0-3s; (b) 0-6s; (c) 0-9s; (d) 0-15s; (e) 3-9s; (f) 3-15s. Time zero is the onset of the signal. The asterisks show the rms noise amplitude measured in a window before signal onset.

The lines are least squares estimates obtained assuming there are no errors in the abscissa. The equations of the lines are given at the top of each figure with the 95% confidence limits on the slope and intercepts. x and y stand for the abscissa and ordinate respectively of the graphs. Triangles show where noise observations fall below the bottom of the graph.

Figure 14 Graphs of various observations taken from the YKA seismograms against m_b^{ML}. (a) rms amplitudes 9-18s (0.5-4.0 Hz) (squares); (b) rms amplitudes 9-18s (1.0-4.0 Hz) (squares); (c) pP-P times. The asterisks show the rms noise amplitude measured in a window before signal onset.

The lines are least squares estimates obtained assuming there are no errors in the abscissa. The equations of the lines are given at the top of each figure with the 95% confidence limits on the slope and intercepts. x and y stand for the abscissa and ordinate respectively of the graphs. Triangles show where noise observations fall below the bottom of the graph.

Figure 15 Graphs of various observations taken from the WRA seismograms against m_b^{ML}. (a) ψ_∞; (b) Pulse rise time; (c) Pulse duration; (d) Pulse fall time. The lines are least squares estimates obtained assuming no errors in the abscissa. The equations of the lines are given at the top of each figure with 95% confidence limits on the slopes and intercepts. x and y stand for abscissa and ordinate respectively of the graphs.

Figure 16 Graphs of various observations taken from the WRA seismograms against m_b^{ML}. (a) Period; (b) Station m_b; (c) Period (0.5-4.0 Hz); (d) Station m_b (0.5-4.0 Hz); (e) Period (1.0-4.0 Hz); (f) Station m_b (1.0-4.0 Hz).

The lines are least squares estimates obtained assuming there are no errors in the abscissa. The equations of the lines are given at the top of each figure with the 95% confidence limits on the slope and intercepts. x and y stand for the abscissa and ordinate respectively of the graphs.

Figure 17 Graphs of various observations taken from the WRA seismograms against maximum-likelihood m_b.

(a) Station m_b computed using logA rather than logA/T;

(b) Station m_b computed using $\log A_o$ where A_o is the ½ peak-to-peak amplitude for a system with a gain of unity at 1 Hz;

(c) Station m_b (0.5-4.0 Hz) computed using logA (0.5-4.0 Hz) rather than logA/T (0.5-4.0 Hz);

(d) Station m_b (0.5-4.0 Hz) computed using $\log A_o$ (0.5-4.0 Hz) where A_o (0.5-4.0 Hz) is the ½ peak-to-peak amplitude for a system with a gain of unity at 1 Hz;

(e) Station m_b (1.0-4.0 Hz) computed using logA (1.0-4.0 Hz) rather than logA/T (1.0-4.0 Hz);

(f) Station m_b (1.0-4.0 Hz) computed using $\log A_o$ (1.0-4.0 Hz) where A_o (1.0-4.0 Hz) is the ½ peak-to-peak amplitude for a system with unit gain at 1 Hz.

The lines are least squares estimates obtained assuming there are no errors in the abscissa. The equations of the lines are given at the top of each figure with the 95% confidence limits on the slope and intercepts. x and y stand for the abscissa and ordinate respectively of the graphs.

Figure 18 Graphs of WRA rms amplitudes in the 0.5-4 Hz band and a number of time windows, against m_b^{ML} (squares). The time windows are: (a) 0-3s; (b) 0-6s; (c) 0-9s; (d) 0-15s; (e) 3-9s; (f) 3-15s. Time zero is the onset of the signal. The asterisks show the rms noise amplitude measured in a window before signal onset.

The lines are least squares estimates obtained assuming there are no errors in the abscissa. The equations of the lines are given at the top of each figure with the 95% confidence limits on the slope and intercepts. x and y stand for the abscissa and ordinate respectively of the graphs.

Figure 19 Graphs of WRA rms amplitudes in the 1.0-4 Hz band and a number of time windows, against m_b^{ML} (squares). The time windows are: (a) 0-3s; (b) 0-6s; (c) 0-9s; (d) 0-15s; (e) 3-9s; (f) 3-15s. Time zero is the onset of the signal. The asterisks show the rms noise amplitude measured in a window before signal onset.

The lines are least squares estimates obtained assuming there are no errors in the abscissa. The equations of the lines are given at the top of each figure with the 95% confidence limits on the slope and intercepts. x and y stand for the abscissa and ordinate respectively of the graphs. Triangles show where noise observations fall below the bottom of the graph.

Figure 20 Graphs of various observations taken from the WRA seismograms against m_b^{ML}. (a) rms amplitudes 9-18s (0.5-4.0 Hz); (b) rms amplitudes 9-18s (1.0-4.0 Hz). The asterisks show the rms noise amplitude measured in a window before signal onset.

The lines are least squares estimates obtained assuming there are no errors in the abscissa. The equations of the lines are given at the top of each figure with the 95% confidence limits on the slope and intercepts. x and y stand for the abscissa and ordinate respectively of the graphs. Triangles show where noise observations fall below the bottom of the graph.

Figure 21 Graphs of various observations taken from the GBA seismograms against m_b^{ML}. (a) Period; (b) Station m_b; (c) Period (0.5-4.0 Hz); (d) Station m_b (0.5-4.0 Hz); (e) Period (1.0-4.0 Hz); (f) Station m_b (1.0-4.0 Hz).

The lines are least squares estimates obtained assuming there are no errors in the abscissa. The equations of the lines are given at the top of each figure with the 95% confidence limits on the slope and intercepts. x and y stand for the abscissa and ordinate respectively of the graphs.

Figure 22 Graphs of various observations taken from the GBA seismograms against m_b^{ML}.

(a) Station m_b computed using logA rather than logA/T;

(b) Station m_b computed using $\log A_0$ where A_0 is the ½ peak-to-peak amplitude for a system with a gain of unity at 1 Hz;

(c) Station m_b (0.5-4.0 Hz) computed using logA (0.5-4.0 Hz) rather than logA/T (0.5-4.0 Hz);

(d) Station m_b (0.5-4.0 Hz) computed using $\log A_0$ (0.5-4.0 Hz), where A_0 (0.5-4.0 Hz) is the ½ peak-to-peak amplitude for a system with a gain of unity at 1 Hz;

(e) Station m_b (1.0-4.0 Hz) computed using logA (1.0-4.0 Hz) rather than logA/T (1.0-4.0 Hz);

(f) Station m_b (1.0-4.0 Hz) computed using $\log A_0$ (1.0-4.0 Hz), where A_0 (1.0-4.0 Hz) is the ½ peak-to-peak amplitude for a system with unit gain at 1 Hz.

The lines are least squares estimates obtained assuming there are no errors in the abscissa. The equations of the lines are given at the top of each figure with the 95% confidence limits on the slope and intercepts. x and y stand for the abscissa and ordinate respectively of the graphs.

Figure 23 Graphs of GBA rms amplitudes in the 0.5-4 Hz band and a number of time windows, against m_b^{ML}. The time windows are: (a) 0-3s; (b) 0-6s; (c) 0-9s; (d) 0-15s; (e) 3-9s; (f) 3-15s. Time zero is the onset of the signal. The asterisks show the rms noise amplitudes measured in a window before signal onset.

The lines are least squares estimates obtained assuming there are no errors in the abscissa. The equations of the lines are given at the top of each figure with the 95% confidence limits on the slope and intercepts. x and y stand for the abscissa and ordinate respectively of the graphs.

Figure 24 Graphs of GBA rms amplitudes in the 1.0-4 Hz band and a number of time windows, against m_b^{ML}. The time windows are: (a) 0-3s; (b) 0-6s; (c) 0-9s; (d) 0-15s; (e) 3-9s; (f) 3-15s. Time zero is the onset of the signal. The asterisks show the rms noise amplitude measured in a window before signal onset.

The lines are least squares estimates obtained assuming there are no errors in the abscissa. The equations of the lines are given at the top of each figure with the 95% confidence limits on the slope and intercepts. x and y stand for the abscissa and ordinate respectively of the graphs.

Figure 25 Graphs of various observations taken from the YKA seismograms against m_b^{ML}. (a) rms amplitudes 9-18s (0.5-4.0 Hz); (b) rms amplitudes 9-18s (1.0-4.0 Hz). The asterisks show the rms noise amplitude measured in a window before signal onset.

The lines are least squares estimates obtained assuming there are no errors in the abscissa. The equations of the lines are given at the top of each figure with the 95% confidence limits on the slope and intercepts. x and y stand for the abscissa and ordinate respectively of the graphs.

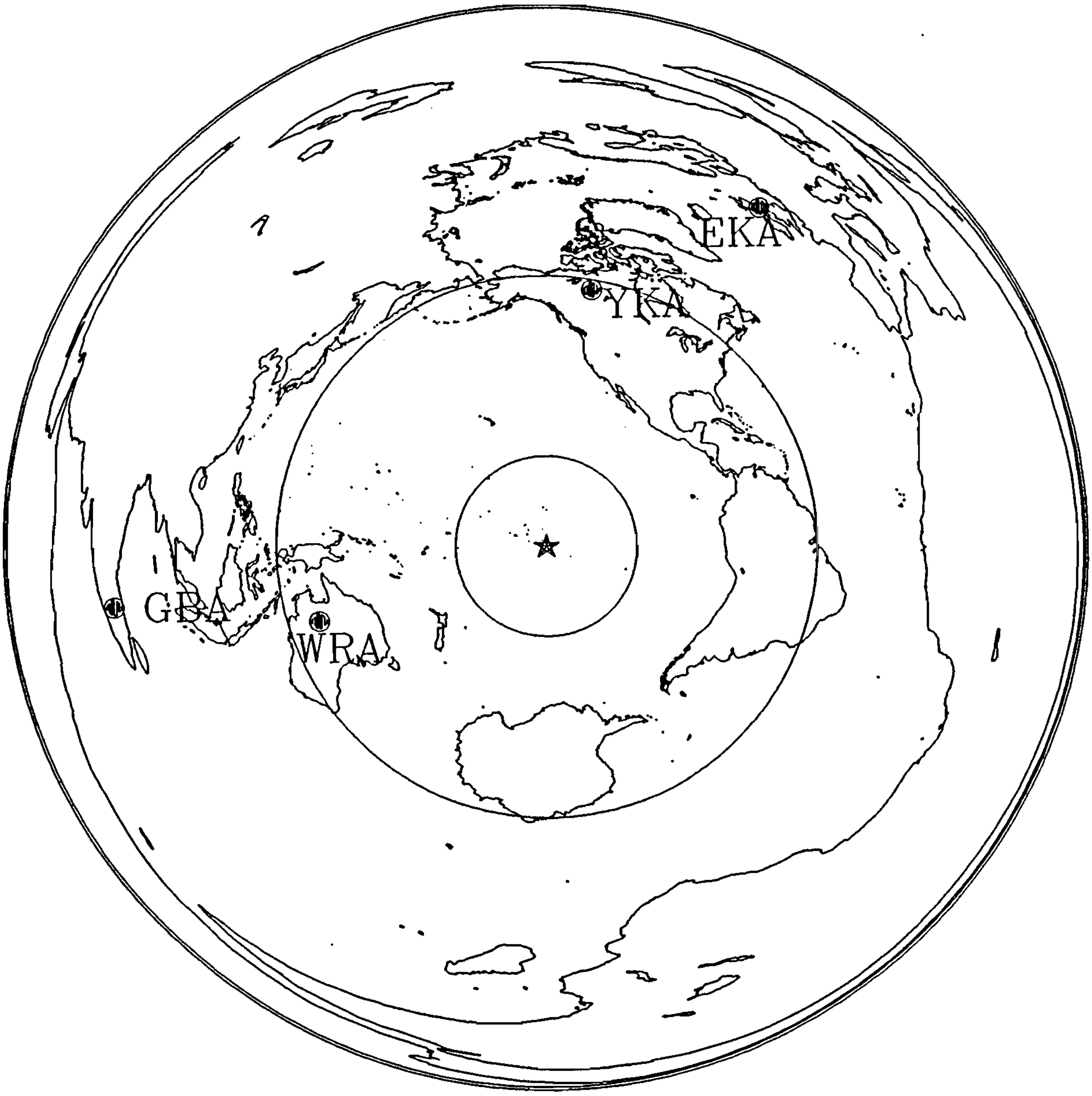

FIGURE 1

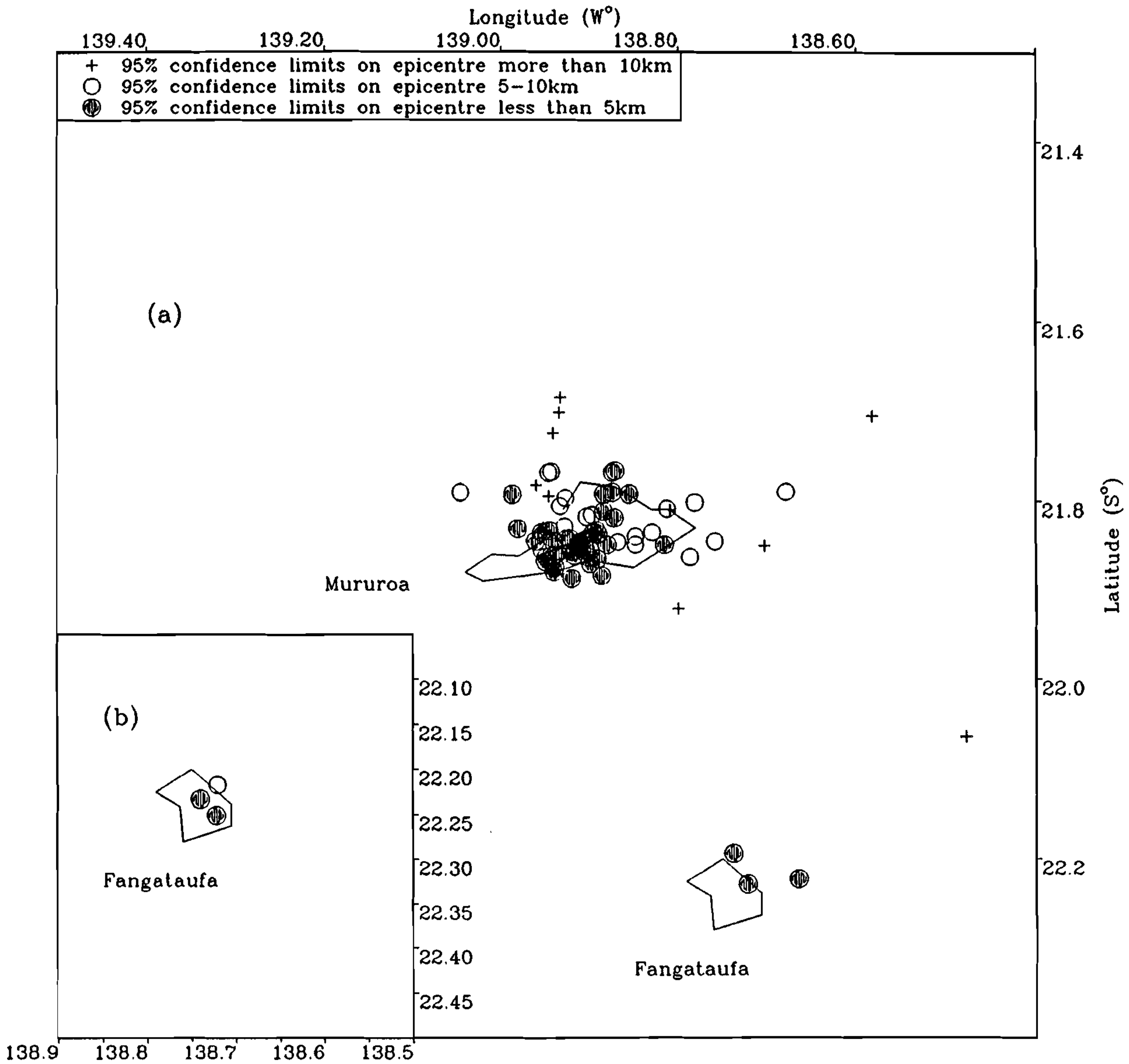
Longitude (W°)
139.40
139.20
139.00
138.80
138.60
+ 95% confidence limits on epicentre more than 10km
○ 95% confidence limits on epicentre 5-10km
95% confidence limits on epicentre less than 5km
21.4
21.6
21.8
22.0
22.2
Latitude (S°)
(a)
Mururoa
Fangataufa
(b)
Fangataufa
22.10
22.15
22.20
22.25
22.30
22.35
22.40
22.45
138.9
138.8
138.7
138.6
138.5

Figure 2

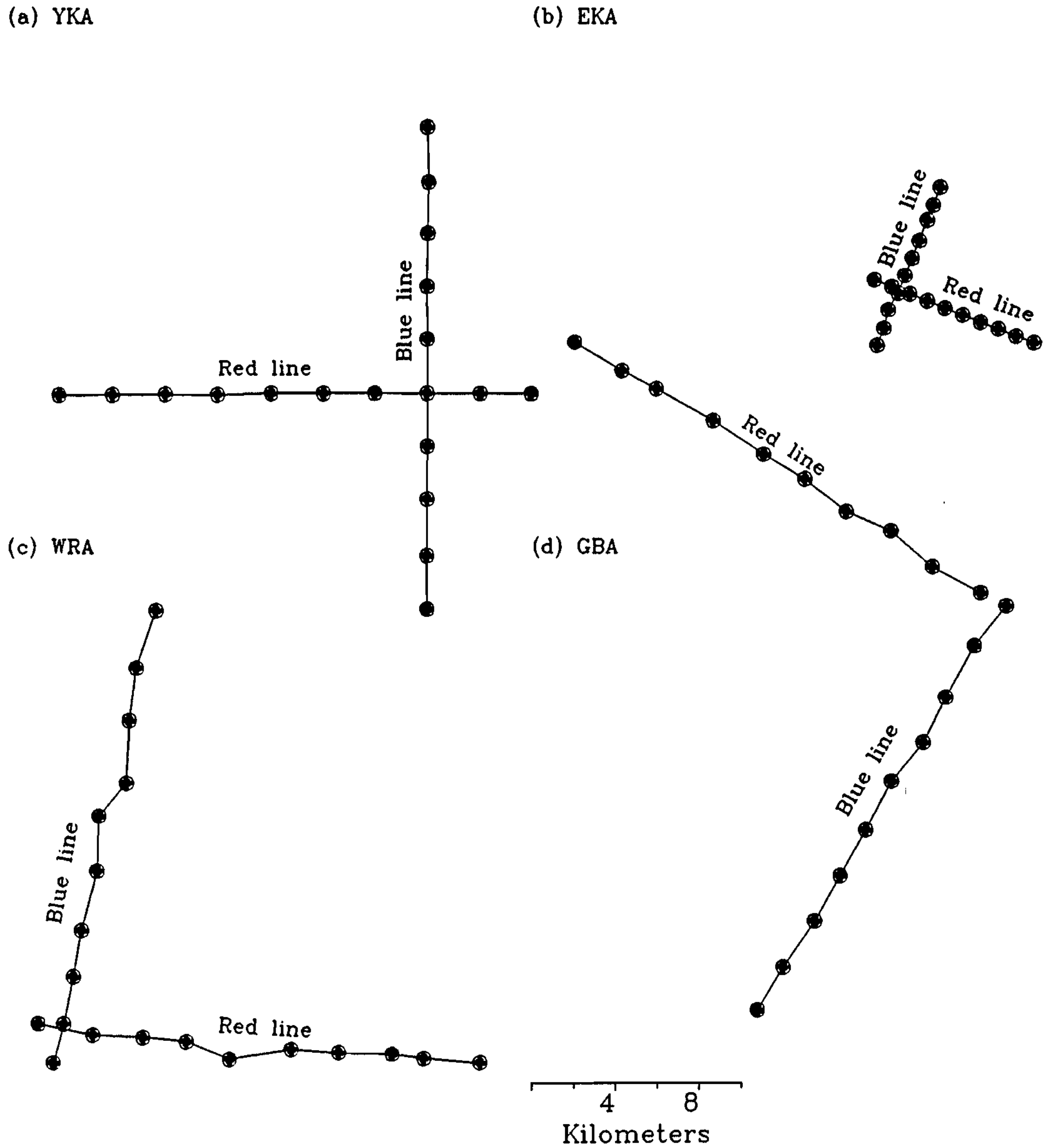
(a) YKA
(b) EKA
(c) WRA
(d) GBA
Blue line
Red line
Blue line
Red line
Blue line
Red line
Red line
Blue line
4
8
Kilometers

Figure 3

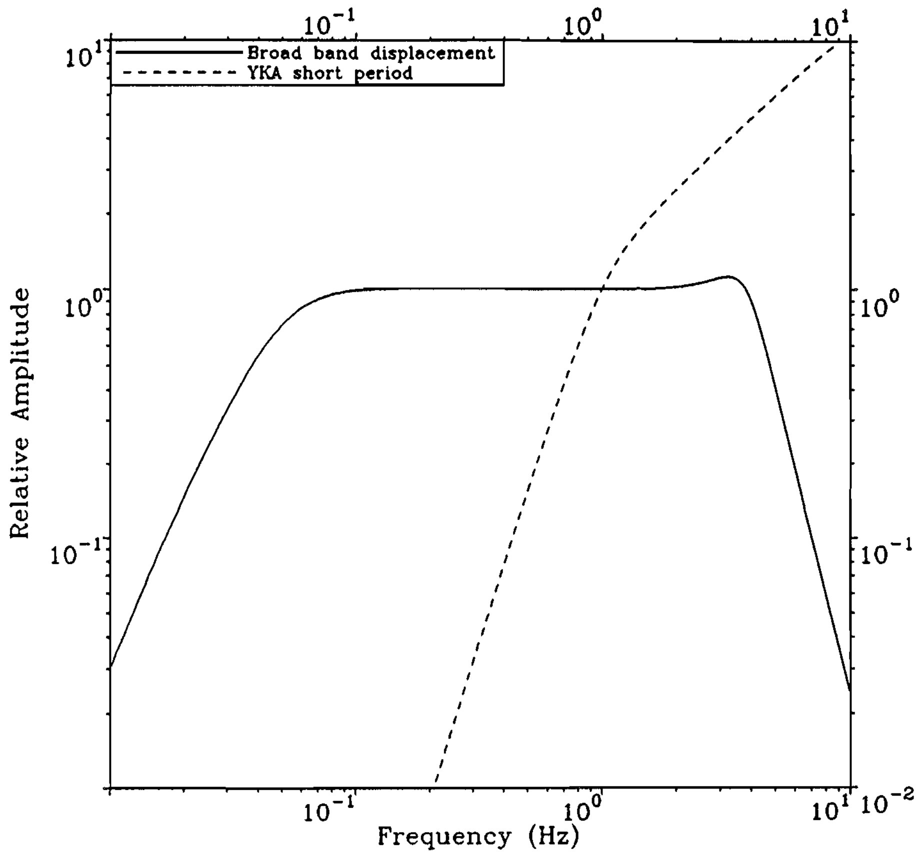

Broad band displacement
YKA short period
Relative Amplitude
Frequency (Hz)
10^{-1}
10^{0}
10^{1}
10^{-2}

Figure 4

Mururoa 25 May 1988 YKA

8-MAY-1995

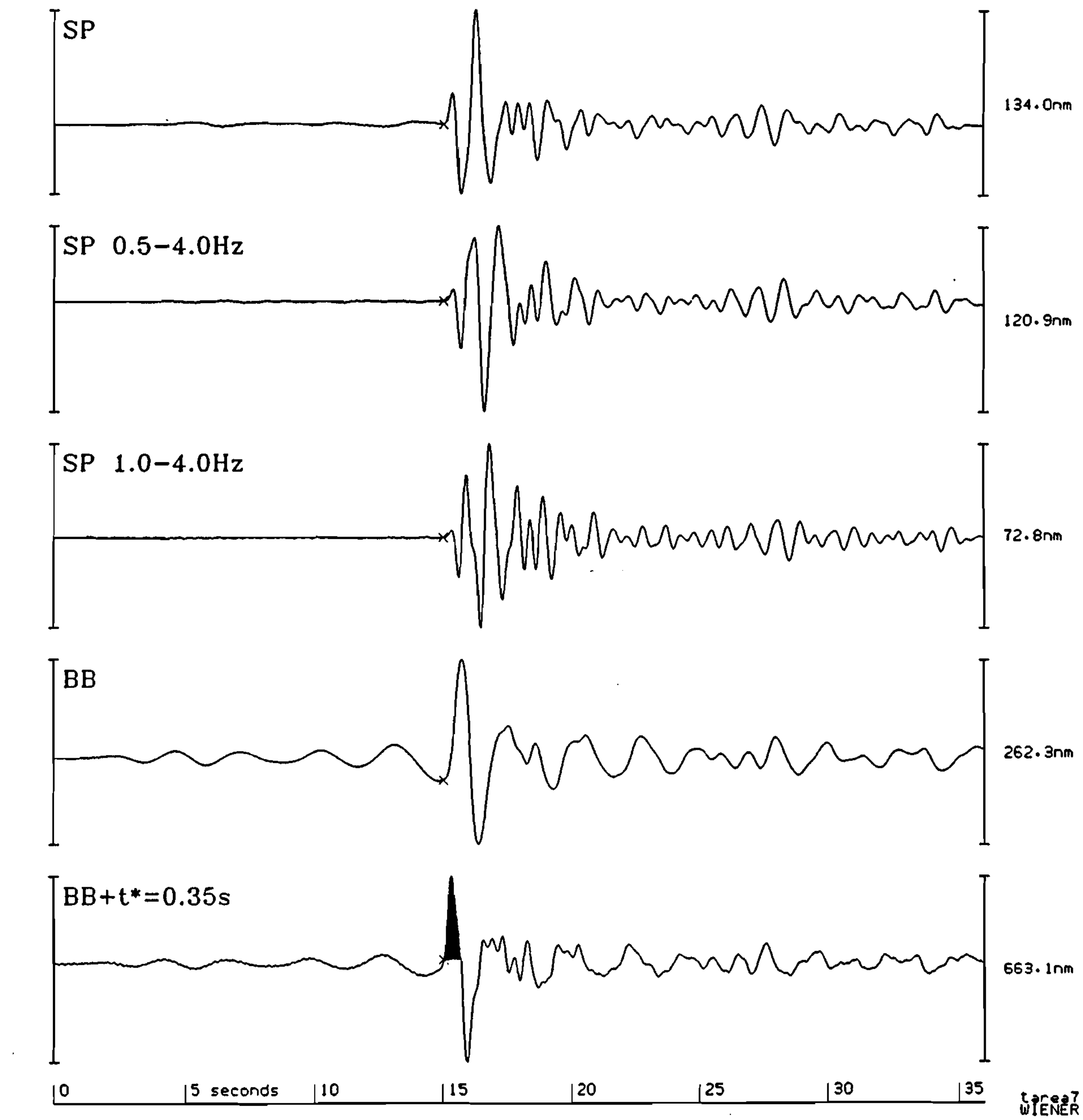

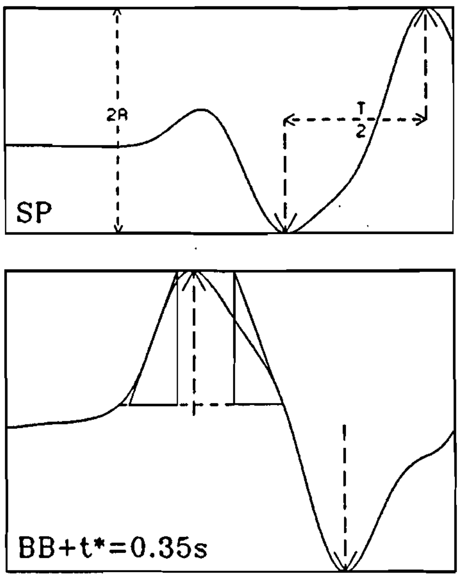


```
FILE=USR$DISK1:[DATA.MURUROA.ROYS]880525_YKA.DAT
Results for picked BB+t*=0.35s channel
     Rise time =0.19s            Pulse area =111.14nm s
     Fall time =0.20s       Rate multiplier =4.00
      Duration =0.66(25)s    P-pP Duration =0.61(25)s
Relative Start =15.03(75)s  Relative Start =15.33(75)s

Results for picked SP channel
Half Pk-Pk (A) =91.00nm  Amp Corr. applied =0.736
    Period (T) =1.15s              Log(A/T) =1.90

Results for 0.5-4.0Hz SP (YKA SP) channel
  RMS 0.0- 3.0 =29.61nm       RMS 0.0- 6.0 =22.36nm
  RMS 0.0- 9.0 =18.37nm       RMS 0.0-15.0 =14.70nm
  RMS 3.0- 9.0 =8.22nm        RMS 3.0-15.0 =7.13nm
  RMS 9.0-18.0 =5.16nm        RMS   Noise  =0.29nm
    Half Pk-Pk =77.98nm  Amp Corr. applied =0.775
        Period =1.13s              Log(A/T) =1.84

Results for 1.0-4.0Hz SP (YKA SP) channel
  RMS 0.0- 3.0 =16.88nm       RMS 0.0- 6.0 =13.16nm
  RMS 0.0- 9.0 =10.90nm       RMS 0.0-15.0 =8.73nm
  RMS 3.0- 9.0 =5.97nm        RMS 3.0-15.0 =4.89nm
  RMS 9.0-18.0 =3.13nm        RMS   Noise  =0.12nm
    Half Pk-Pk =19.00nm  Amp Corr. applied =1.915
        Period =0.65s              Log(A/T) =1.47
```

Figure 5

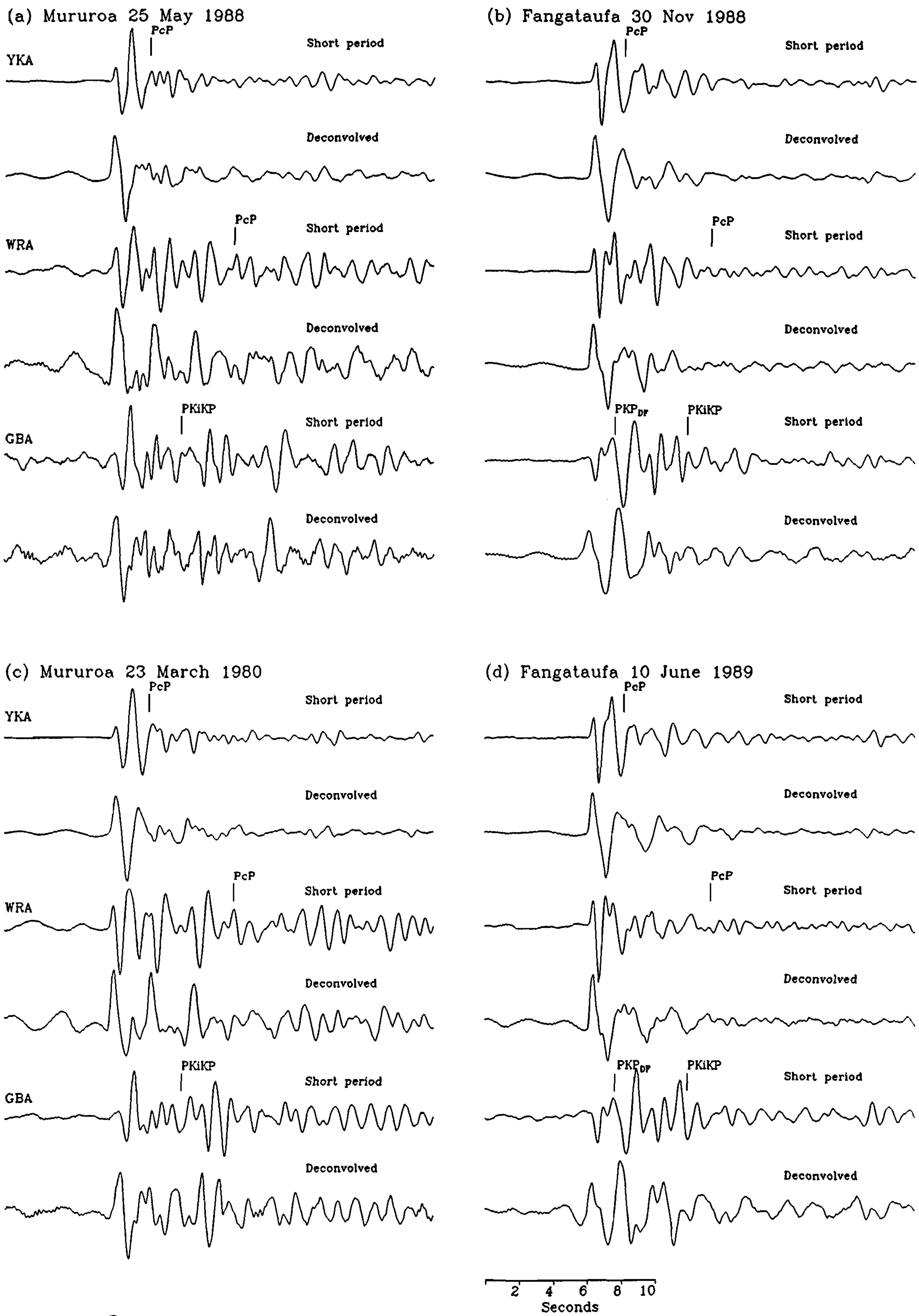

(a) Mururoa 25 May 1988
PcP
Short period
YKA
Deconvolved
PcP
Short period
WRA
Deconvolved
PKiKP
Short period
GBA
Deconvolved
(b) Fangataufa 30 Nov 1988
PcP
Short period
Deconvolved
PcP
Short period
Deconvolved
PKP DF
PKiKP
Short period
Deconvolved
(c) Mururoa 23 March 1980
PcP
Short period
YKA
Deconvolved
PcP
Short period
WRA
Deconvolved
PKiKP
Short period
GBA
Deconvolved
(d) Fangataufa 10 June 1989
PcP
Short period
Deconvolved
PcP
Short period
Deconvolved
PKP DF
PKiKP
Short period
Deconvolved
2 4 6 8 10
Seconds

Figure 6

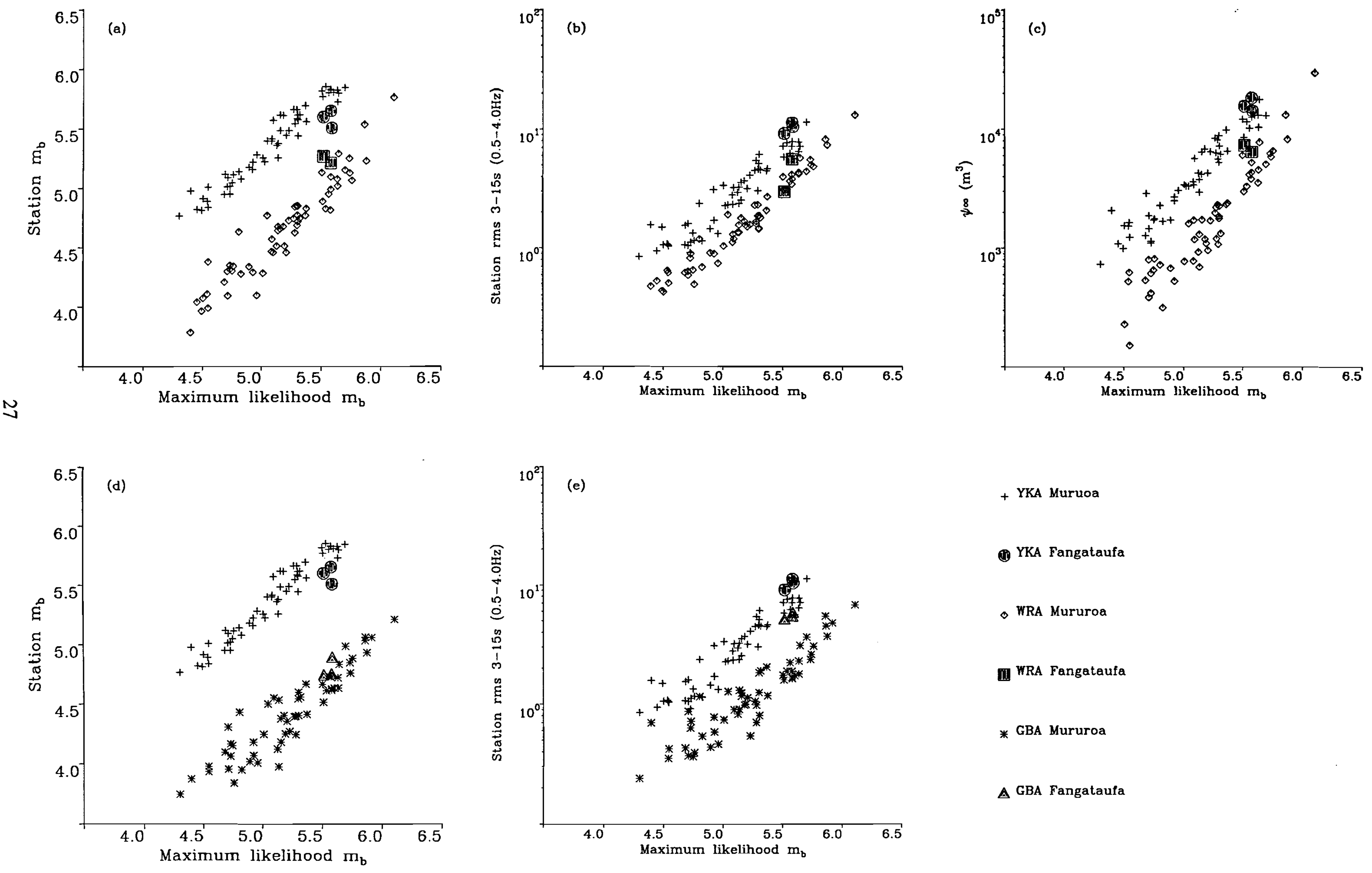

(a)
Station m_b
Maximum likelihood m_b
(b)
Station rms 3-15s (0.5-4.0Hz)
Maximum likelihood m_b
(c)
ψ_∞ (m^3)
Maximum likelihood m_b
(d)
Station m_b
Maximum likelihood m_b
(e)
Station rms 3-15s (0.5-4.0Hz)
Maximum likelihood m_b
YKA Muruoa
YKA Fangataufa
WRA Mururoa
WRA Fangataufa
GBA Mururoa
GBA Fangataufa

Figure 7

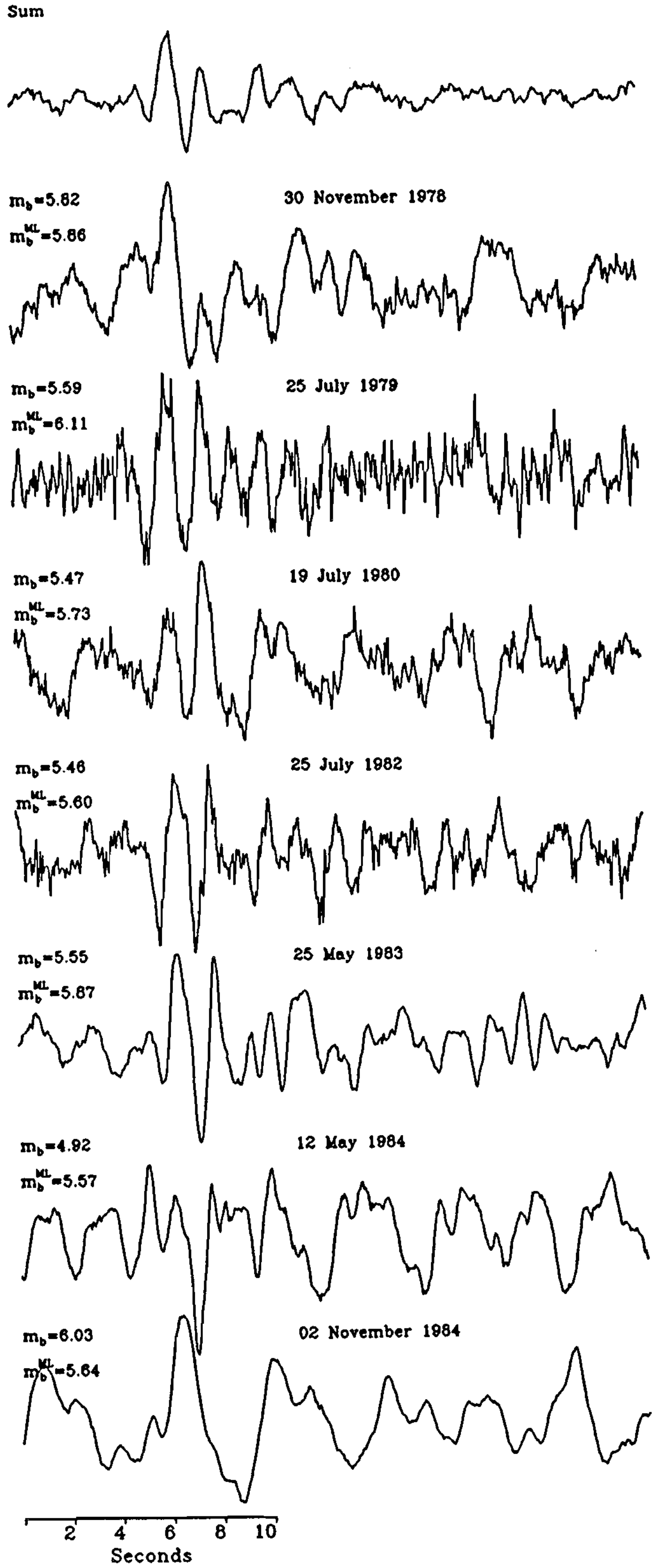

Sum
m_b=5.82
m_b^{ML}=5.86
30 November 1978
m_b=5.59
m_b^{ML}=6.11
25 July 1979
m_b=5.47
m_b^{ML}=5.73
19 July 1980
m_b=5.46
m_b^{ML}=5.60
25 July 1982
m_b=5.55
m_b^{ML}=5.67
25 May 1983
m_b=4.92
m_b^{ML}=5.57
12 May 1984
m_b=6.03
m_b^{ML}=5.64
02 November 1984
2 4 6 8 10
Seconds

Figure 8

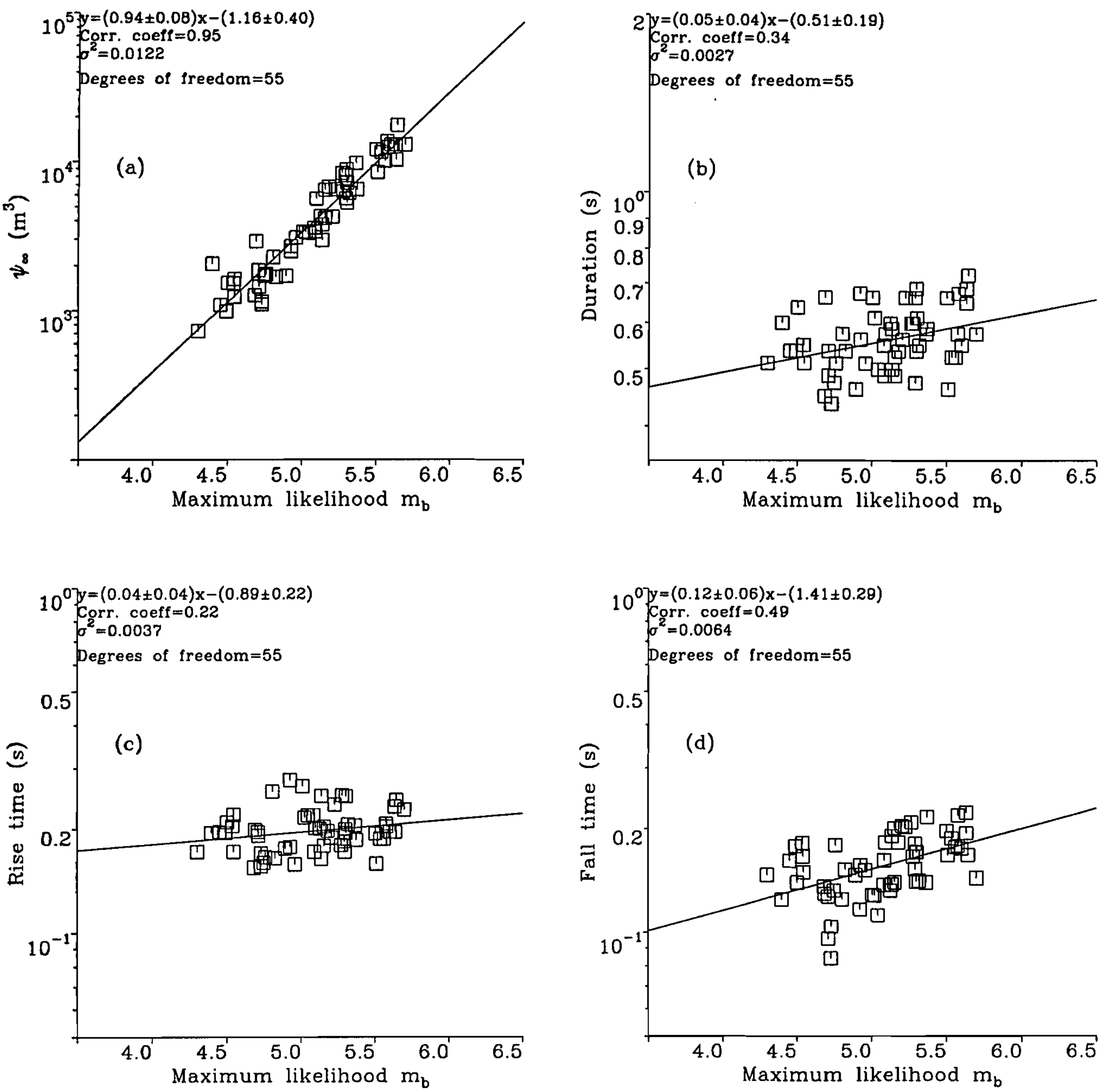
y=(0.94±0.08)x−(1.16±0.40)
Corr. coeff=0.95
σ²=0.0122
Degrees of freedom=55
(a)
ψ∞ (m³)
Maximum likelihood m_b
y=(0.05±0.04)x−(0.51±0.19)
Corr. coeff=0.34
σ²=0.0027
Degrees of freedom=55
(b)
Duration (s)
Maximum likelihood m_b
y=(0.04±0.04)x−(0.89±0.22)
Corr. coeff=0.22
σ²=0.0037
Degrees of freedom=55
(c)
Rise time (s)
Maximum likelihood m_b
y=(0.12±0.06)x−(1.41±0.29)
Corr. coeff=0.49
σ²=0.0064
Degrees of freedom=55
(d)
Fall time (s)
Maximum likelihood m_b

Figure 9

9 MY

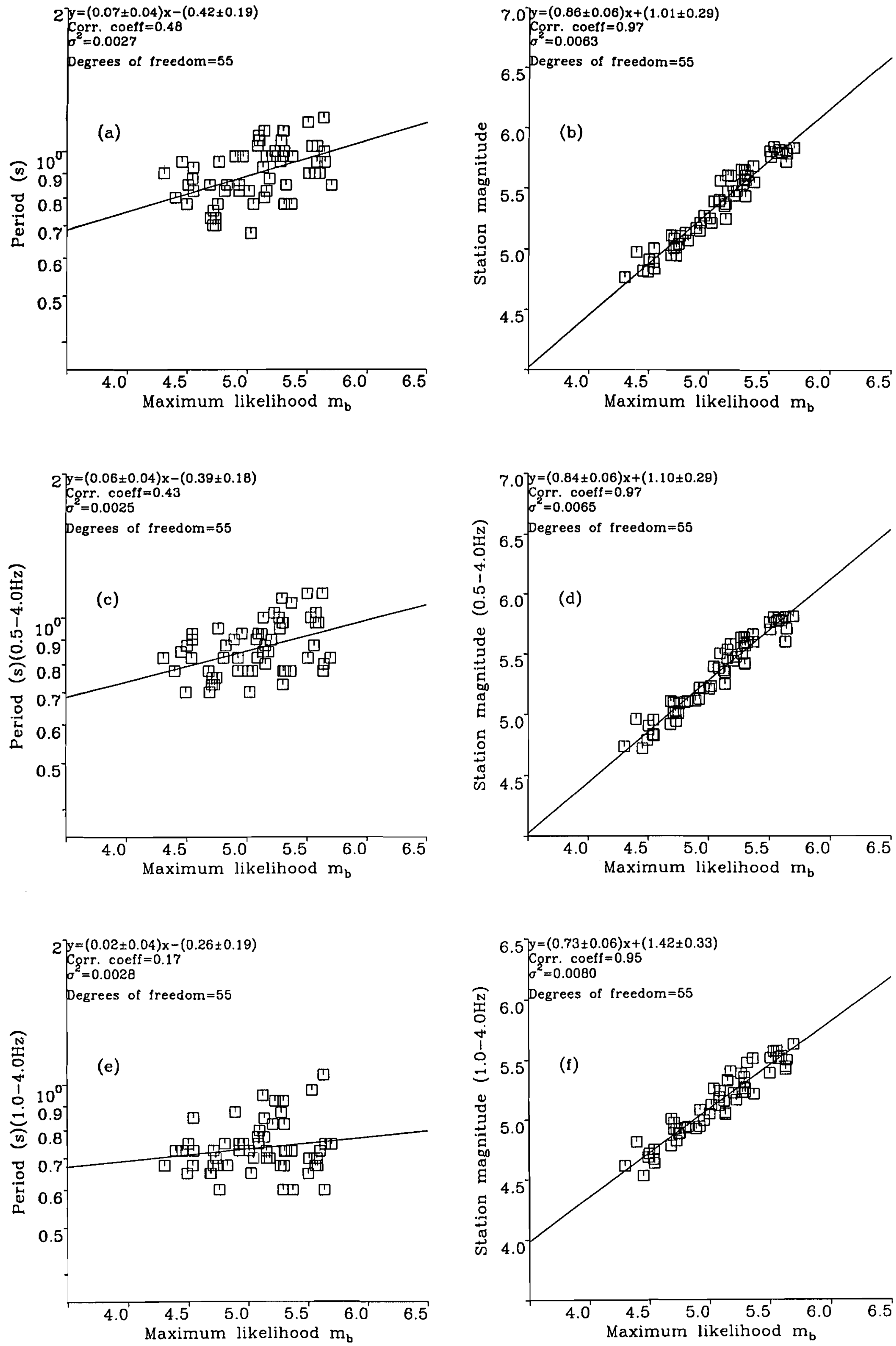

Figure 10

10MY

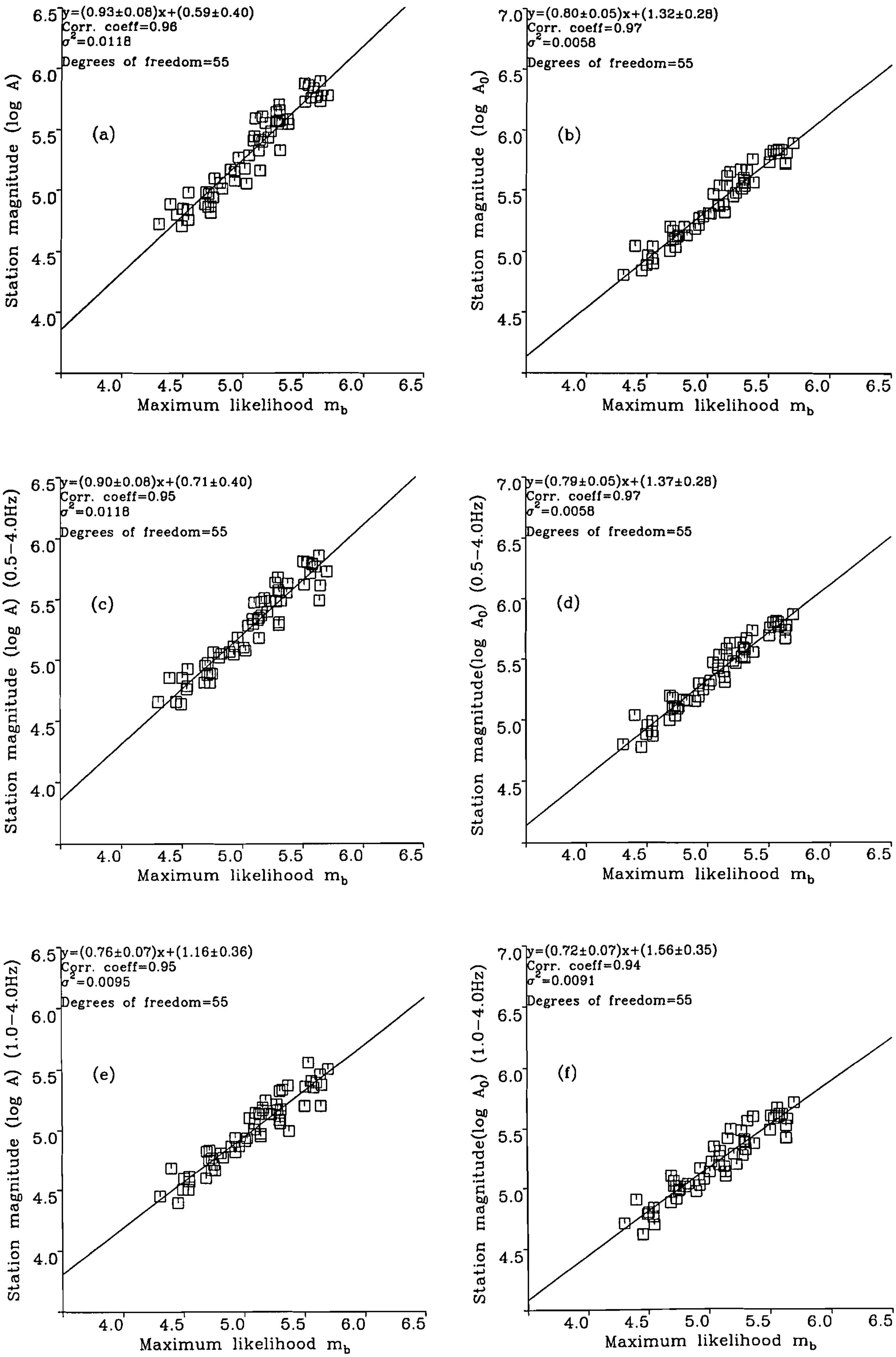
y=(0.93±0.08)x+(0.59±0.40)
Corr. coeff=0.96
σ²=0.0118
Degrees of freedom=55
(a)
Station magnitude (log A)
Maximum likelihood m_b
y=(0.80±0.05)x+(1.32±0.28)
Corr. coeff=0.97
σ²=0.0058
Degrees of freedom=55
(b)
Station magnitude (log A0)
Maximum likelihood m_b
y=(0.90±0.08)x+(0.71±0.40)
Corr. coeff=0.95
σ²=0.0118
Degrees of freedom=55
(c)
Station magnitude (log A) (0.5−4.0Hz)
Maximum likelihood m_b
y=(0.79±0.05)x+(1.37±0.28)
Corr. coeff=0.97
σ²=0.0058
Degrees of freedom=55
(d)
Station magnitude(log A0) (0.5−4.0Hz)
Maximum likelihood m_b
y=(0.76±0.07)x+(1.16±0.36)
Corr. coeff=0.95
σ²=0.0095
Degrees of freedom=55
(e)
Station magnitude (log A) (1.0−4.0Hz)
Maximum likelihood m_b
y=(0.72±0.07)x+(1.56±0.35)
Corr. coeff=0.94
σ²=0.0091
Degrees of freedom=55
(f)
Station magnitude(log A0) (1.0−4.0Hz)
Maximum likelihood m_b

Figure 11

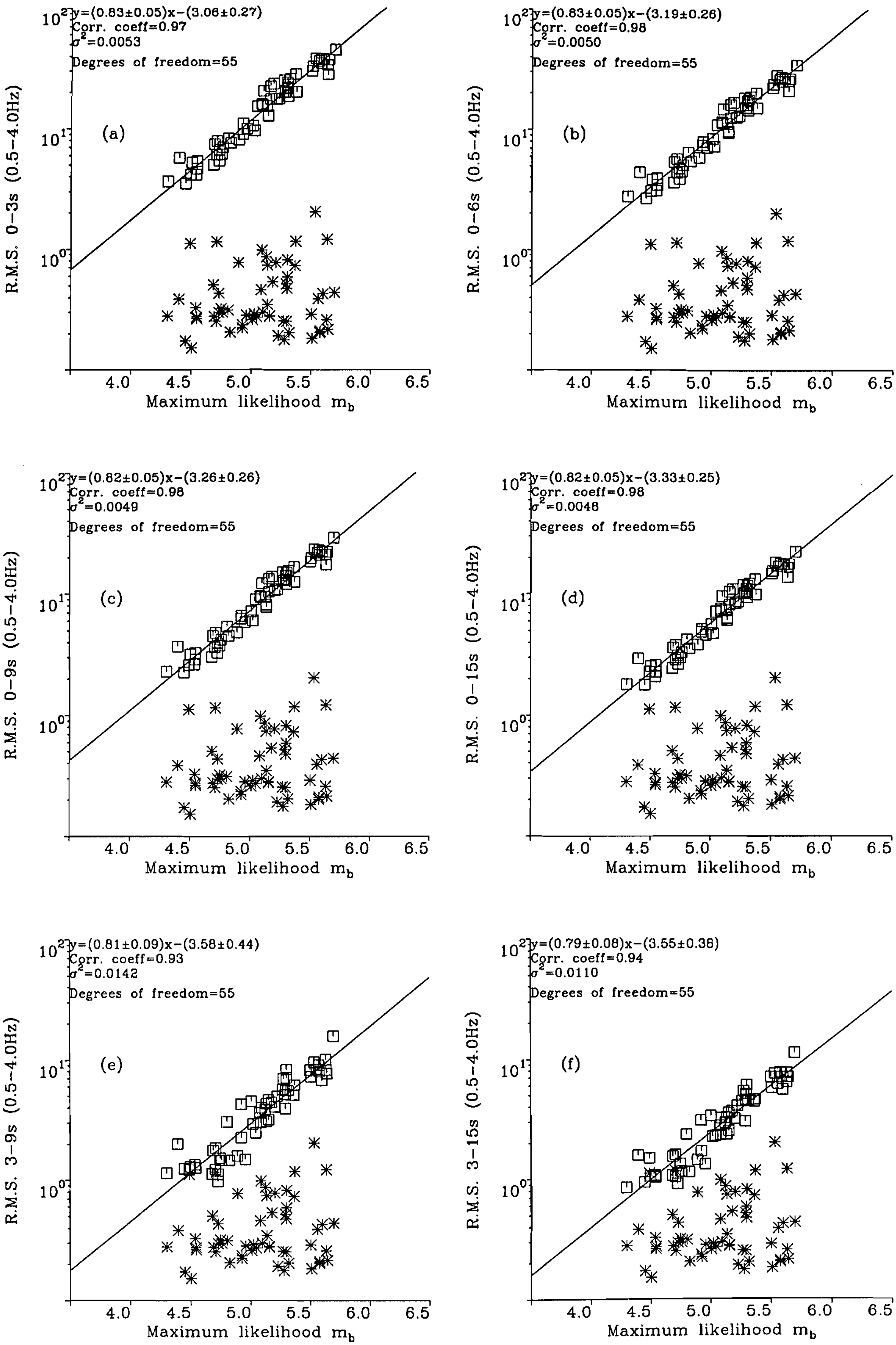

Figure 12

12MY

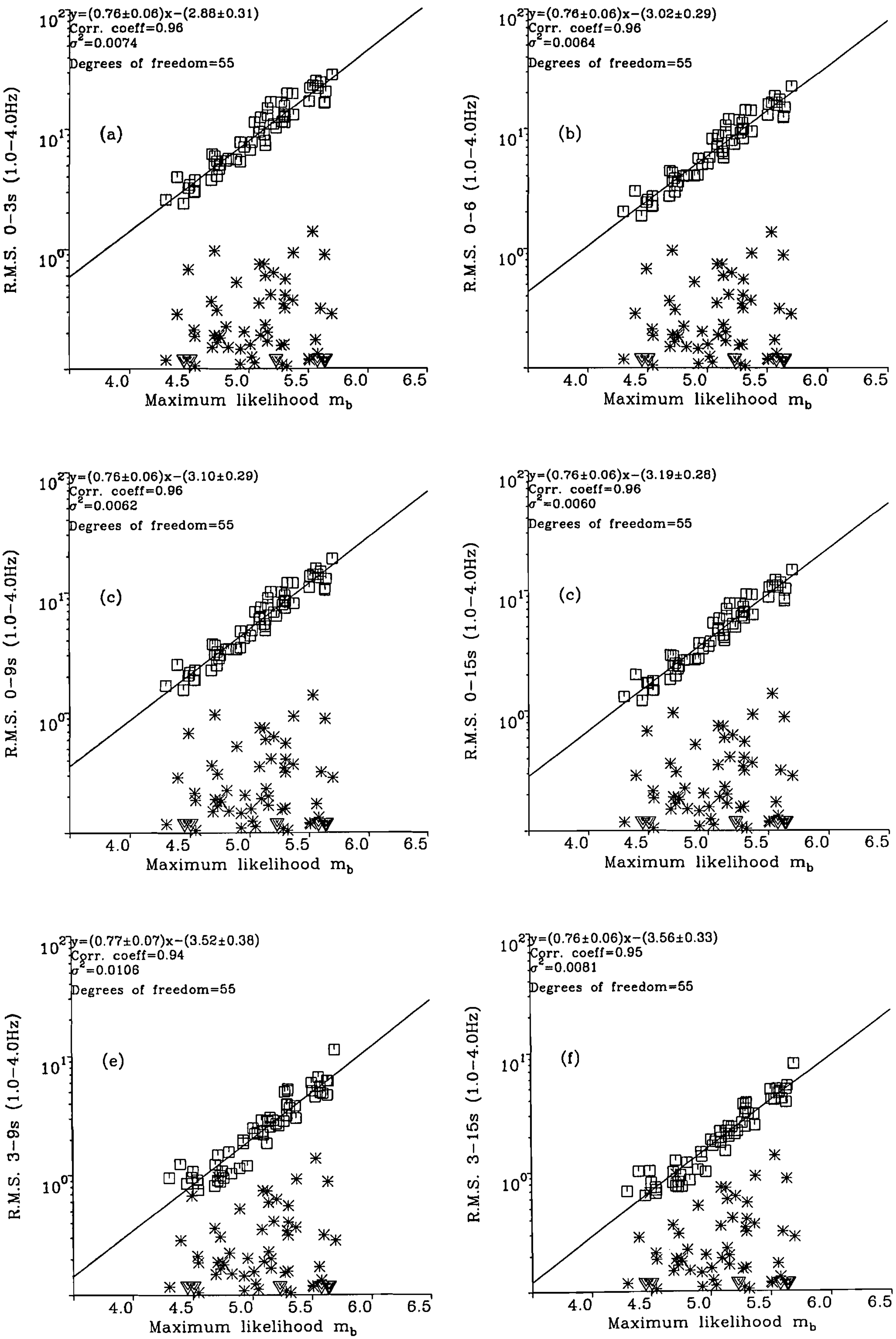

Figure 13

13MY

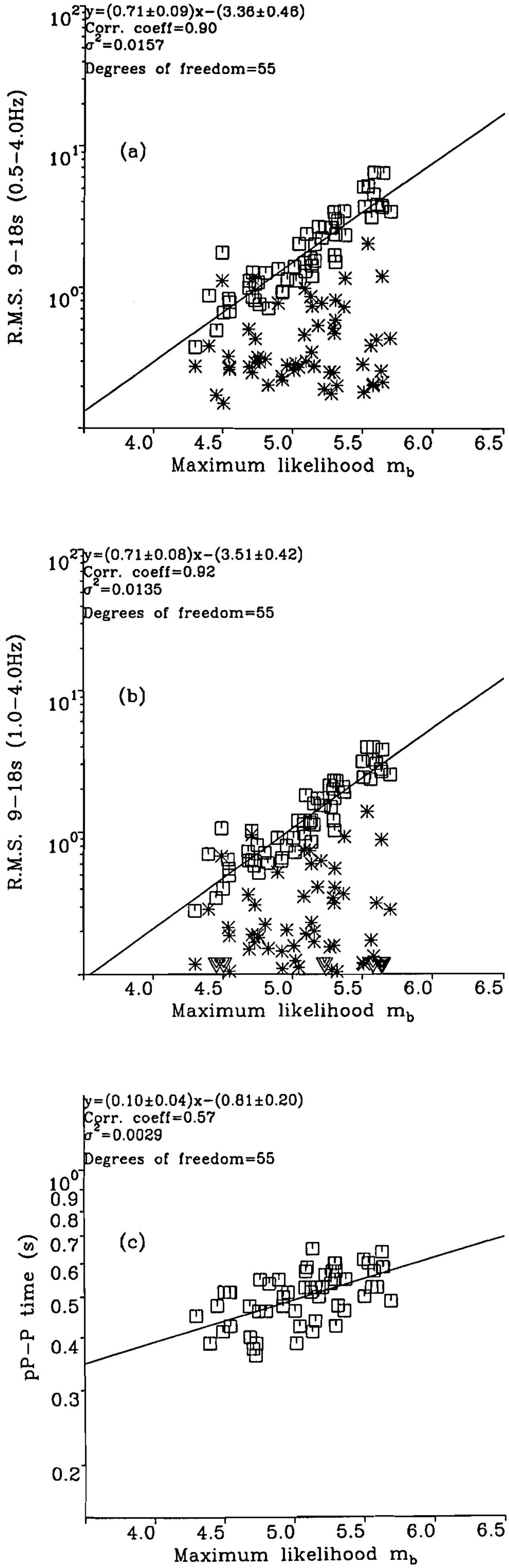

Figure 14

14MY

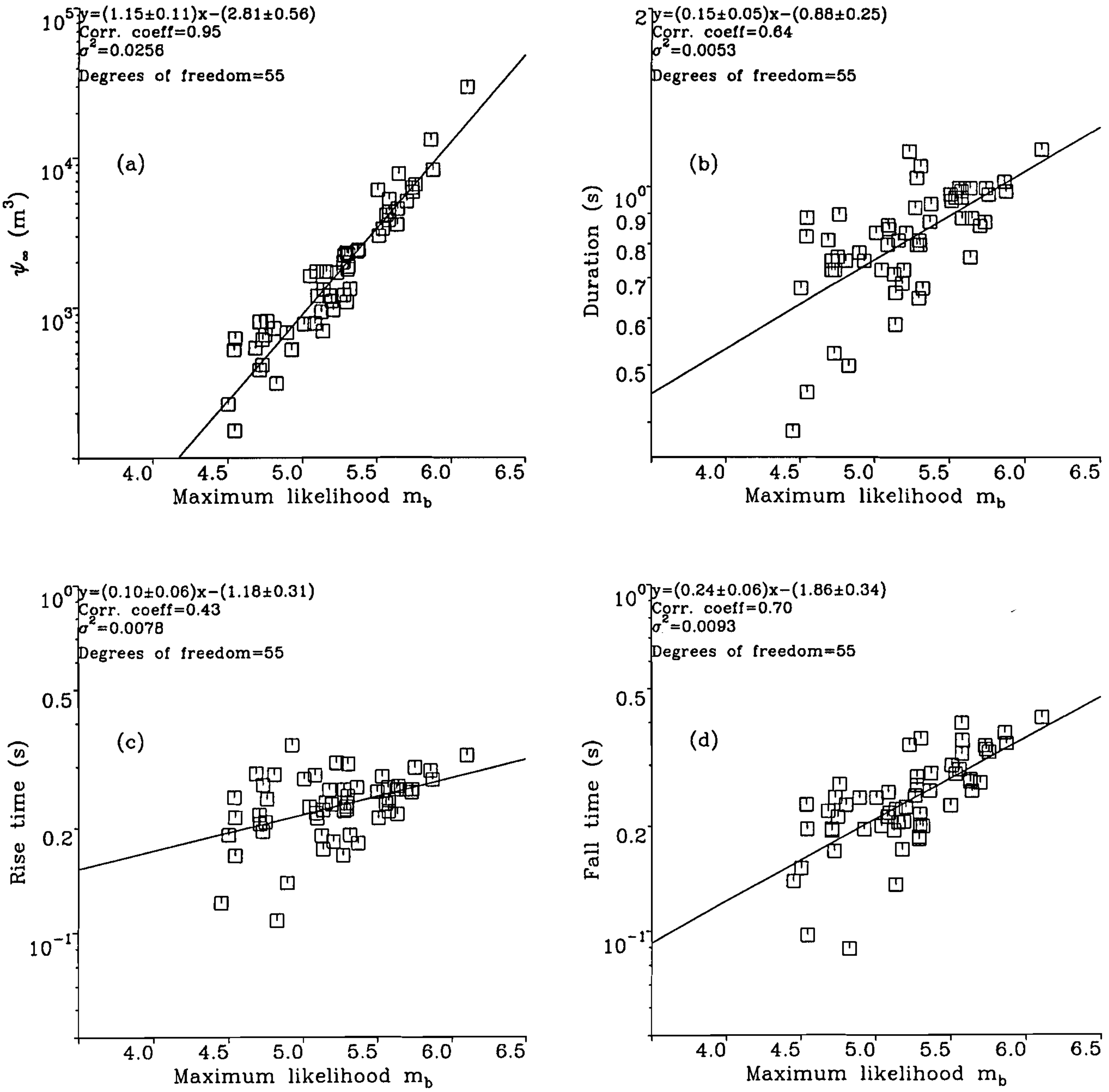

y=(1.15±0.11)x−(2.81±0.56)
Corr. coeff=0.95
σ²=0.0256
Degrees of freedom=55
(a)
ψ∞ (m³)
Maximum likelihood m_b
y=(0.15±0.05)x−(0.88±0.25)
Corr. coeff=0.64
σ²=0.0053
Degrees of freedom=55
(b)
Duration (s)
Maximum likelihood m_b
y=(0.10±0.06)x−(1.18±0.31)
Corr. coeff=0.43
σ²=0.0078
Degrees of freedom=55
(c)
Rise time (s)
Maximum likelihood m_b
y=(0.24±0.06)x−(1.86±0.34)
Corr. coeff=0.70
σ²=0.0093
Degrees of freedom=55
(d)
Fall time (s)
Maximum likelihood m_b

Figure 15

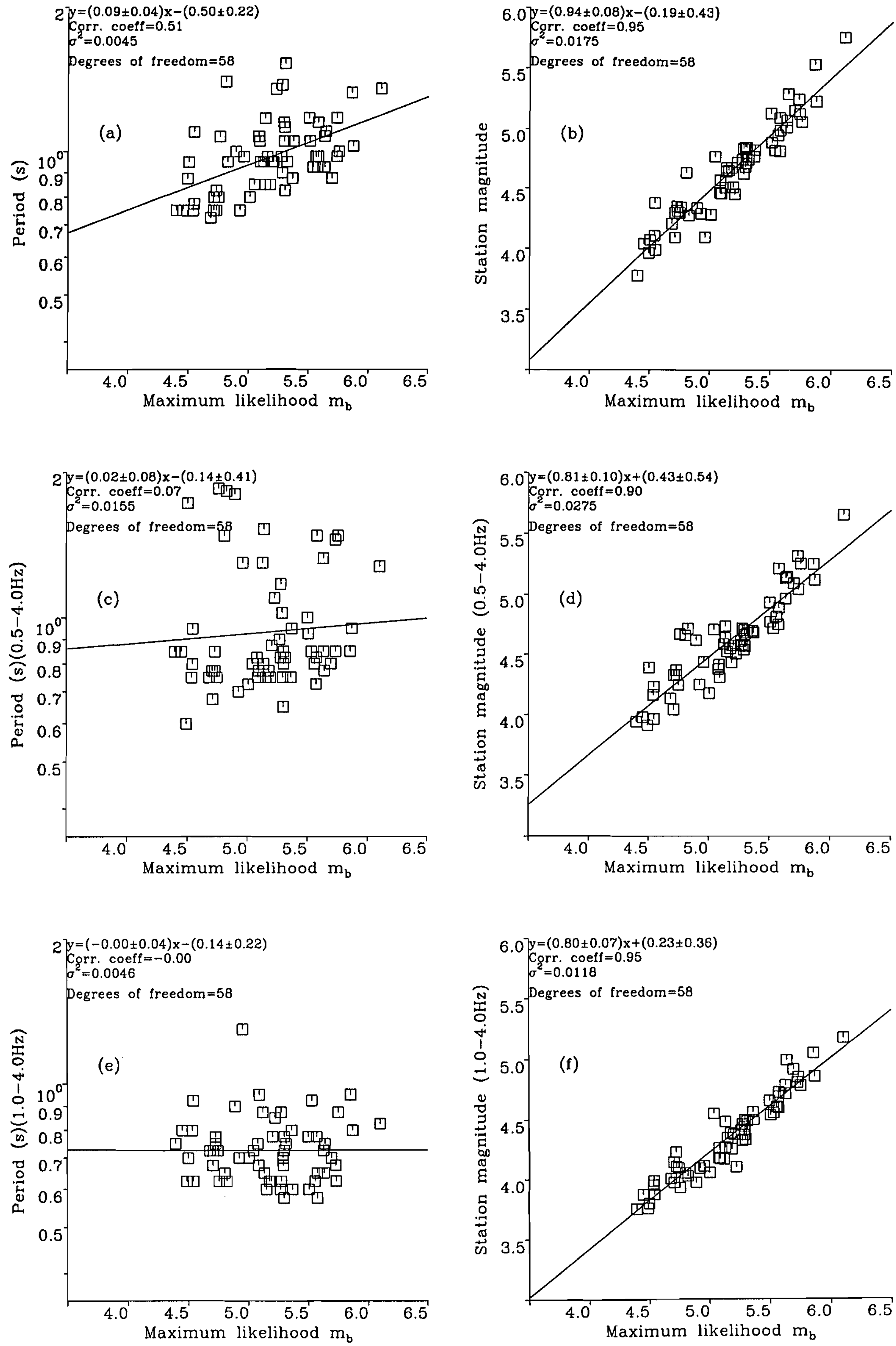

Figure 16

16MW

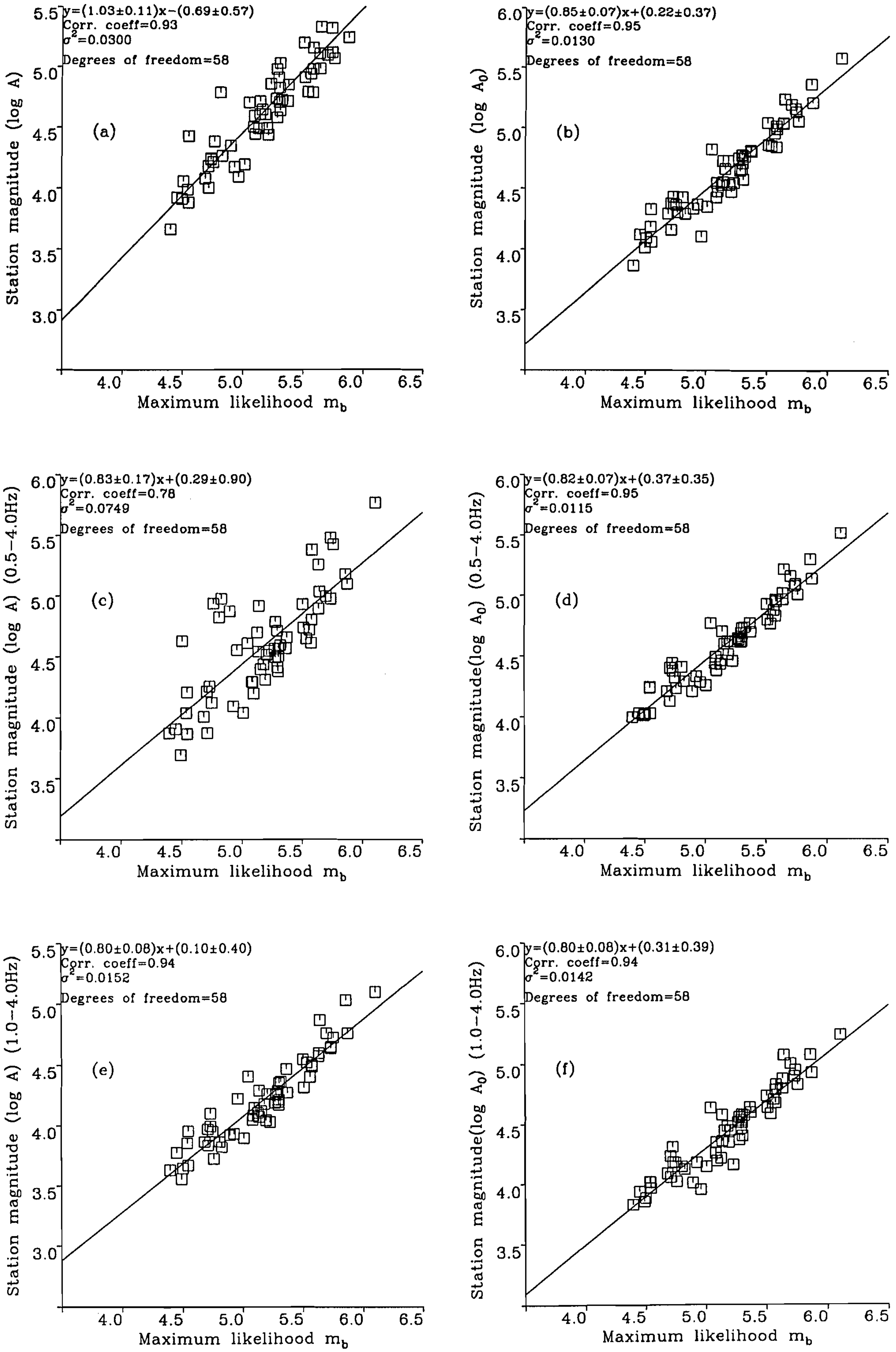
y=(1.03±0.11)x−(0.69±0.57)
Corr. coeff=0.93
σ²=0.0300
Degrees of freedom=58
(a)
Station magnitude (log A)
Maximum likelihood m_b
y=(0.85±0.07)x+(0.22±0.37)
Corr. coeff=0.95
σ²=0.0130
Degrees of freedom=58
(b)
Station magnitude (log A0)
Maximum likelihood m_b
y=(0.83±0.17)x+(0.29±0.90)
Corr. coeff=0.78
σ²=0.0749
Degrees of freedom=58
(c)
Station magnitude (log A) (0.5−4.0Hz)
Maximum likelihood m_b
y=(0.82±0.07)x+(0.37±0.35)
Corr. coeff=0.95
σ²=0.0115
Degrees of freedom=58
(d)
Station magnitude(log A0) (0.5−4.0Hz)
Maximum likelihood m_b
y=(0.80±0.08)x+(0.10±0.40)
Corr. coeff=0.94
σ²=0.0152
Degrees of freedom=58
(e)
Station magnitude (log A) (1.0−4.0Hz)
Maximum likelihood m_b
y=(0.80±0.08)x+(0.31±0.39)
Corr. coeff=0.94
σ²=0.0142
Degrees of freedom=58
(f)
Station magnitude(log A0) (1.0−4.0Hz)
Maximum likelihood m_b

Figure 17

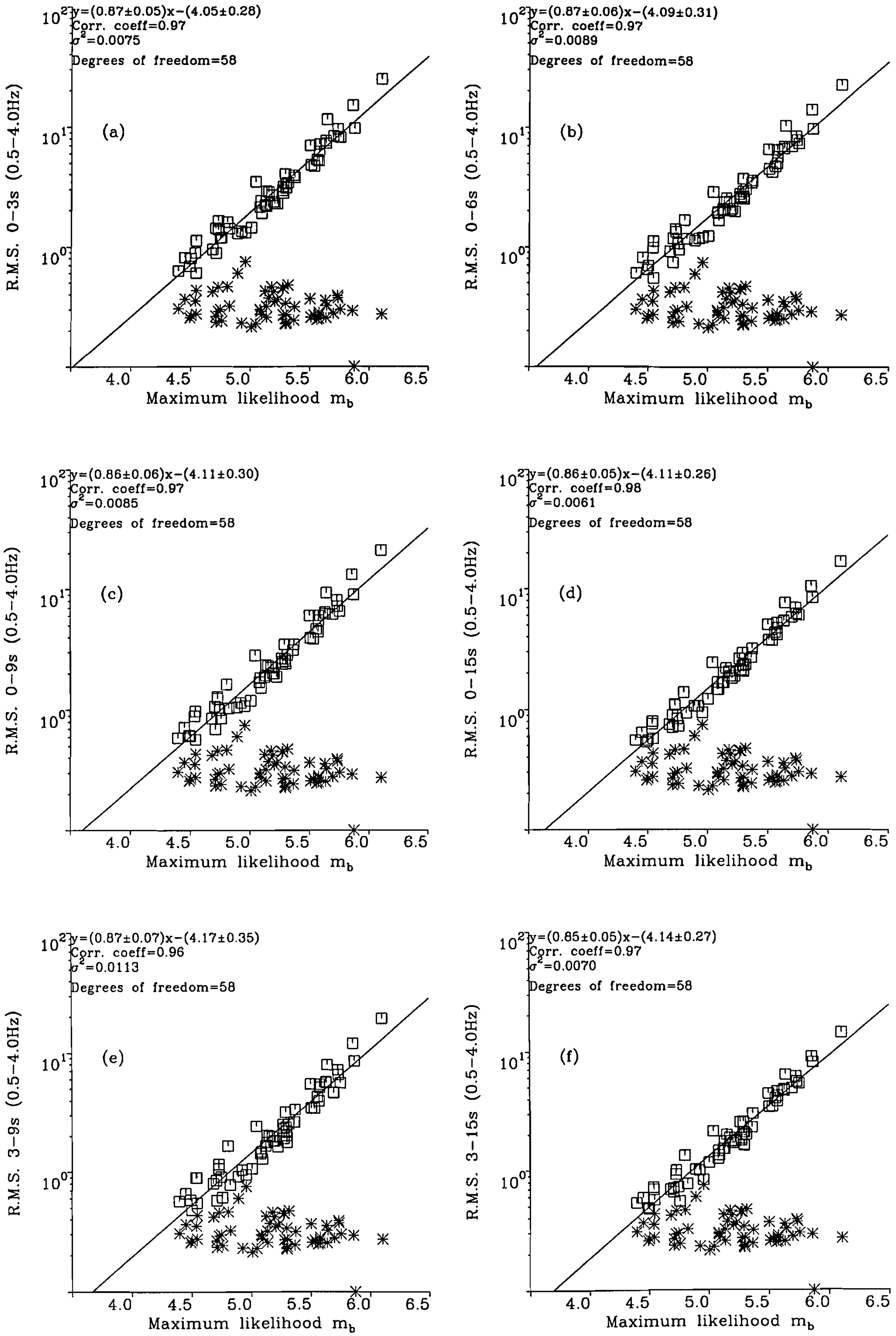

Figure 18

18MW

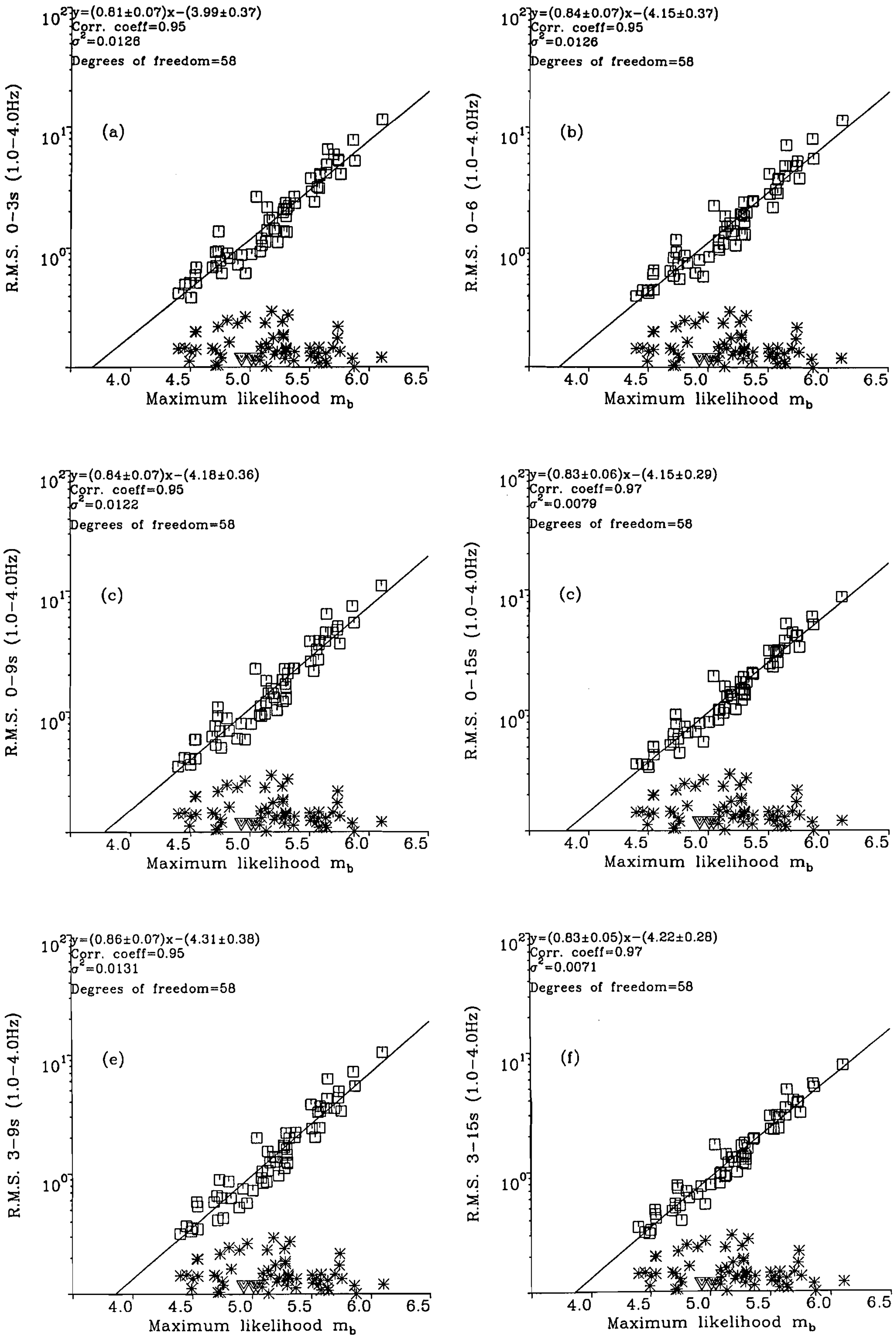

Figure 19

19MW

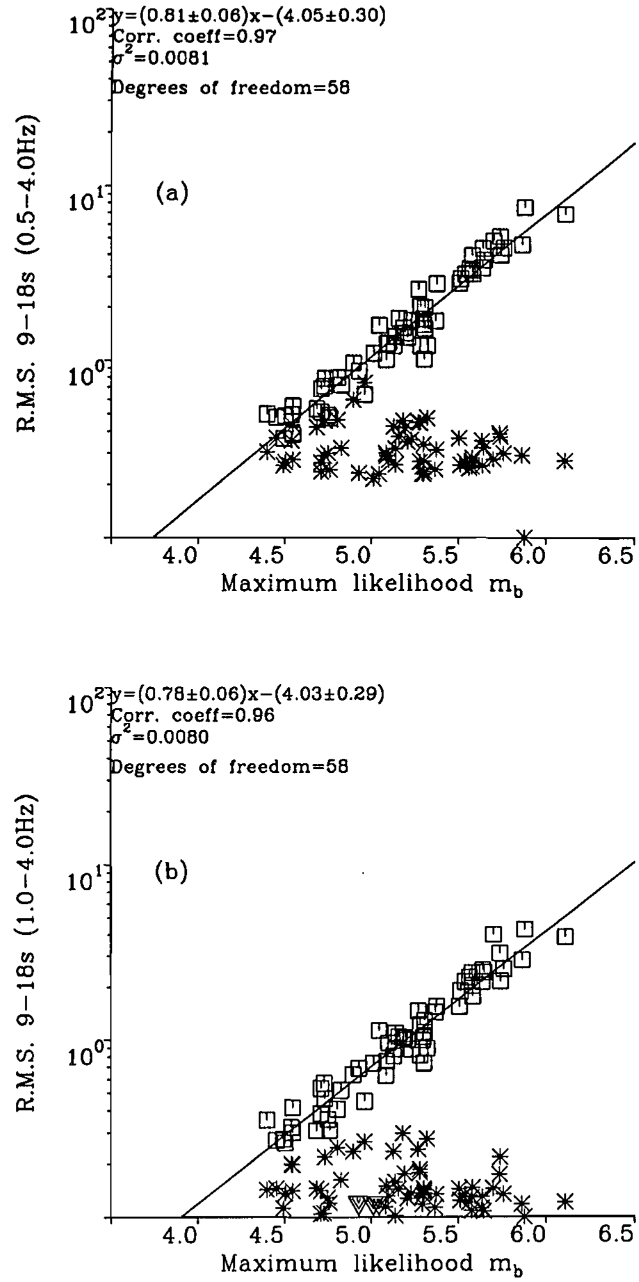

Figure 20

20MW

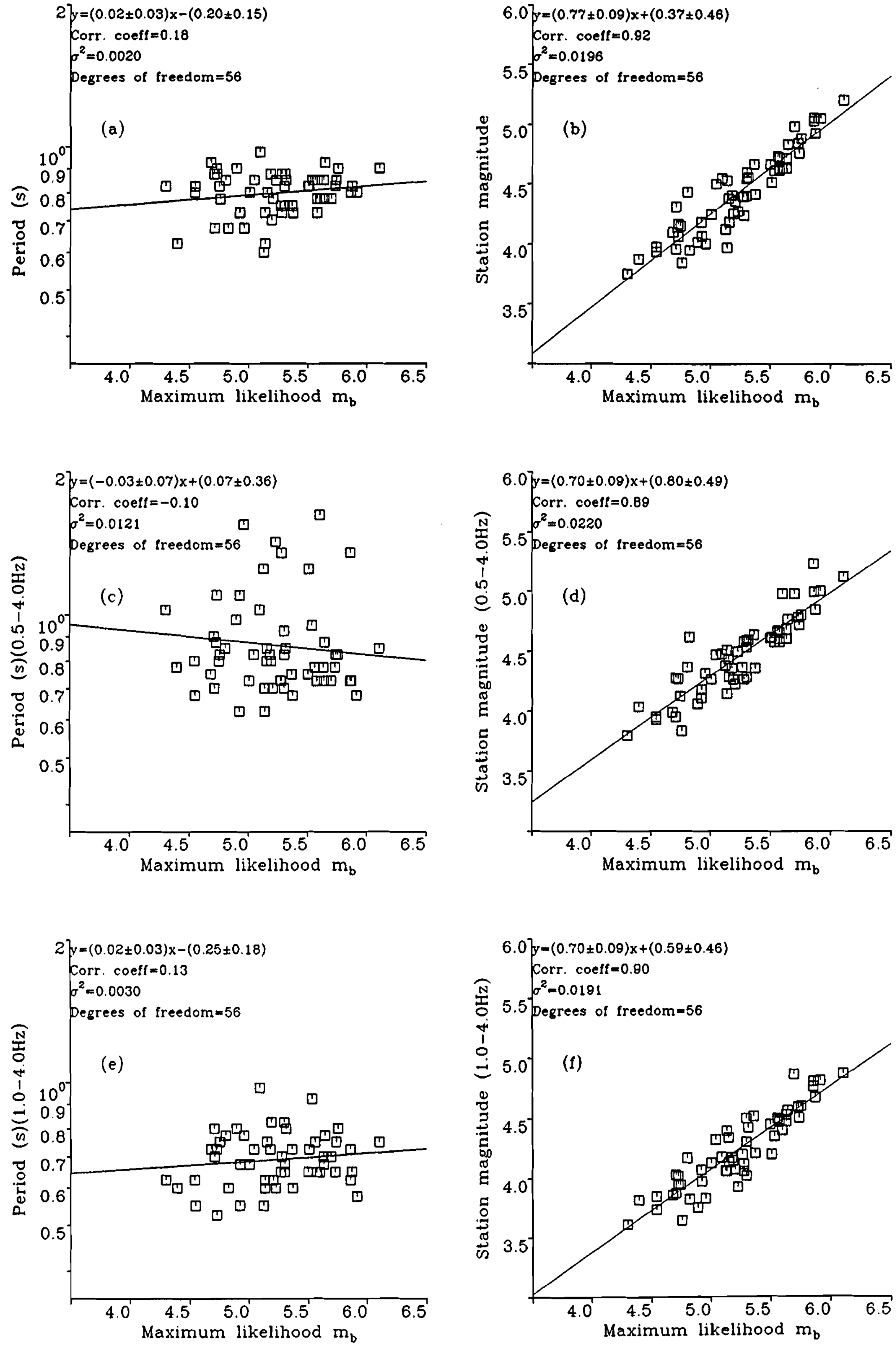

Figure 21

21MG

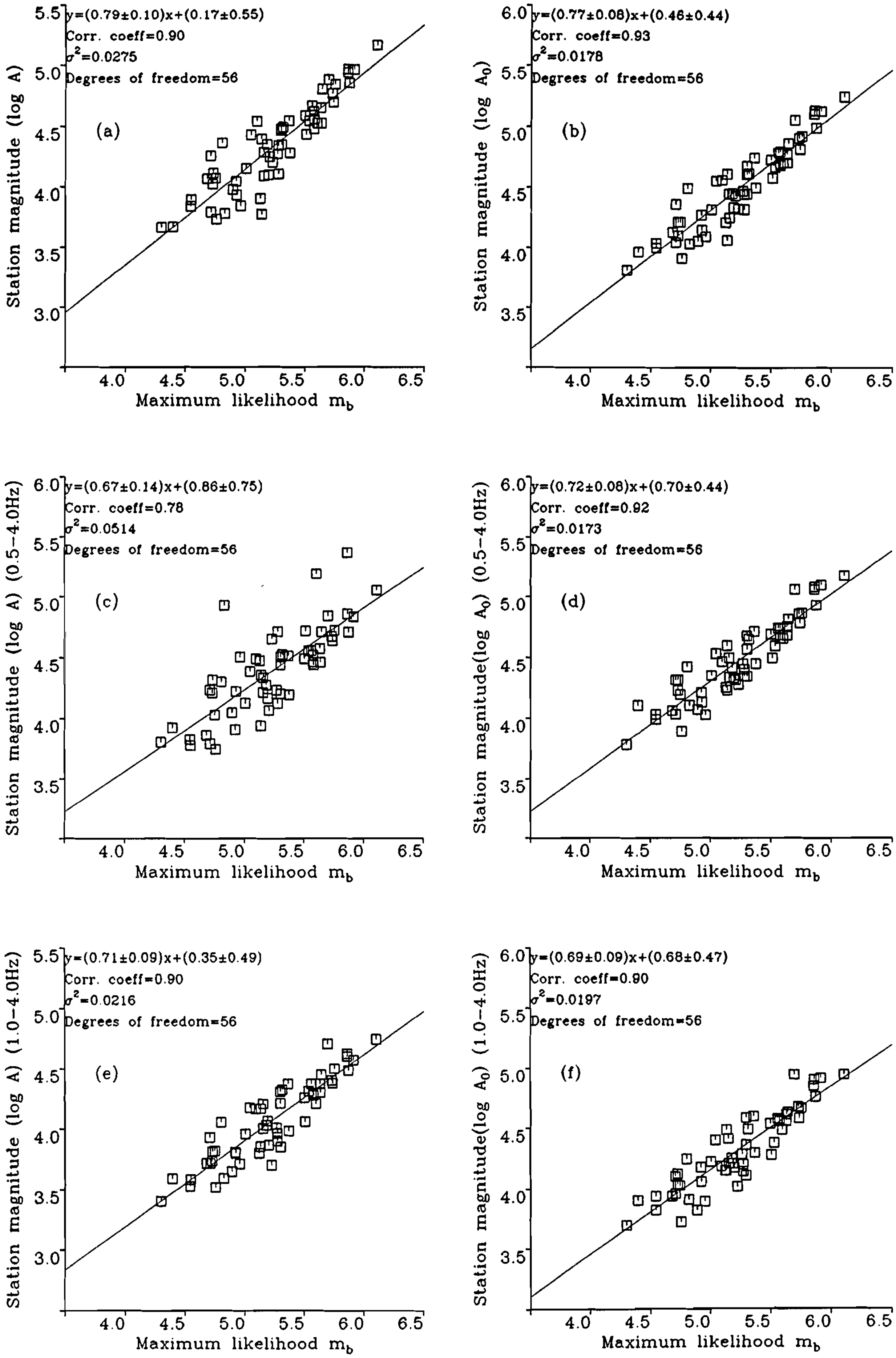

Figure 22

22MG

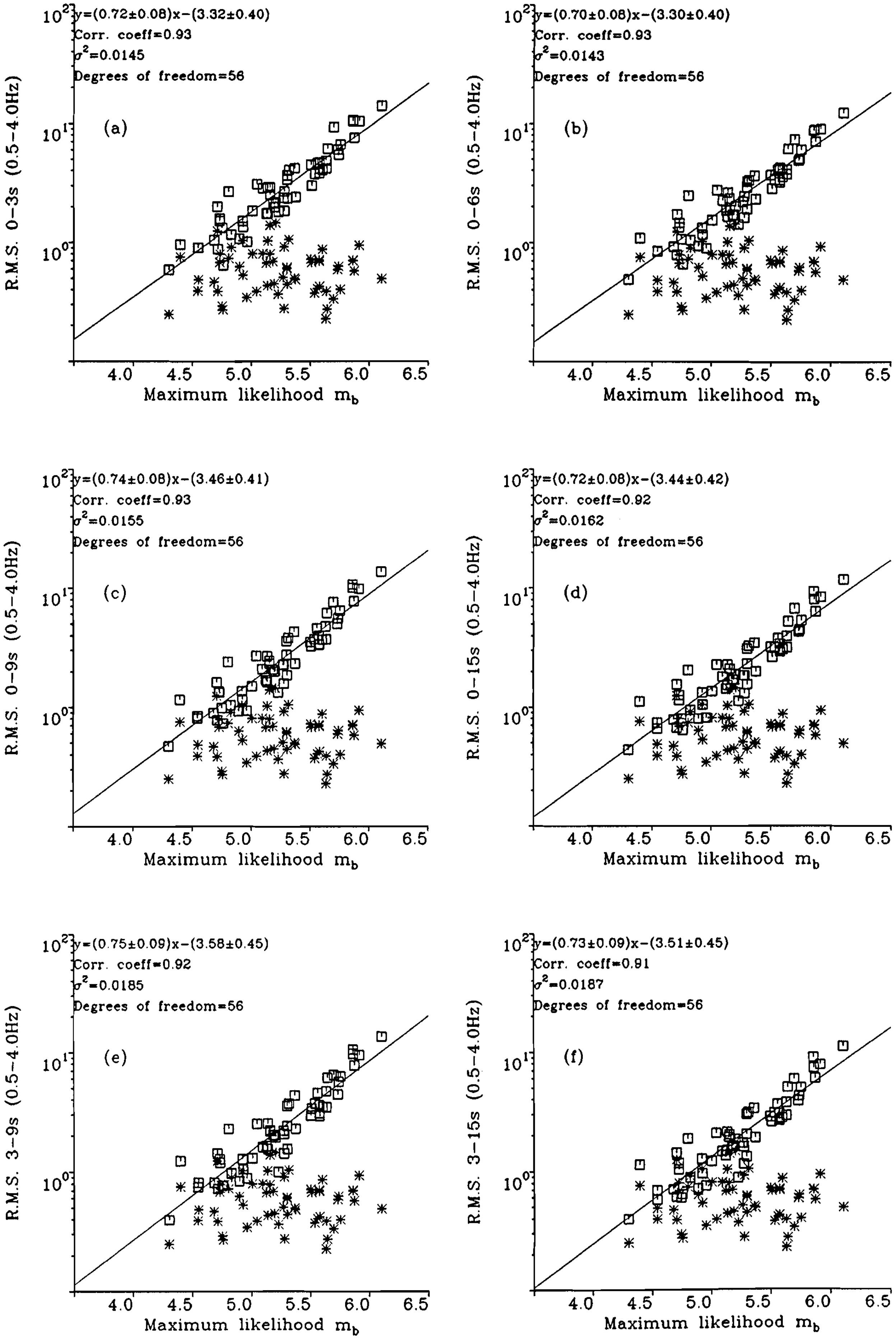

Figure 23

23MG

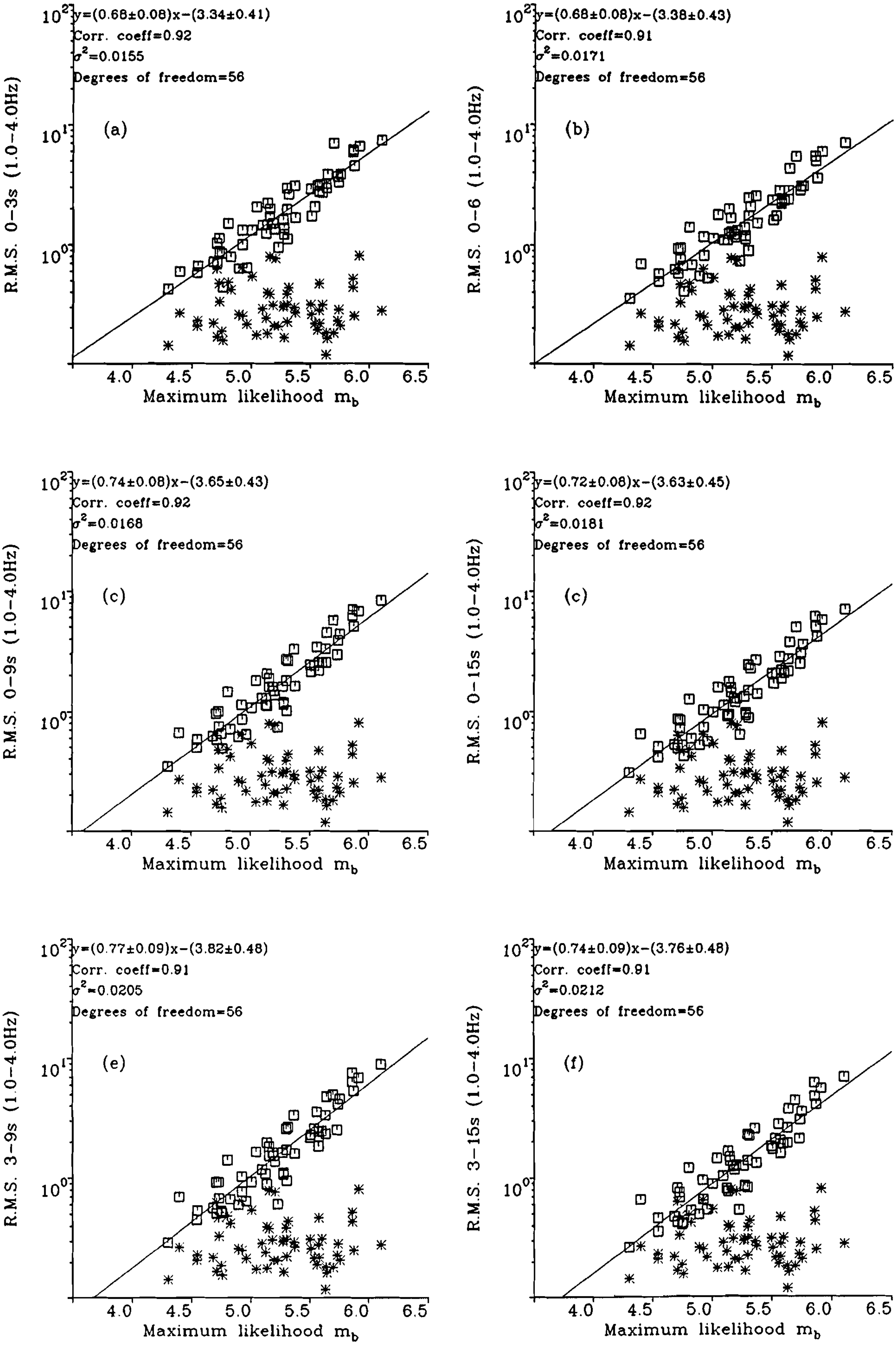

Figure 24

24MG

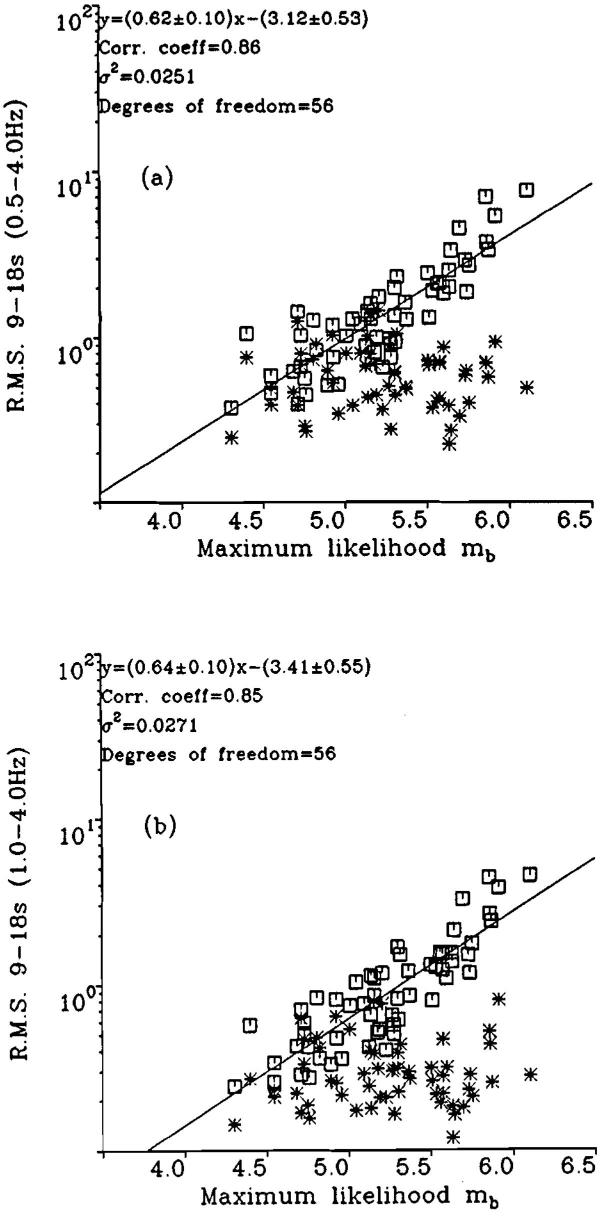

Figure 25

25MG

APPENDIX A

SEISMOGRAMS FOR THE MURUROA EXPLOSIONS

YKA

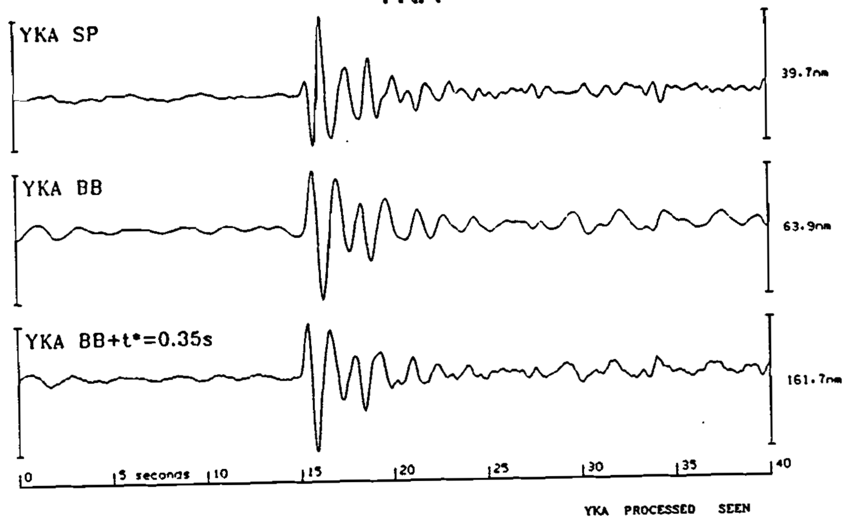

GBA

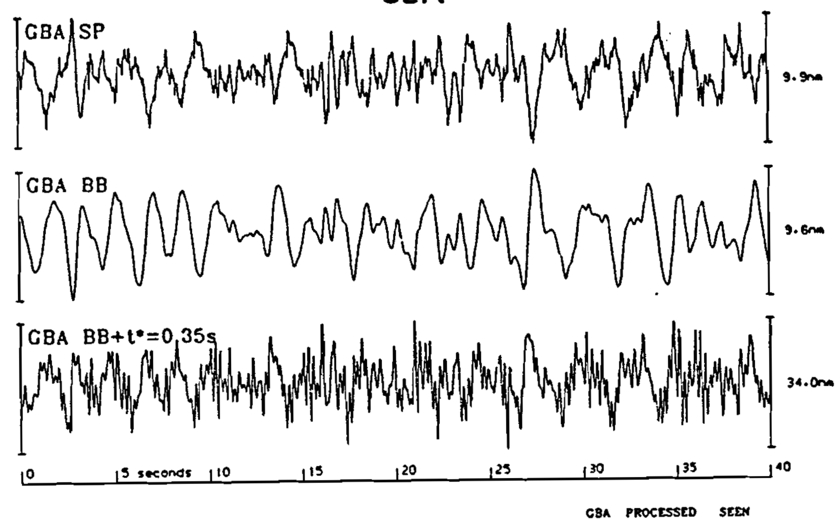

WRA

WRA NOT PROCESSED NO TAPE

EKA

EKA NOT PROCESSED

Figure A1 Short period, broad band and deconvolved P seismograms from the Mururoa explosion of 11 July 1976.

YKA

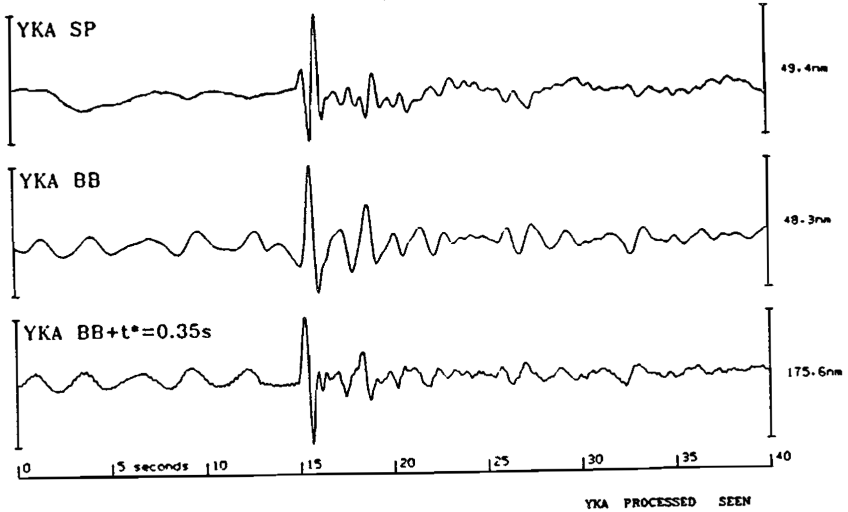

GBA

GBA NOT PROCESSED NO TAPE

WRA

WRA NOT PROCESSED NO TAPE

EKA

EKA NOT PROCESSED

Figure A2 Short period, broad band and deconvolved P seismograms from the Mururoa explosion of 19 February 1977.

YKA

YKA PROCESSED SEEN OVERLOADED

WRA

WRA NOT PROCESSED NO TAPE

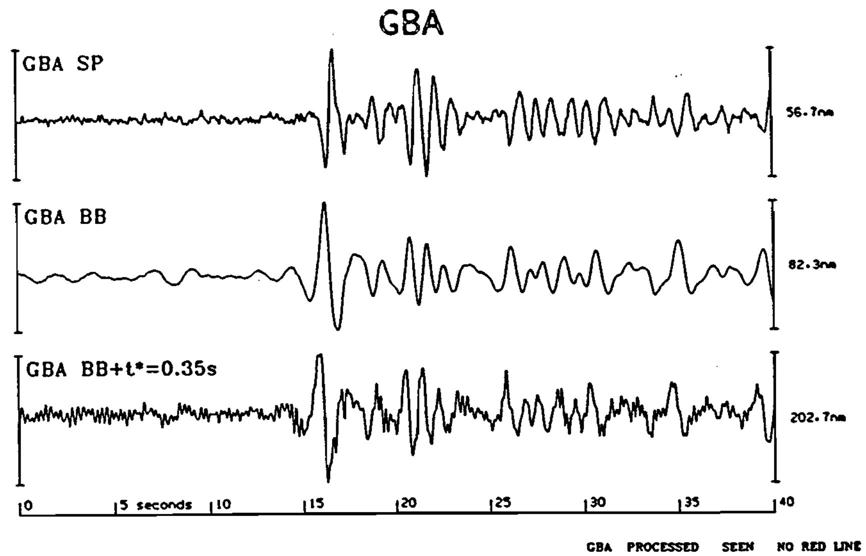

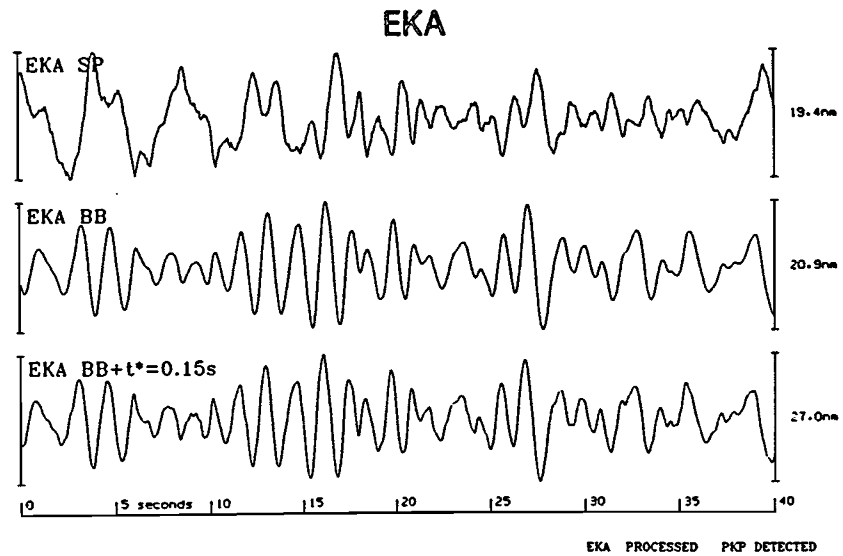

Figure A3 Short period, broad band and deconvolved P seismograms from the Mururoa explosion of 19 March 1977.

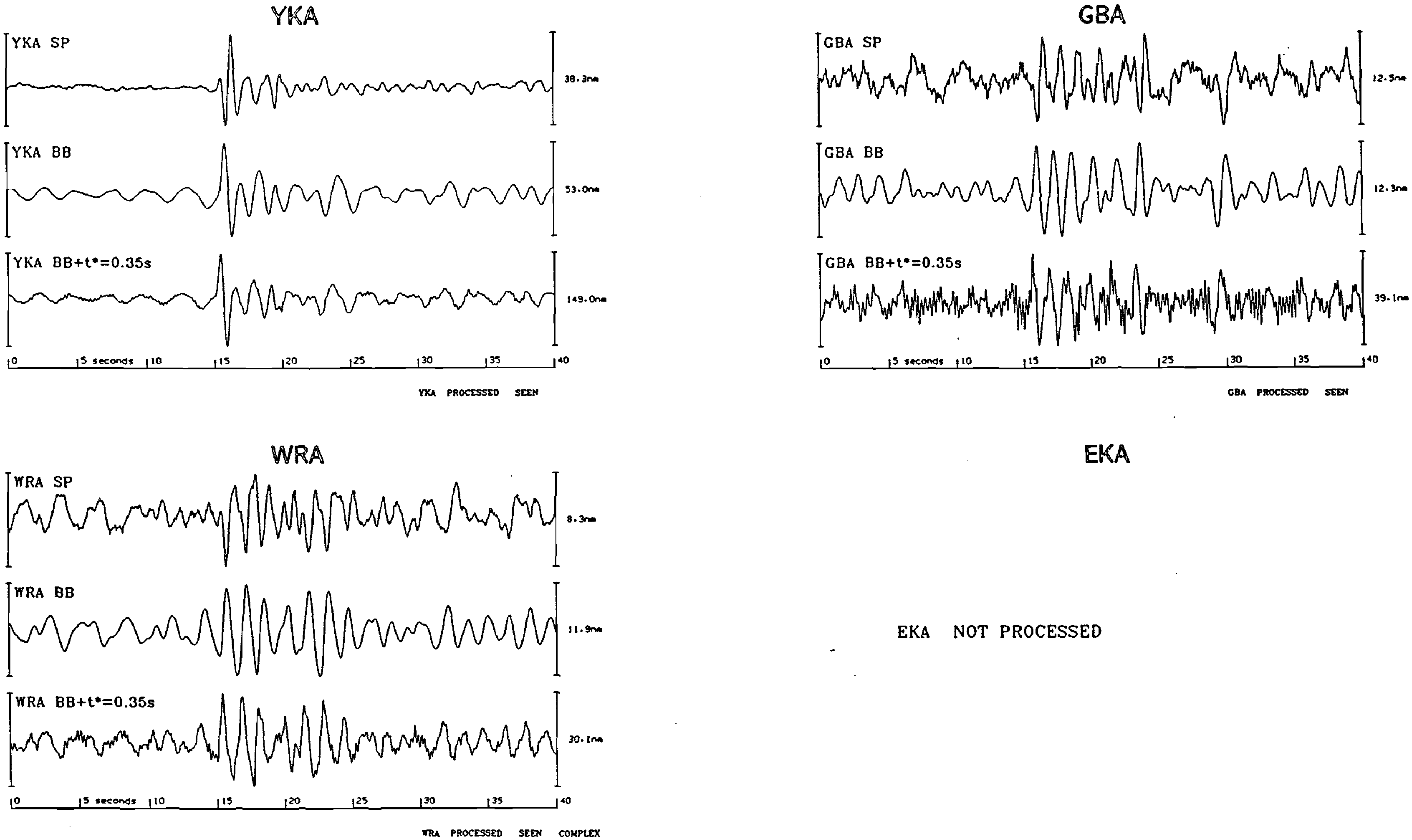

Figure A4 Short period, broad band and deconvolved P seismograms from the Mururoa explosion of 6 July 1977.

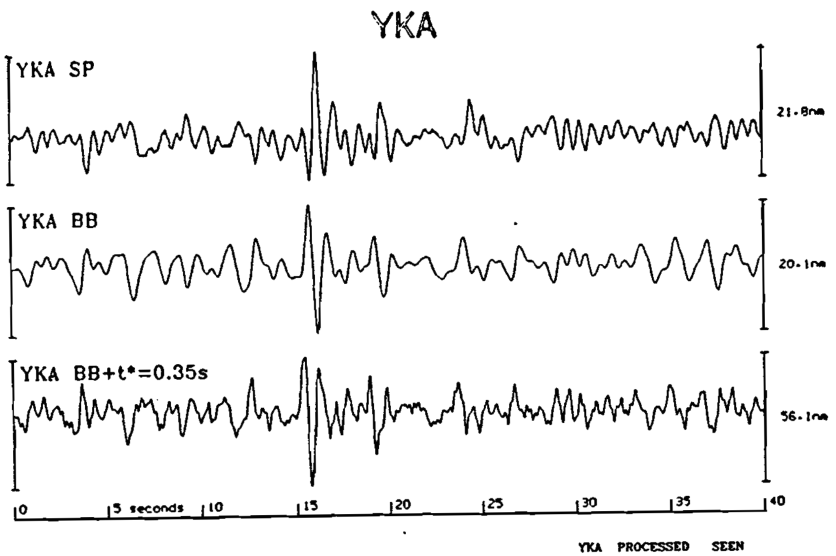

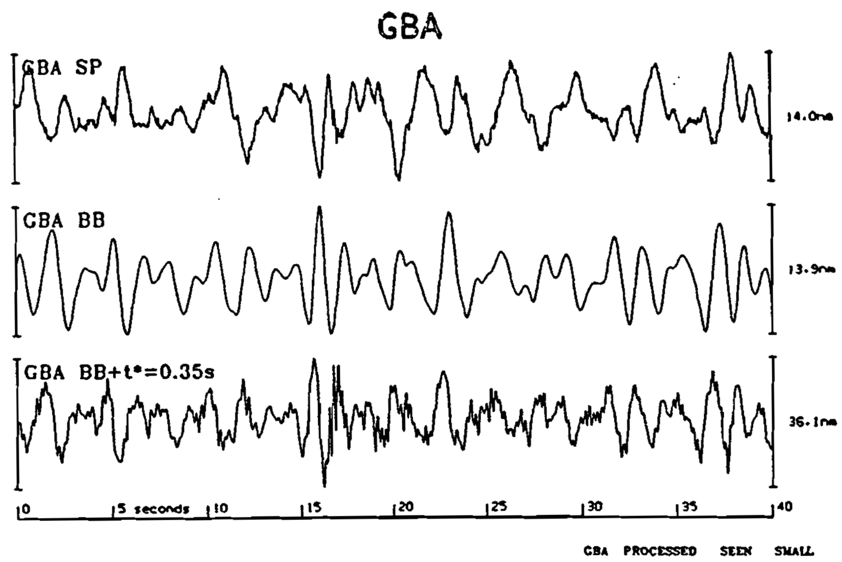

WRA

WRA NOT PROCESSED NOT AVAILABLE

EKA

EKA NOT PROCESSED

Figure A5 Short period, broad band and deconvolved P seismograms from the Mururoa explosion of 12 November 1977.

YKA

YKA NOT PROCESSED NOT AVAILABLE

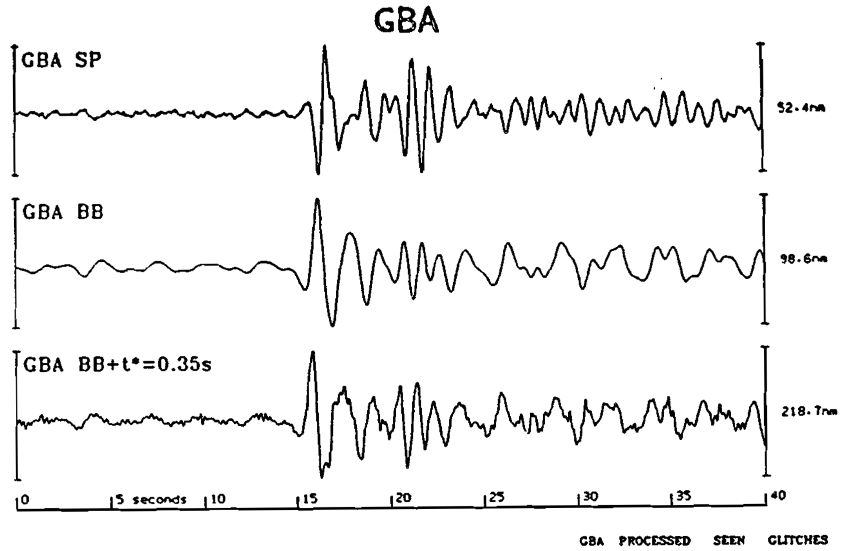

WRA

WRA NOT PROCESSED NOT AVAILABLE

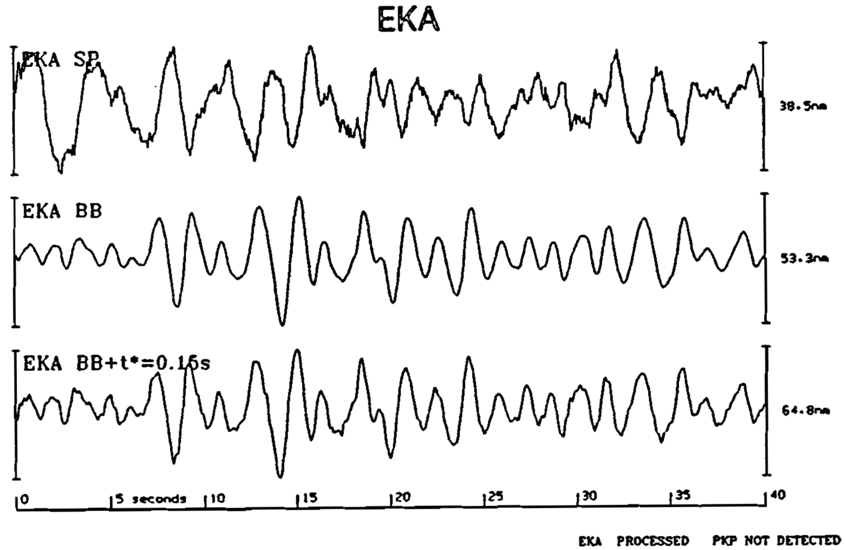

Figure A6 Short period, broad band and deconvolved P seismograms from the Mururoa explosion of 24 November 1977.

YKA

YKA NOT PROCESSED NOT AVAILABLE

GBA

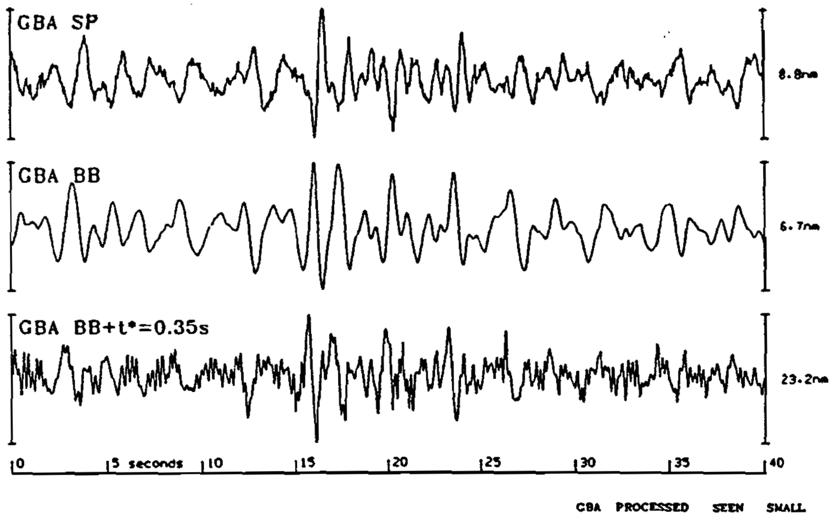

WRA

WRA NOT PROCESSED NOT AVAILABLE

EKA

EKA NOT PROCESSED

Figure A7 Short period, broad band and deconvolved P seismograms from the Mururoa explosion of 17 December 1977.

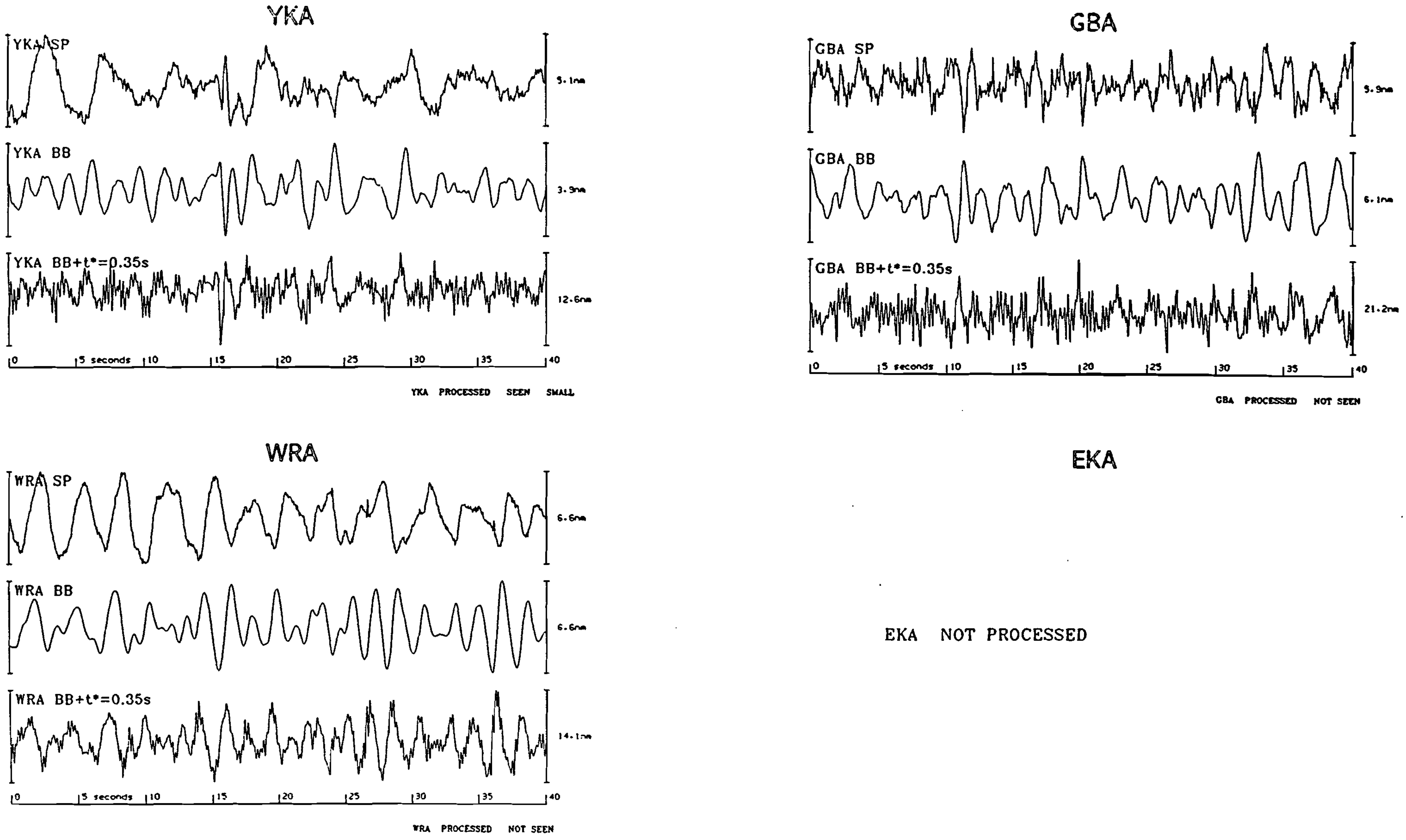

Figure A8 Short period, broad band and deconvolved P seismograms from the Mururoa explosion of 27 February 1978.

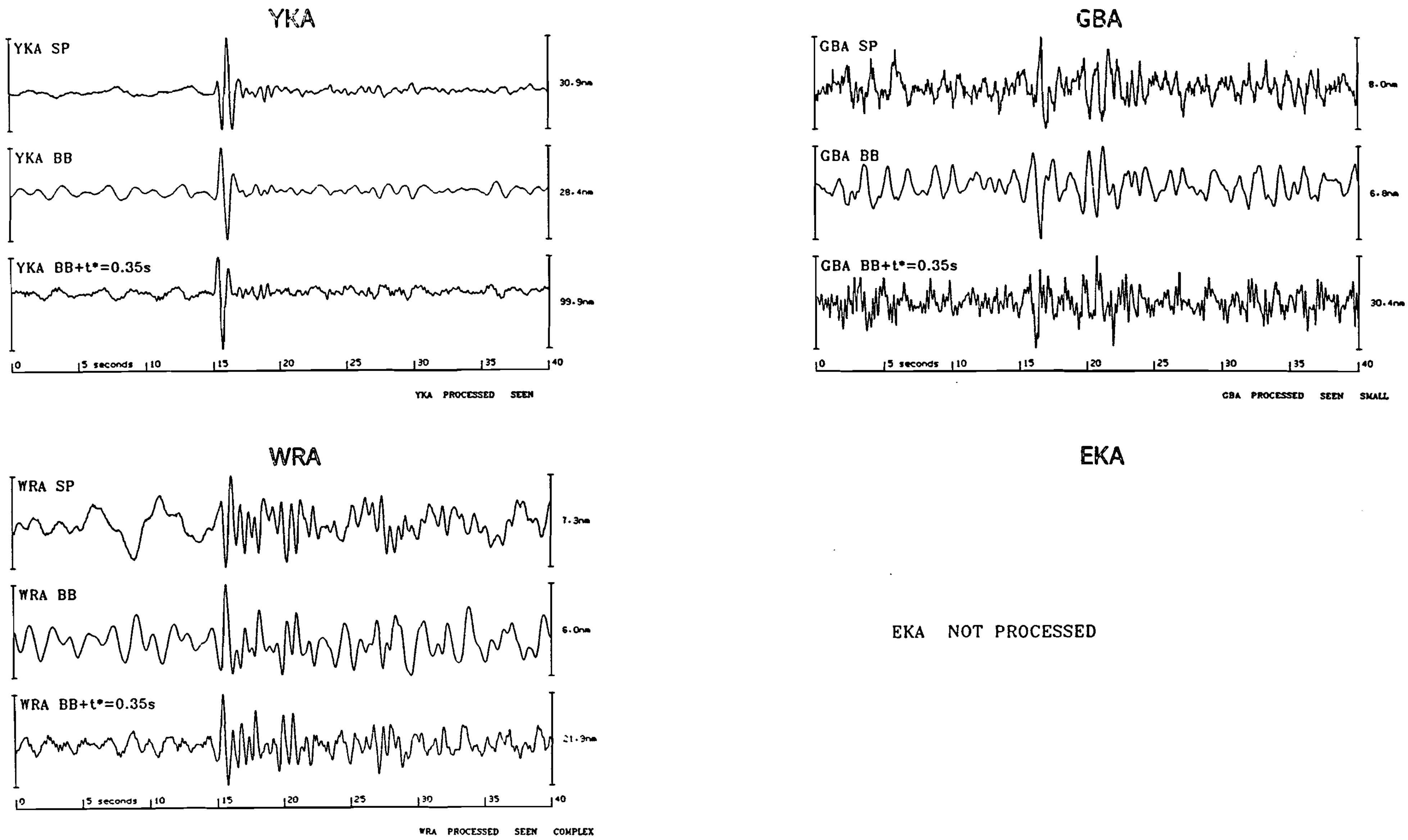

Figure A9 Short period, broad band and deconvolved P seismograms from the Mururoa explosion of 22 March 1978.

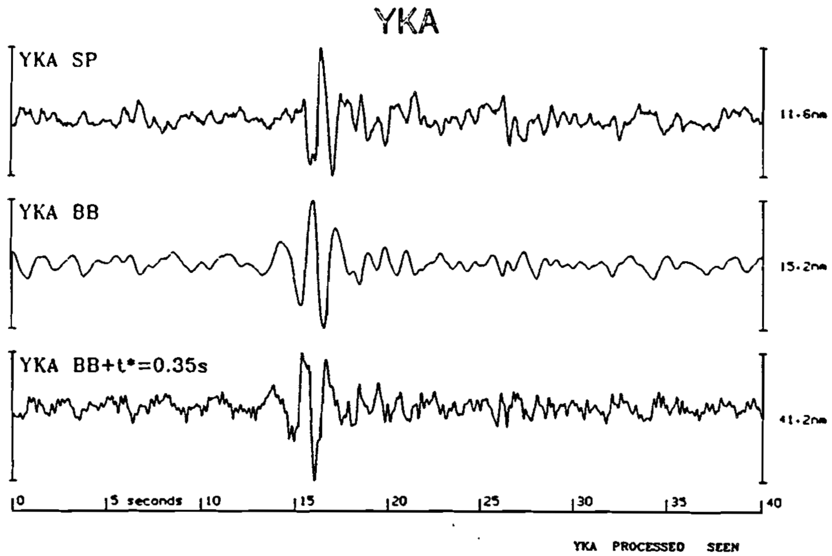

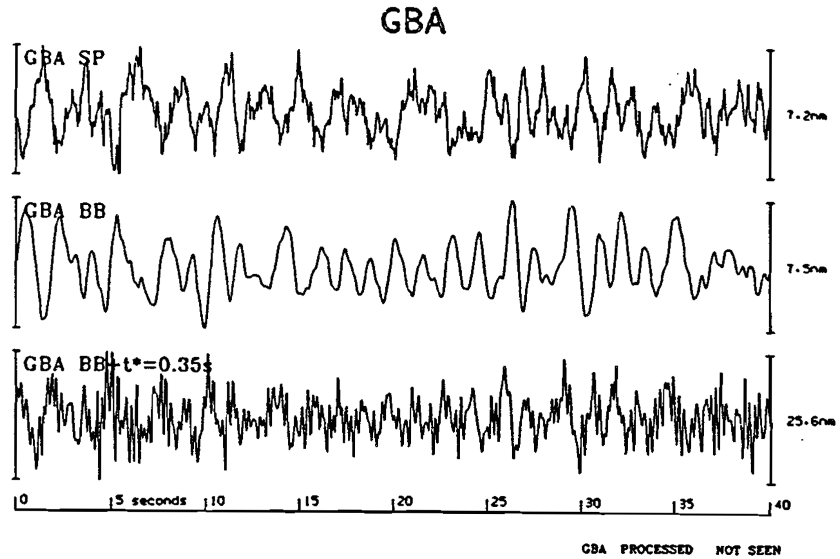

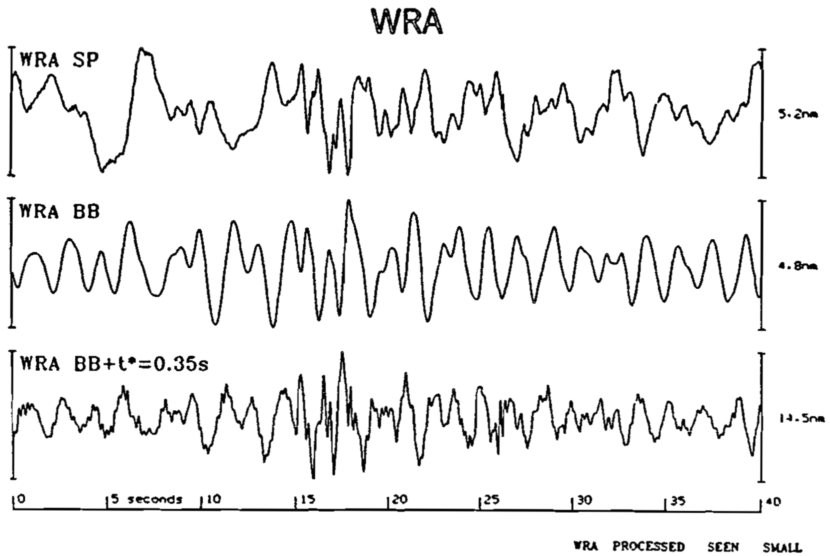

EKA

EKA NOT PROCESSED

Figure A10 Short period, broad band and deconvolved P seismograms from the Mururoa explosion of 19 July 1978.

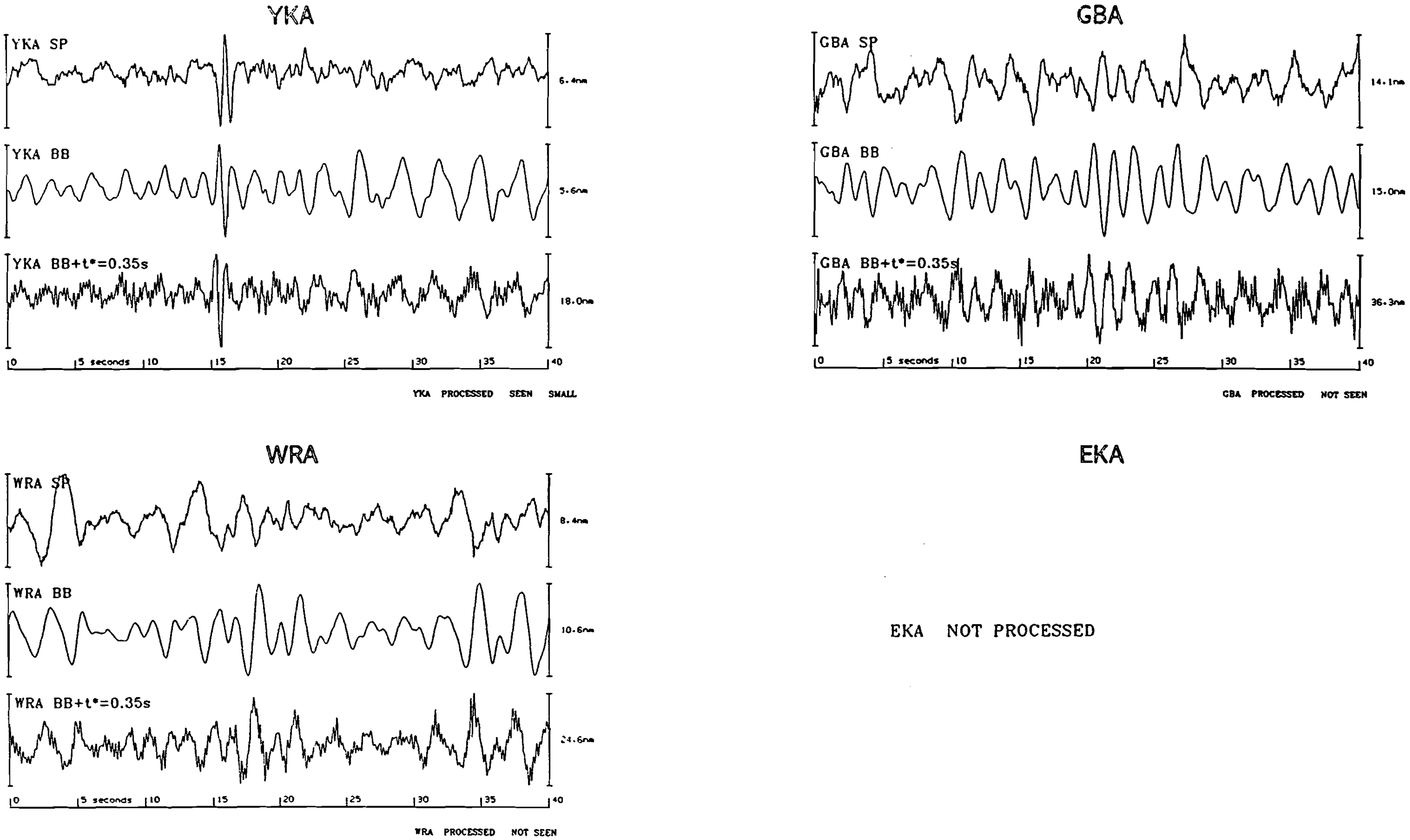

Figure A11 Short period, broad band and deconvolved P seismograms from the Mururoa explosion of 26 July 1978.

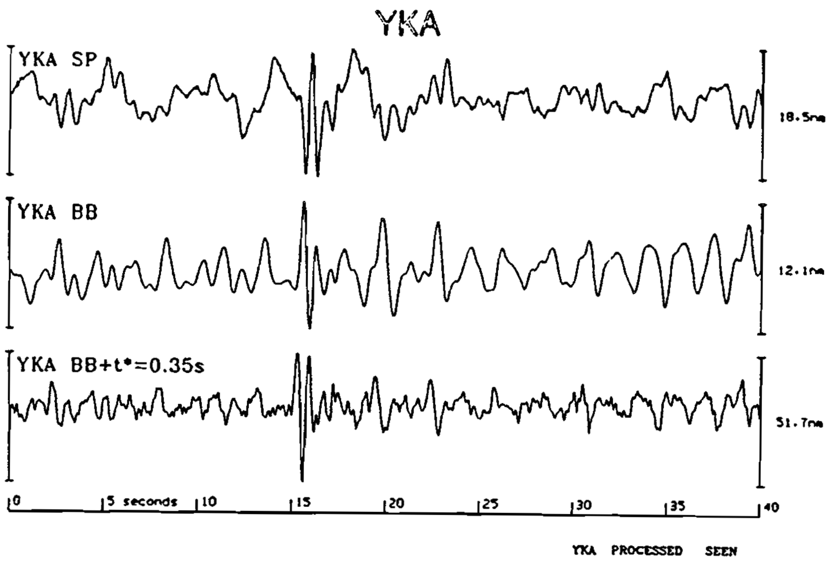

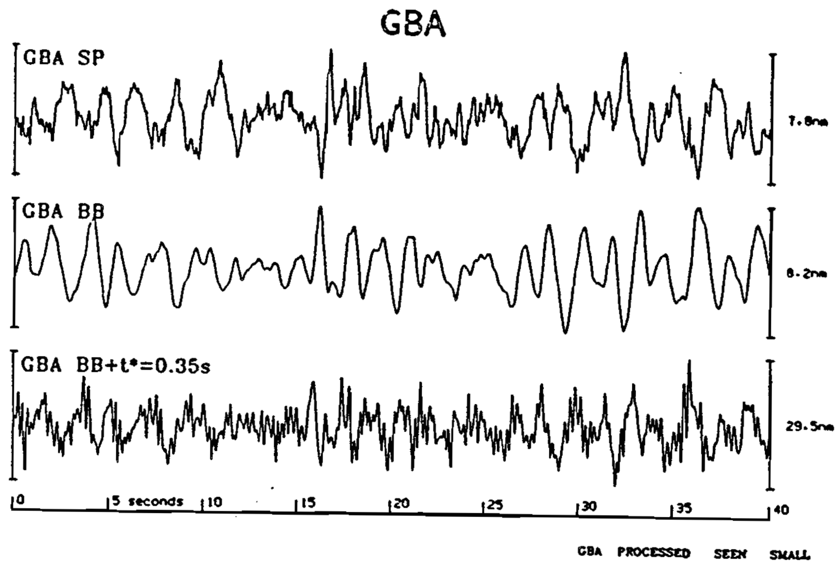

WRA

WRA NOT PROCESSED NOT AVAILABLE

EKA

EKA NOT PROCESSED

Figure A12 Short period, broad band and deconvolved P seismograms from the Mururoa explosion of 2 November 1978.

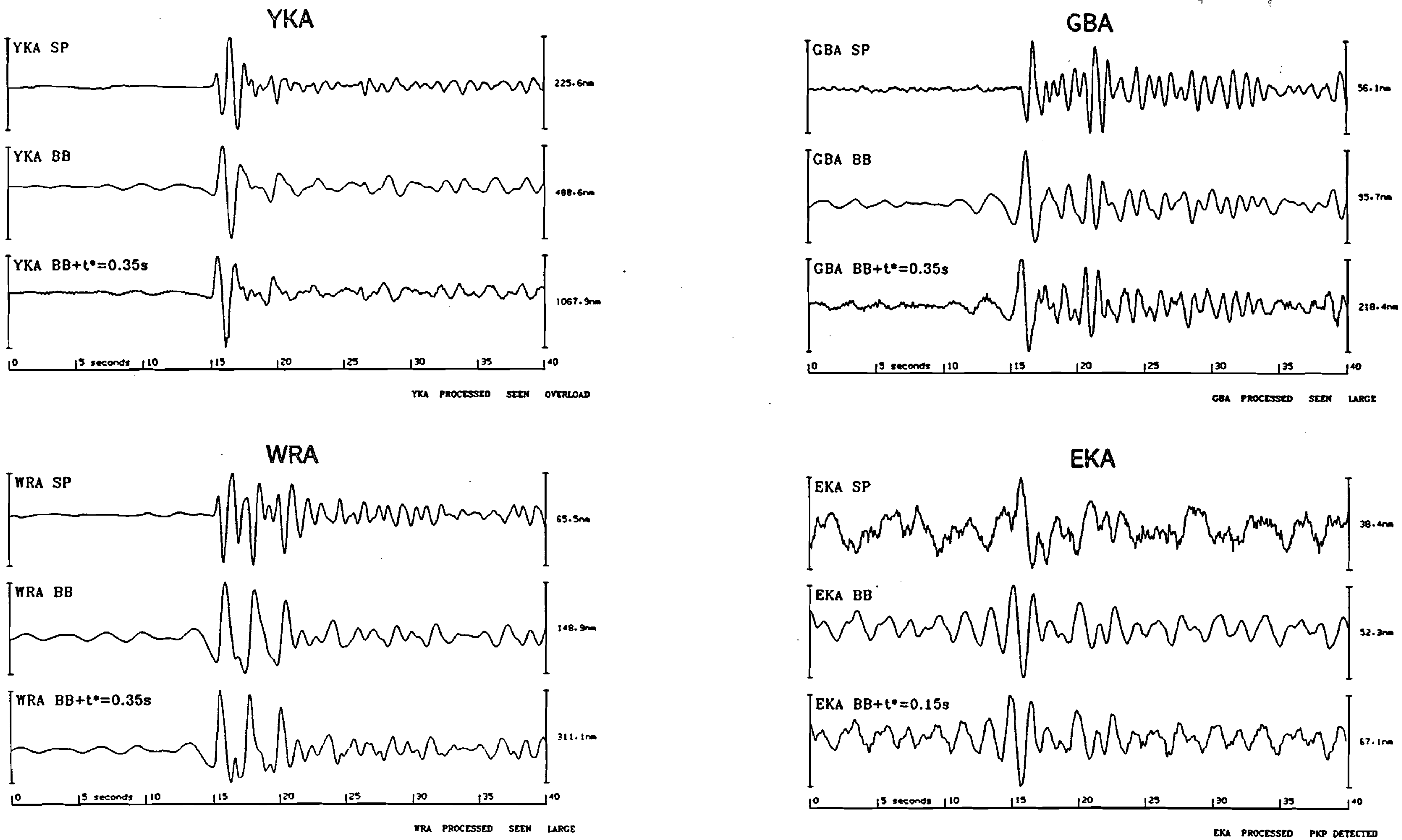

Figure A13 Short period, broad band and deconvolved P seismograms from the Mururoa explosion of 30 November 1978.

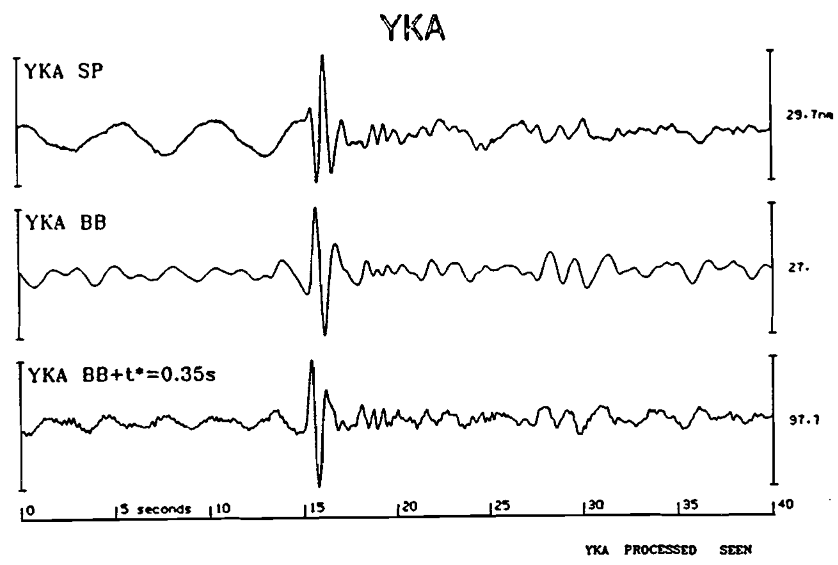

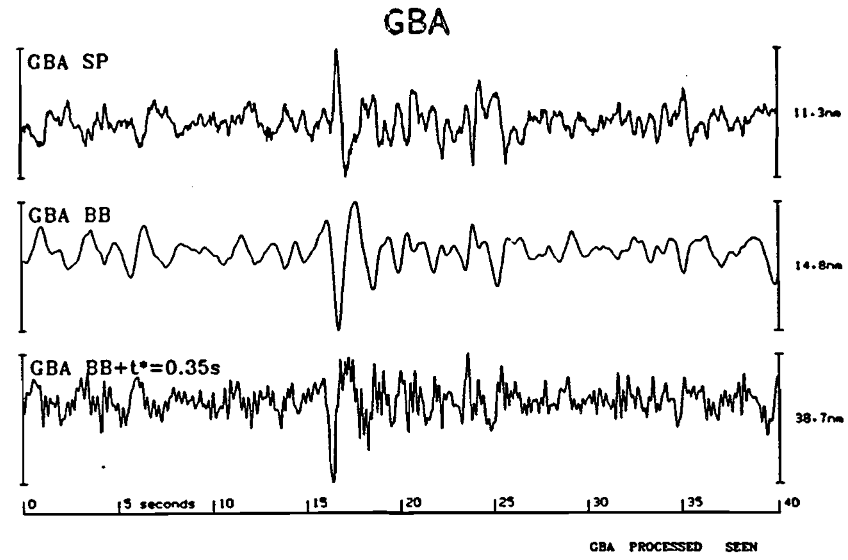

WRA

WRA NOT PROCESSED NO TAPE

EKA

EKA NOT PROCESSED

Figure A14 Short period, broad band and deconvolved P seismograms from the Mururoa explosion of 17 December 1978.

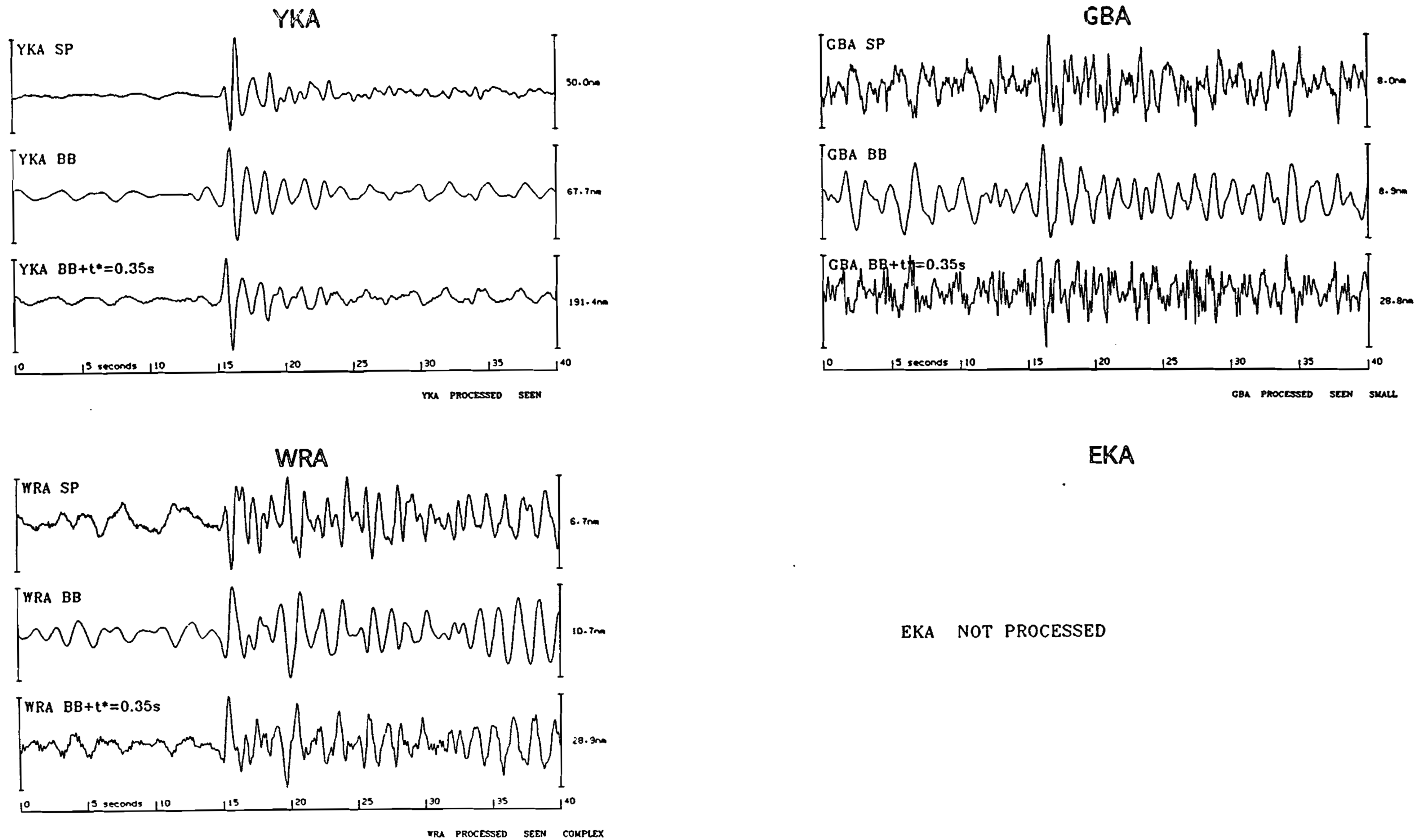

Figure A15 Short period, broad band and deconvolved P seismograms from the Mururoa explosion of 19 December 1978.

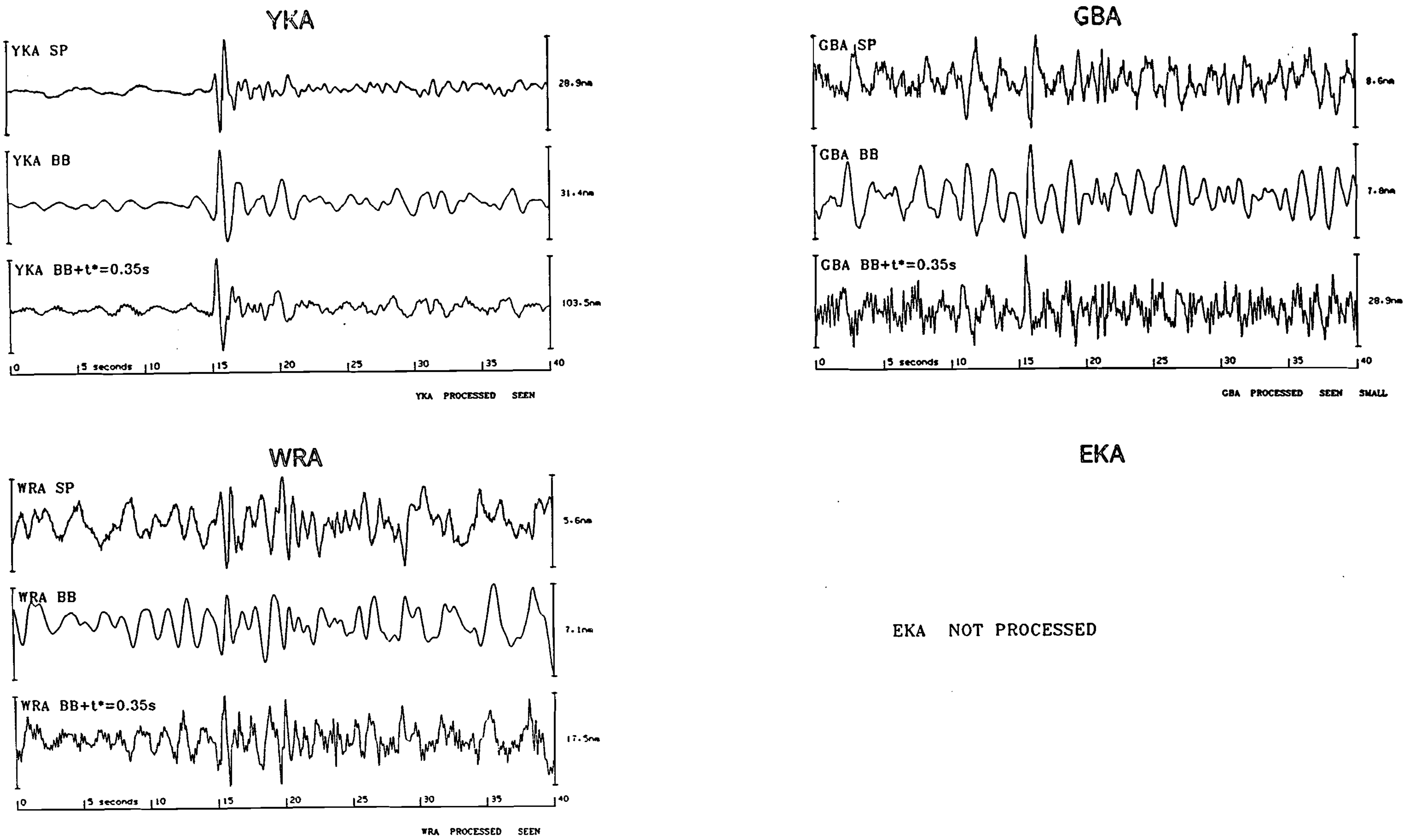

Figure A16 Short period, broad band and deconvolved P seismograms from the Mururoa explosion of 1 March 1979.

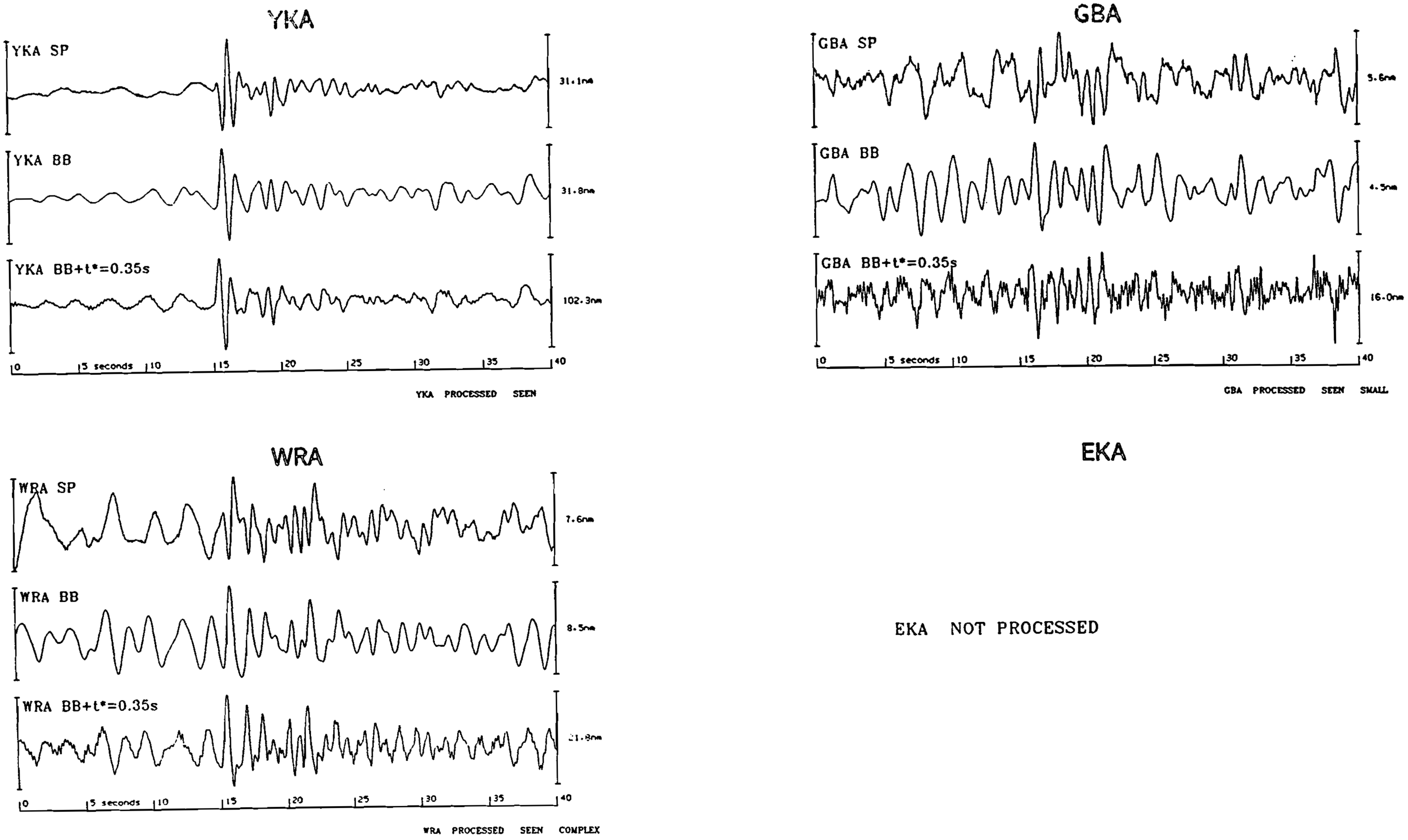

Figure A17 Short period, broad band and deconvolved P seismograms from the Mururoa explosion of 9 March 1979.

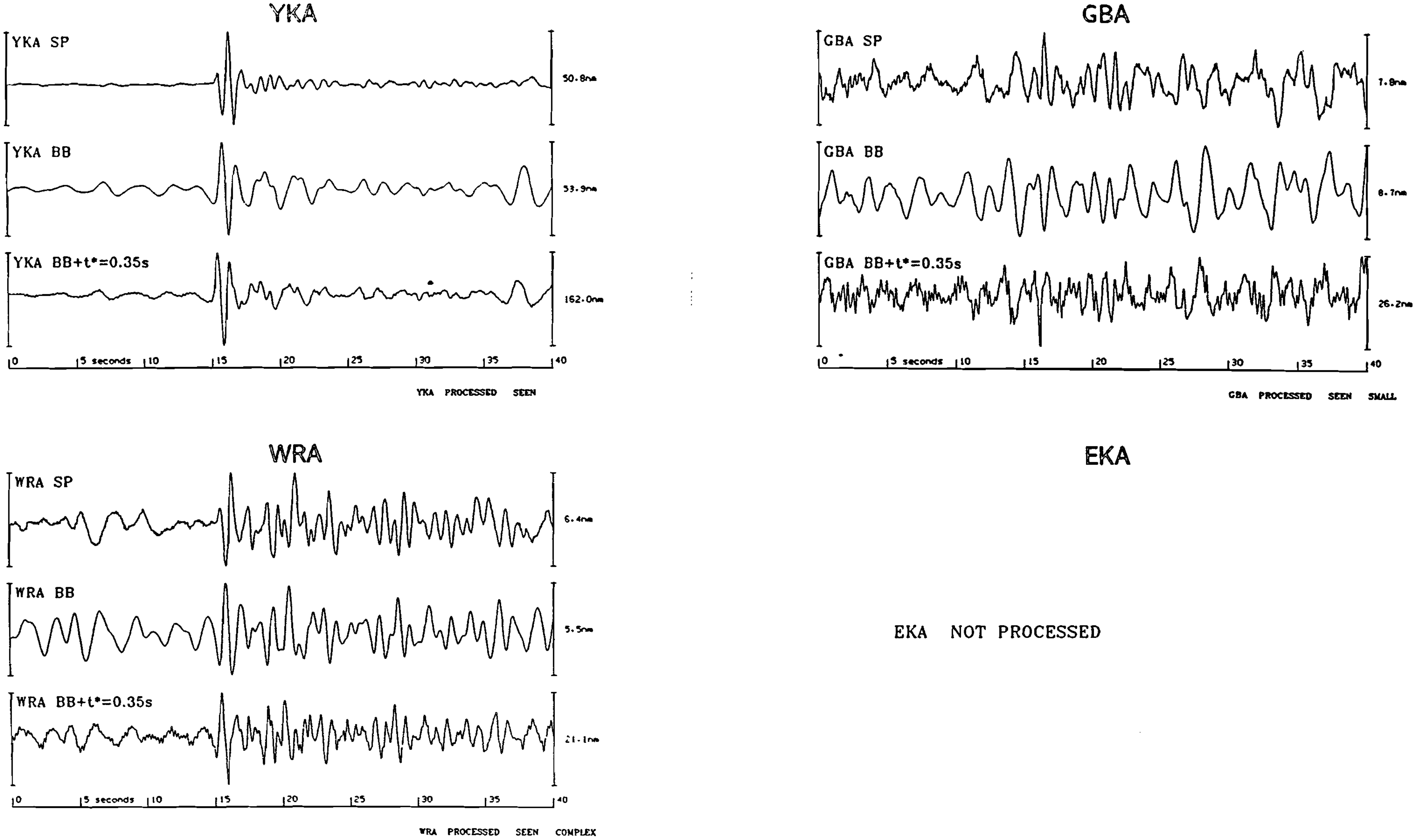

Figure A18 Short period, broad band and deconvolved P seismograms from the Mururoa explosion of 24 March 1979.

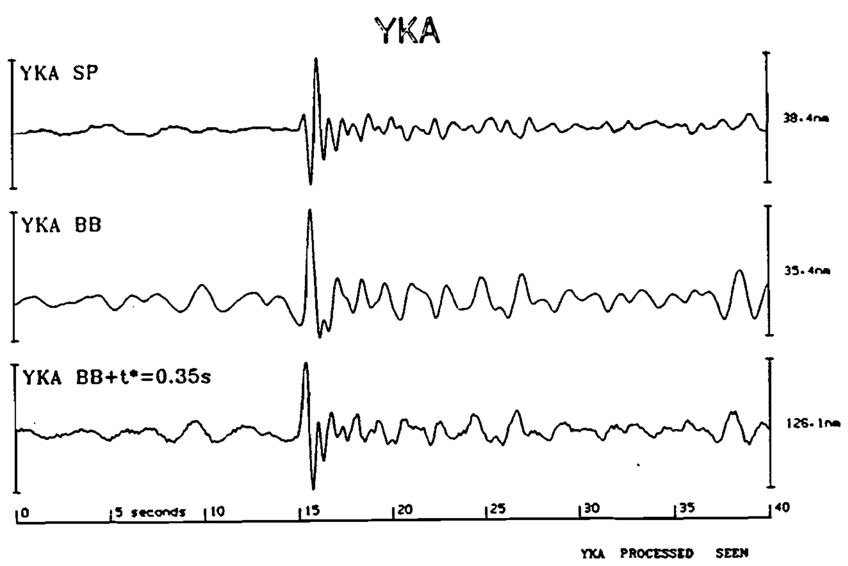

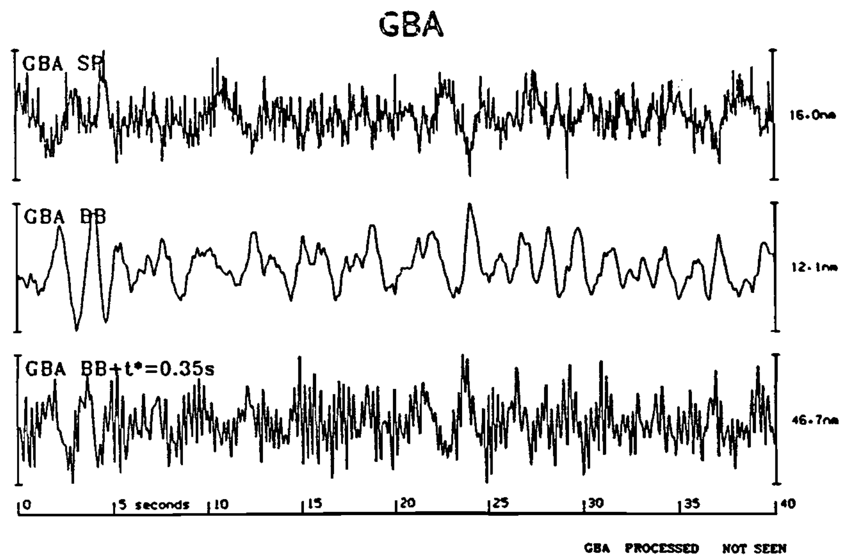

WRA

WRA NOT PROCESSED NOT AVAILABLE

EKA

EKA NOT PROCESSED

Figure A19 Short period, broad band and deconvolved P seismograms from the Mururoa explosion of 4 April 1979.

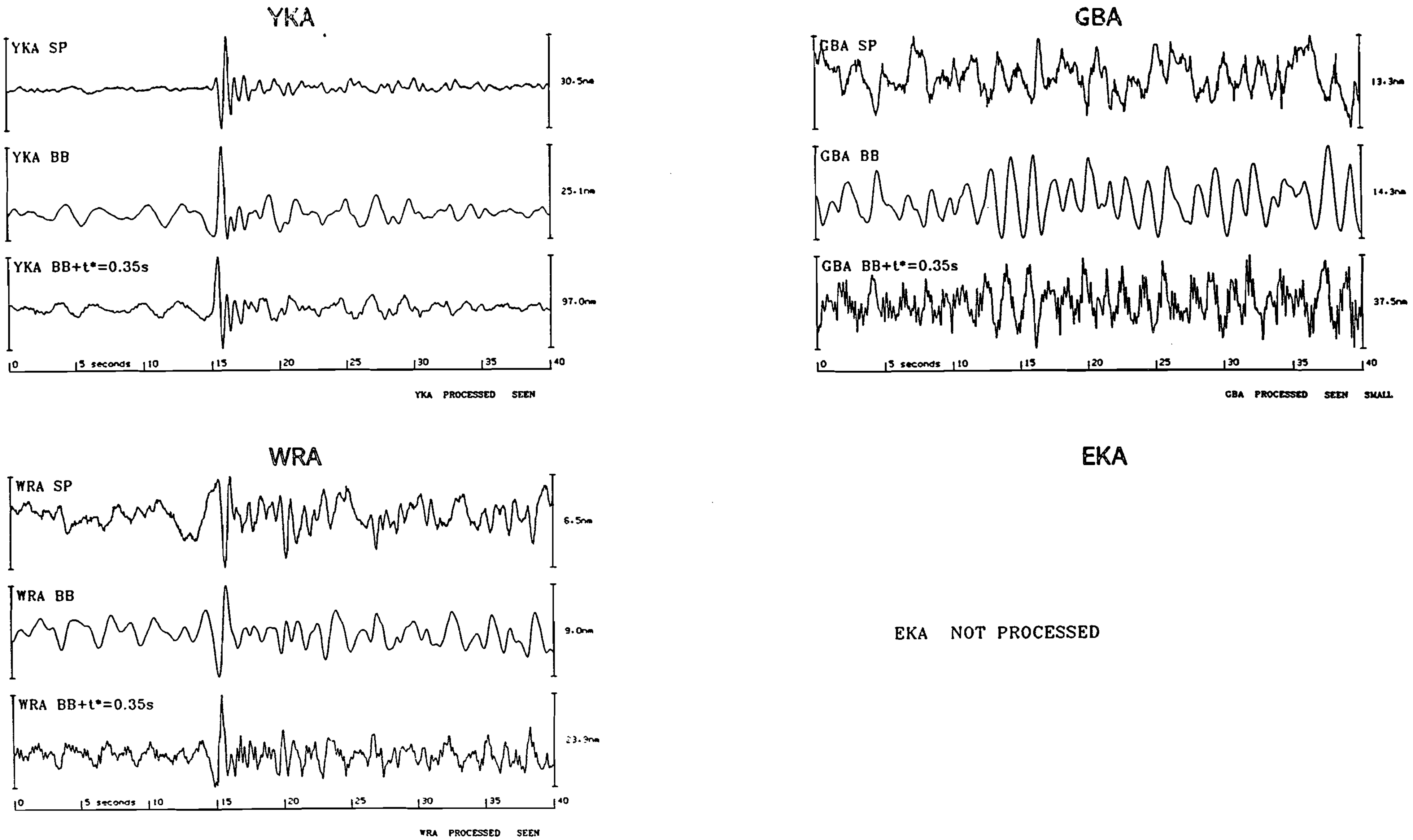

Figure A20 Short period, broad band and deconvolved P seismograms from the Mururoa explosion of 18 June 1979.

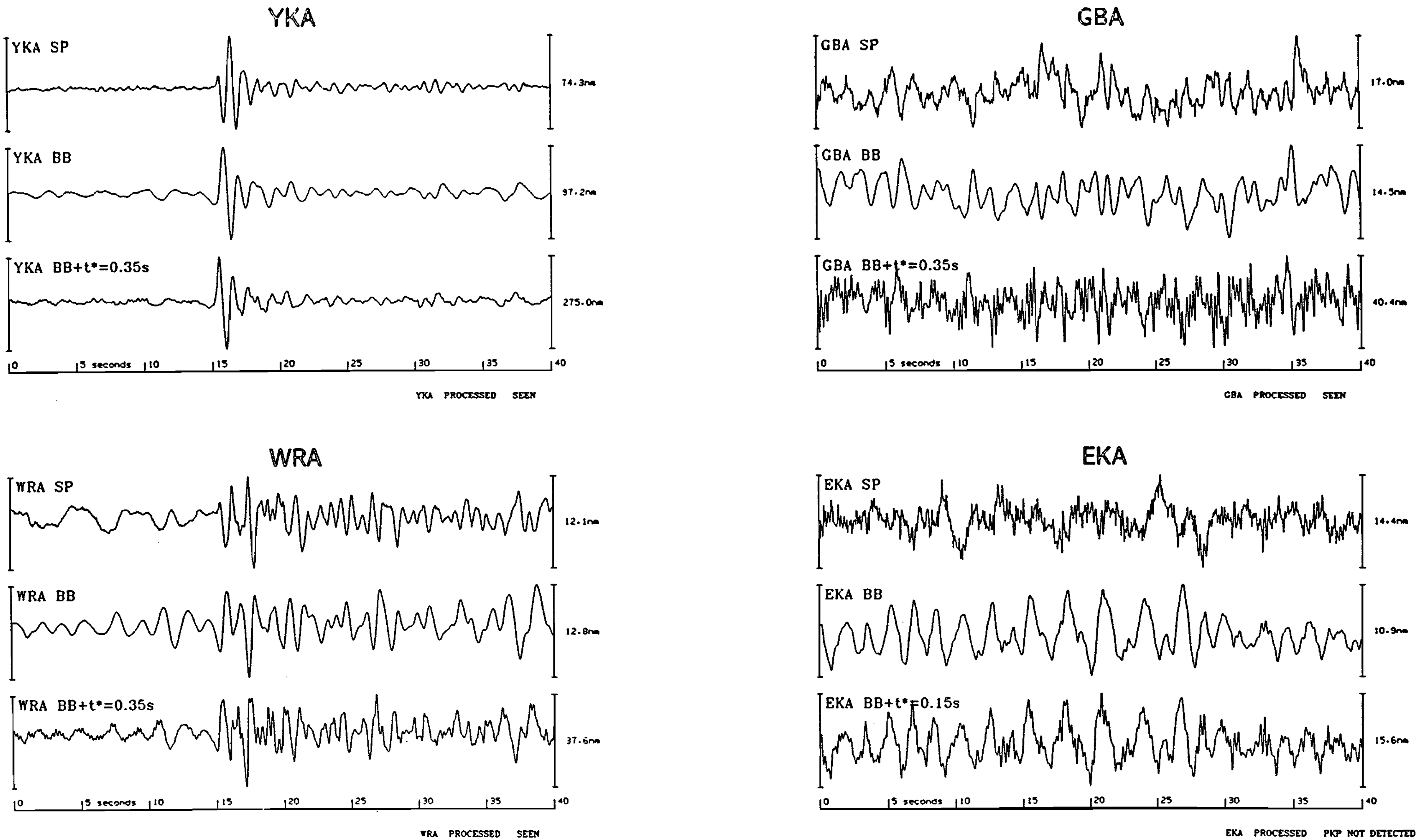

Figure A21 Short period, broad band and deconvolved P seismograms from the Mururoa explosion of 29 June 1979.

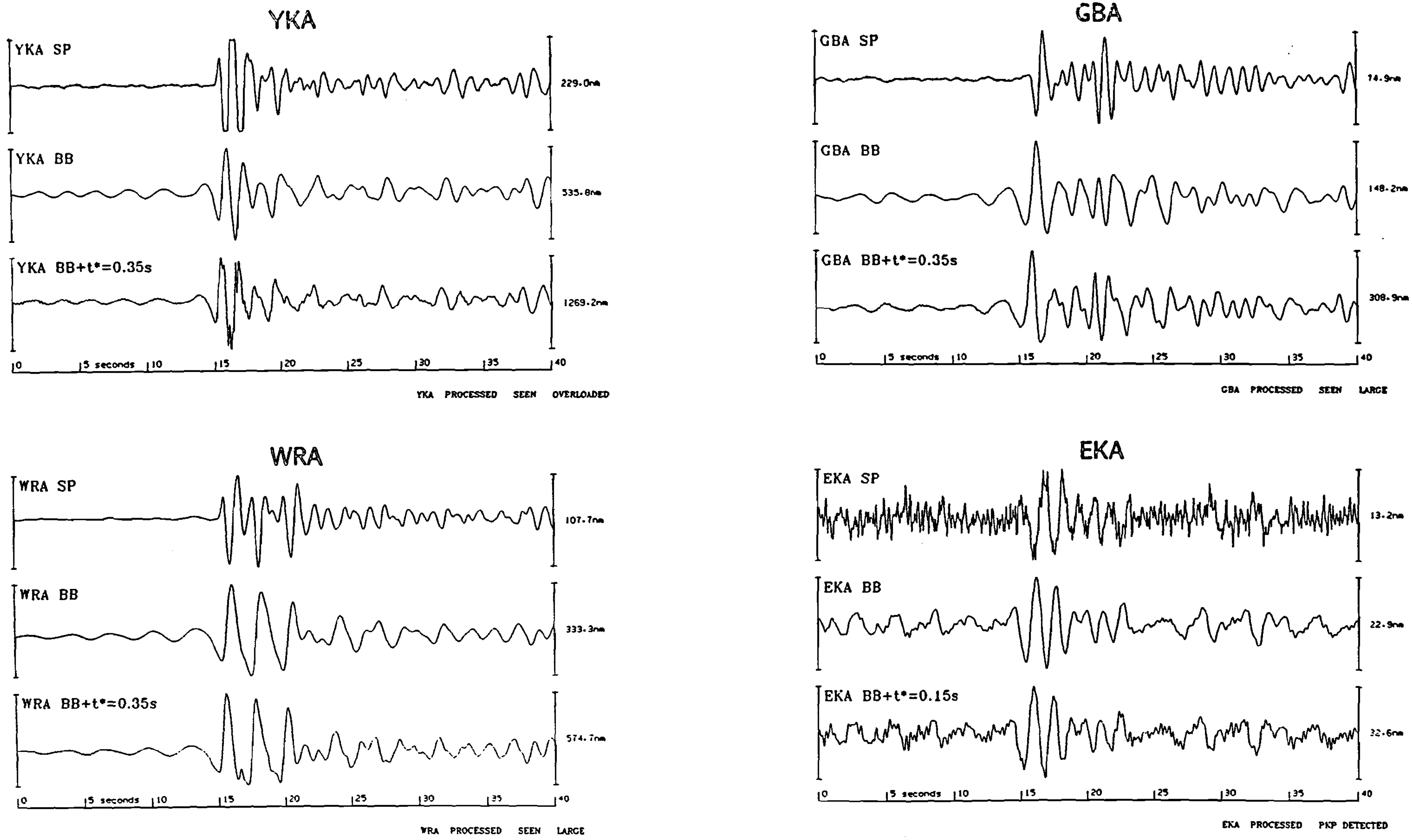

Figure A22 Short period, broad band and deconvolved P seismograms from the Mururoa explosion of 25 July 1979.

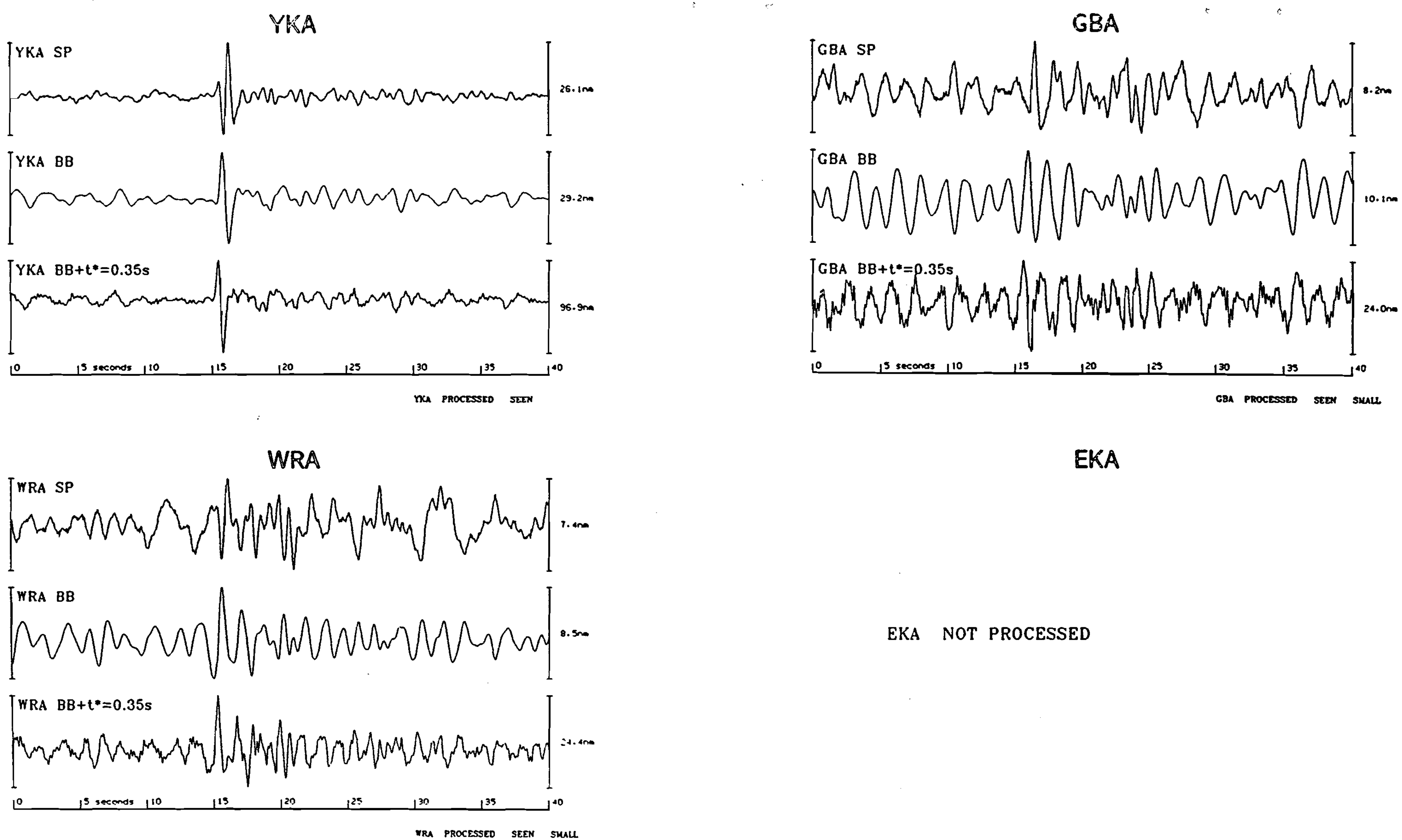

Figure A23 Short period, broad band and deconvolved P seismograms from the Mururoa explosion of 28 July 1979.

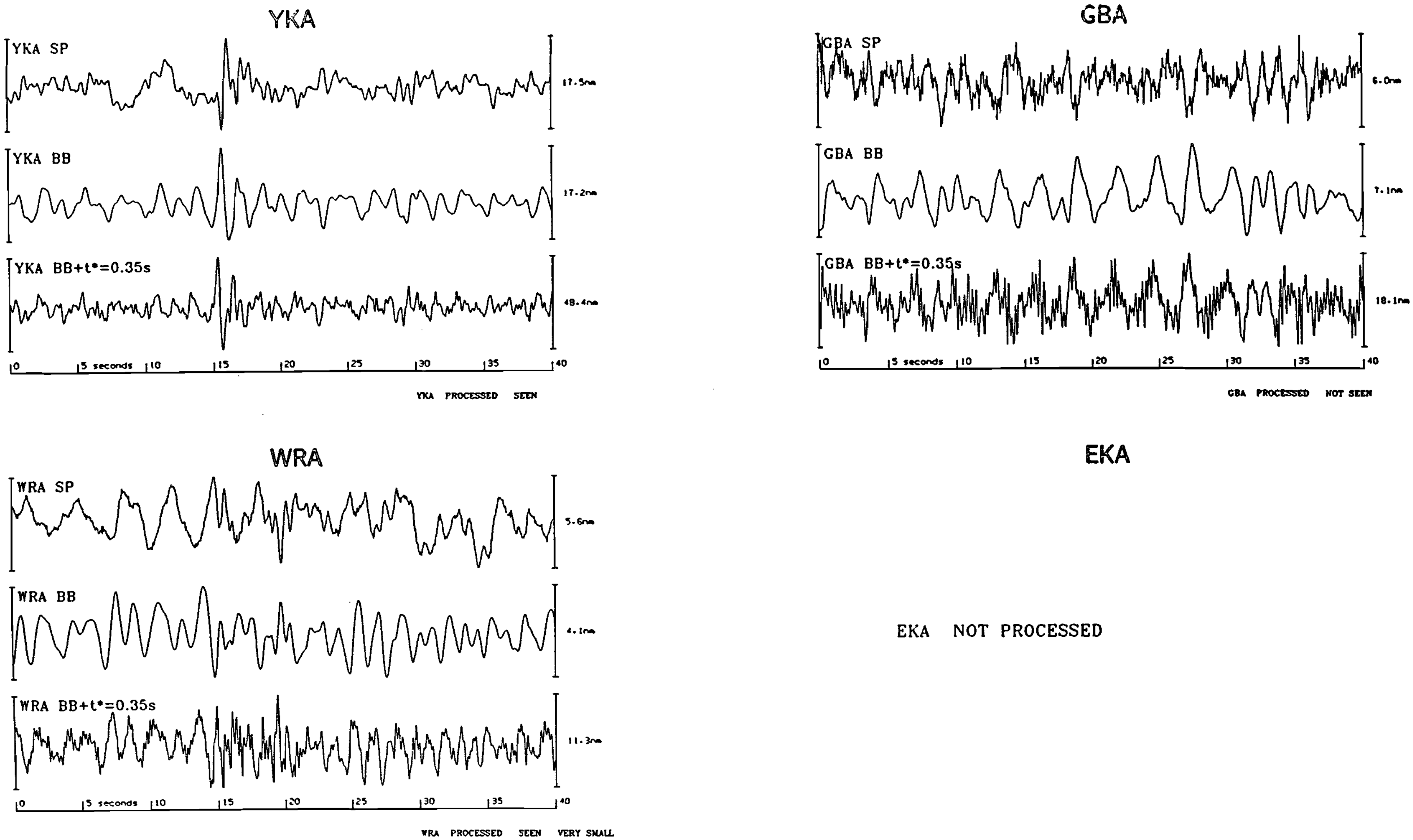

Figure A24 Short period, broad band and deconvolved P seismograms from the Mururoa explosion of 22 November 1979.

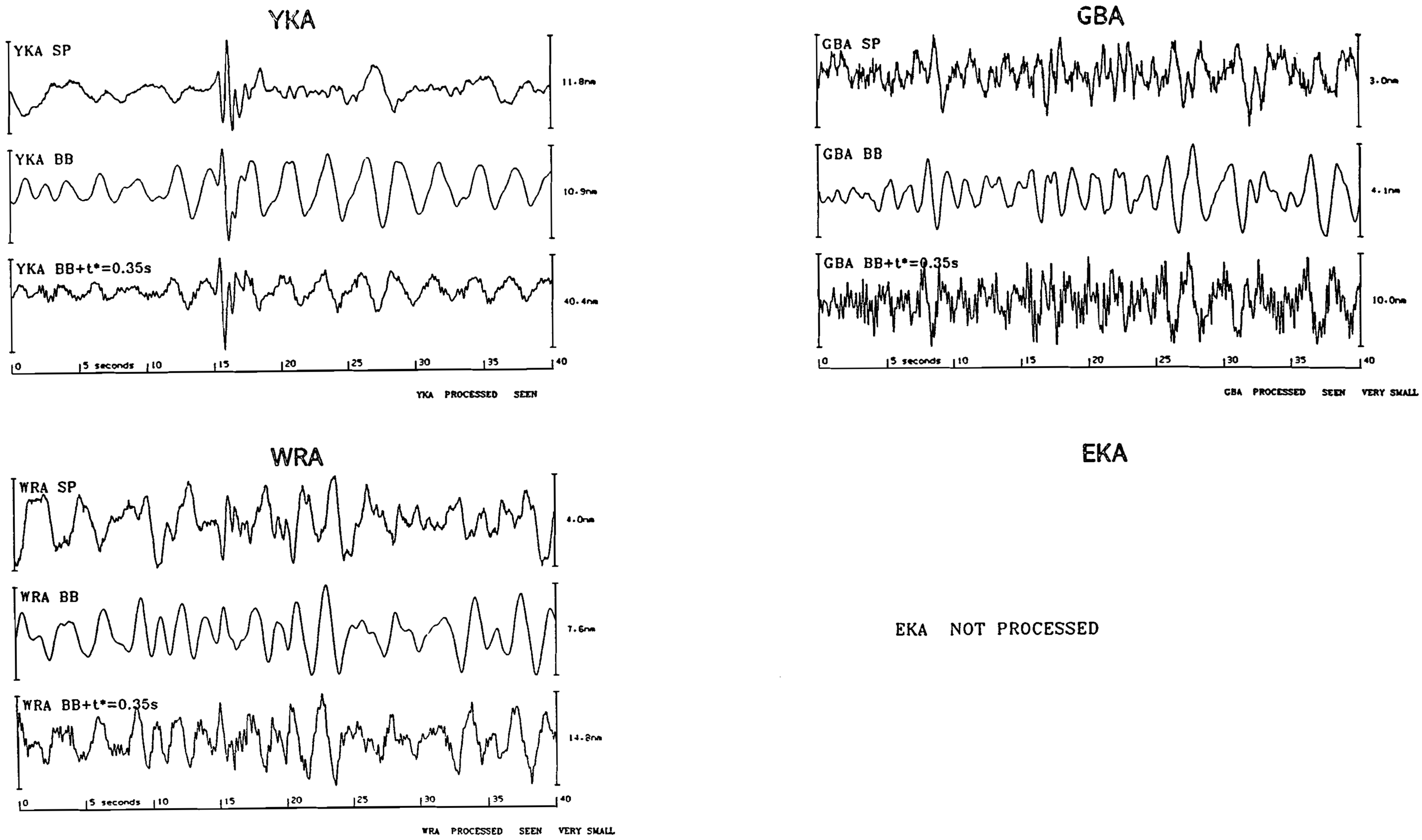

Figure A25 Short period, broad band and deconvolved P seismograms from the Mururoa explosion of 23 February 1980.

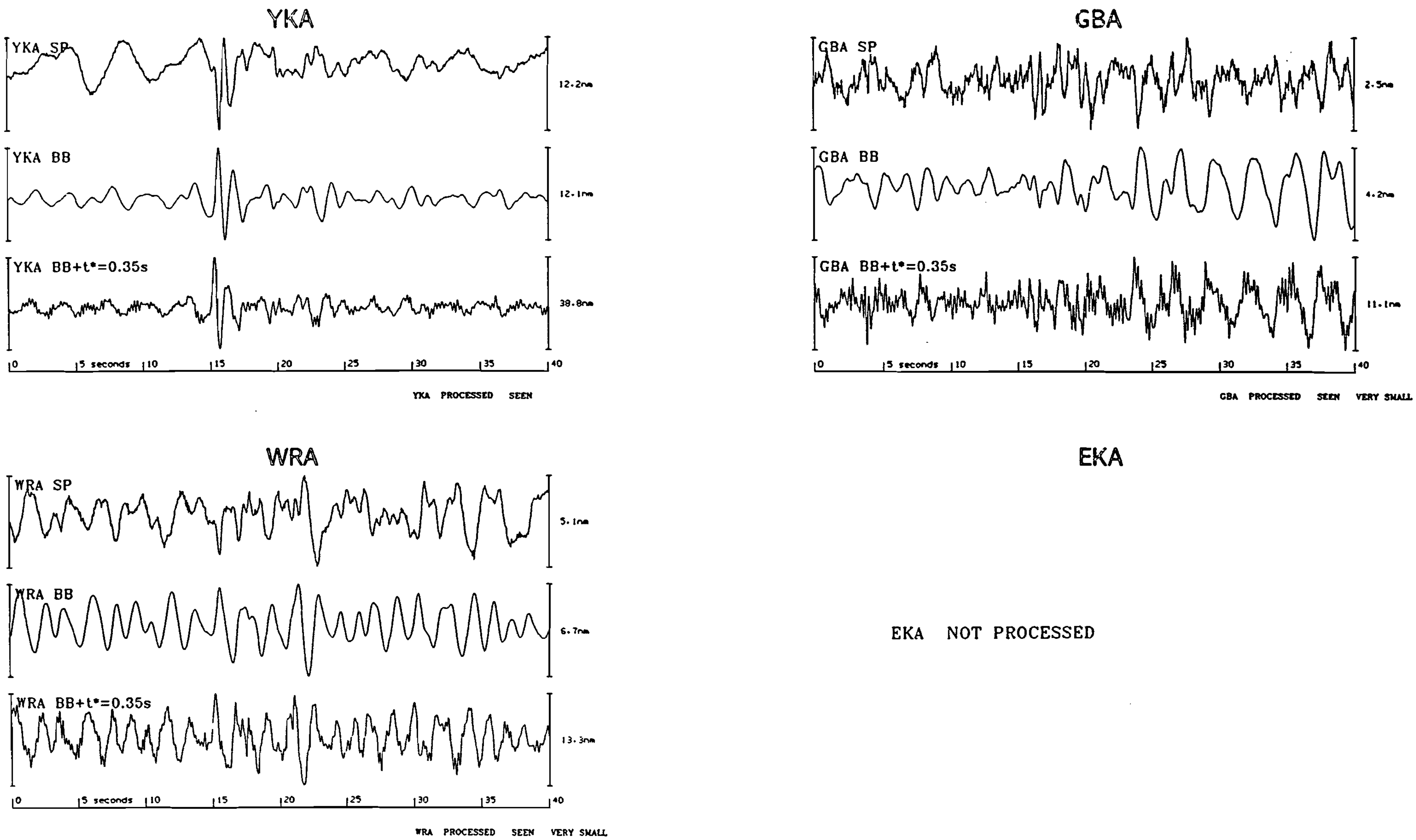

Figure A26 Short period, broad band and deconvolved P seismograms from the Mururoa explosion of 3 March 1980.

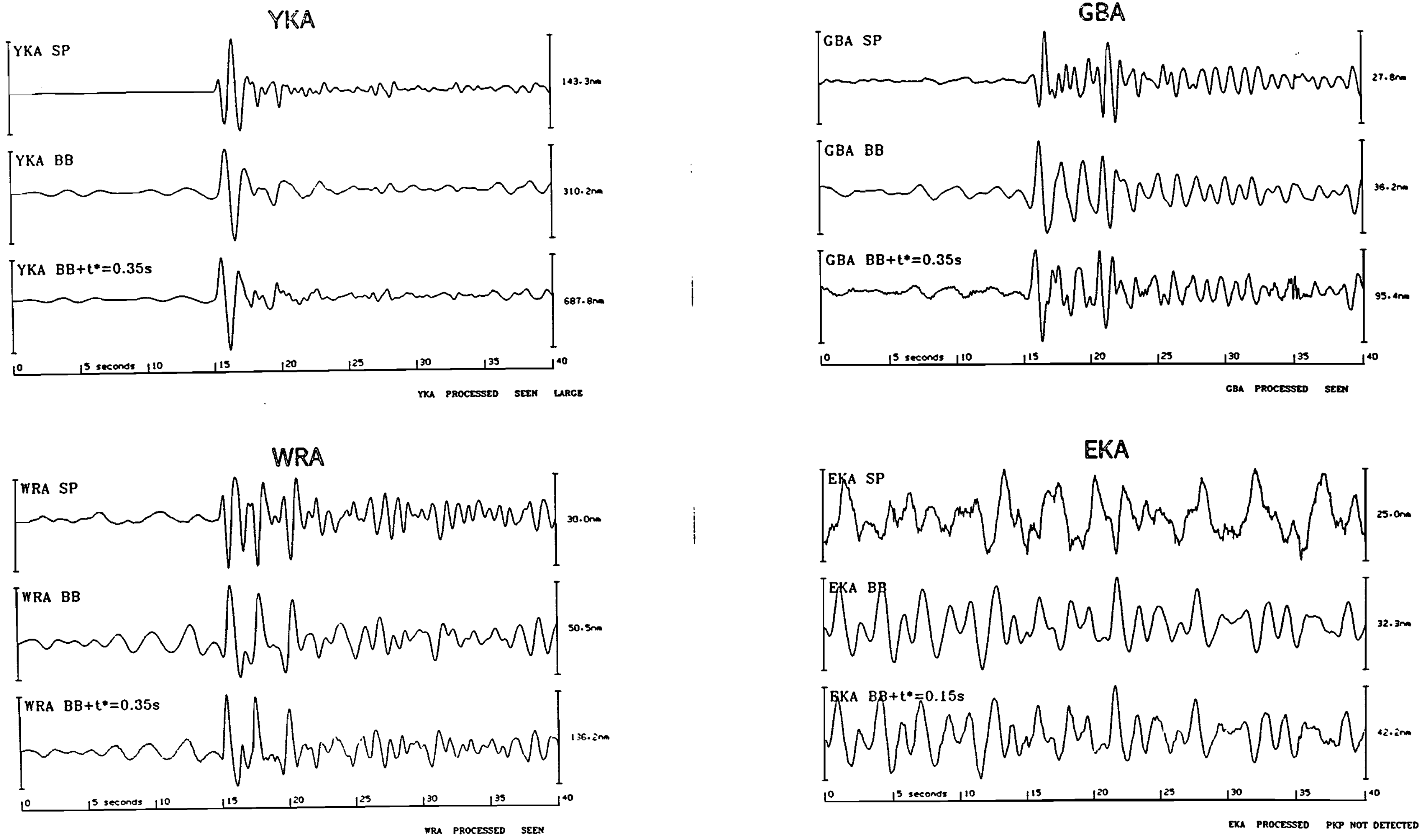

Figure A27 Short period, broad band and deconvolved P seismograms from the Mururoa explosion of 23 March 1980.

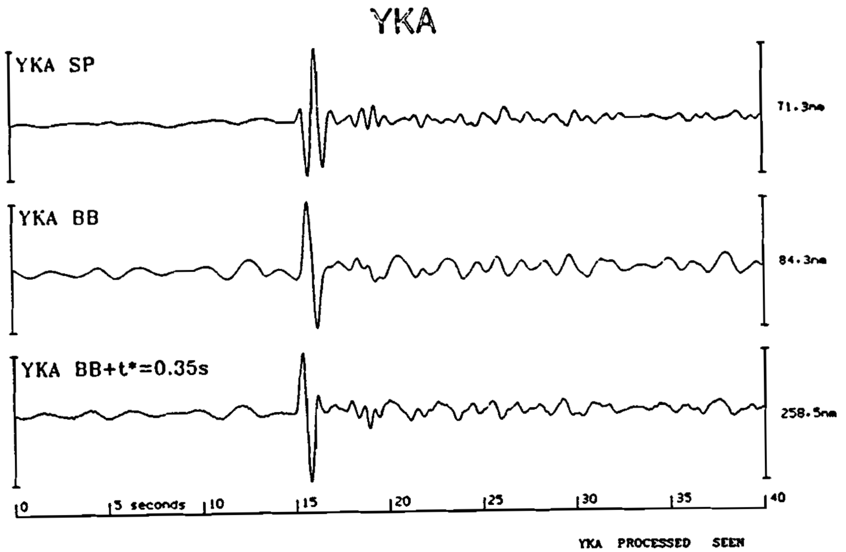

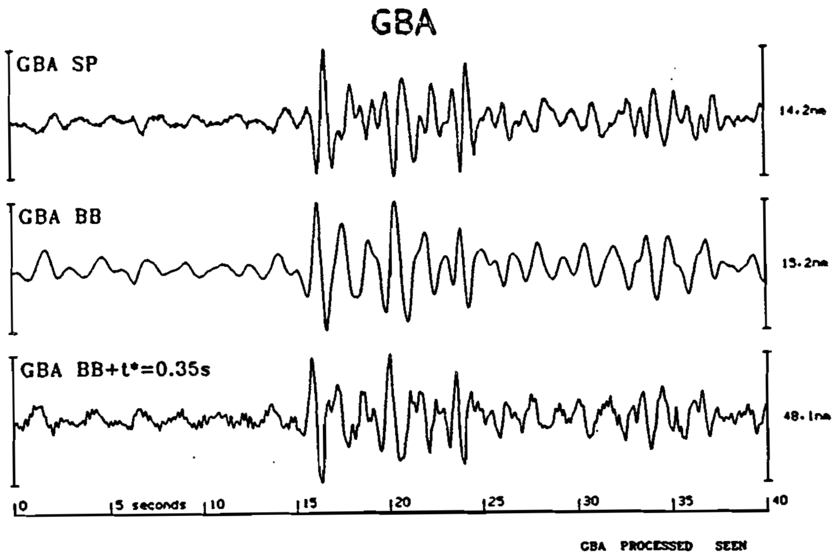

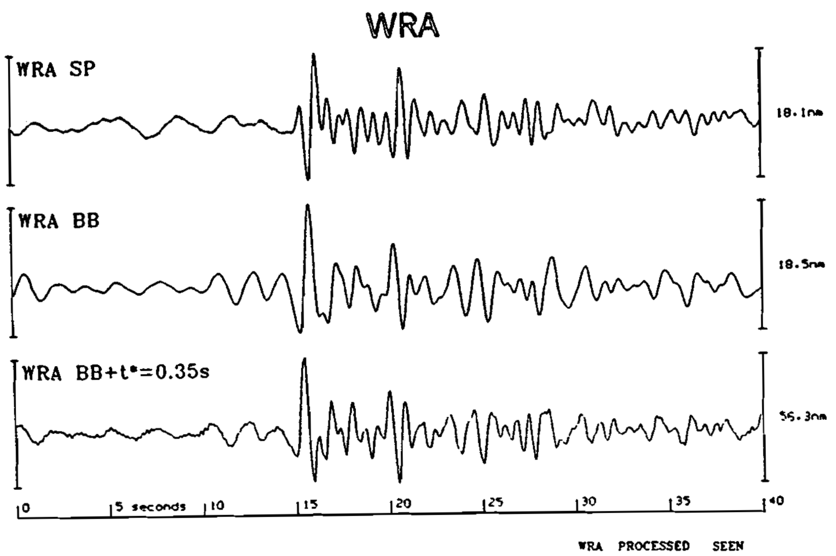

EKA

EKA NOT PROCESSED

Figure A28 Short period, broad band and deconvolved P seismograms from the Mururoa explosion of 1 April 1980.

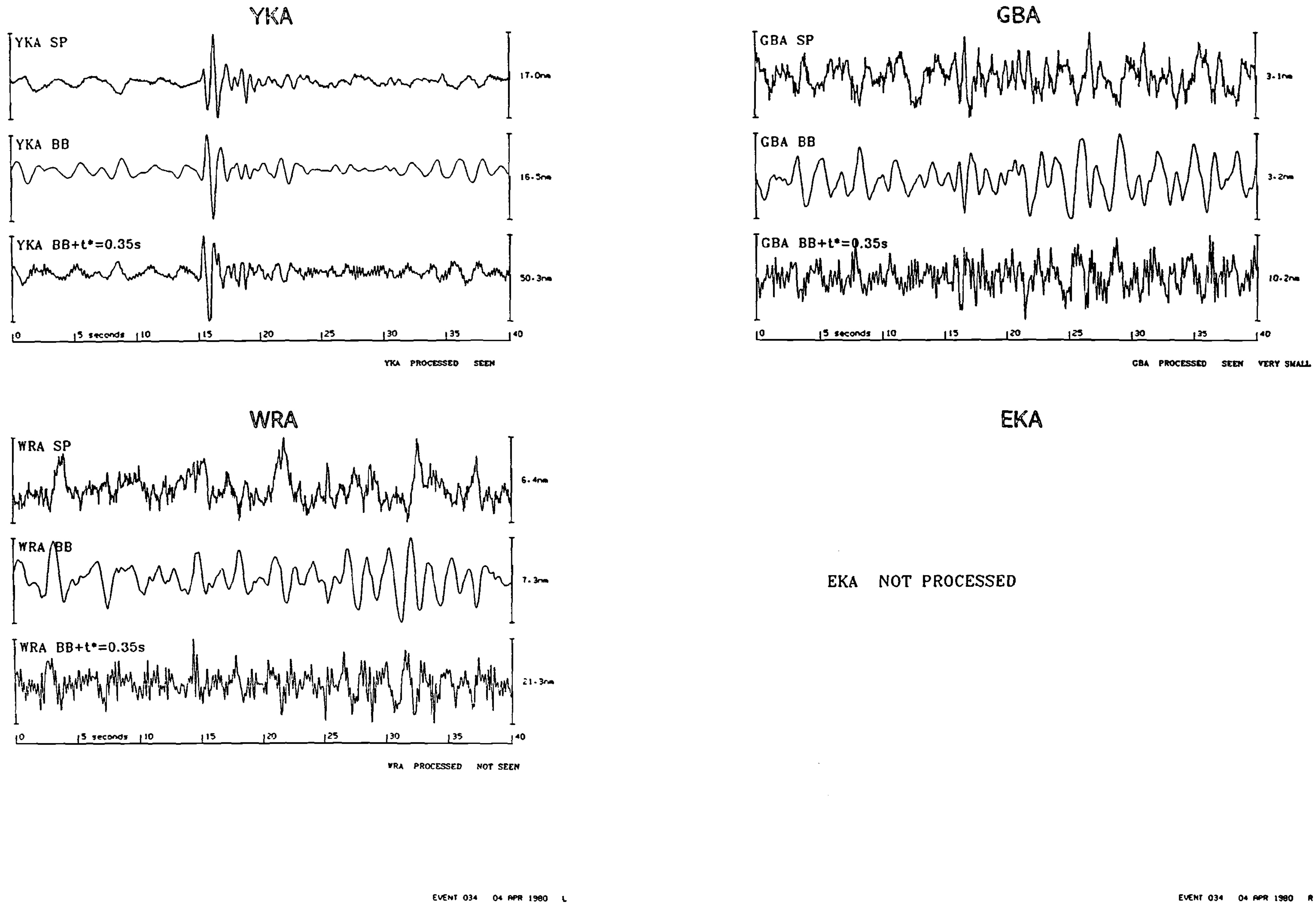

Figure A29 Short period, broad band and deconvolved P seismograms from the Mururoa explosion of 4 April 1980.

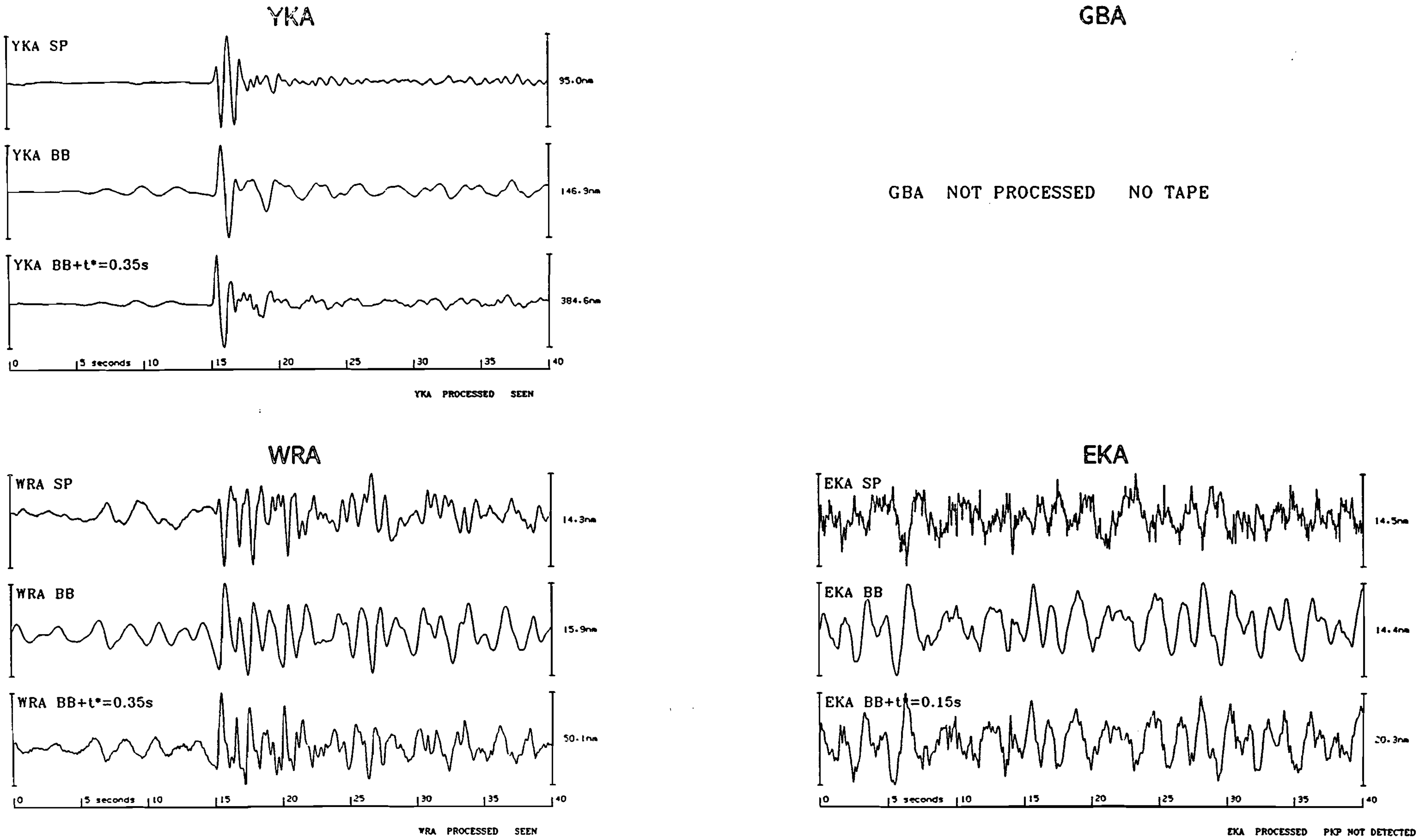

Figure A30 Short period, broad band and deconvolved P seismograms from the Mururoa explosion of 16 June 1980.

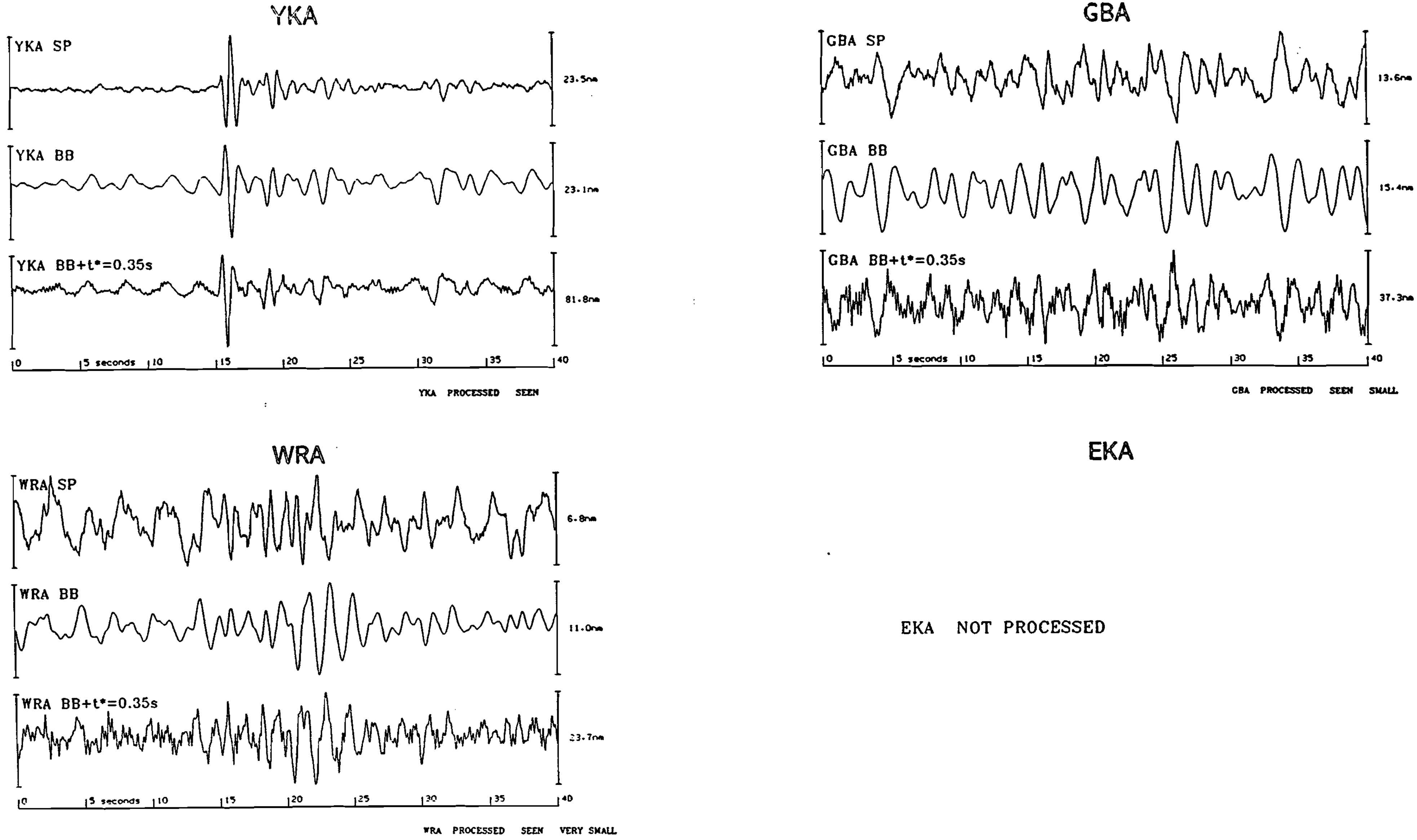

Figure A31 Short period, broad band and deconvolved P seismograms from the Mururoa explosion of 21 June 1980.

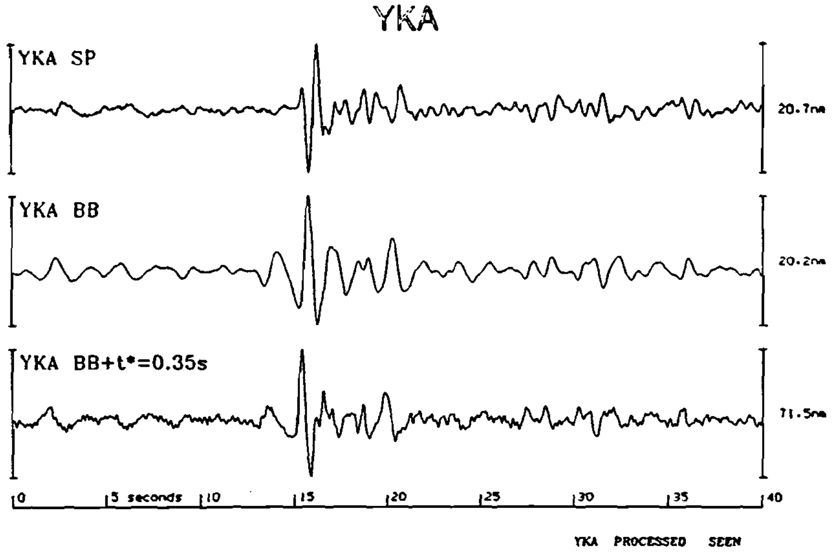

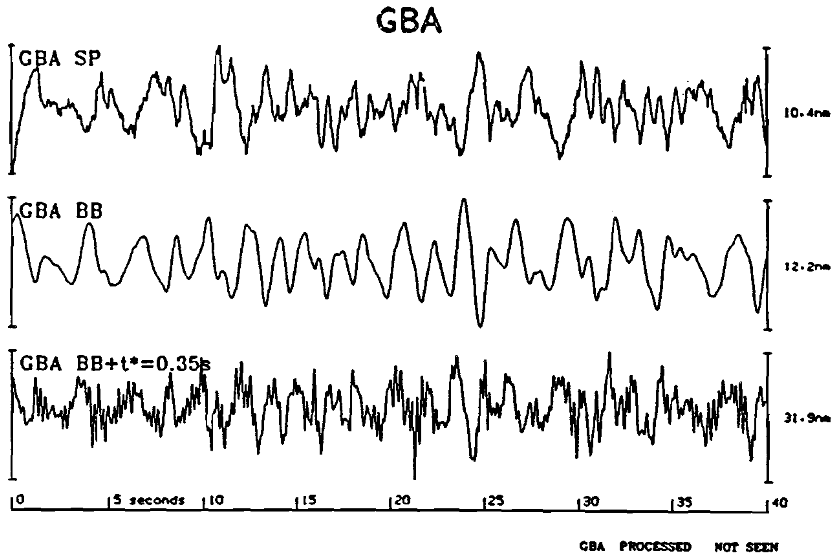

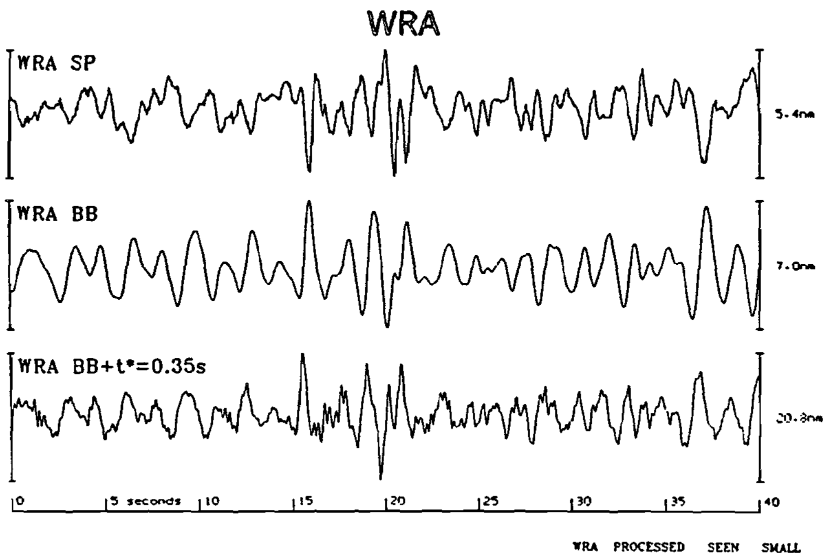

EKA

EKA NOT PROCESSED

Figure A32 Short period, broad band and deconvolved P seismograms from the Mururoa explosion of 6 July 1980.

YKA

YKA PROCESSED SEEN VBB ONLY

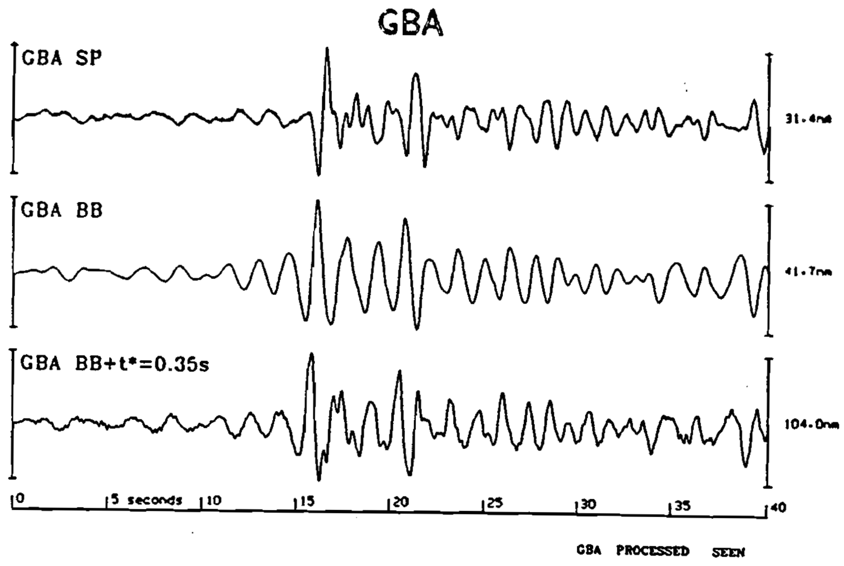

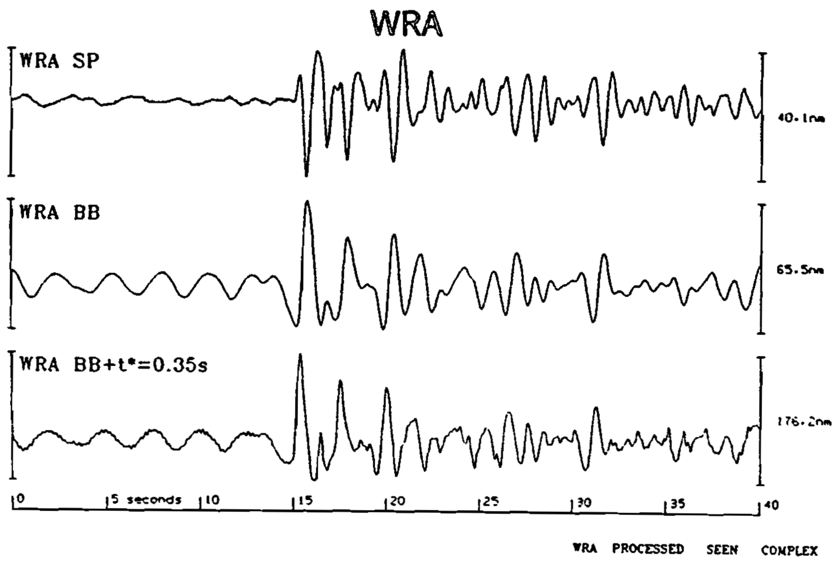

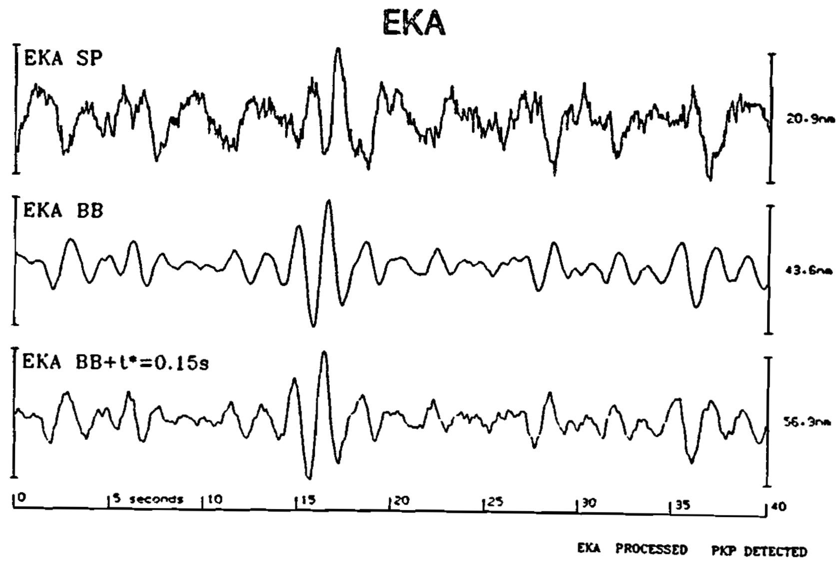

Figure A33 Short period, broad band and deconvolved P seismograms from the Mururoa explosion of 19 July 1980.

YKA

YKA NOT PROCESSED NO TAPE

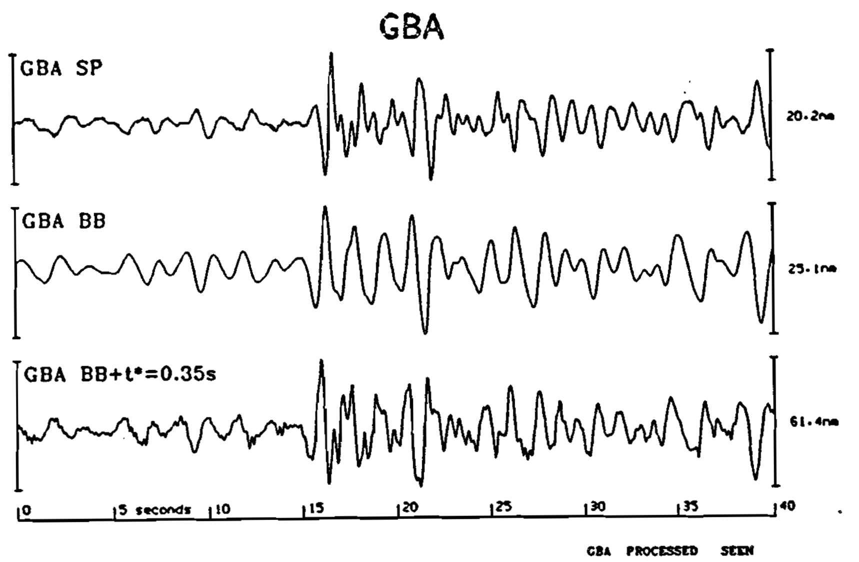

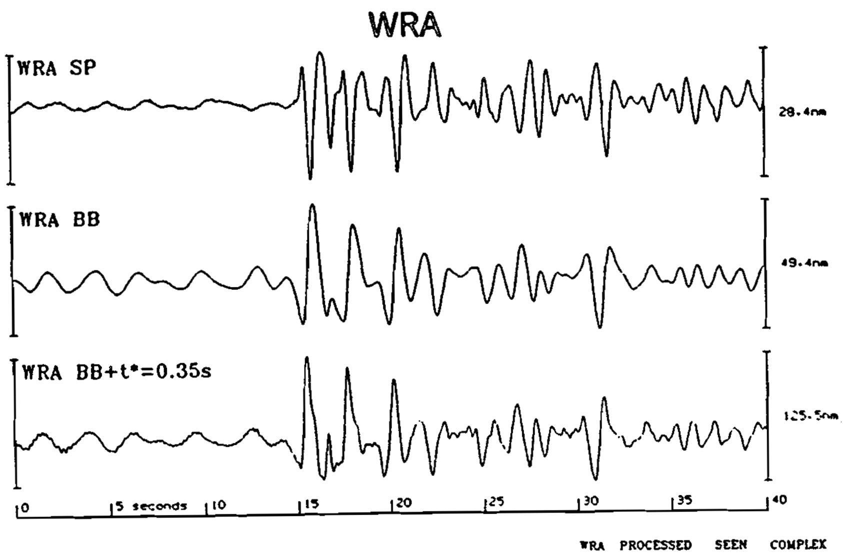

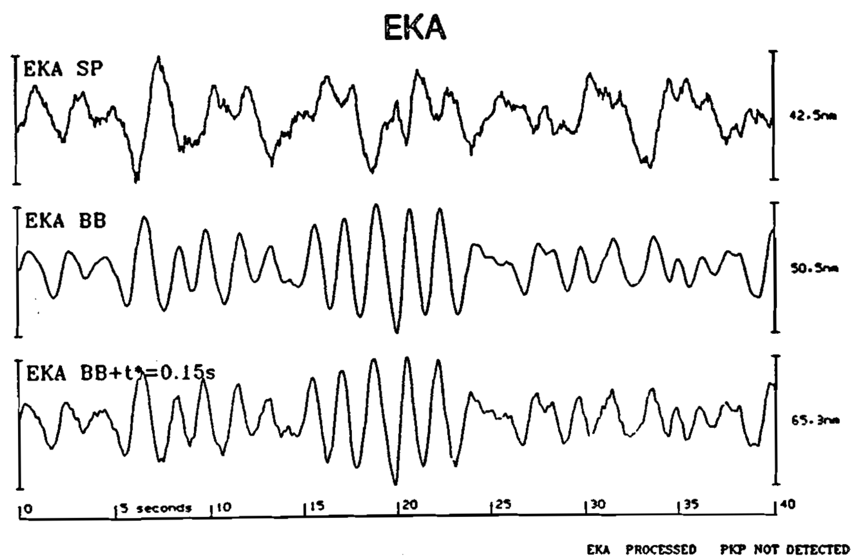

Figure A34 Short period, broad band and deconvolved P seismograms from the Mururoa explosion of 3 December 1980.

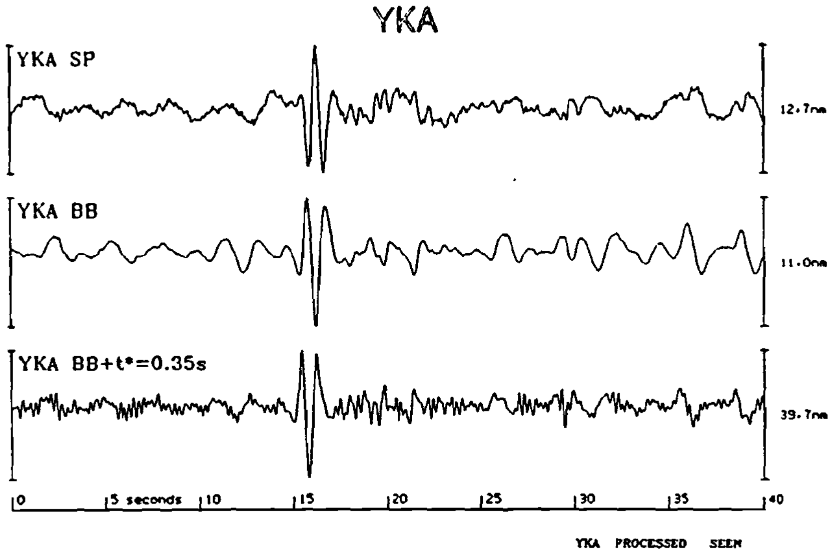

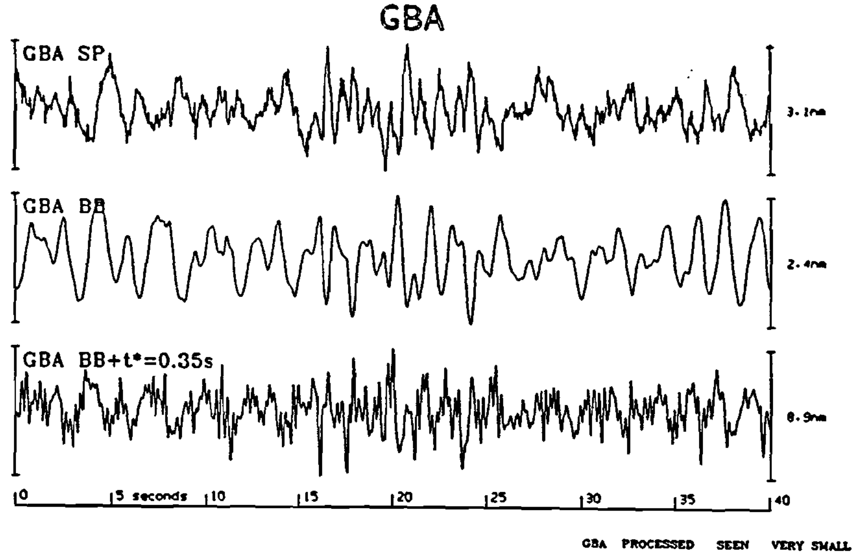

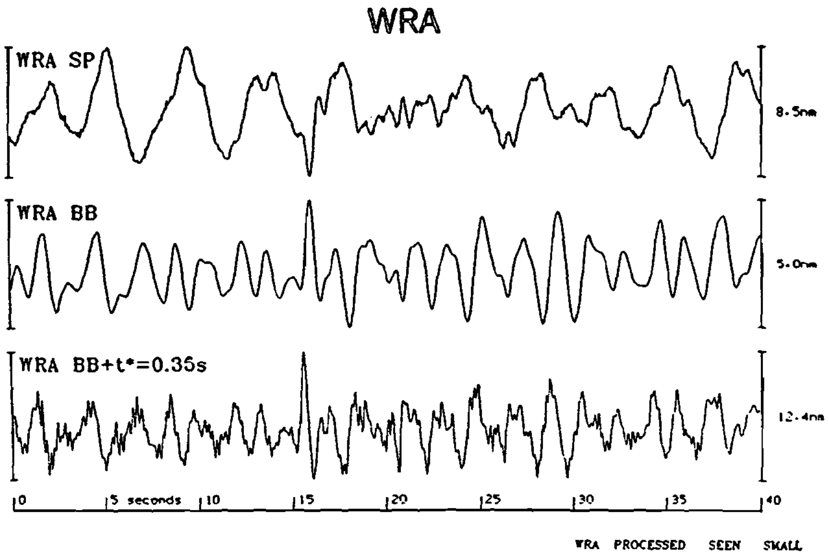

EKA

EKA NOT PROCESSED

Figure A35 Short period, broad band and deconvolved P seismograms from the Mururoa explosion of 27 February 1981.

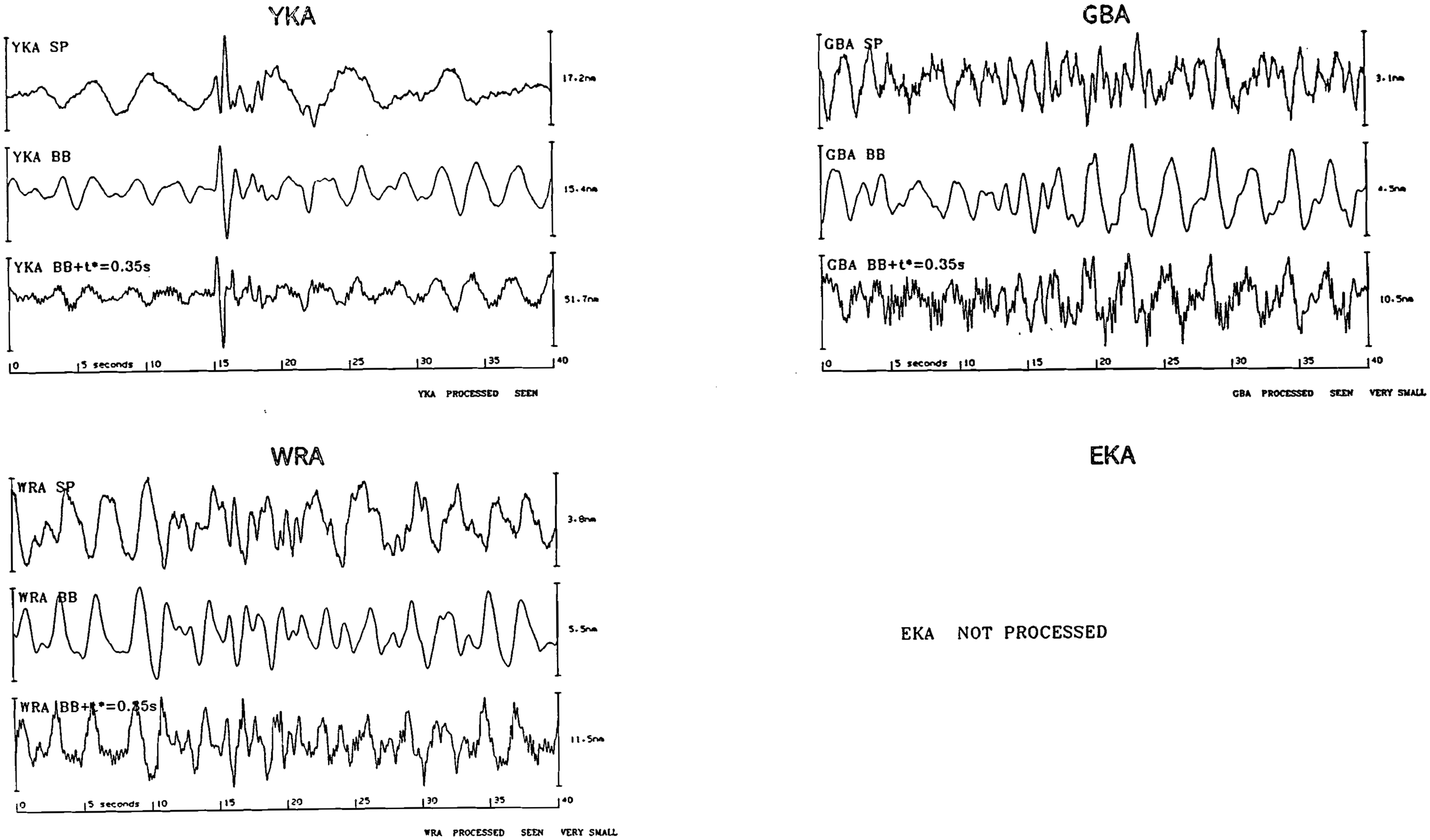

Figure A36 Short period, broad band and deconvolved P seismograms from the Mururoa explosion of 6 March 1981.

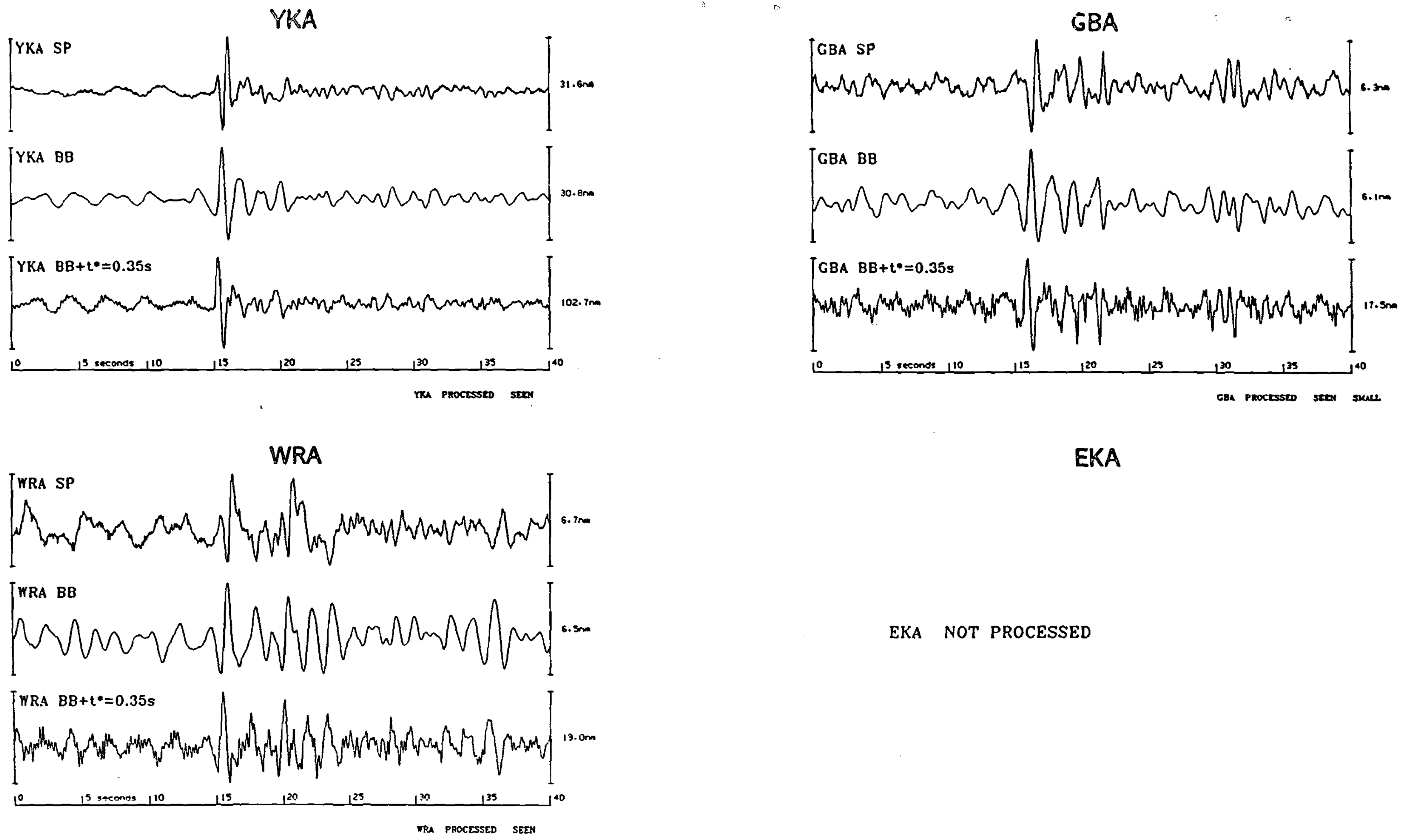

Figure A37 Short period, broad band and deconvolved P seismograms from the Mururoa explosion of 28 March 1981.

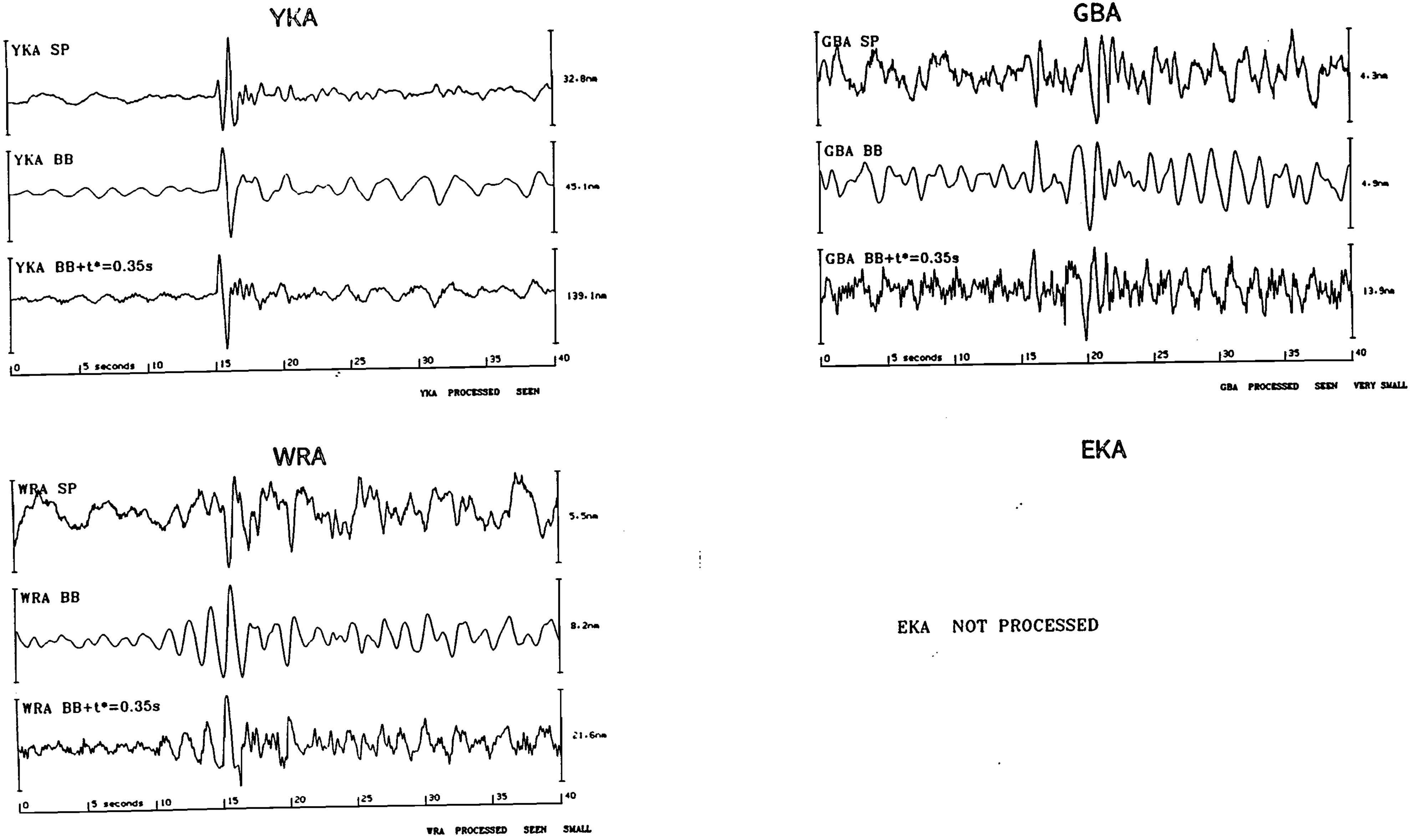

Figure A38 Short period, broad band and deconvolved P seismograms from the Mururoa explosion of 10 April 1981.

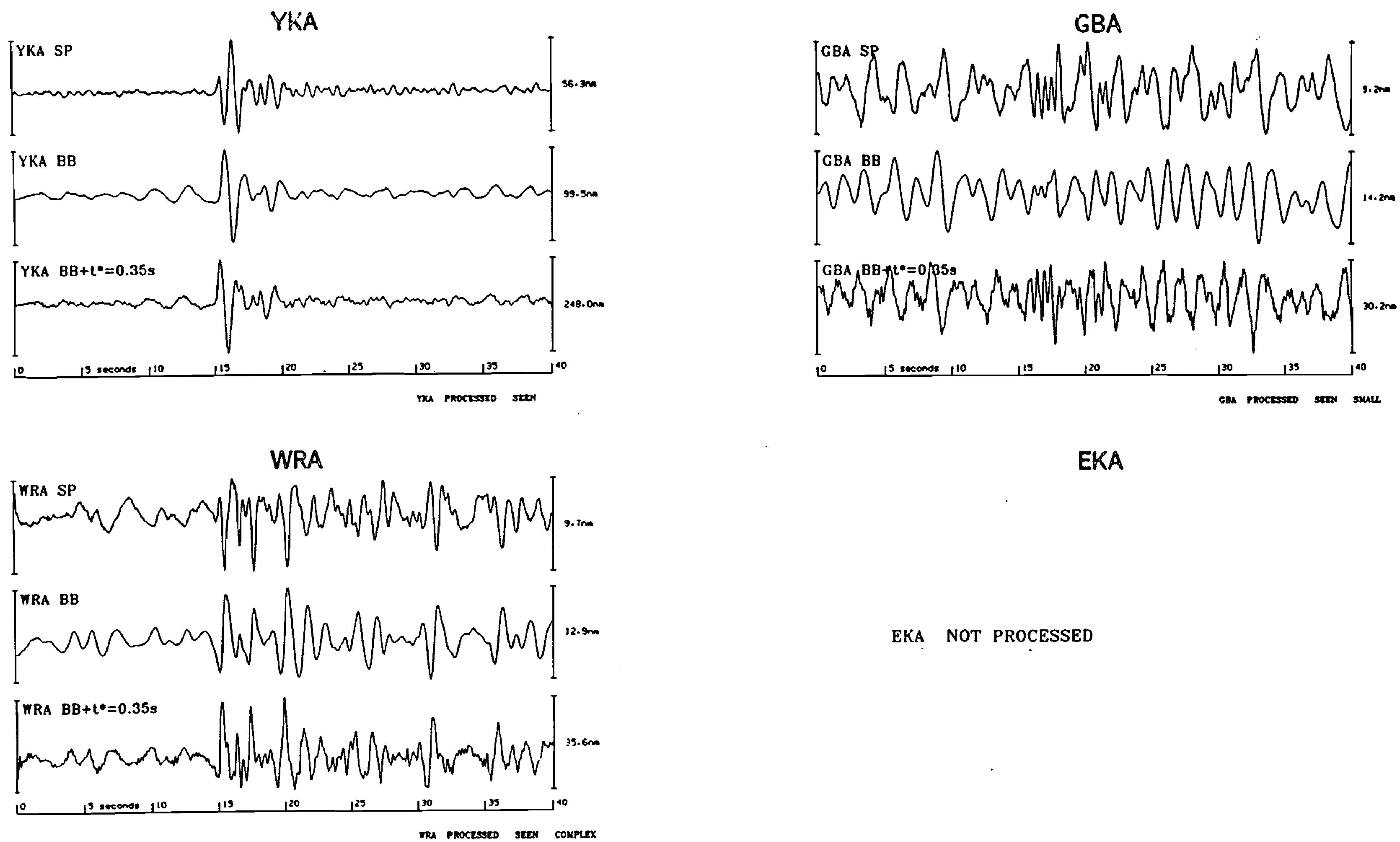

Figure A39 Short period, broad band and deconvolved P seismograms from the Mururoa explosion of 8 July 1981.

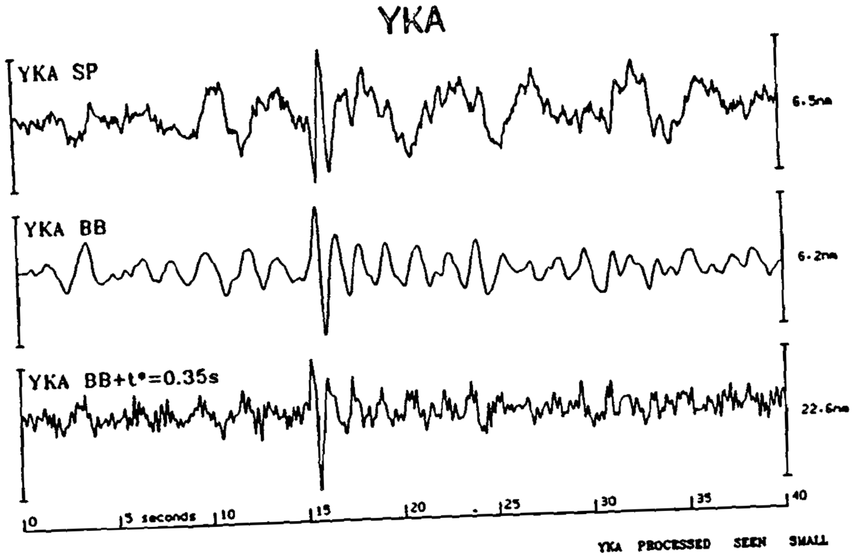

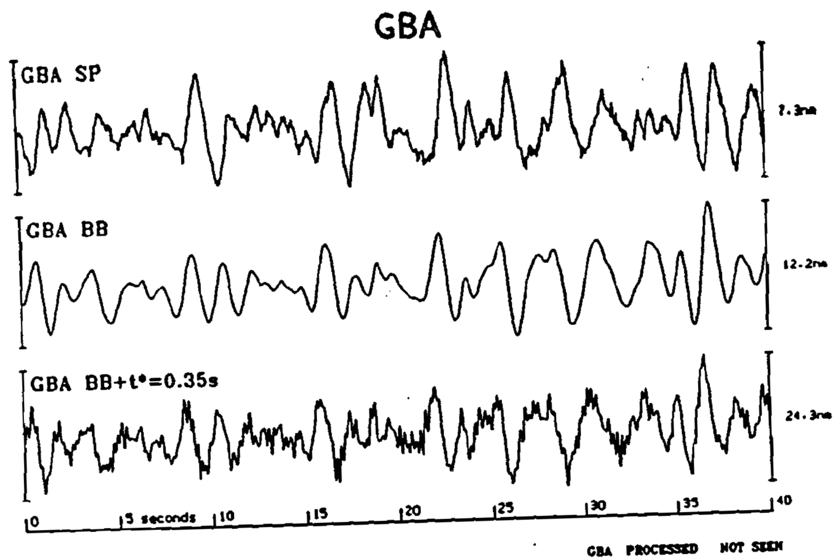

WRA

WRA NOT PROCESSED NO TAPE

EKA

EKA NOT PROCESSED

Figure A40 Short period, broad band and deconvolved P seismograms from the Mururoa explosion of 11 July 1981.

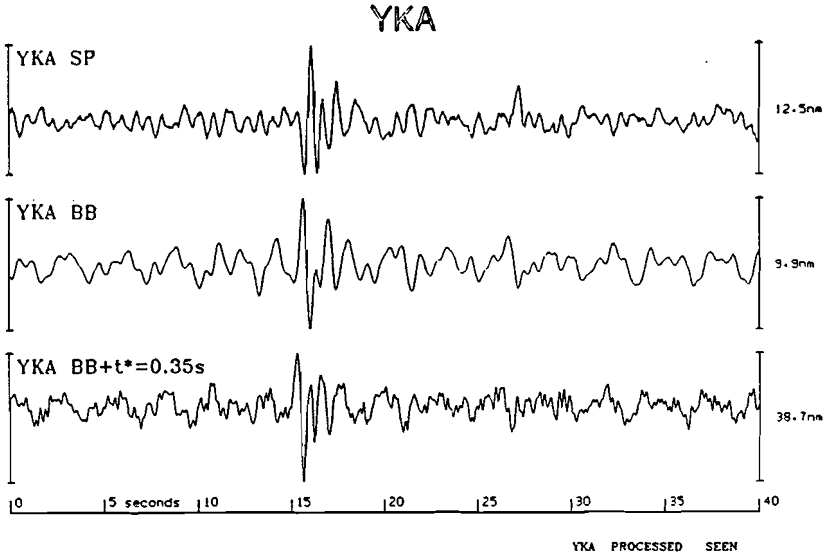

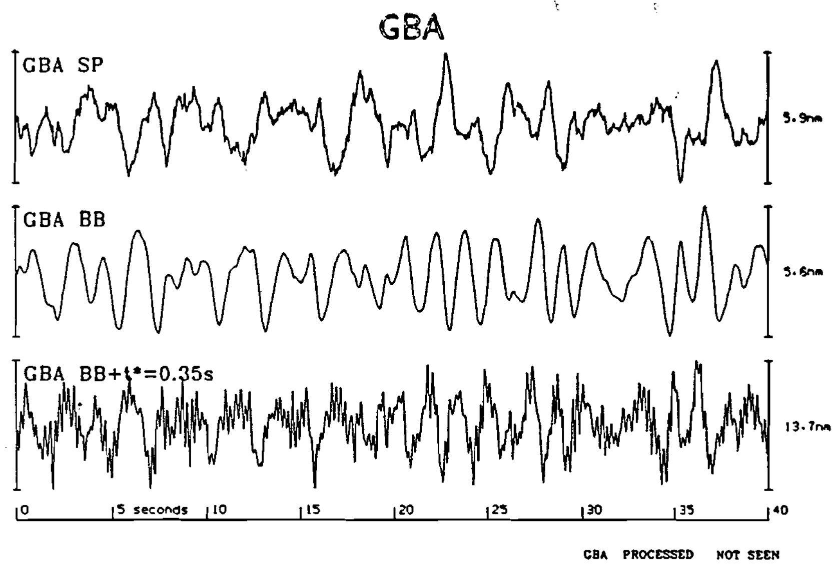

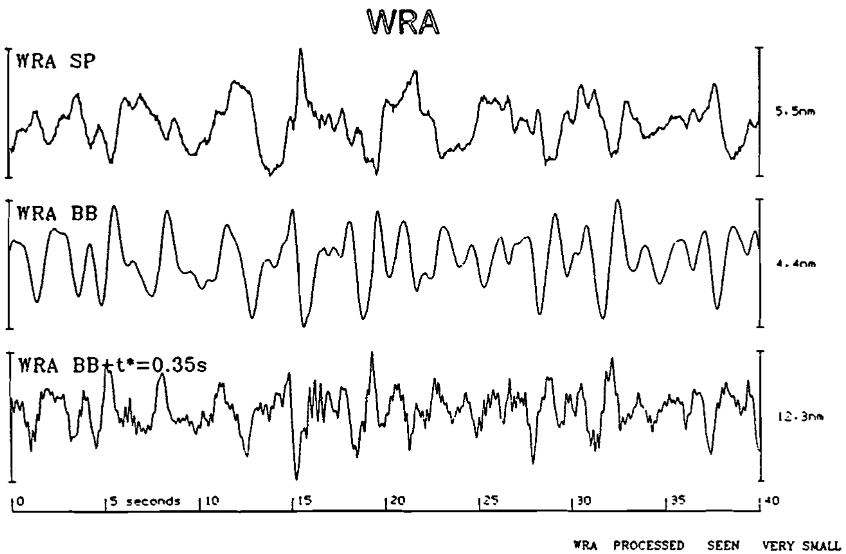

EKA

EKA NOT PROCESSED

Figure A41 Short period, broad band and deconvolved P seismograms from the Mururoa explosion of 18 July 1981.

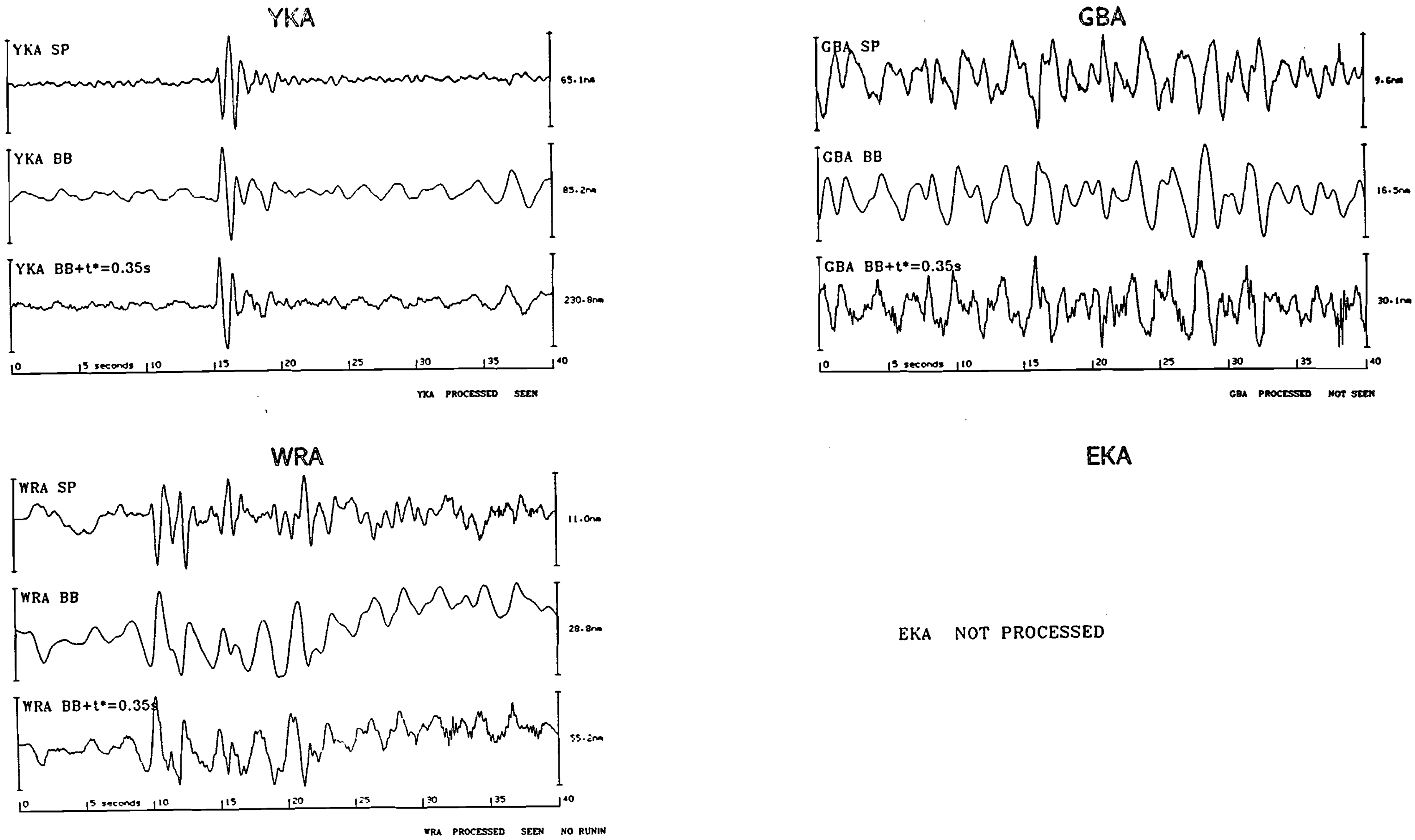

Figure A42 Short period, broad band and deconvolved P seismograms from the Mururoa explosion of 3 August 1981.

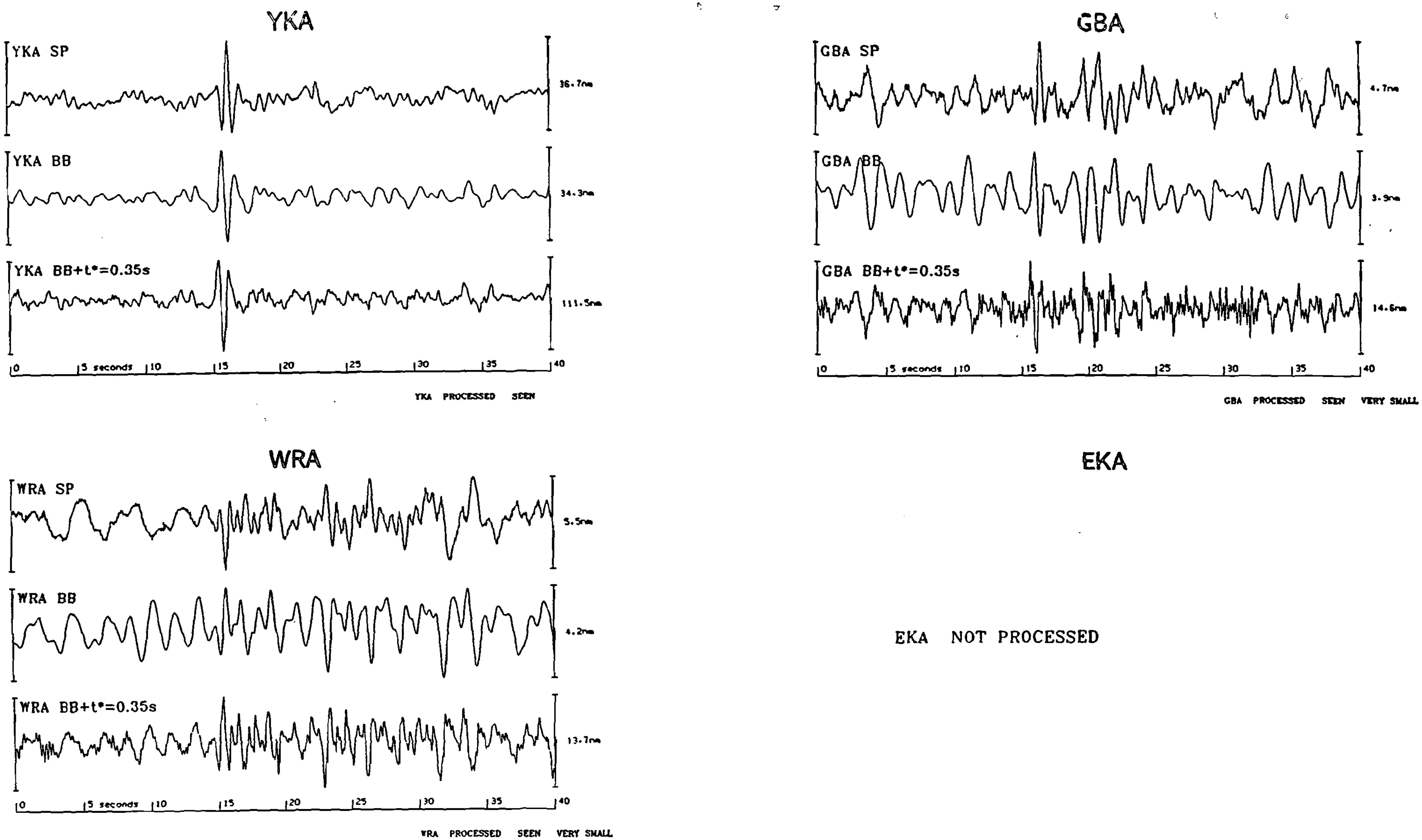

Figure A43 Short period, broad band and deconvolved P seismograms from the Mururoa explosion of 11 November 1981.

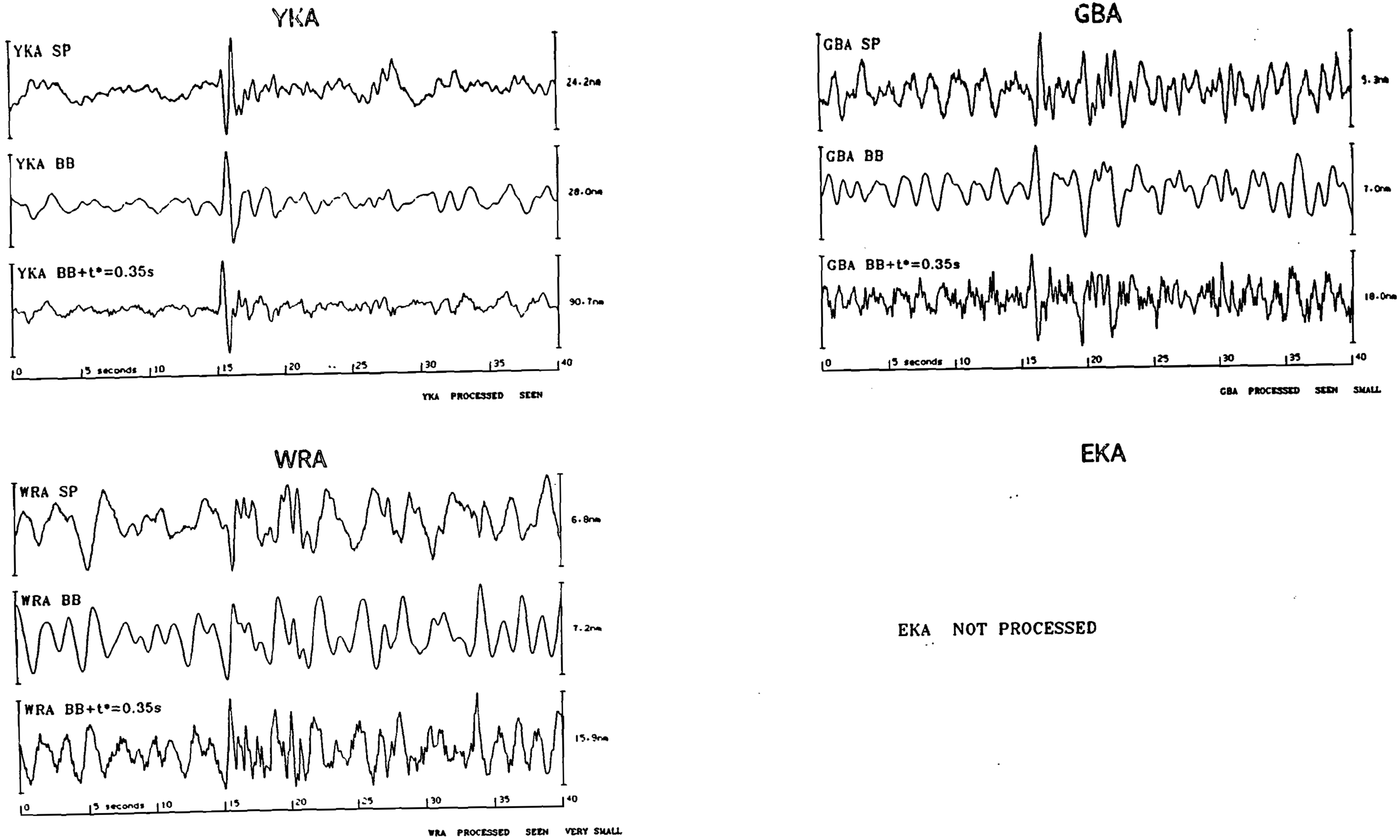

Figure A44 Short period, broad band and deconvolved P seismograms from the Mururoa explosion of 5 December 1981.

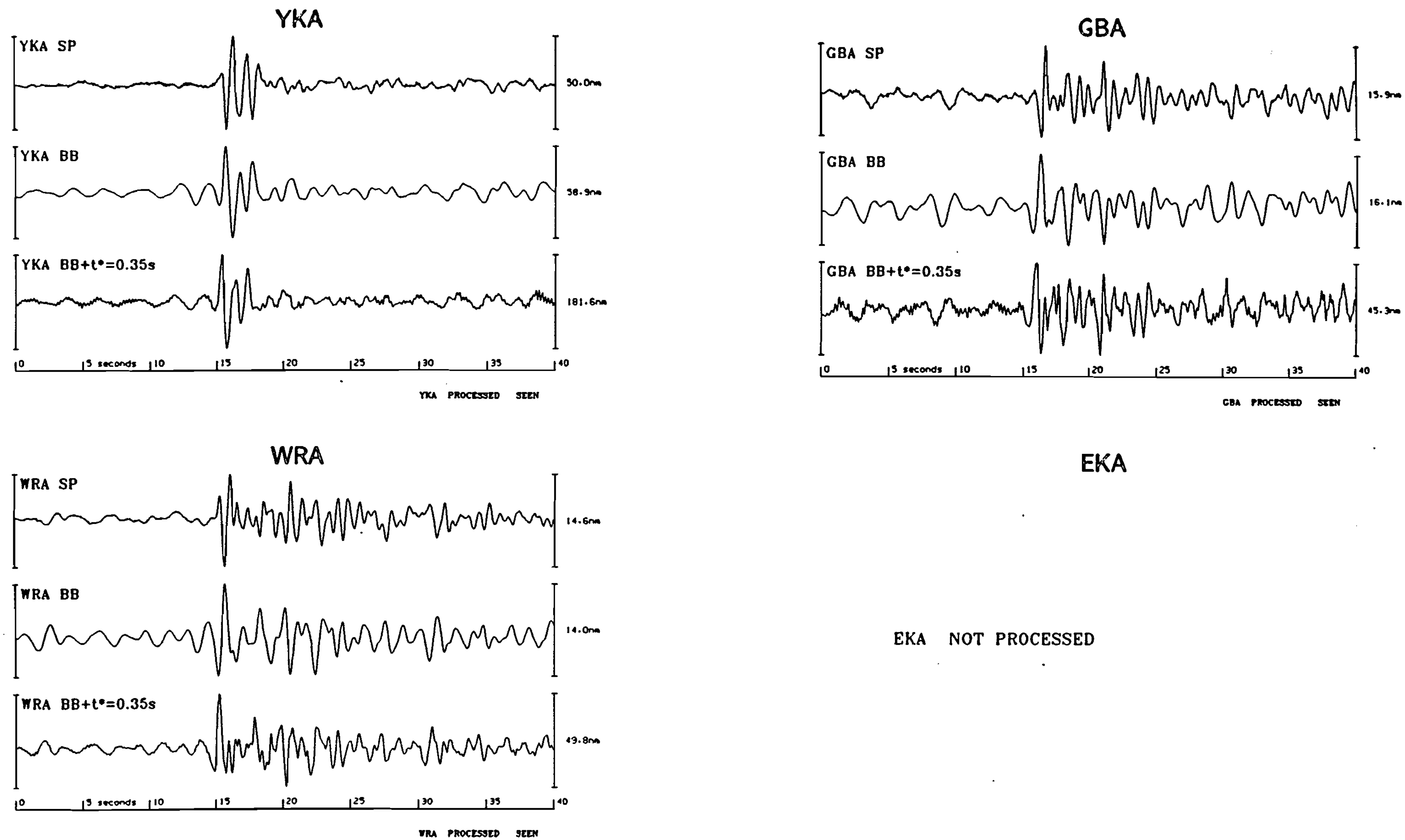

Figure A45 Short period, broad band and deconvolved P seismograms from the Mururoa explosion of 8 December 1981.

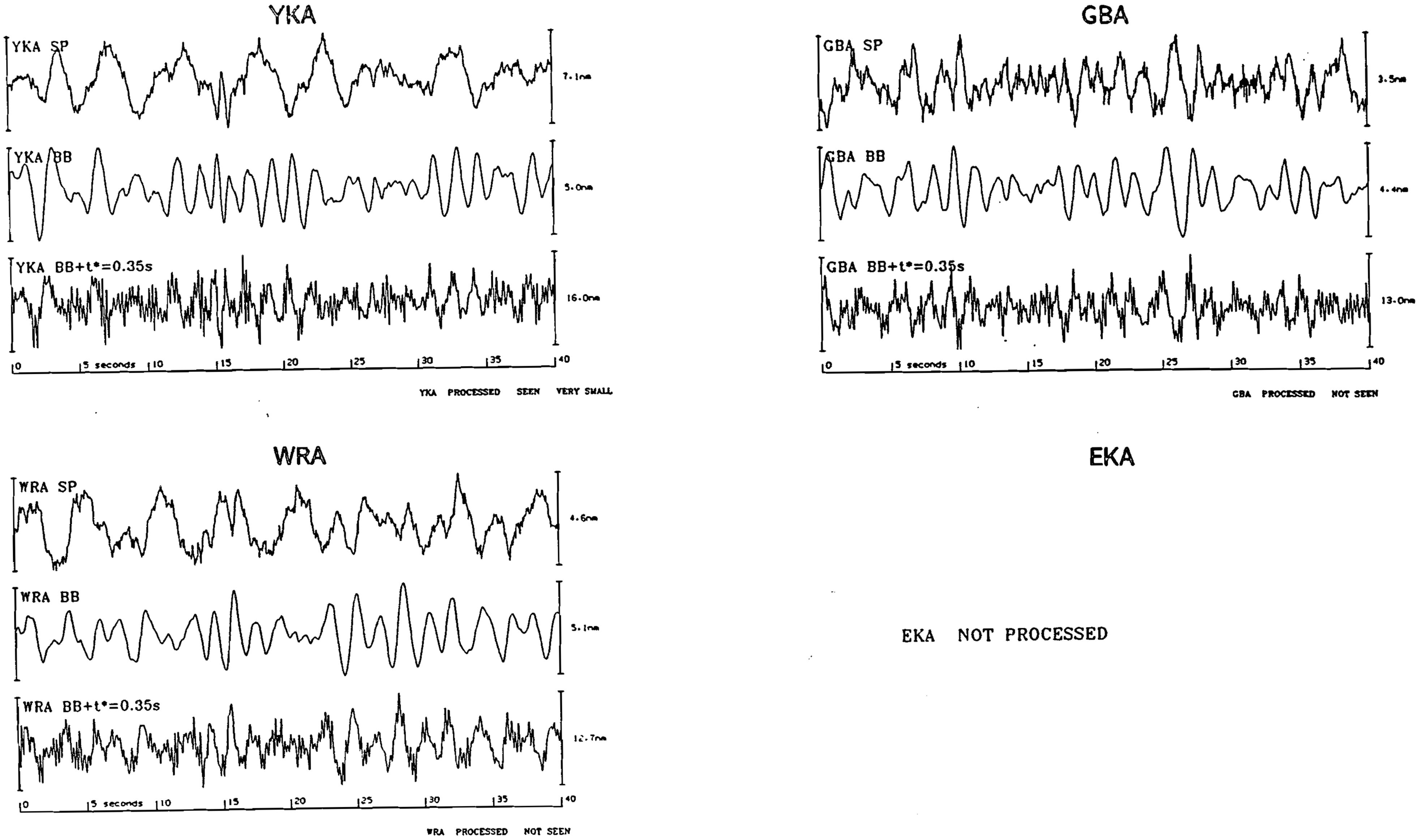

Figure A46 Short period, broad band and deconvolved P seismograms from the Mururoa explosion of 20 February 1982.

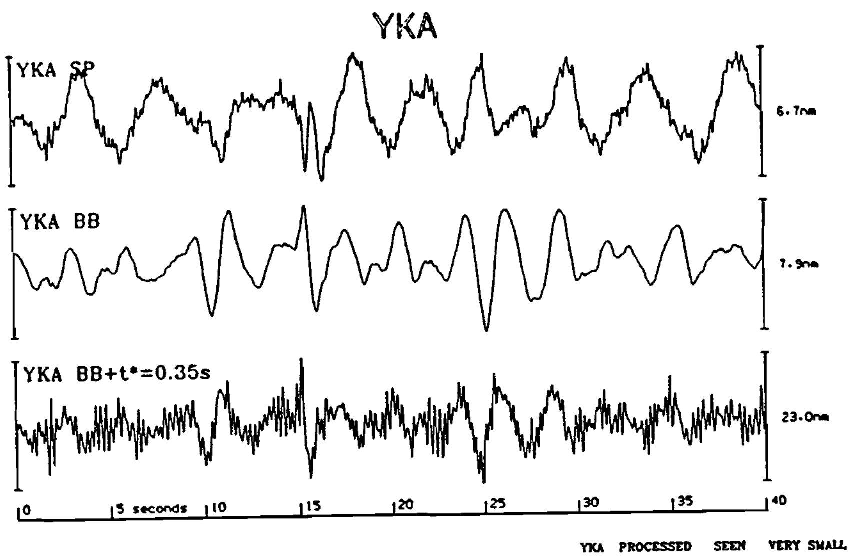

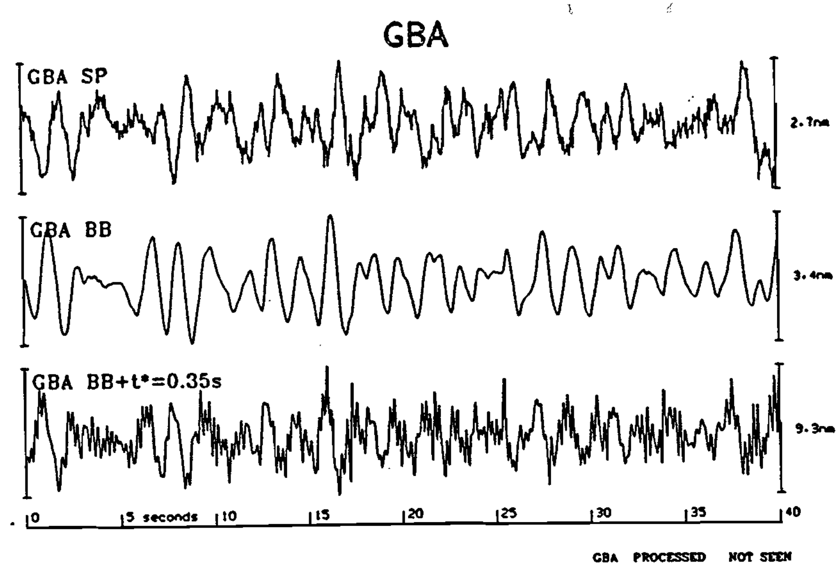

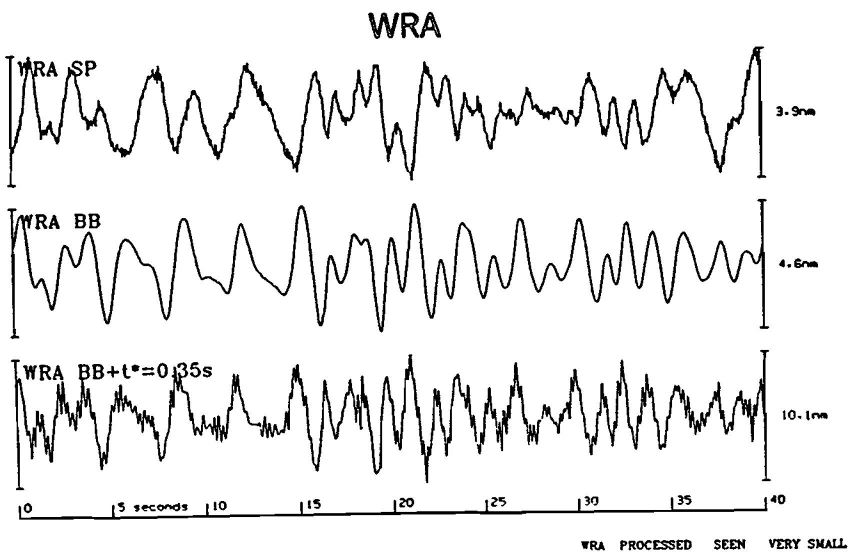

EKA

EKA NOT PROCESSED

Figure A47 Short period, broad band and deconvolved P seismograms from the Mururoa explosion of 24 February 1982.

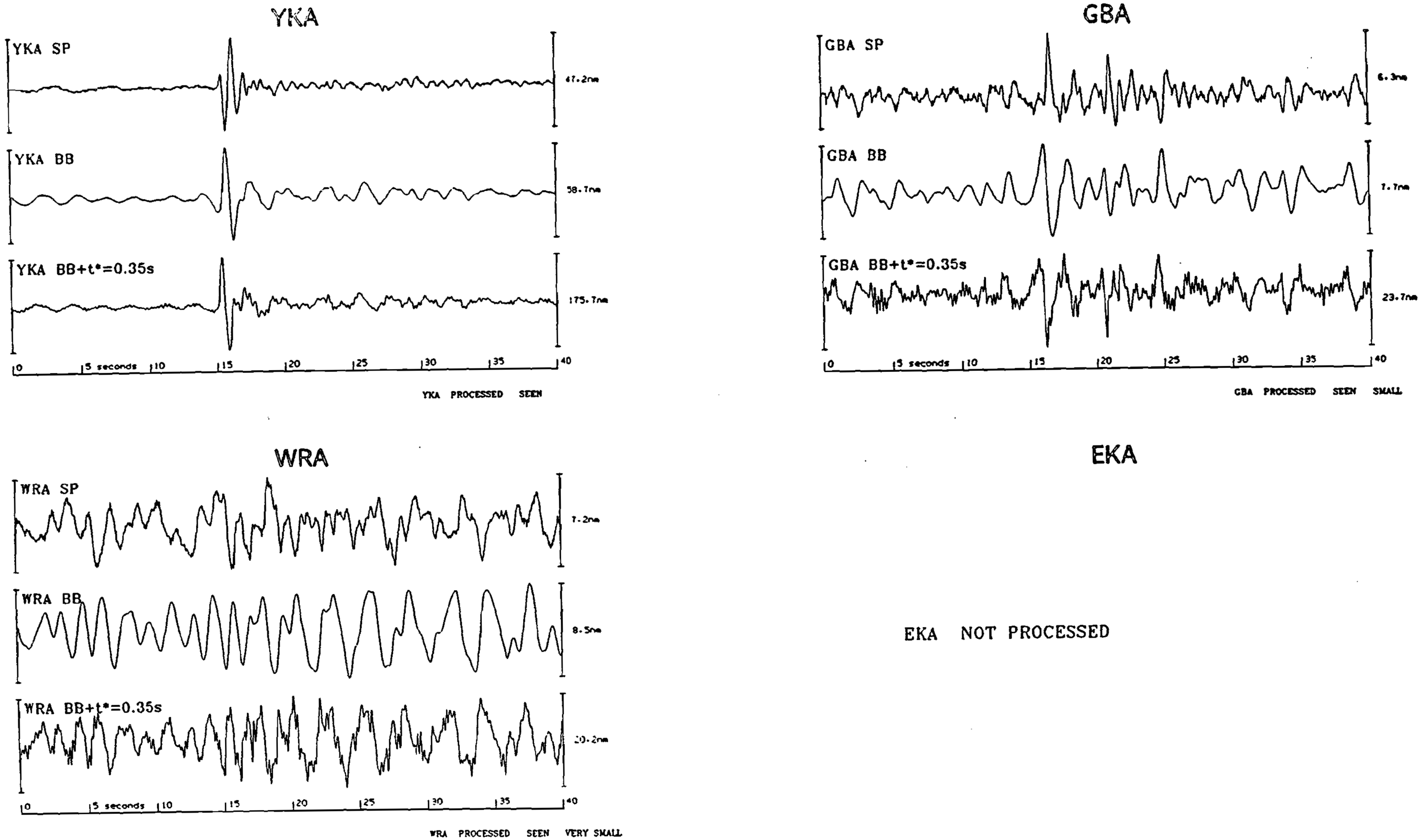

Figure A48 Short period, broad band and deconvolved P seismograms from the Mururoa explosion of 20 March 1982.

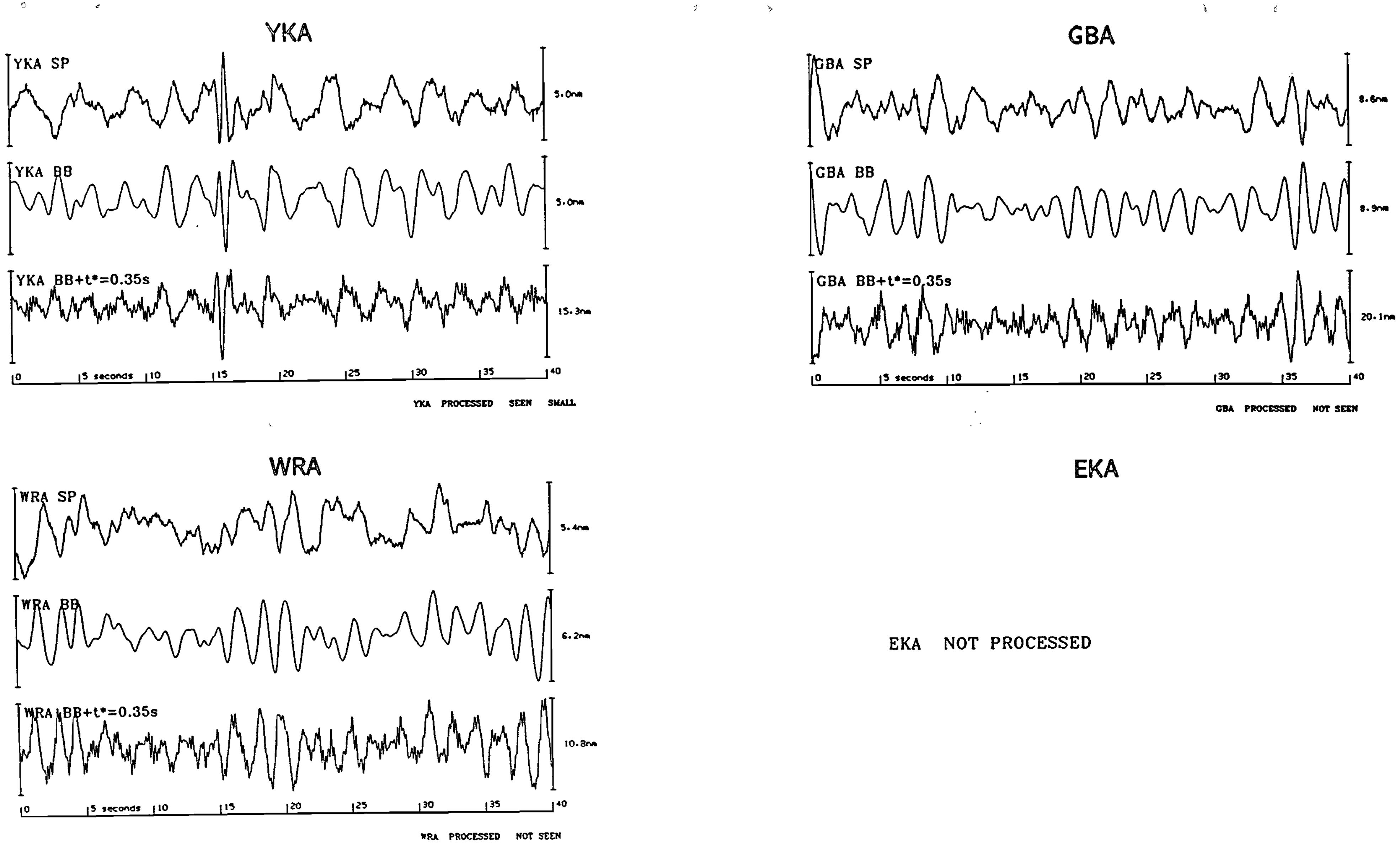

Figure A49 Short period, broad band and deconvolved P seismograms from the Mururoa explosion of 27 June 1982.

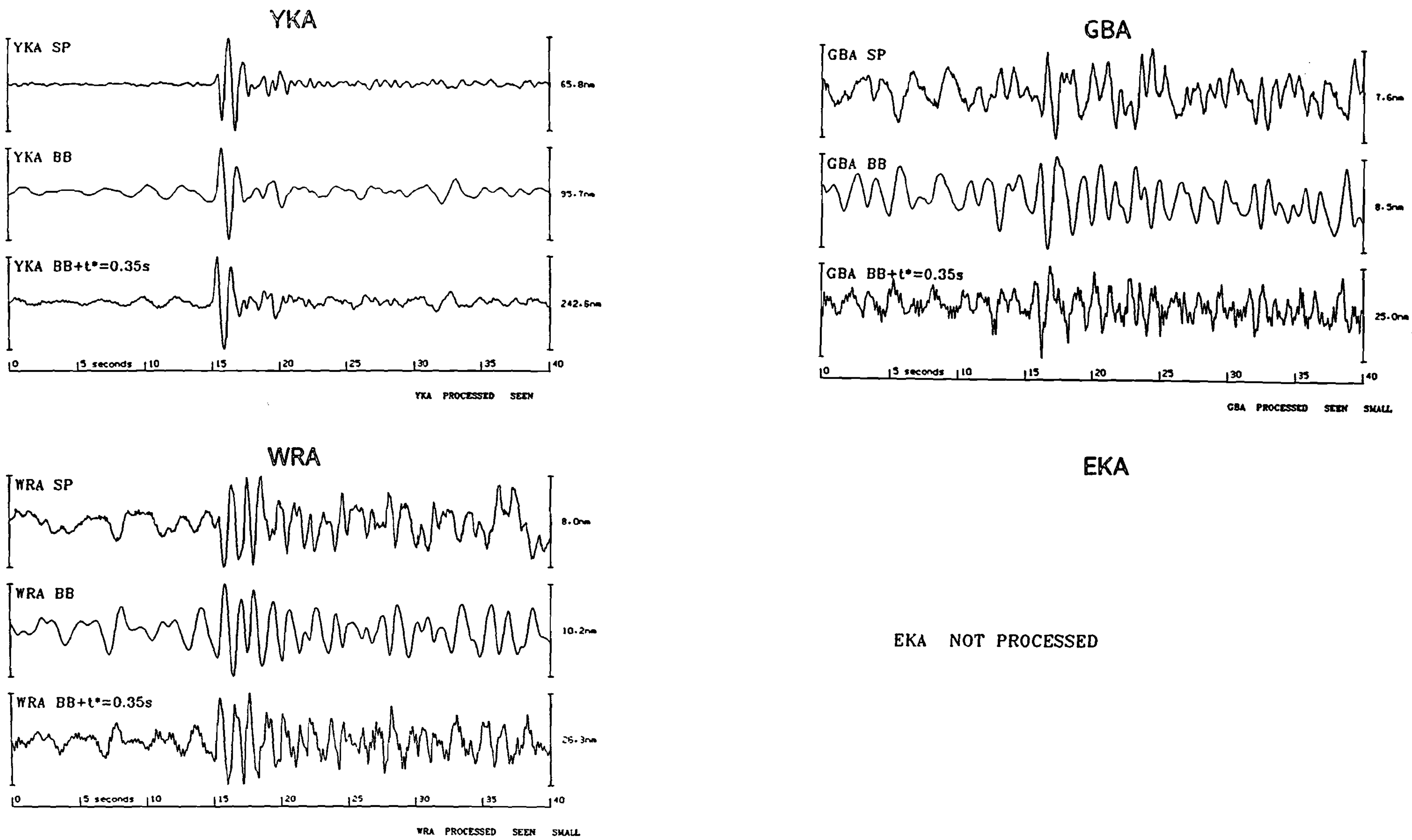

Figure A50 Short period, broad band and deconvolved P seismograms from the Mururoa explosion of 1 July 1982.

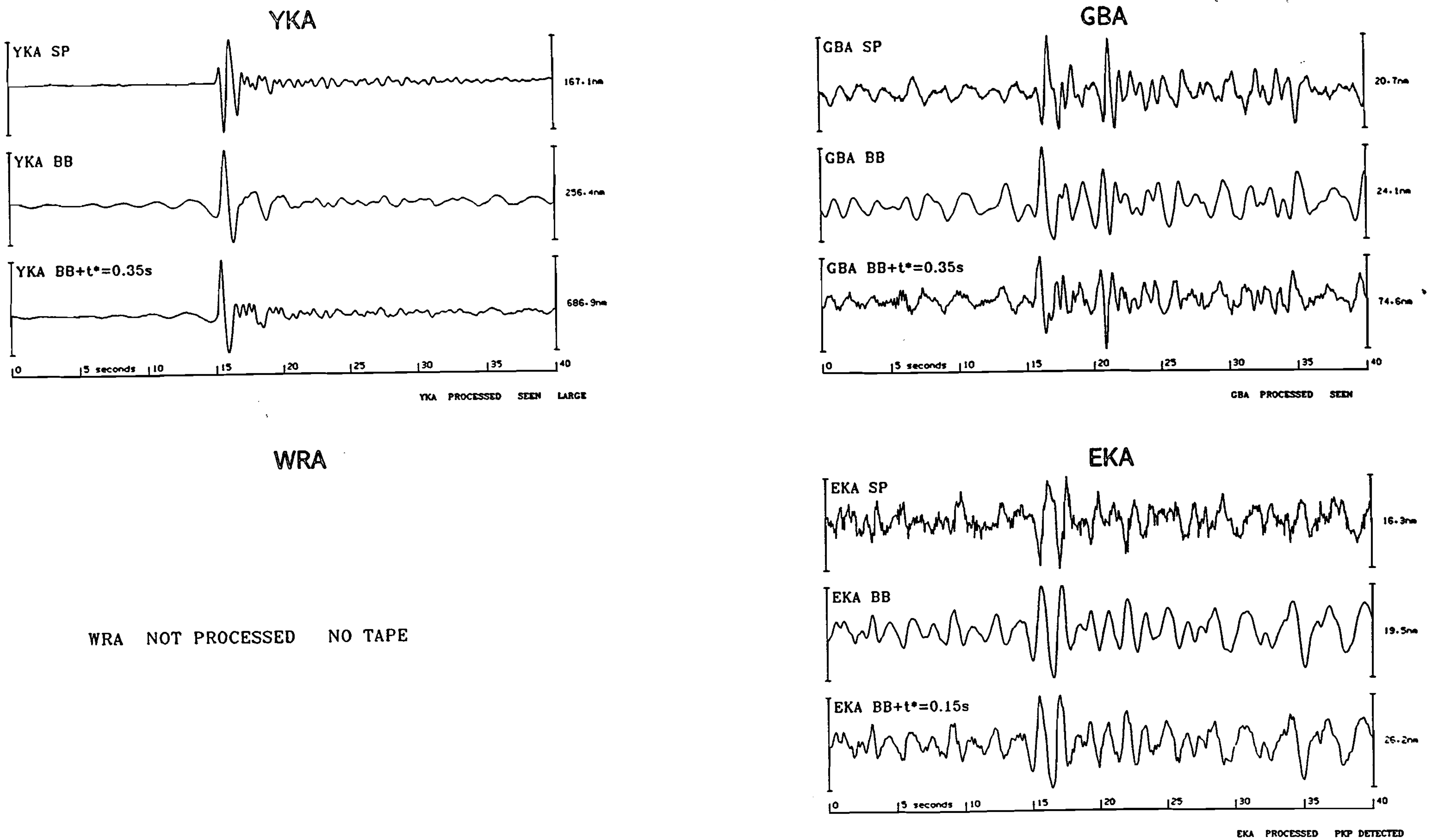

Figure A51 Short period, broad band and deconvolved P seismograms from the Mururoa explosion of 25 July 1982.

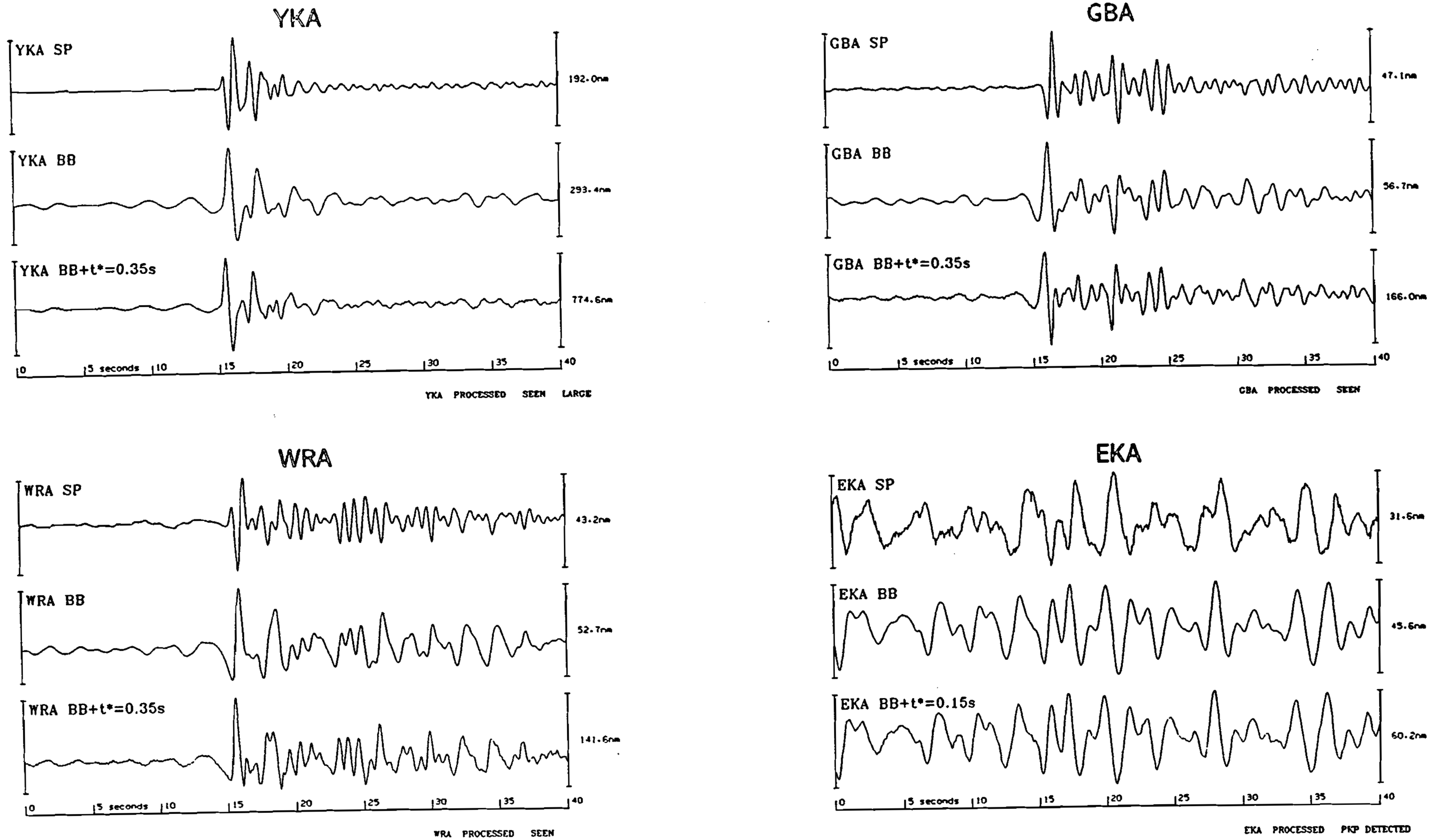

Figure A52 Short period, broad band and deconvolved P seismograms from the Mururoa explosion of 19 April 1983.

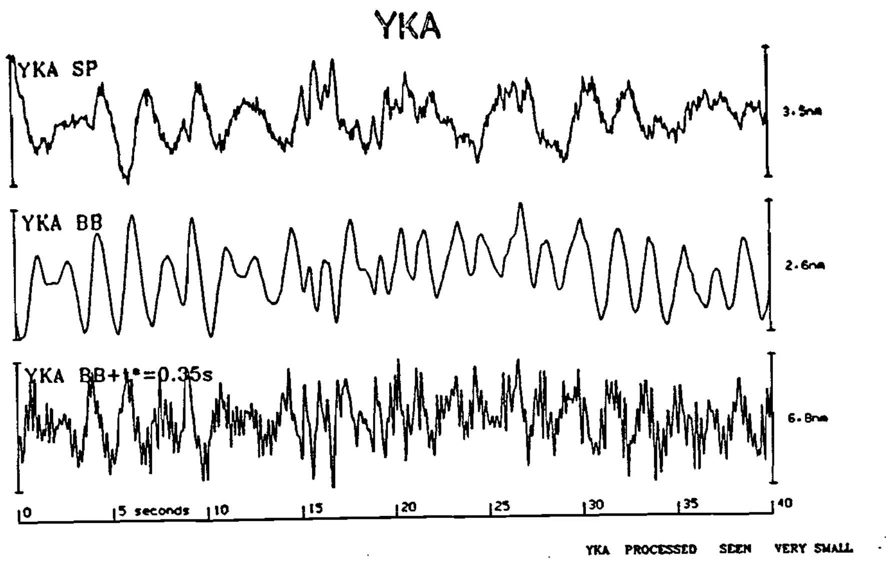

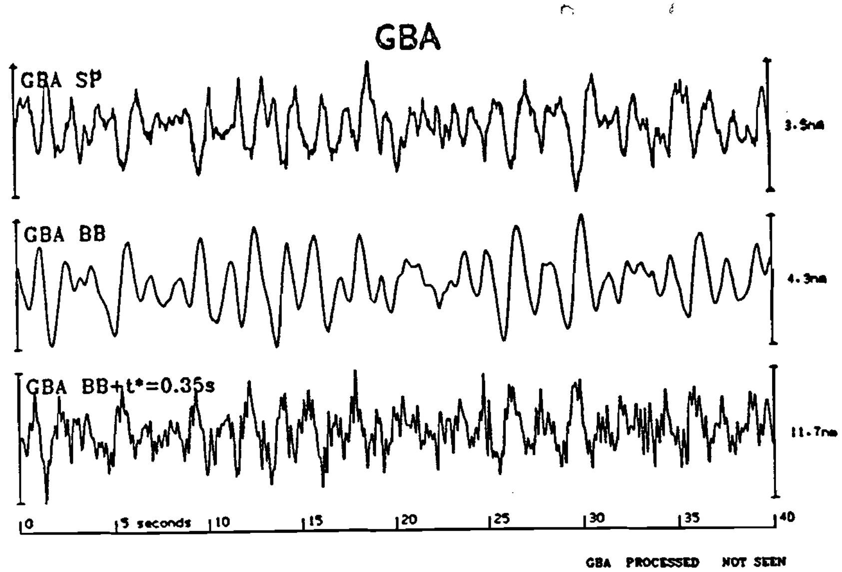

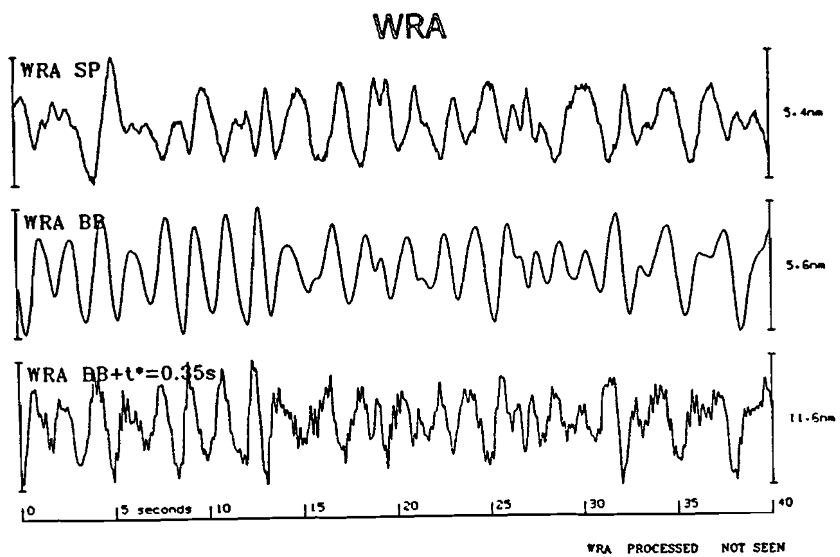

EKA

EKA NOT PROCESSED

Figure A53 Short period, broad band and deconvolved P seismograms from the Mururoa explosion of 25 April 1983.

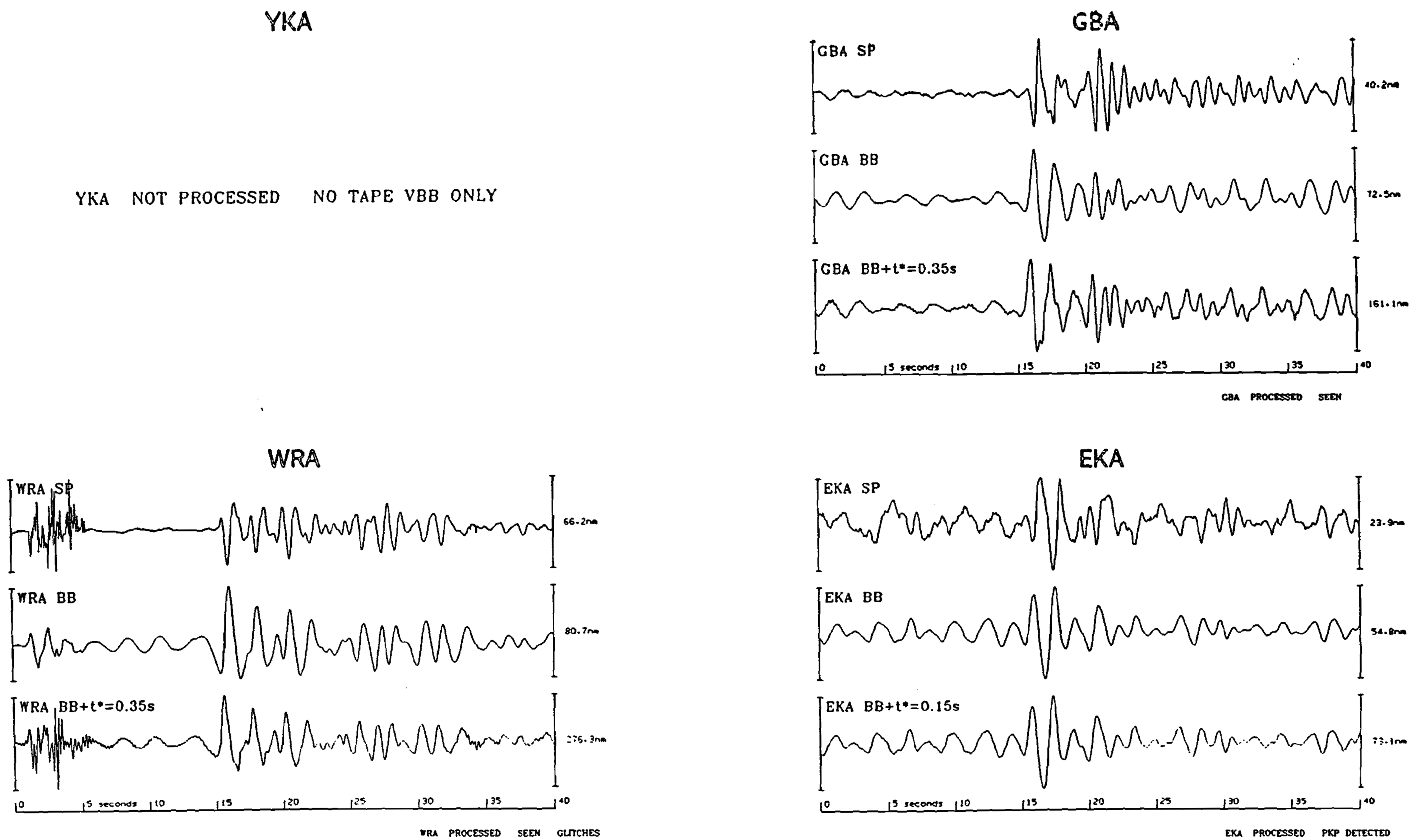

Figure A54 Short period, broad band and deconvolved P seismograms from the Mururoa explosion of 25 May 1983.

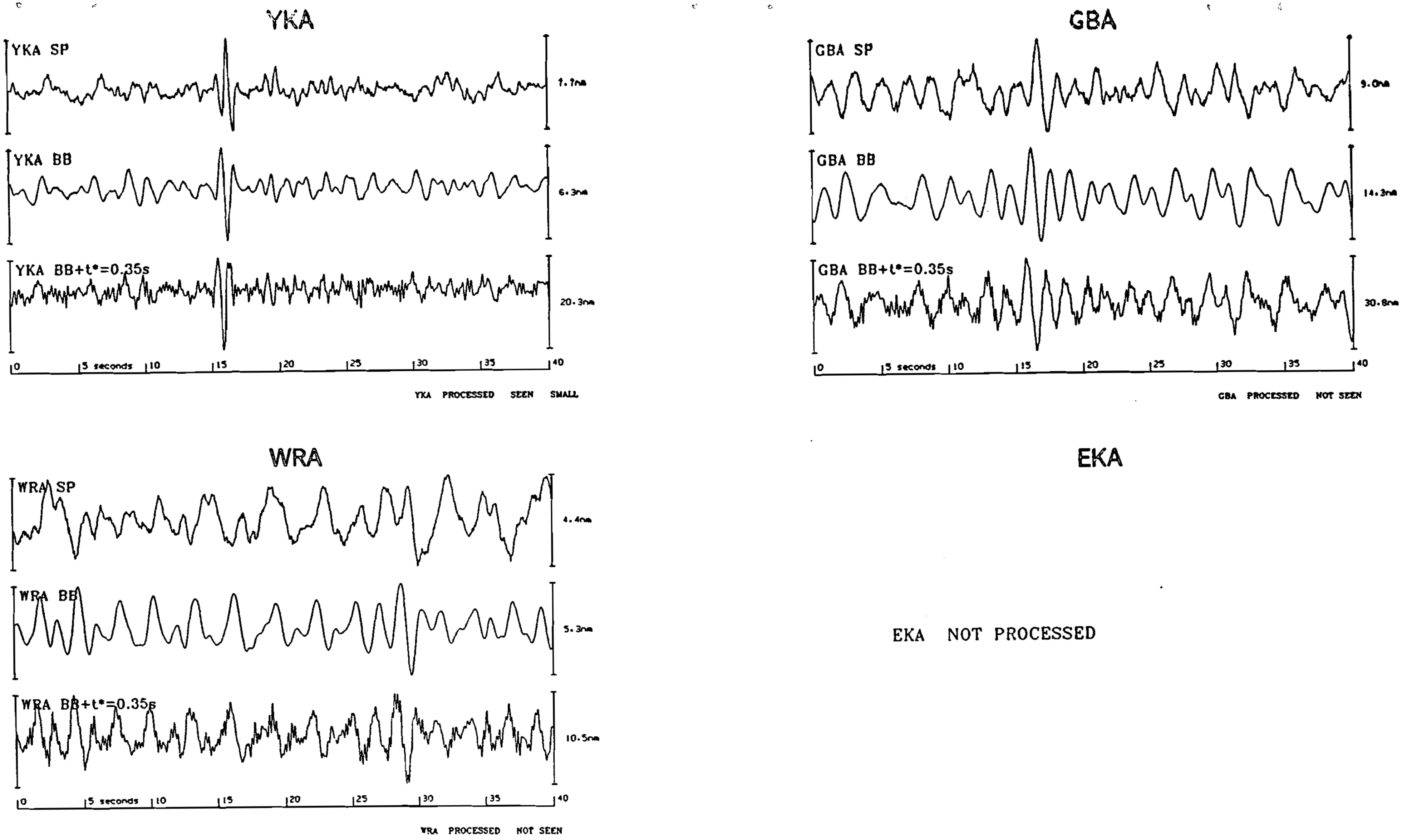

Figure A55 Short period, broad band and deconvolved P seismograms from the Mururoa explosion of 18 June 1983.

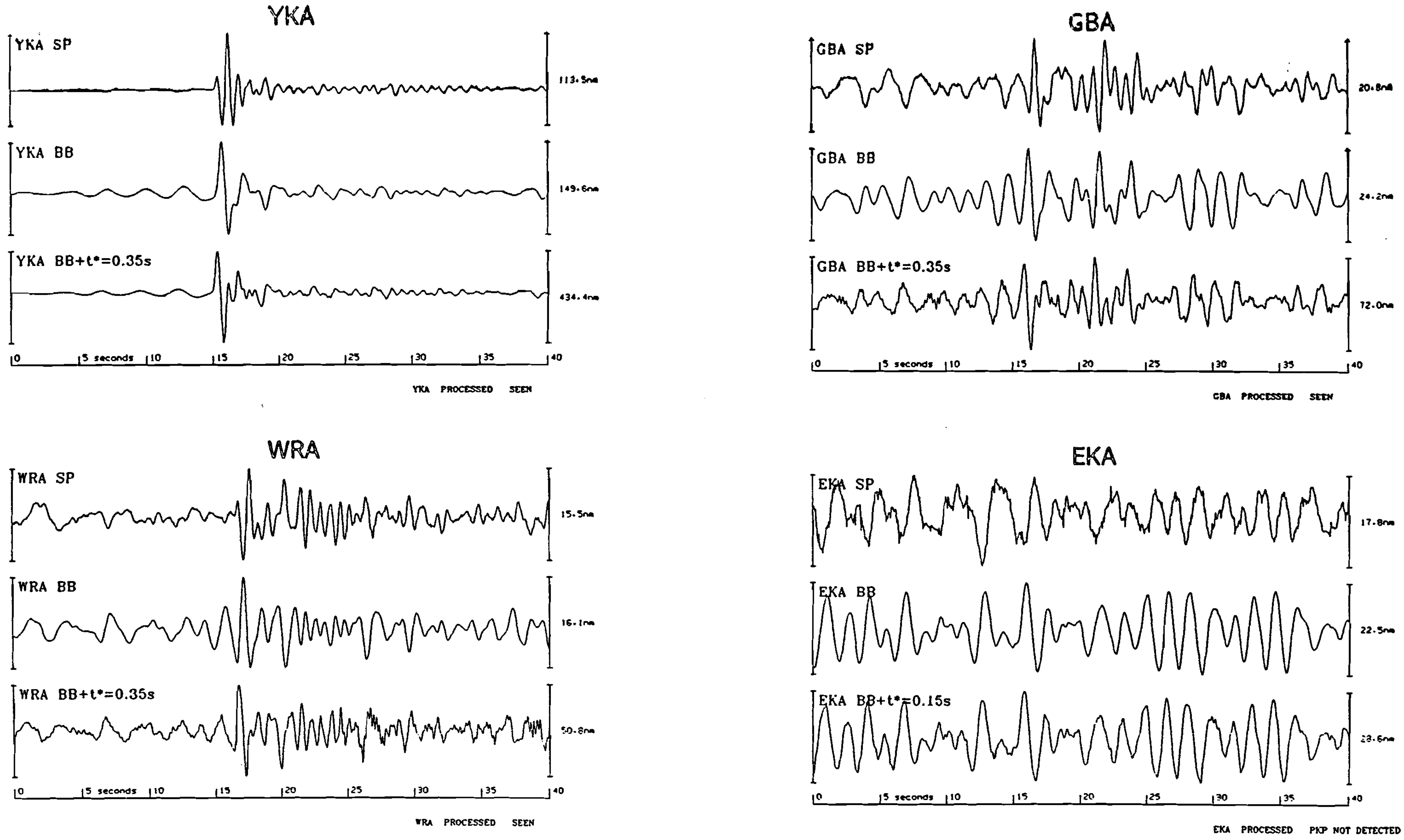

Figure A56 Short period, broad band and deconvolved P seismograms from the Mururoa explosion of 28 June 1983.

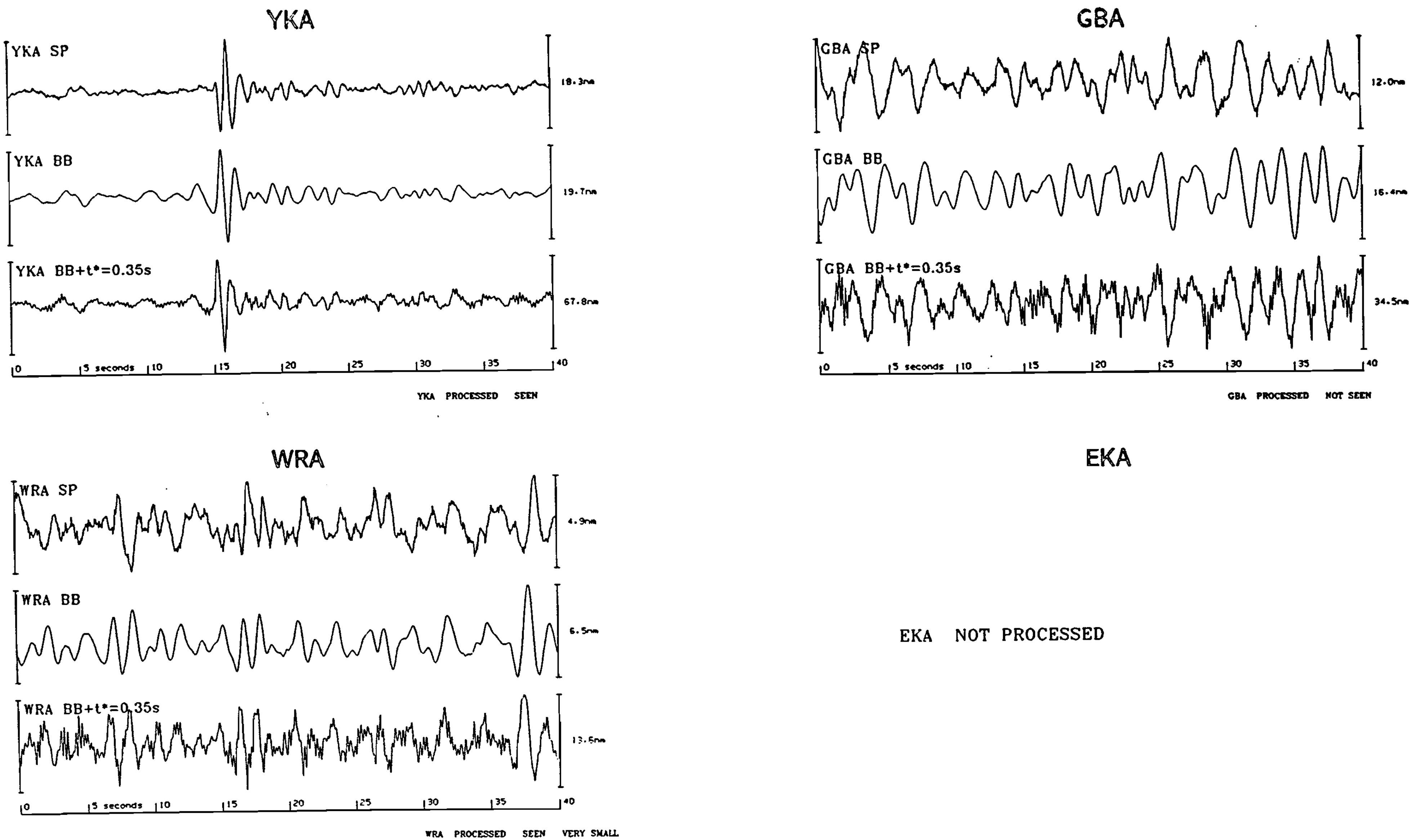

Figure A57 Short period, broad band and deconvolved P seismograms from the Mururoa explosion of 20 July 1983.

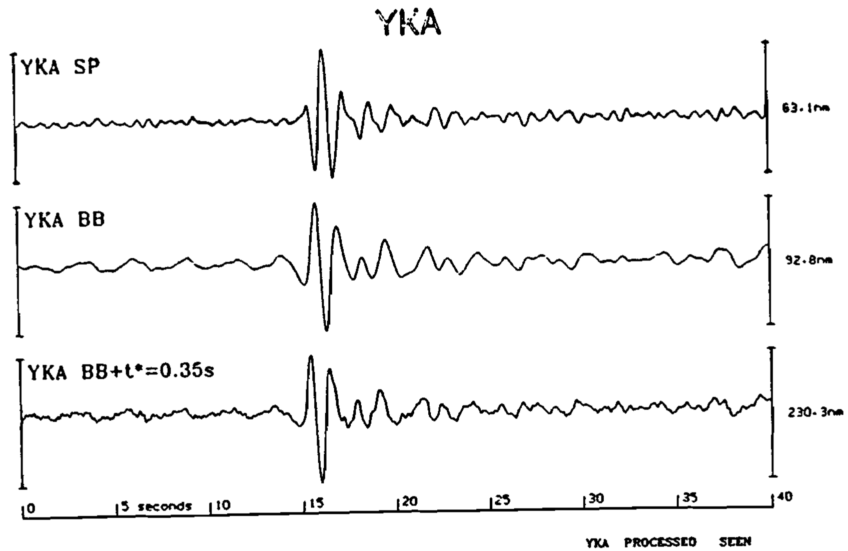

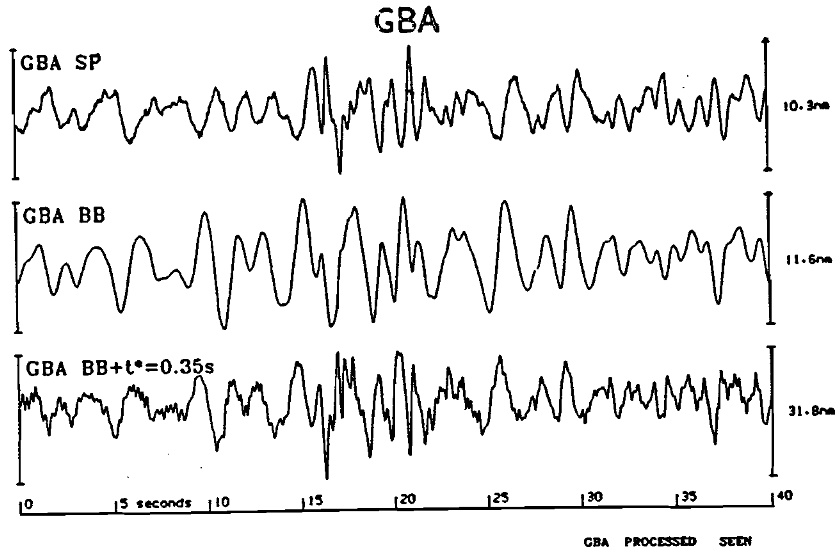

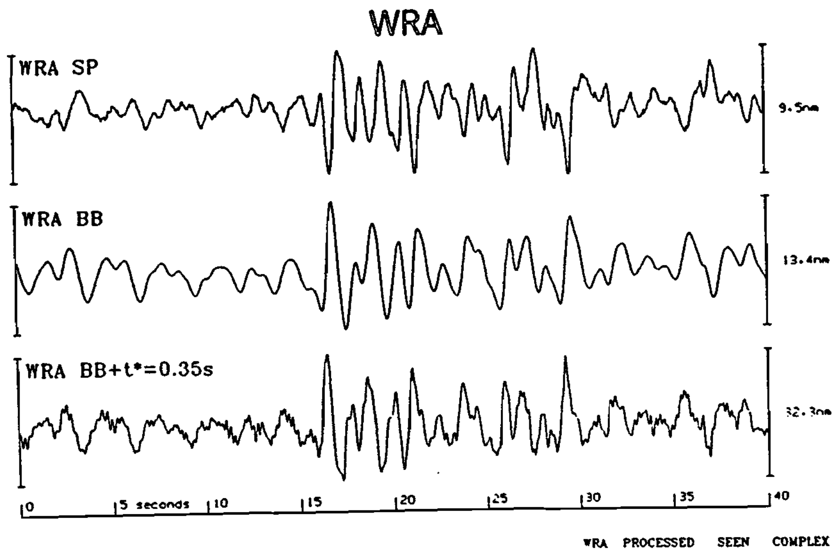

EKA

EKA NOT PROCESSED

Figure A58 Short period, broad band and deconvolved P seismograms from the Mururoa explosion of 4 August 1983.

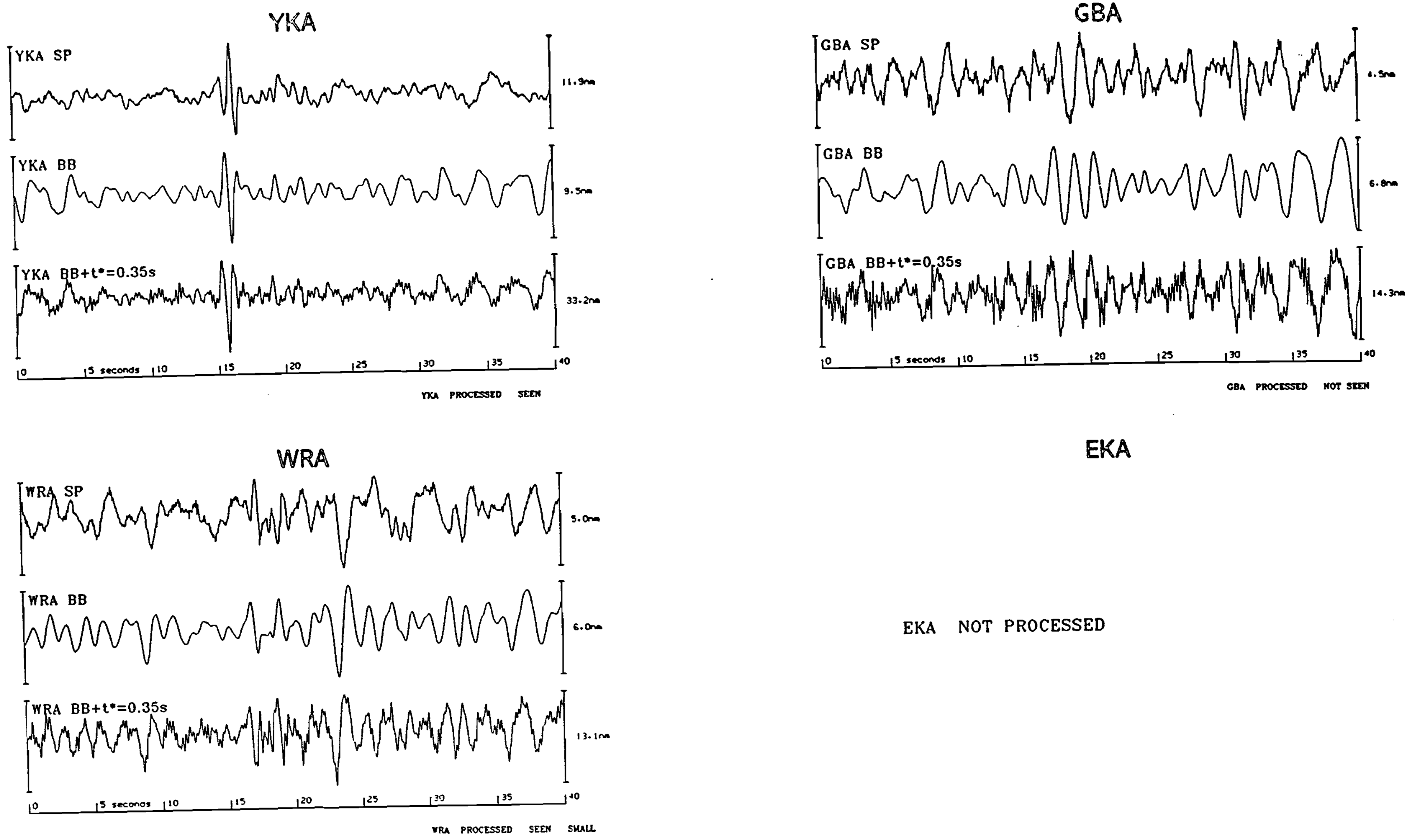

Figure A59 Short period, broad band and deconvolved P seismograms from the Mururoa explosion of 3 December 1983.

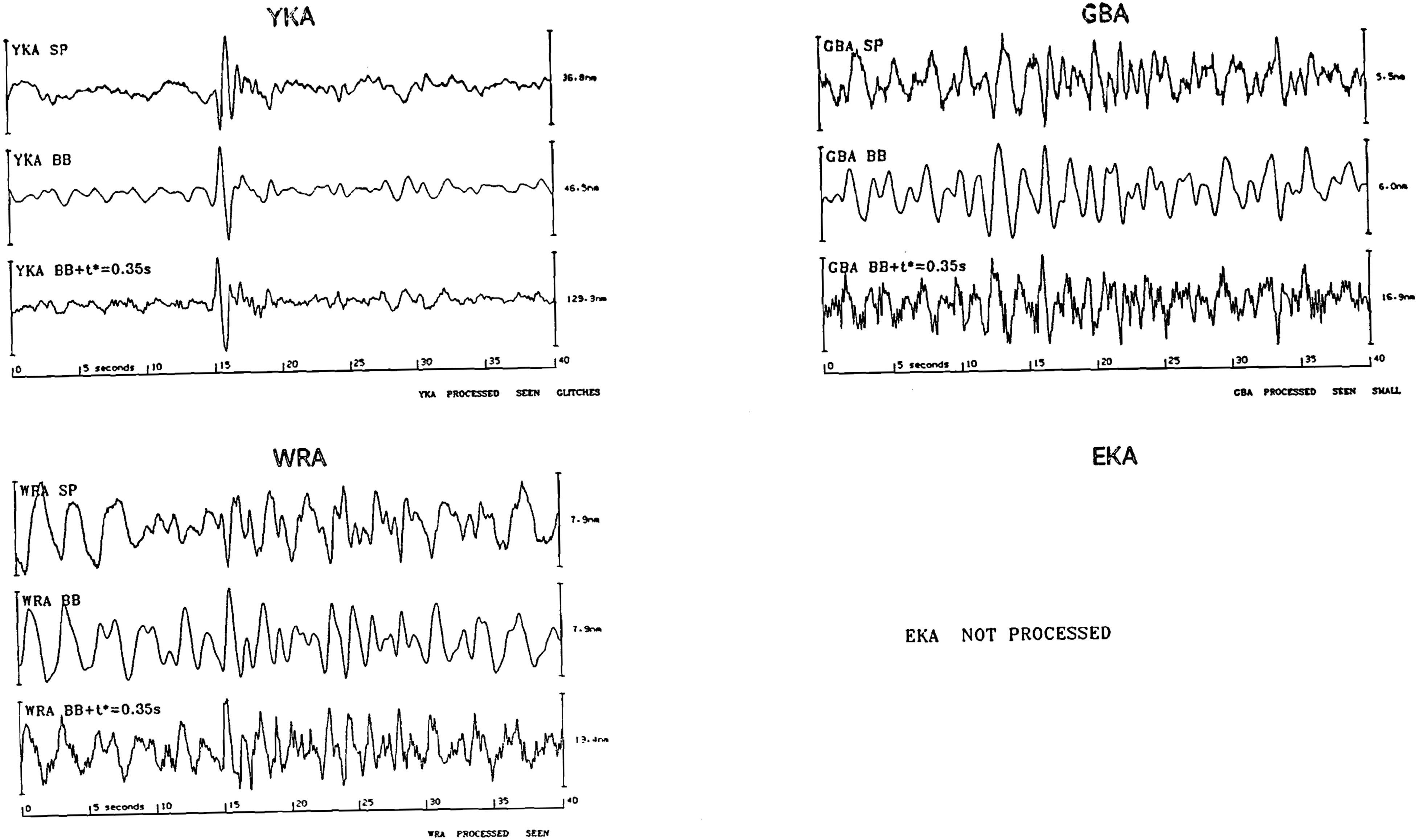

Figure A60 Short period, broad band and deconvolved P seismograms from the Mururoa explosion of 7 December 1983.

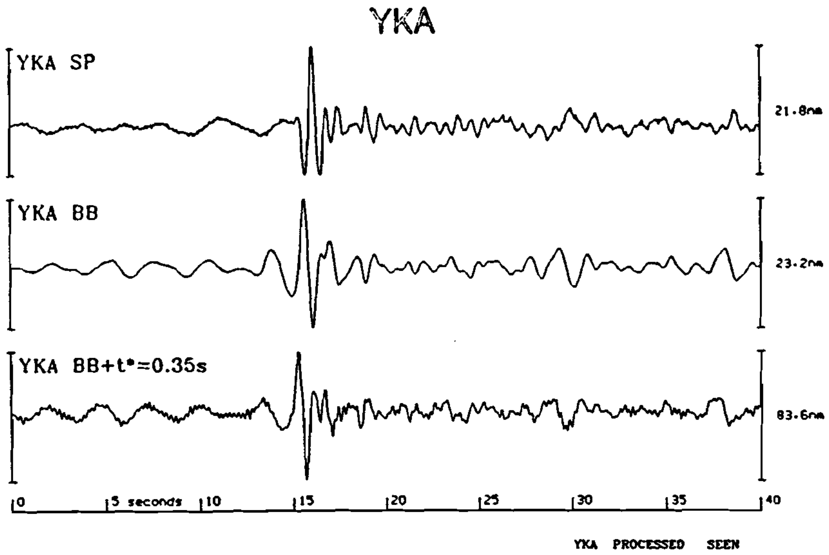

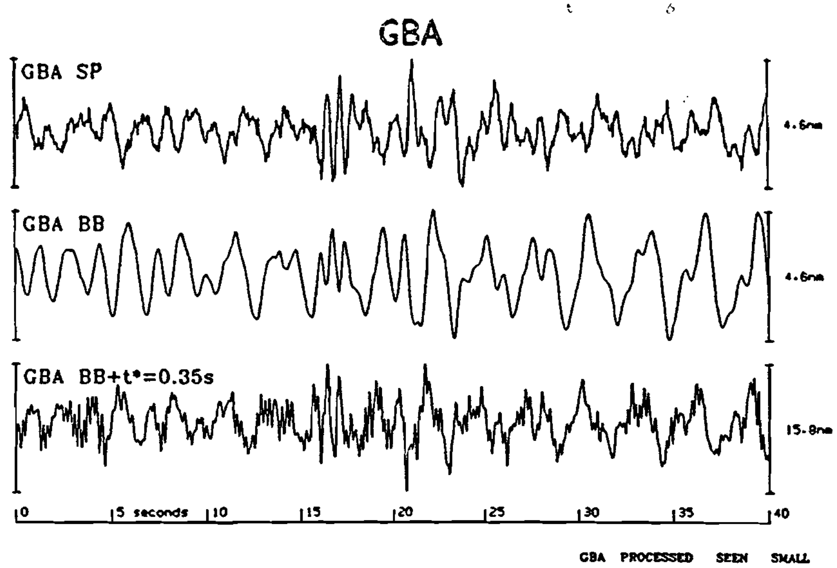

WRA

WRA NOT PROCESSED NO TAPE

EKA

EKA NOT PROCESSED

Figure A61 Short period, broad band and deconvolved P seismograms from the Mururoa explosion of 8 May 1984.

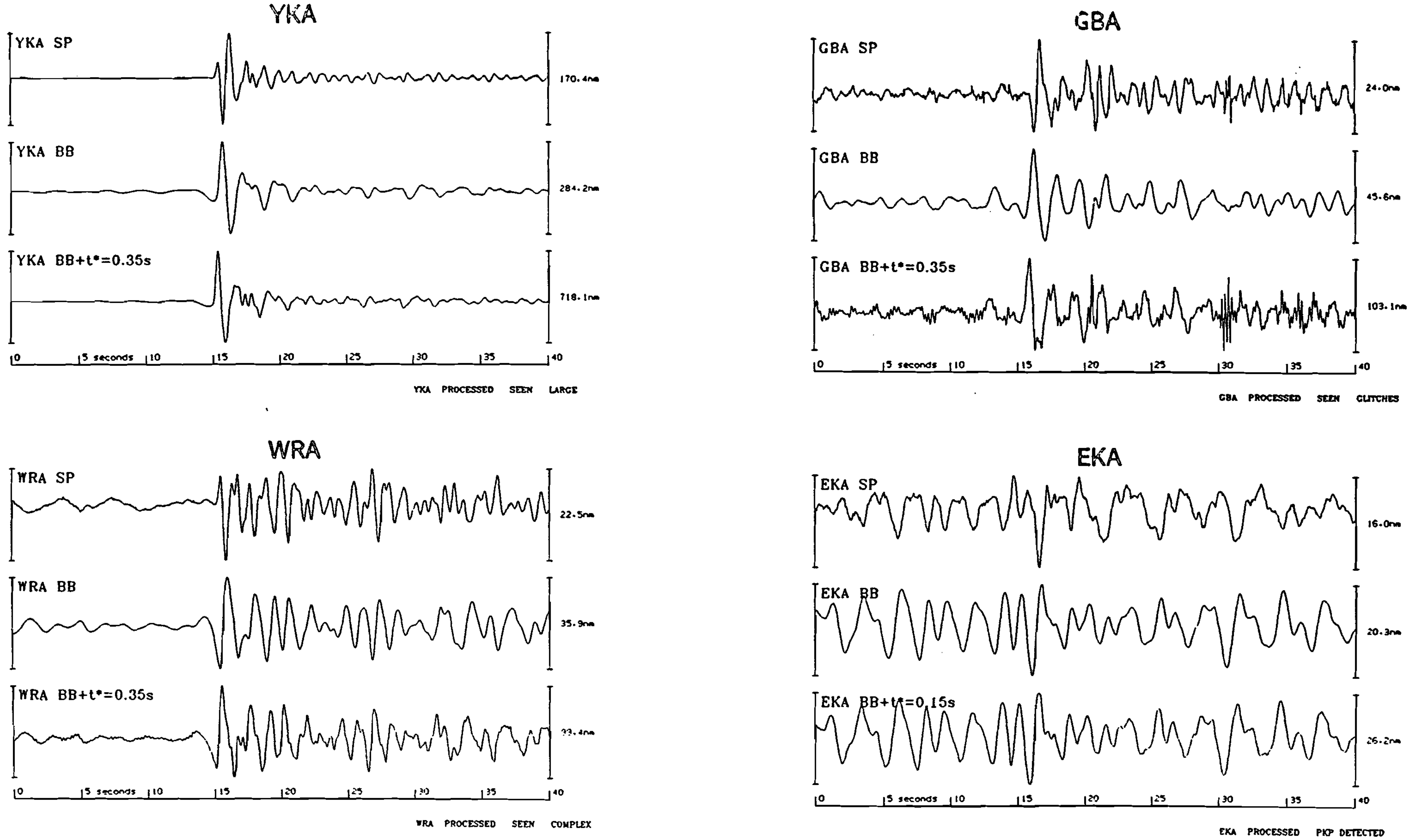

Figure A62 Short period, broad band and deconvolved P seismograms from the Mururoa explosion of 12 May 1984.

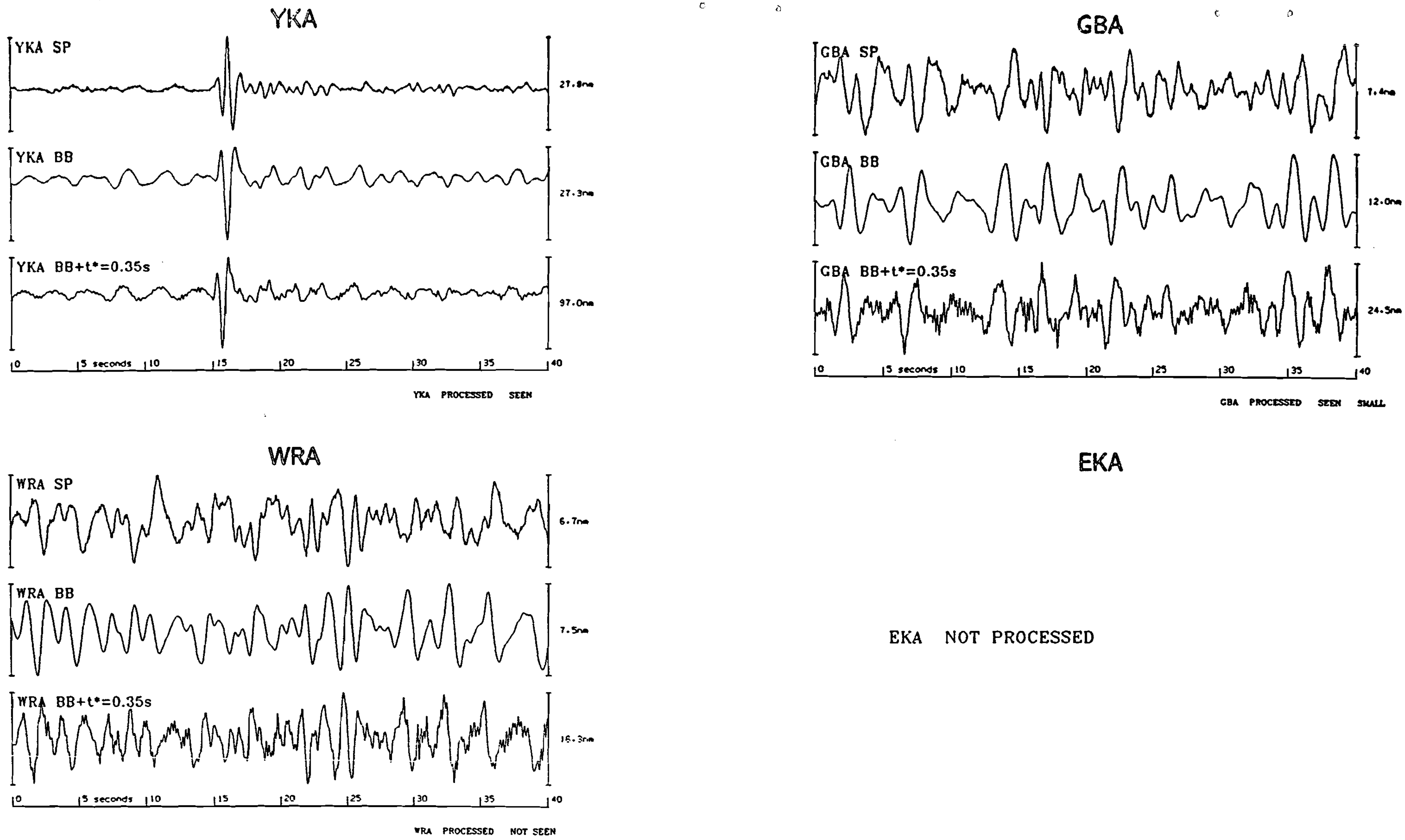

Figure A63 Short period, broad band and deconvolved P seismograms from the Mururoa explosion of 12 June 1984.

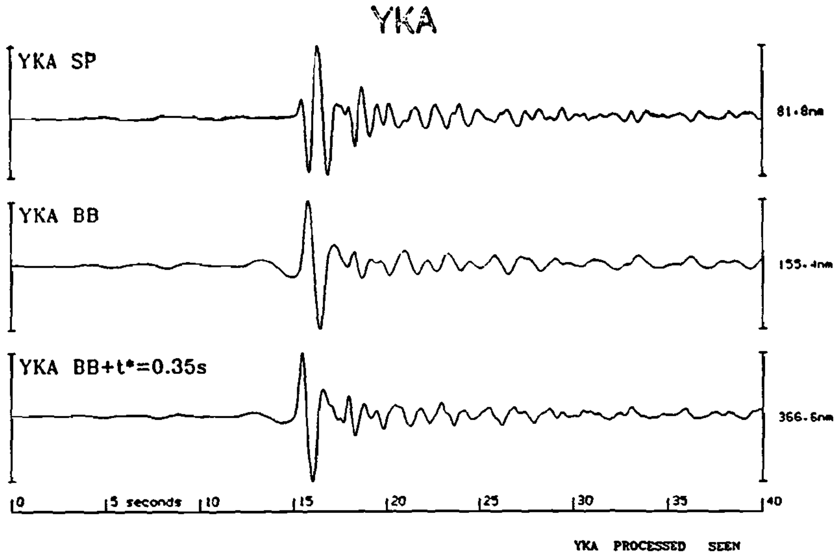

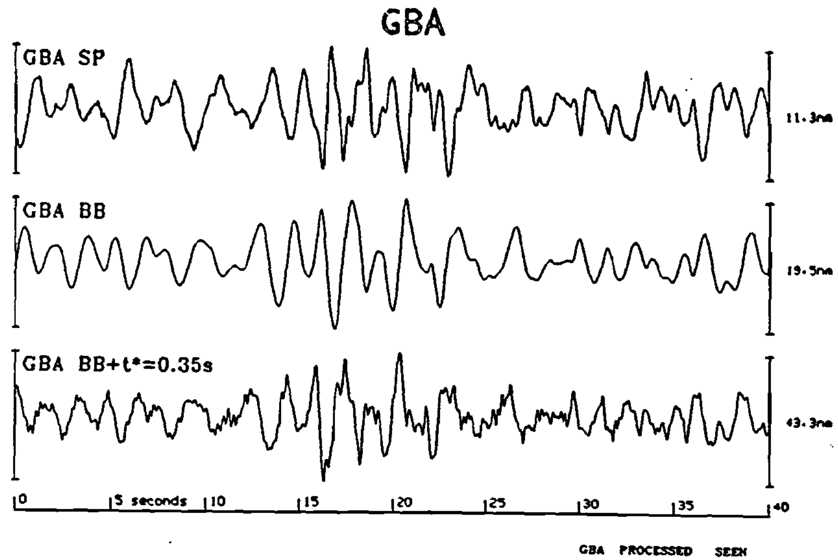

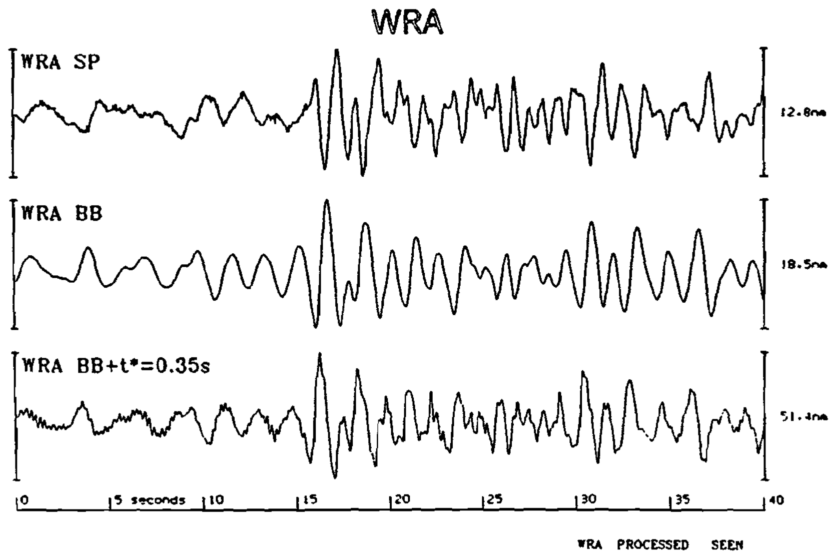

EKA

EKA NOT PROCESSED

Figure A64 Short period, broad band and deconvolved P seismograms from the Mururoa explosion of 16 June 1984.

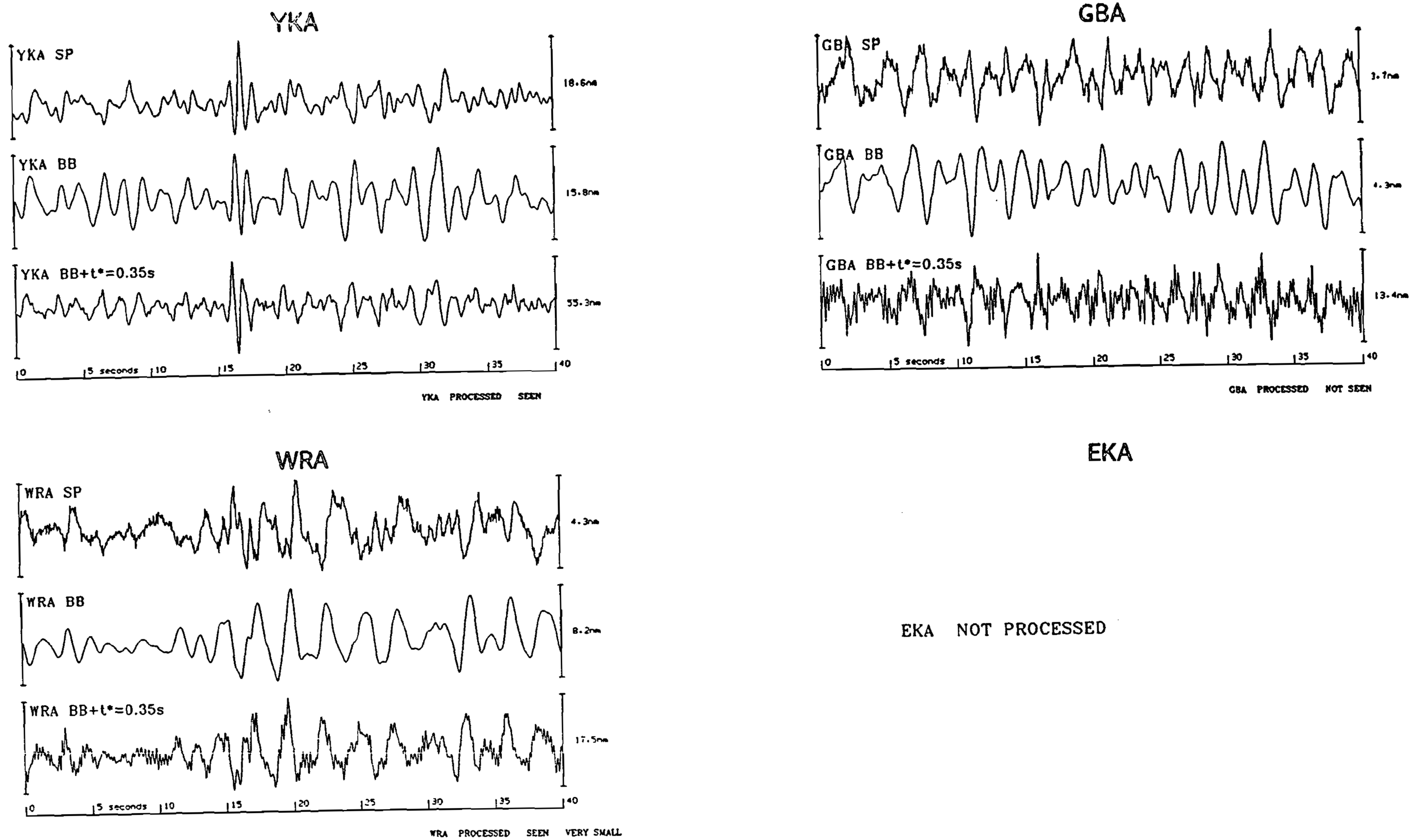

Figure A65 Short period, broad band and deconvolved P seismograms from the Mururoa explosion of 27 October 1984.

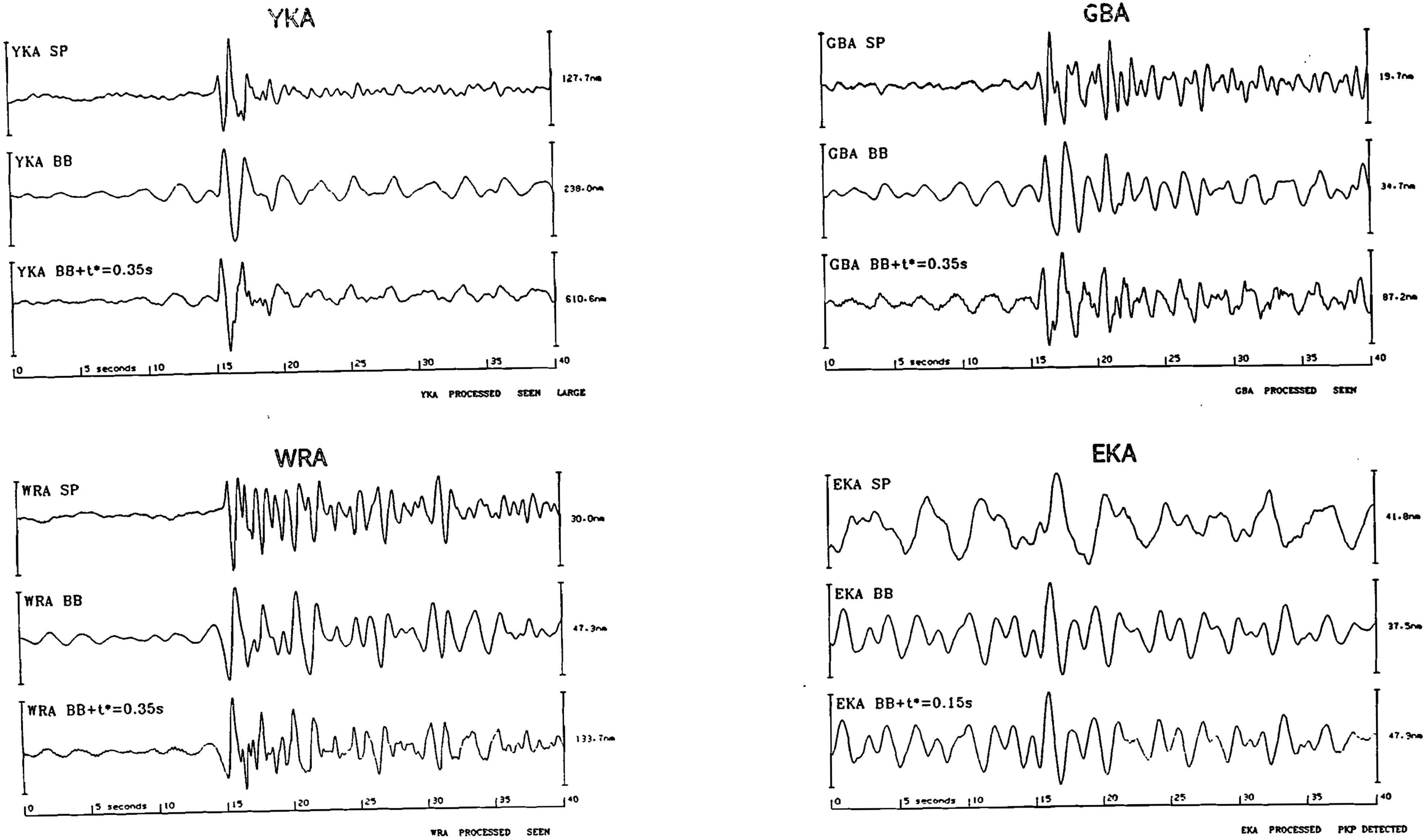

Figure A66 Short period, broad band and deconvolved P seismograms from the Mururoa explosion of 2 November 1984.

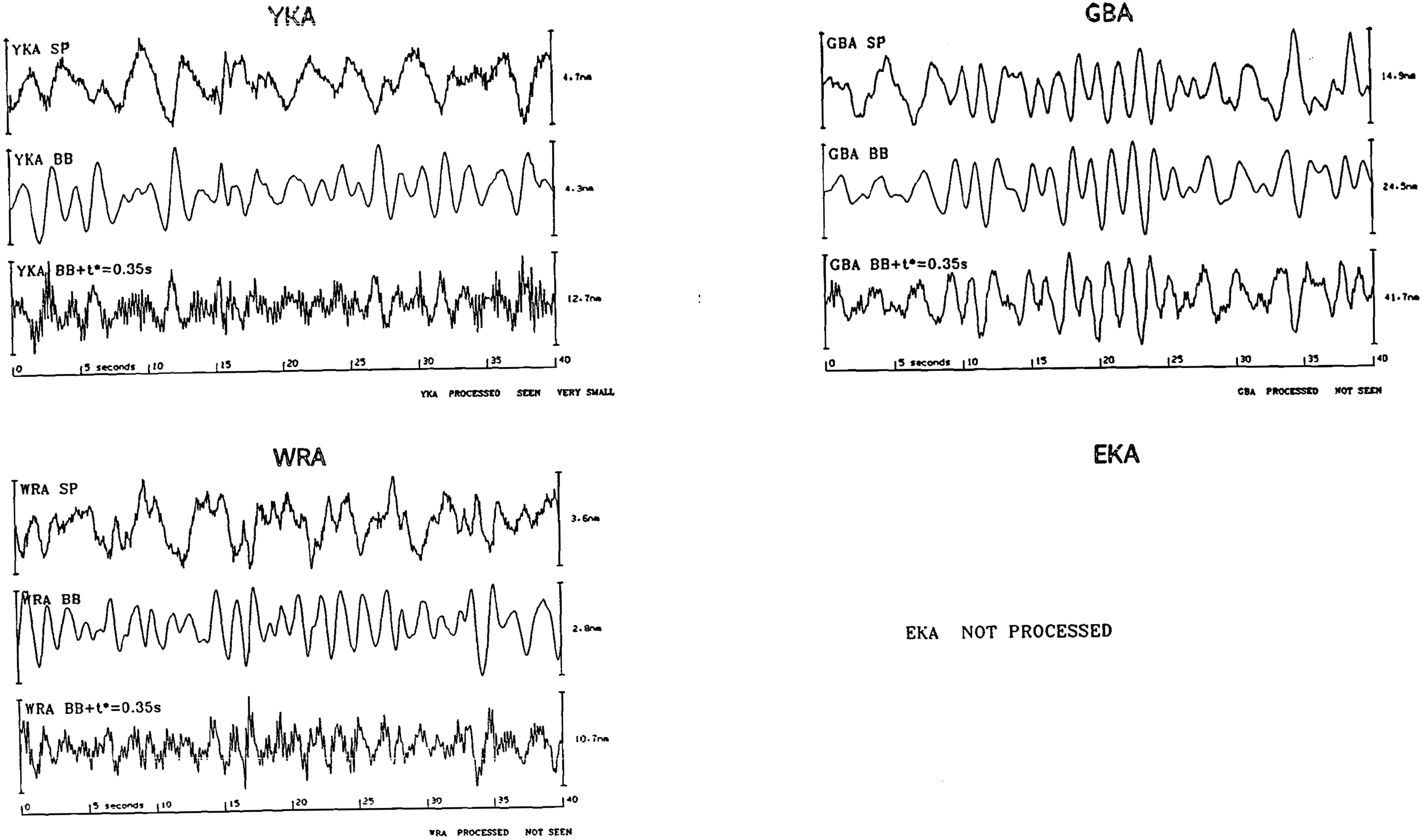

Figure A67 Short period, broad band and deconvolved P seismograms from the Mururoa explosion of 1 December 1984.

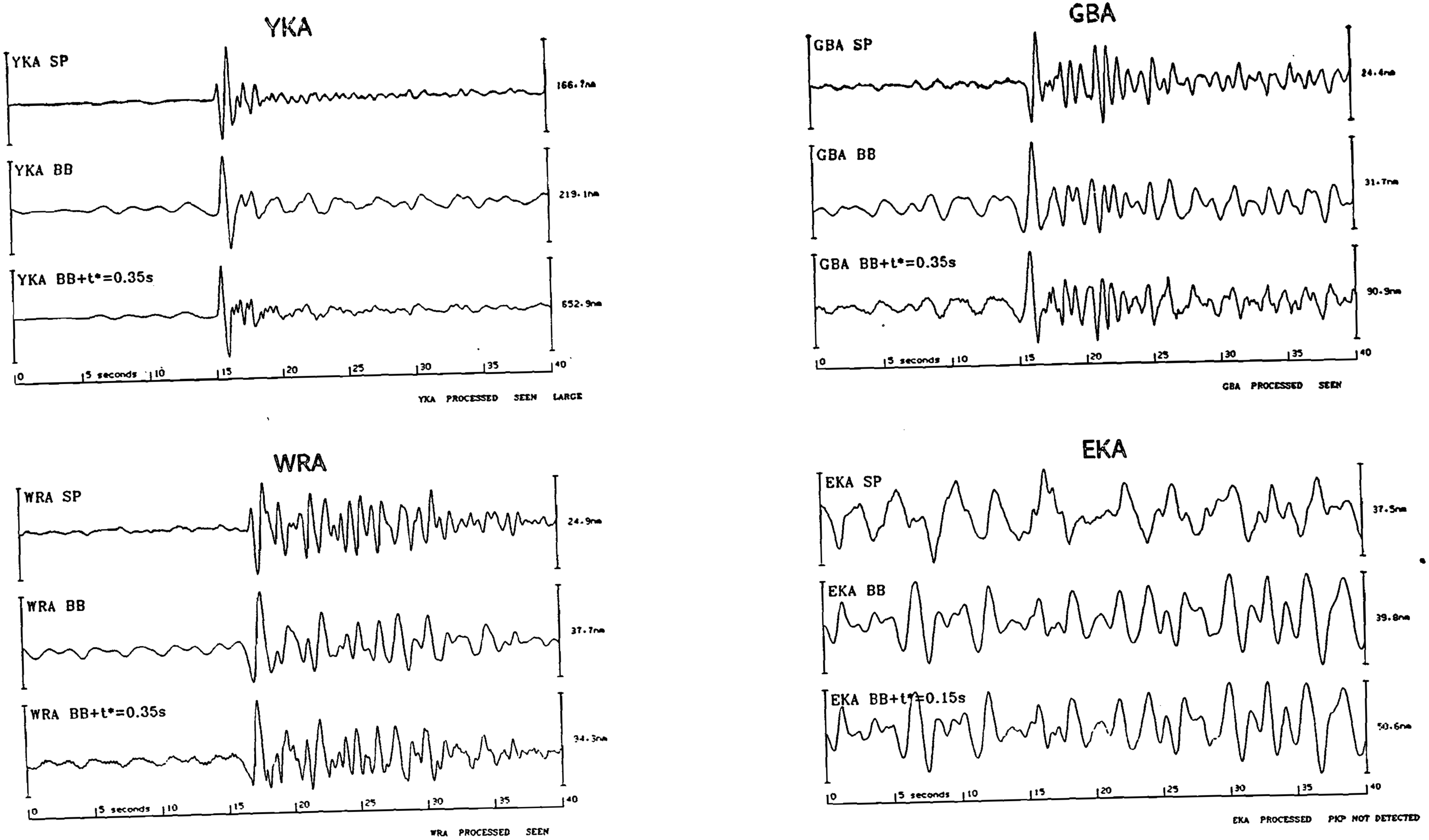

Figure A68 Short period, broad band and deconvolved P seismograms from the Mururoa explosion of 6 December 1984.

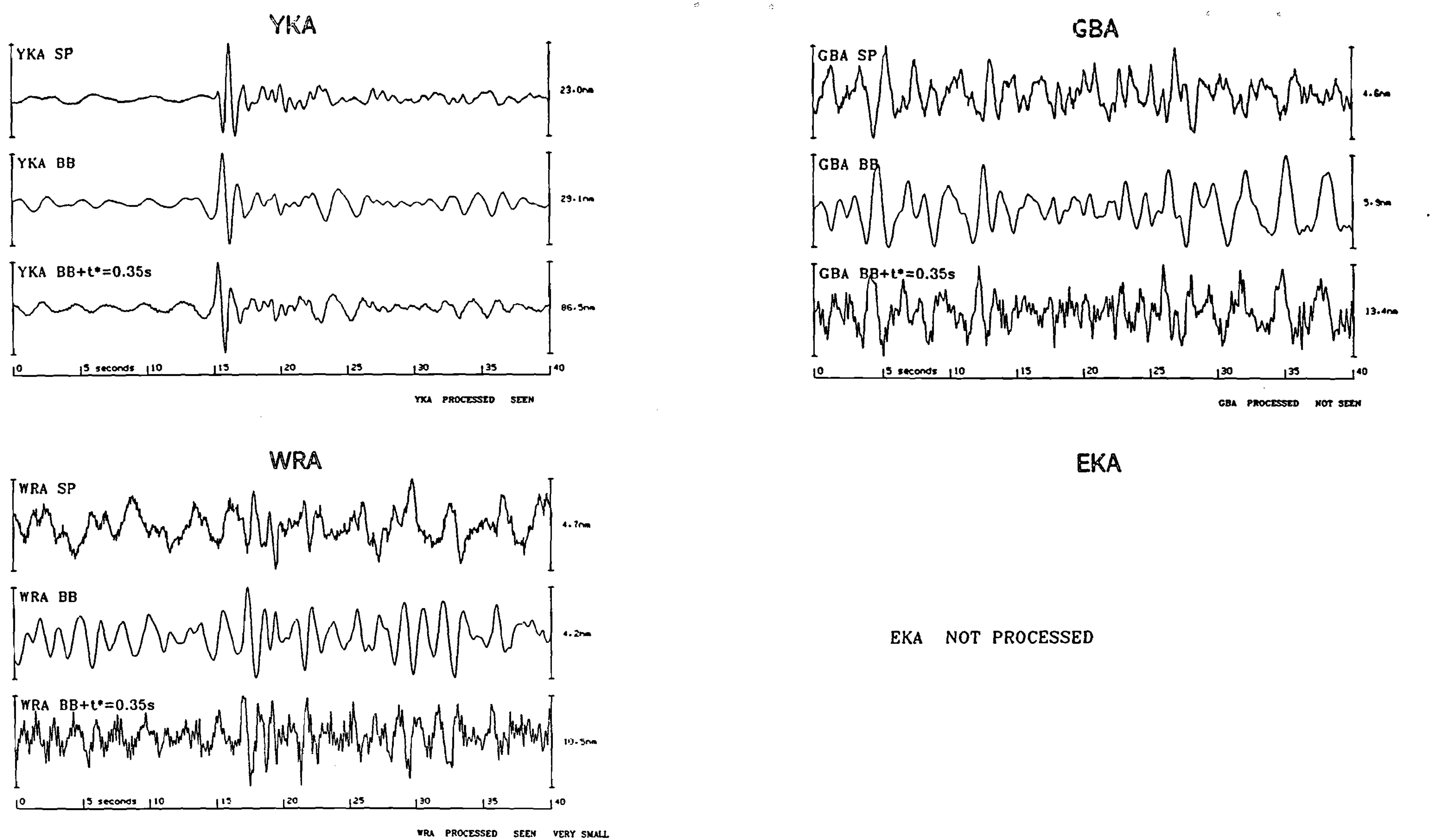

Figure A69 Short period, broad band and deconvolved P seismograms from the Mururoa explosion of 30 April 1985.

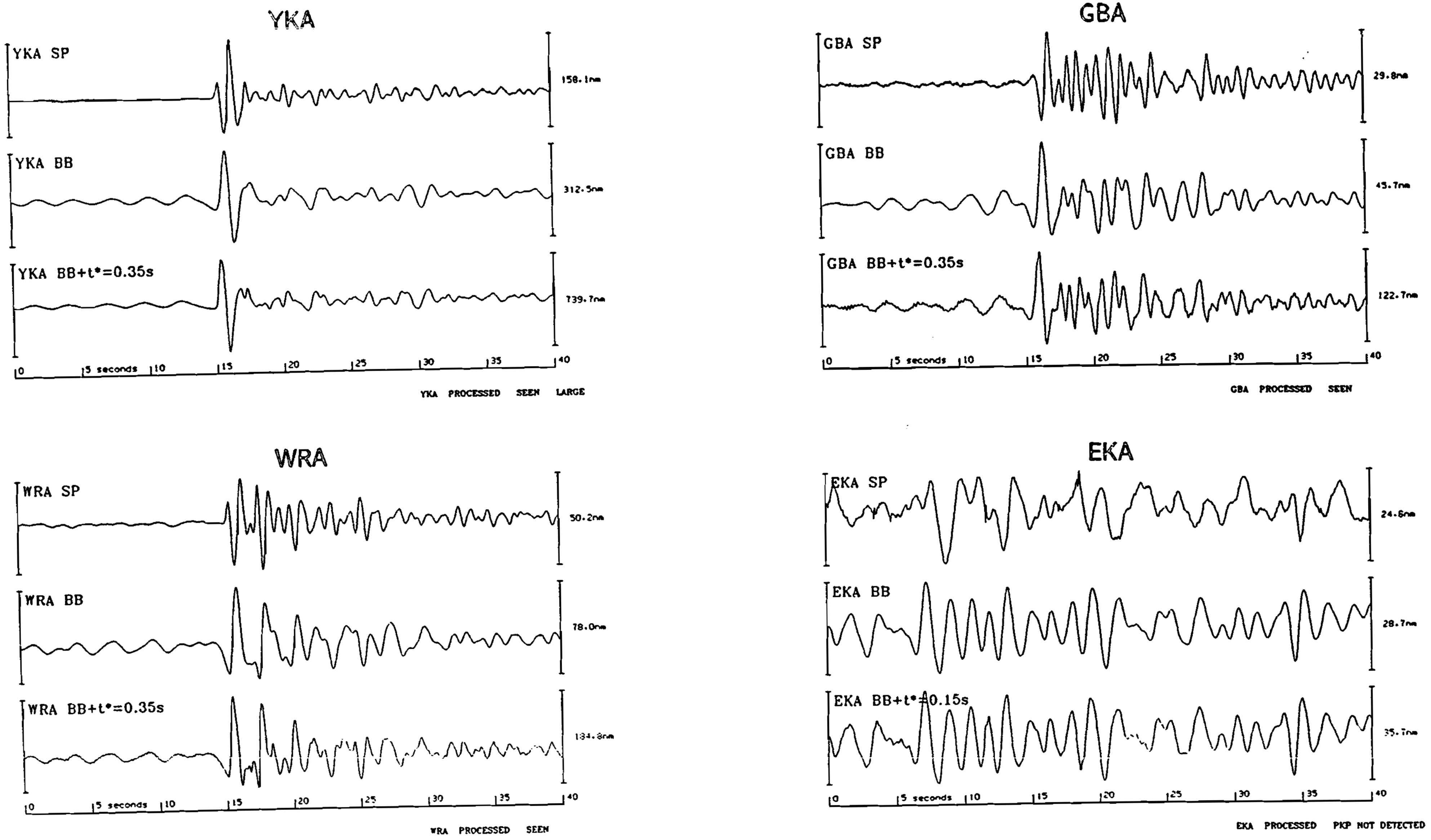

Figure A70 Short period, broad band and deconvolved P seismograms from the Mururoa explosion of 8 May 1985.

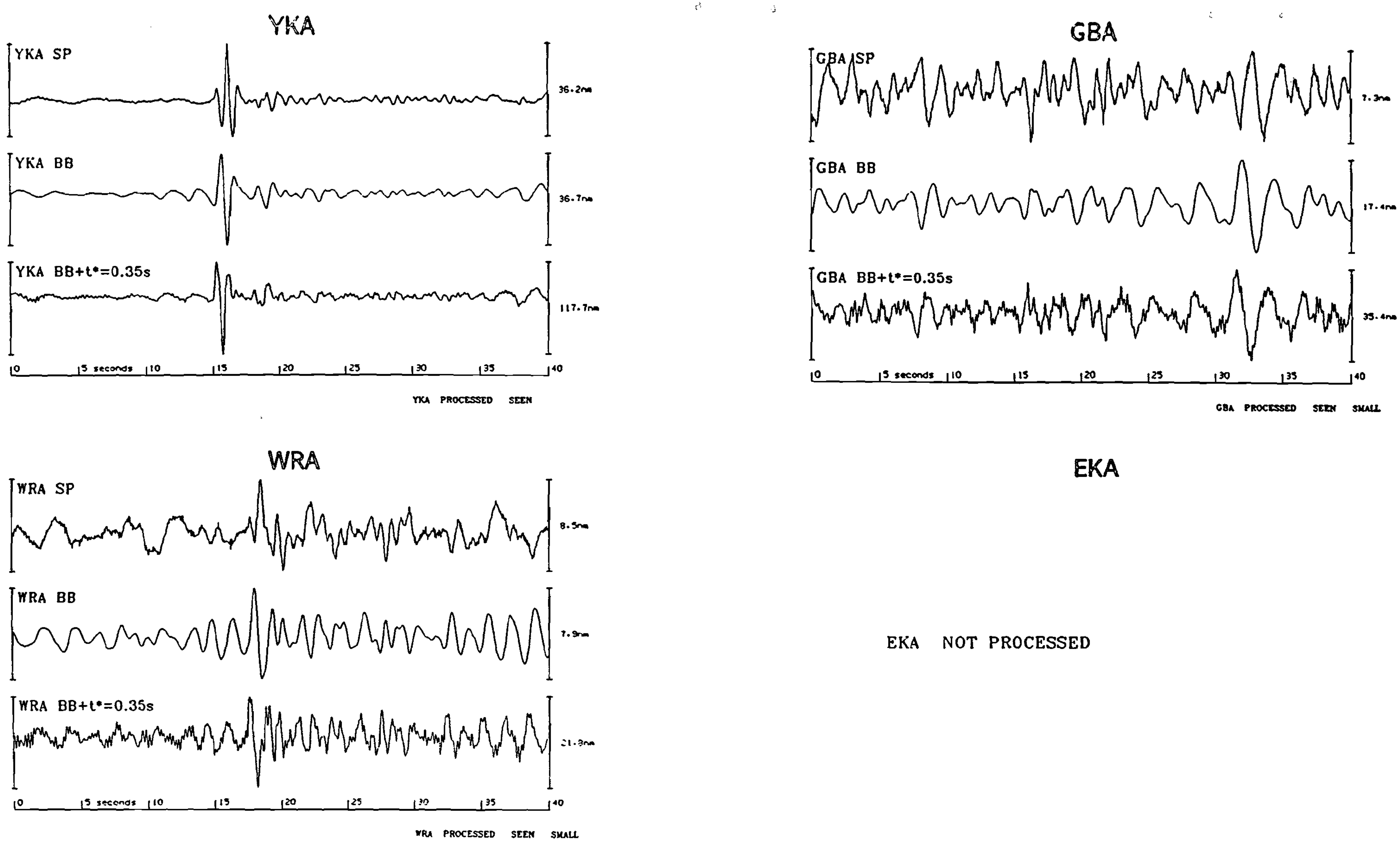

Figure A71 Short period, broad band and deconvolved P seismograms from the Mururoa explosion of 3 June 1985.

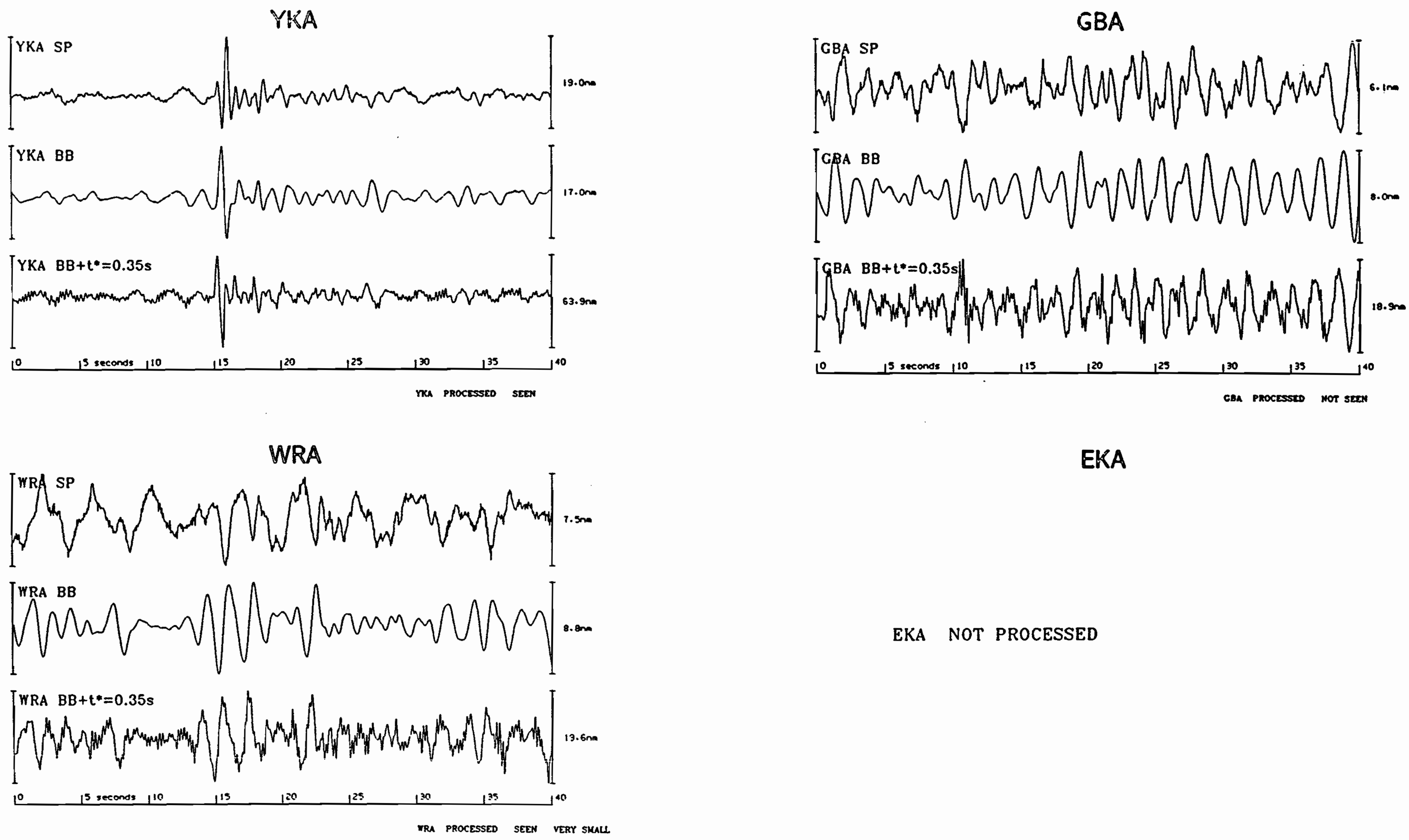

Figure A72 Short period, broad band and deconvolved P seismograms from the Mururoa explosion of 7 June 1985.

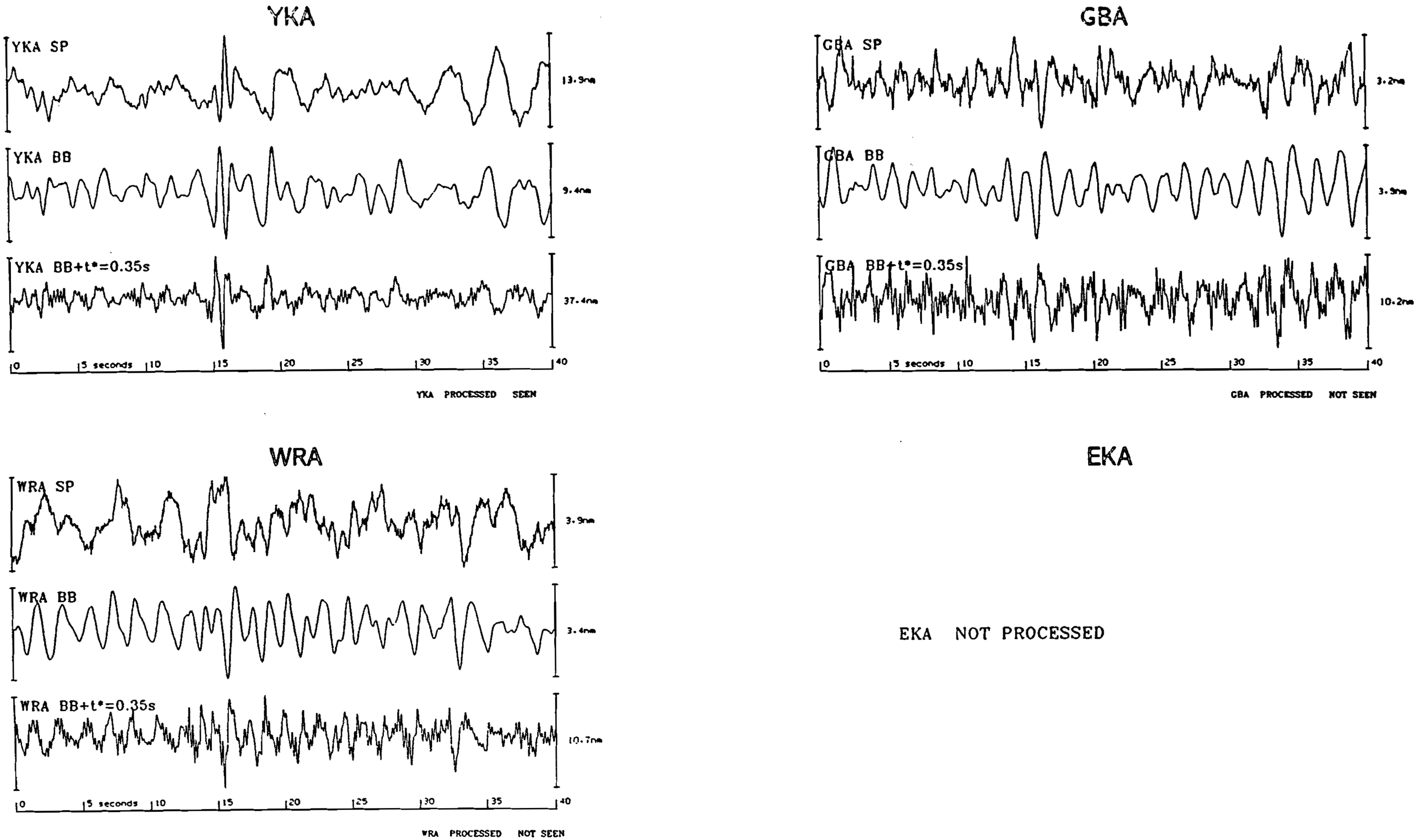

Figure A73 Short period, broad band and deconvolved P seismograms from the Mururoa explosion of 24 October 1985.

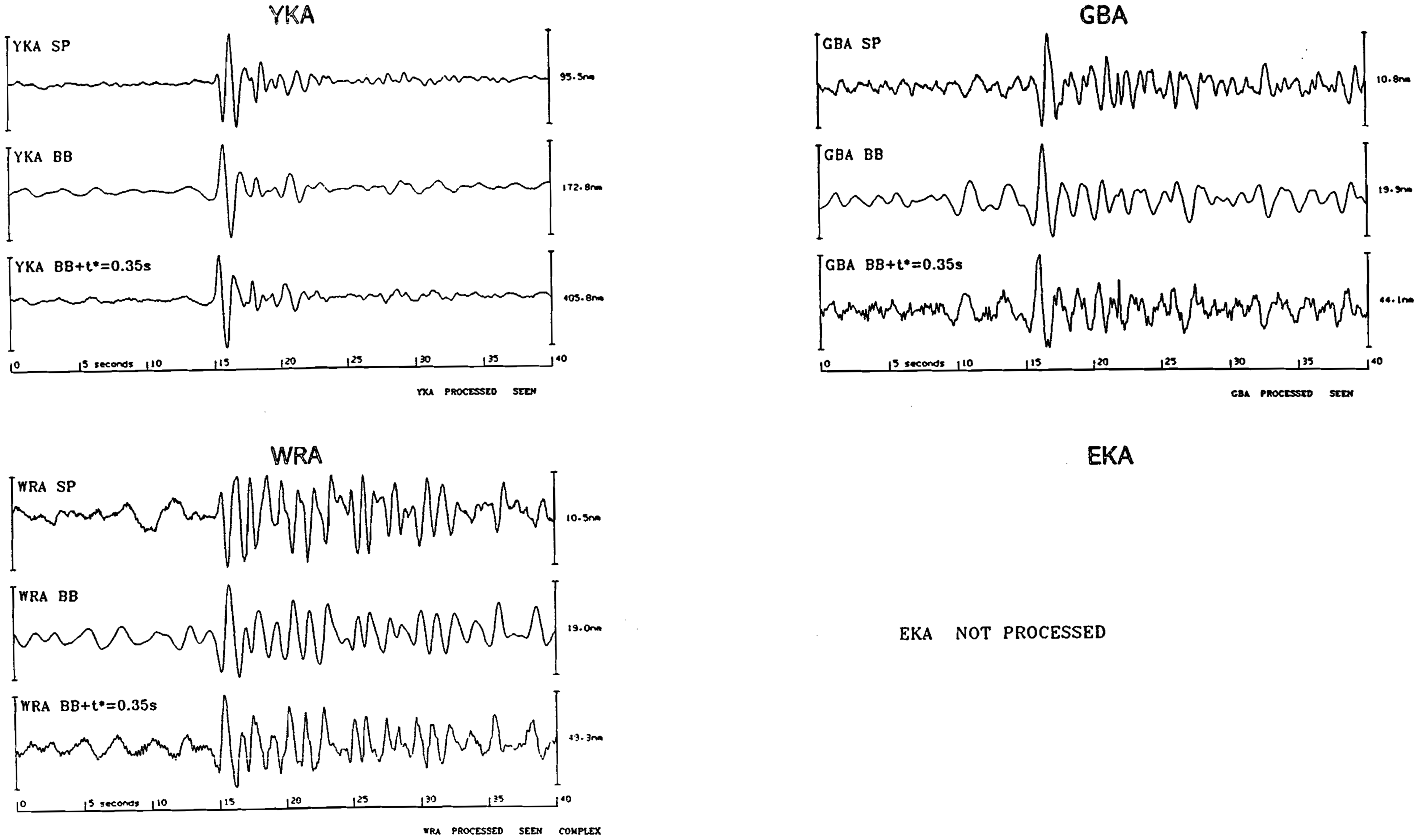

Figure A74 Short period, broad band and deconvolved P seismograms from the Mururoa explosion of 26 October 1985.

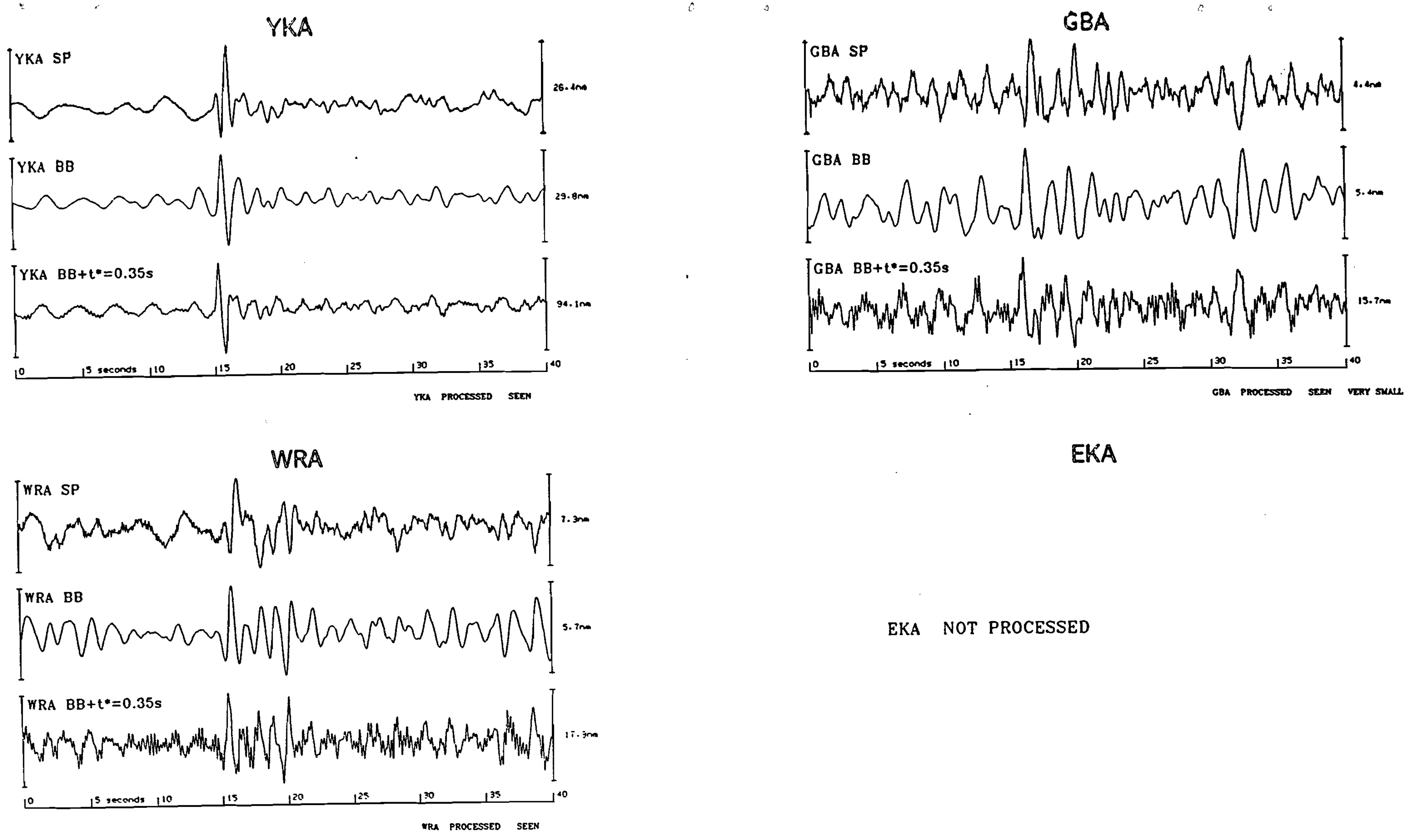

Figure A75 Short period, broad band and deconvolved P seismograms from the Mururoa explosion of 24 November 1985.

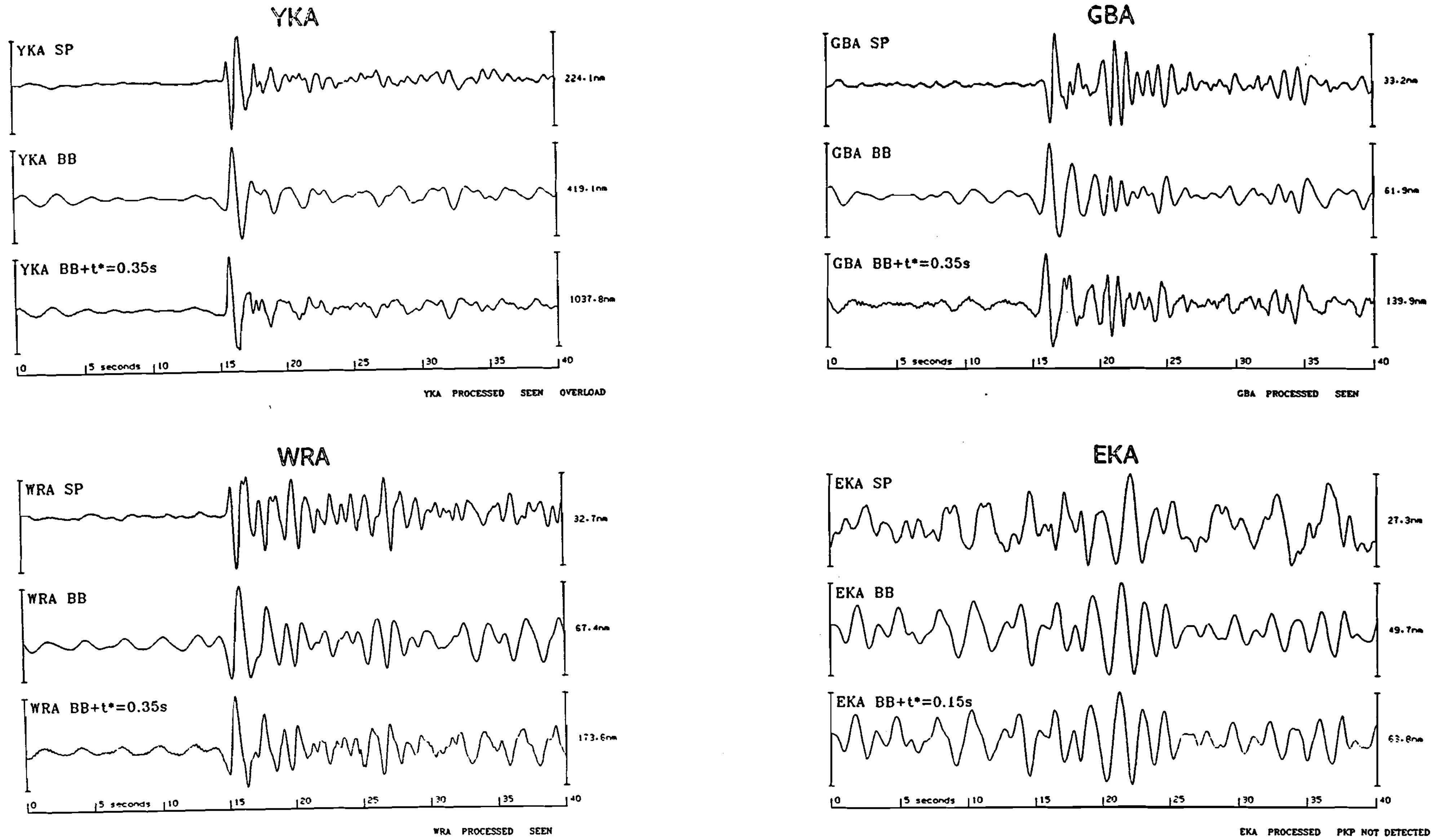

Figure A76 Short period, broad band and deconvolved P seismograms from the Mururoa explosion of 26 November 1985.

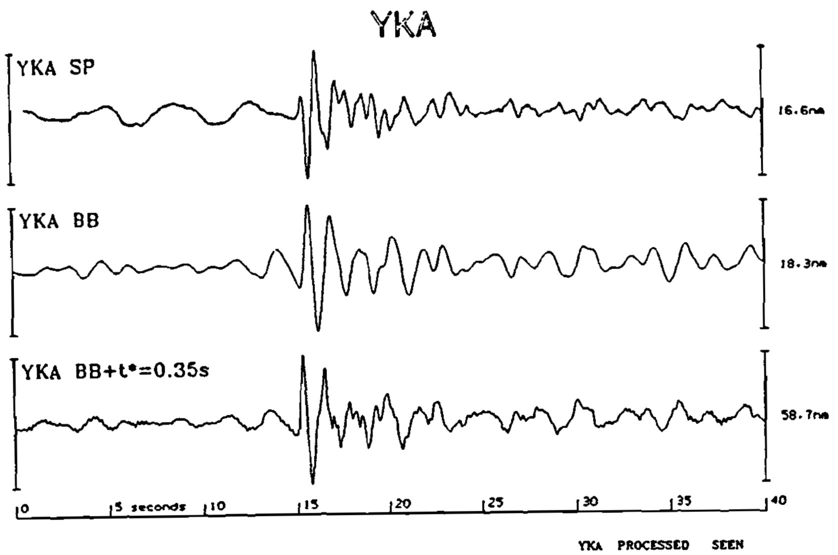

GBA

GBA NOT PROCESSED TAPE ERRORS

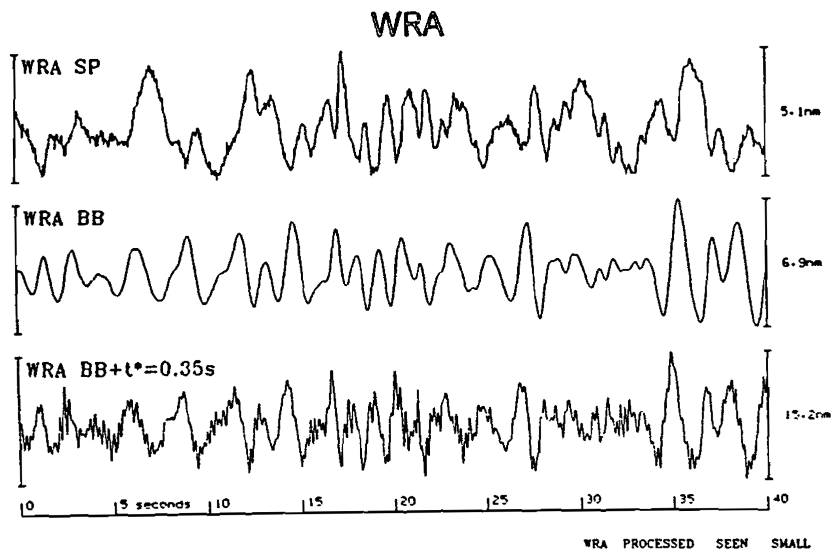

EKA

EKA NOT PROCESSED

Figure A77 Short period, broad band and deconvolved P seismograms from the Mururoa explosion of 26 April 1986.

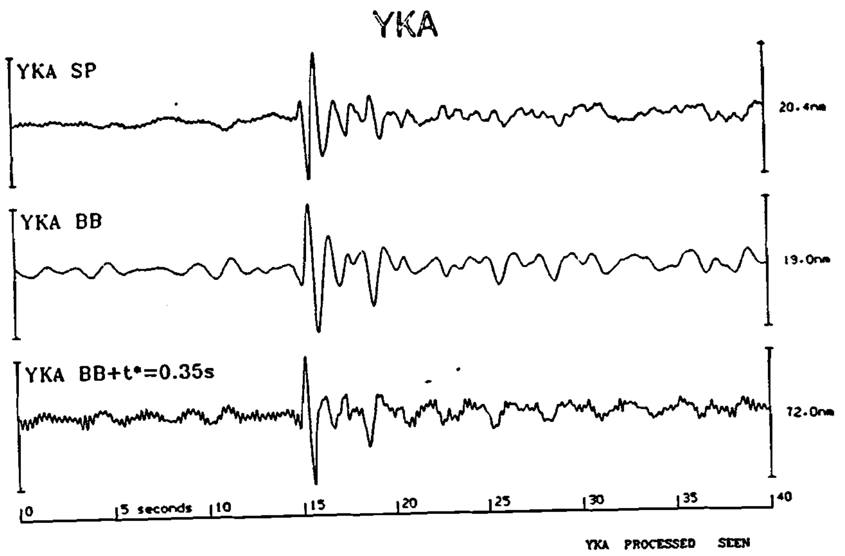

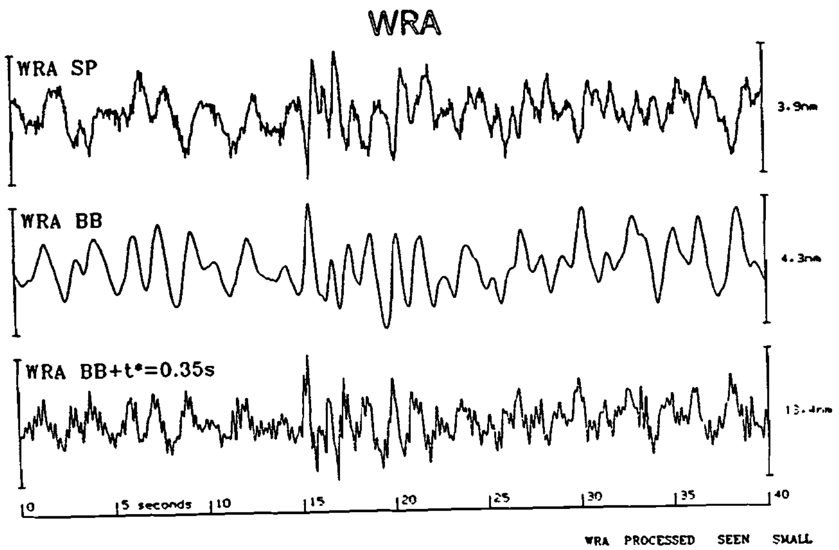

GBA

GBA NOT PROCESSED TAPE ERRORS

EKA

EKA NOT PROCESSED

Figure A78 Short period, broad band and deconvolved P seismograms from the Mururoa explosion of 6 May 1986.

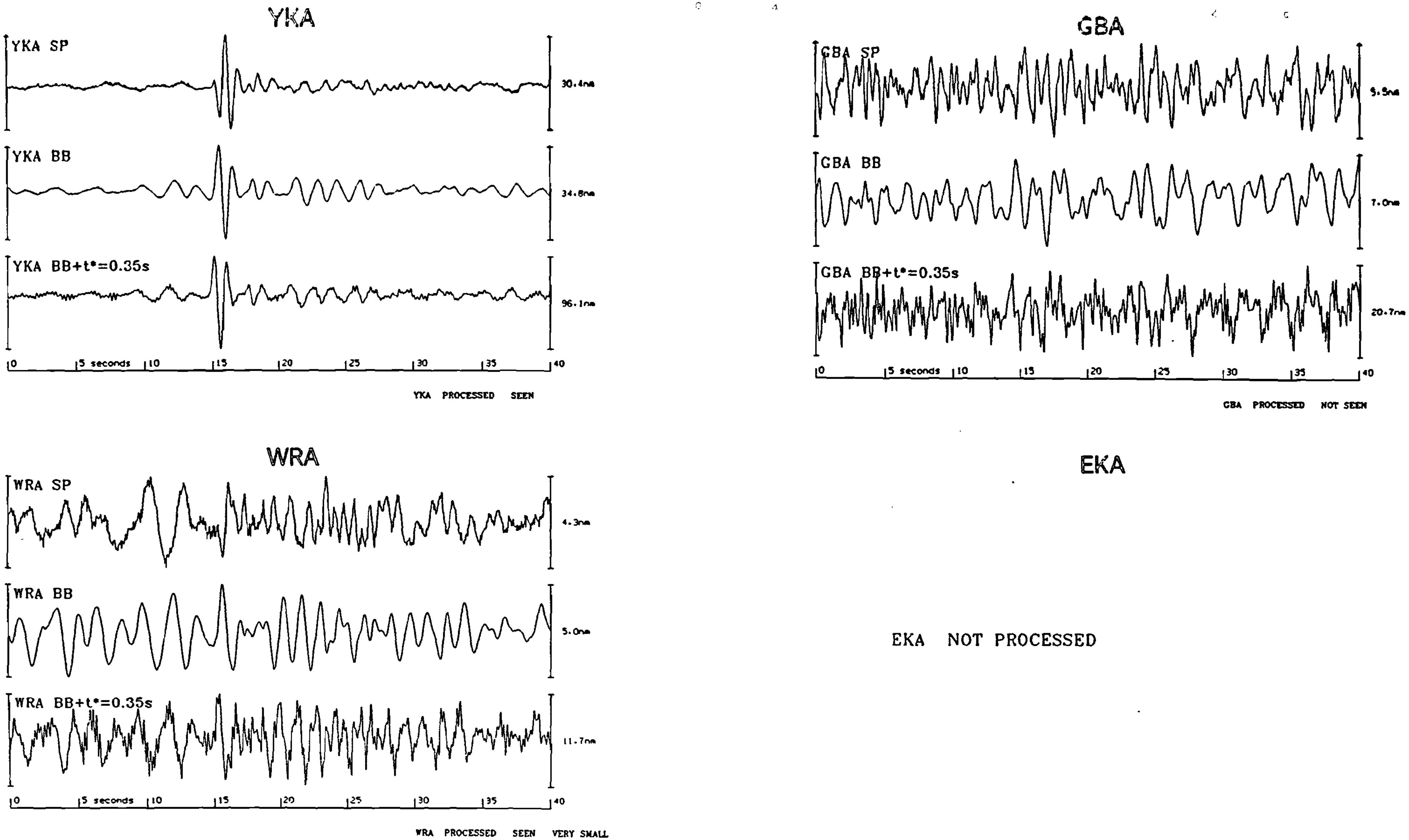

Figure A79 Short period, broad band and deconvolved P seismograms from the Mururoa explosion of 27 May 1986.

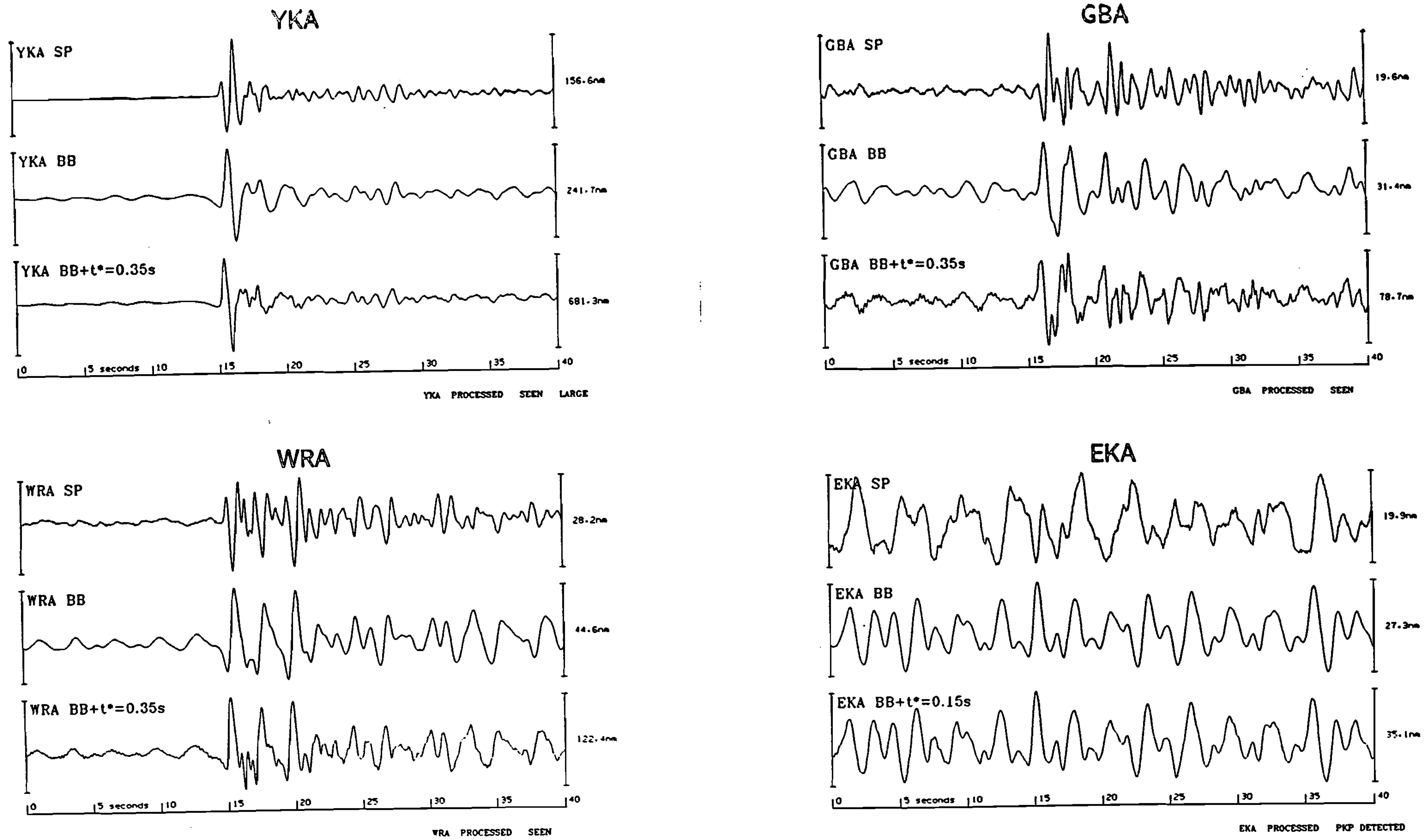

Figure A80 Short period, broad band and deconvolved P seismograms from the Mururoa explosion of 30 May 1986.

YKA

YKA NOT PROCESSED NO TAPE

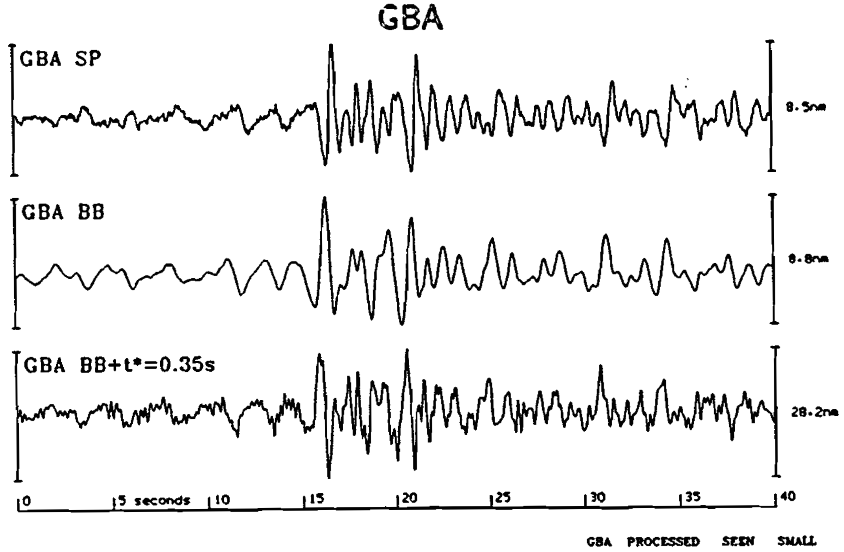

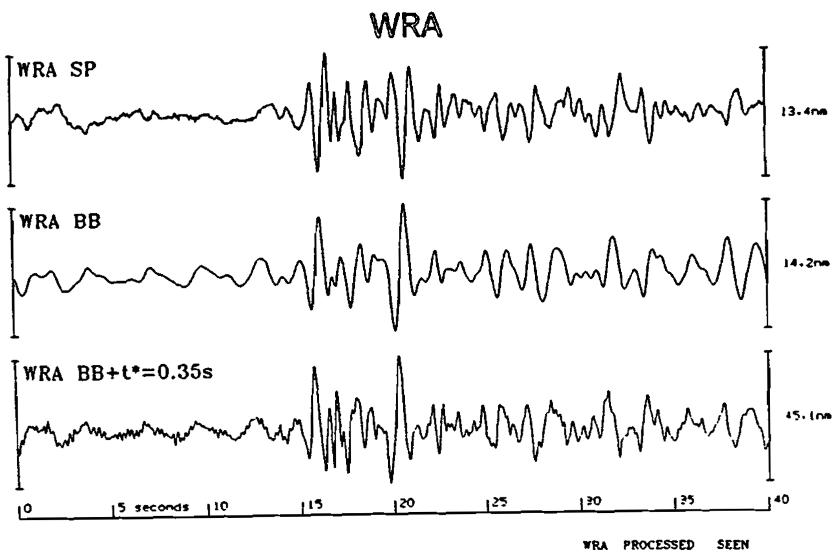

EKA

EKA NOT PROCESSED

Figure A81 Short period, broad band and deconvolved P seismograms from the Mururoa explosion of 12 November 1986.

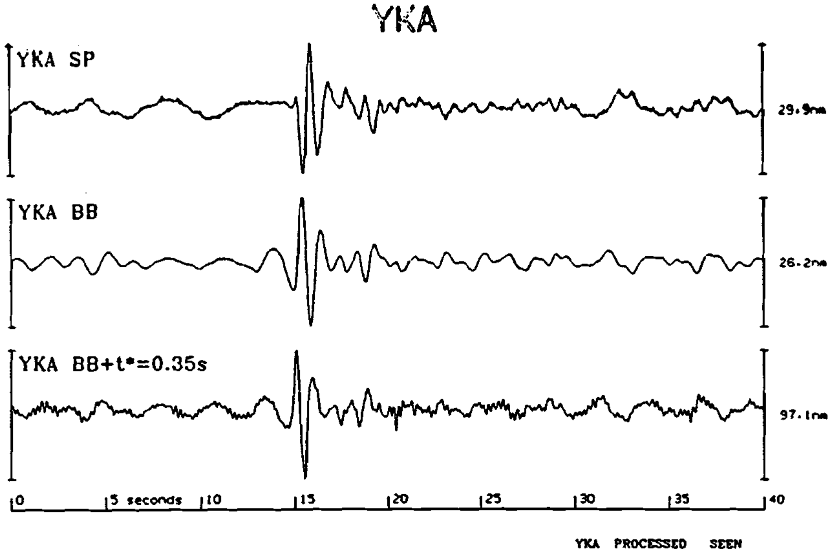

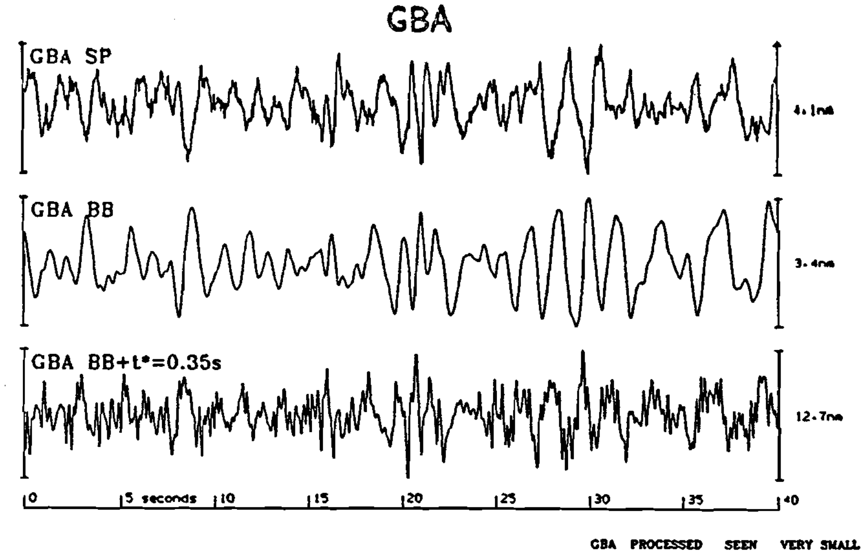

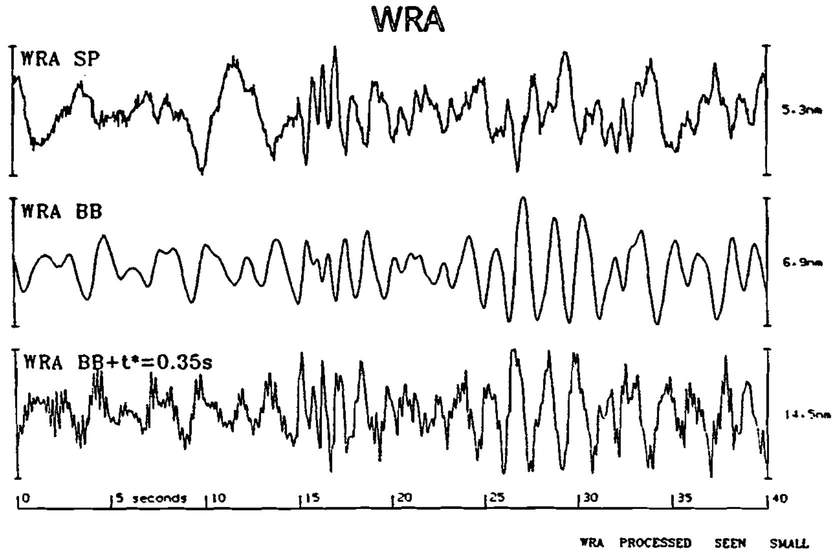

EKA

EKA NOT PROCESSED

Figure A82 Short period, broad band and deconvolved P seismograms from the Mururoa explosion of 6 December 1986.

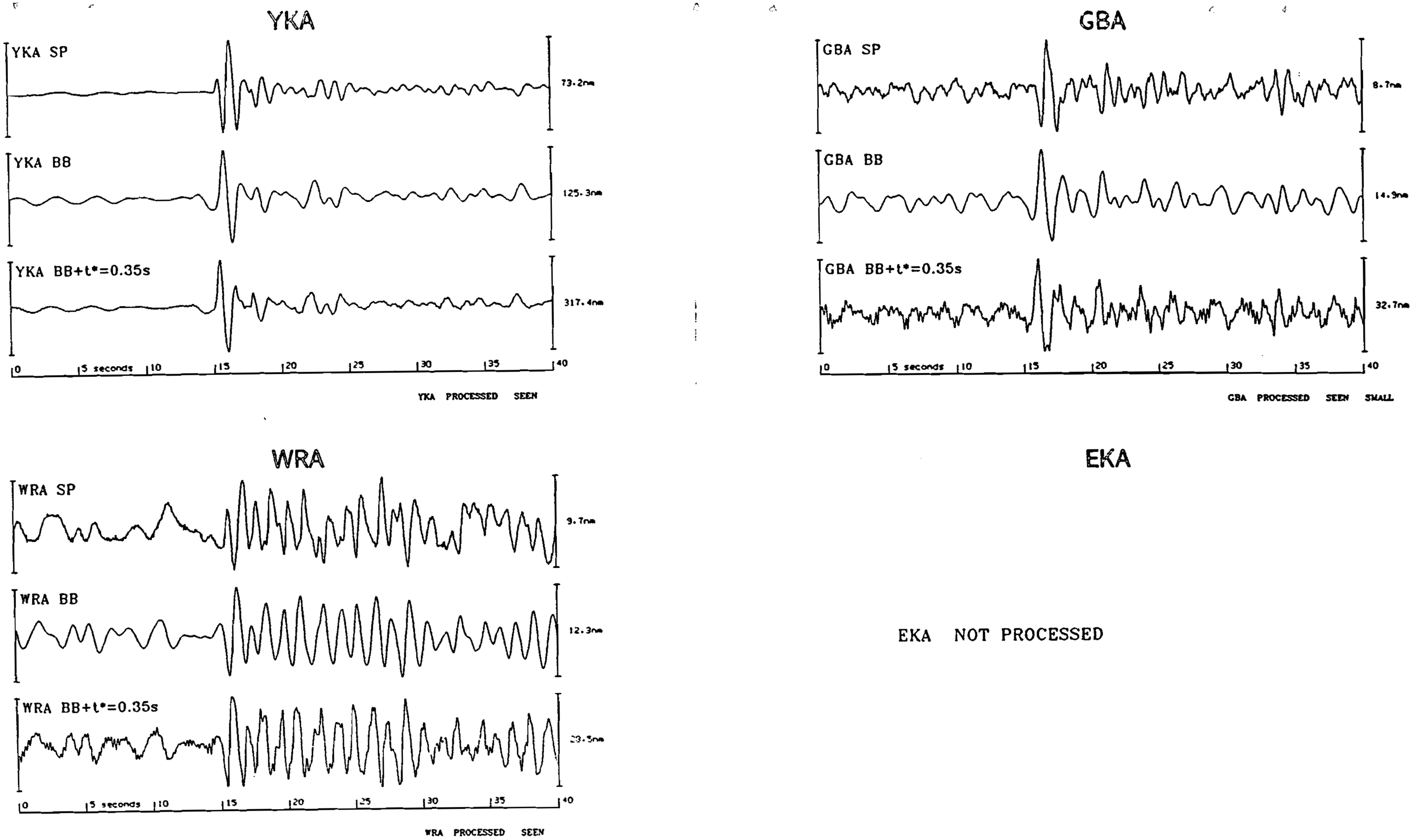

Figure A83 Short period, broad band and deconvolved P seismograms from the Mururoa explosion of 10 December 1986.

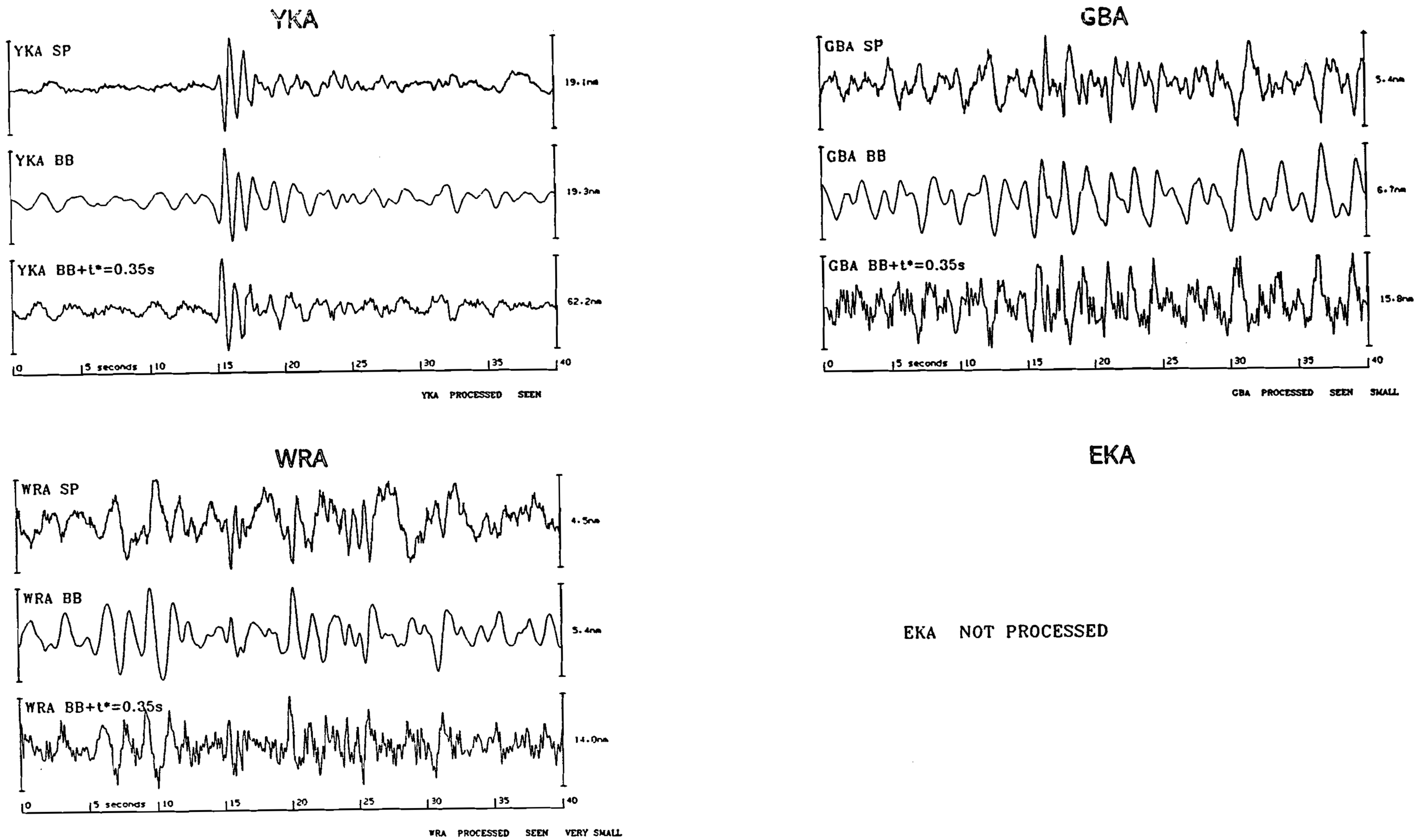

Figure A84 Short period, broad band and deconvolved P seismograms from the Mururoa explosion of 5 May 1987.

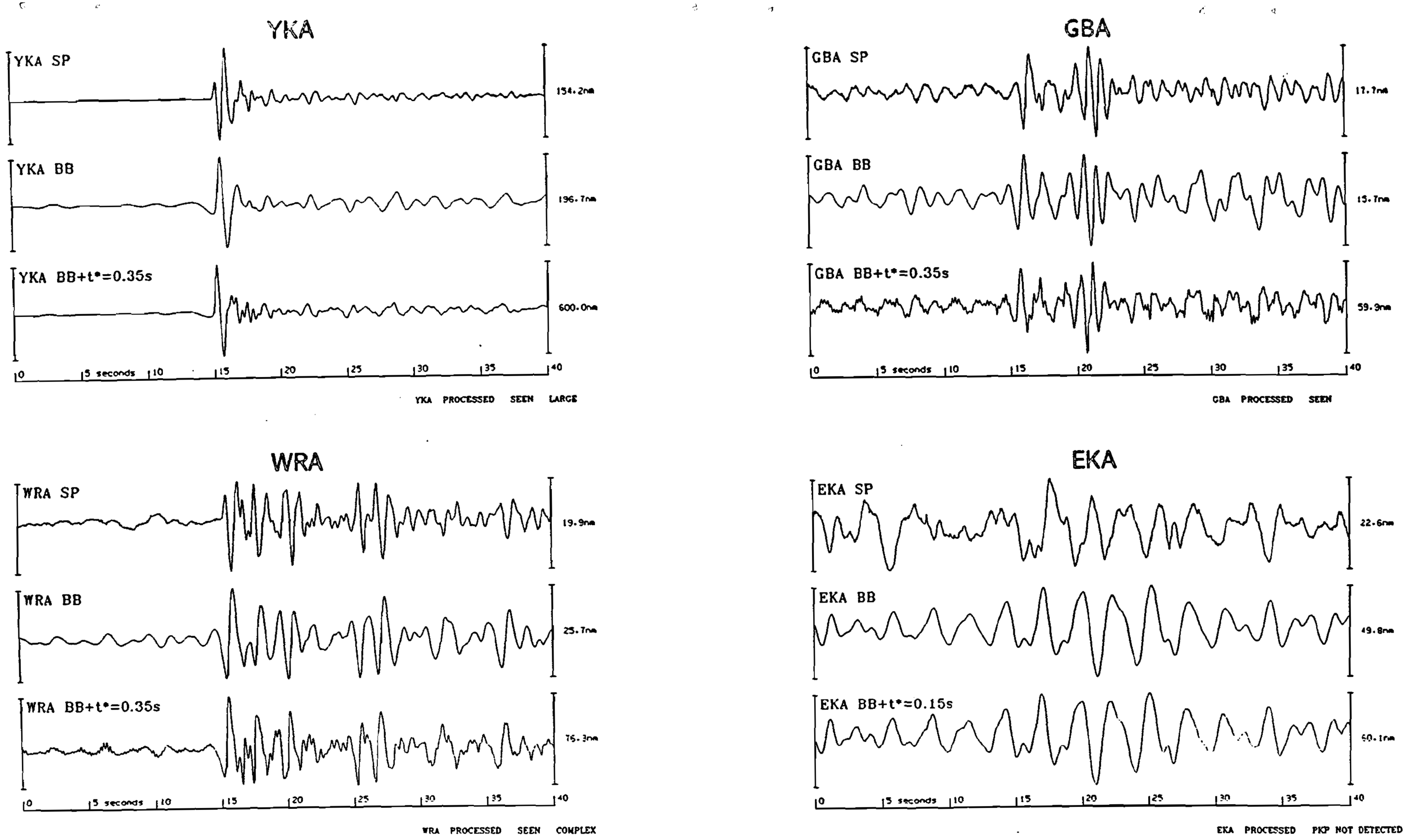

Figure A85 Short period, broad band and deconvolved P seismograms from the Mururoa explosion of 20 May 1987.

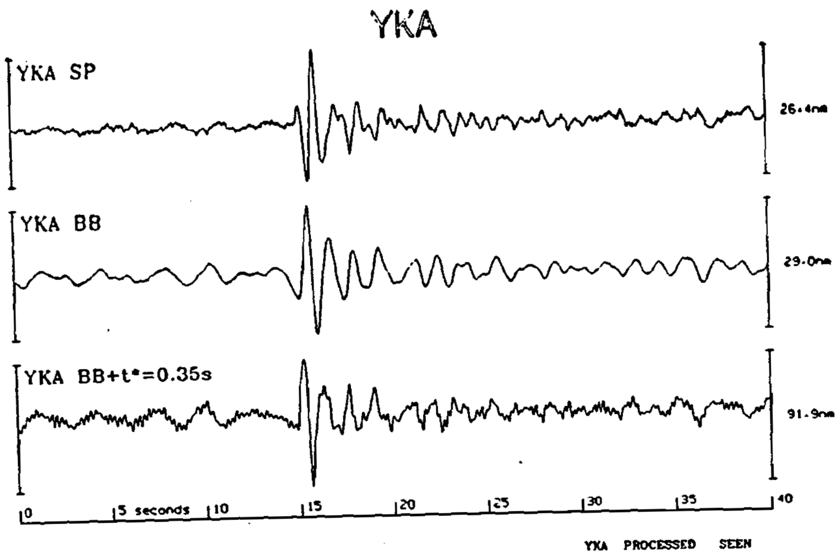

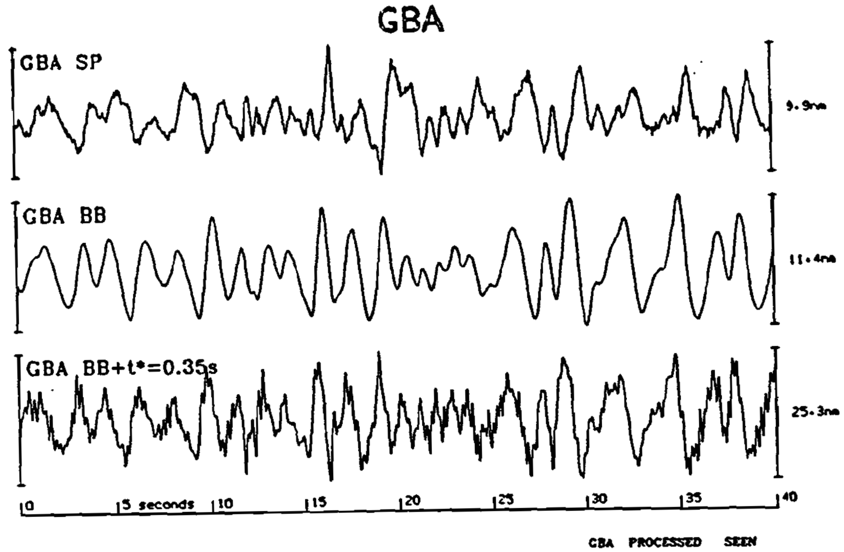

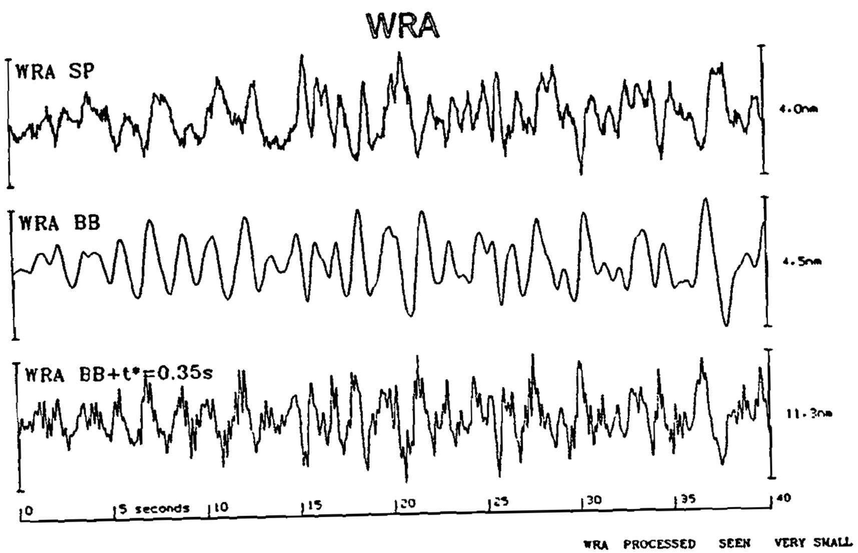

EKA

EKA NOT PROCESSED

Figure A86 Short period, broad band and deconvolved P seismograms from the Mururoa explosion of 6 June 1987.

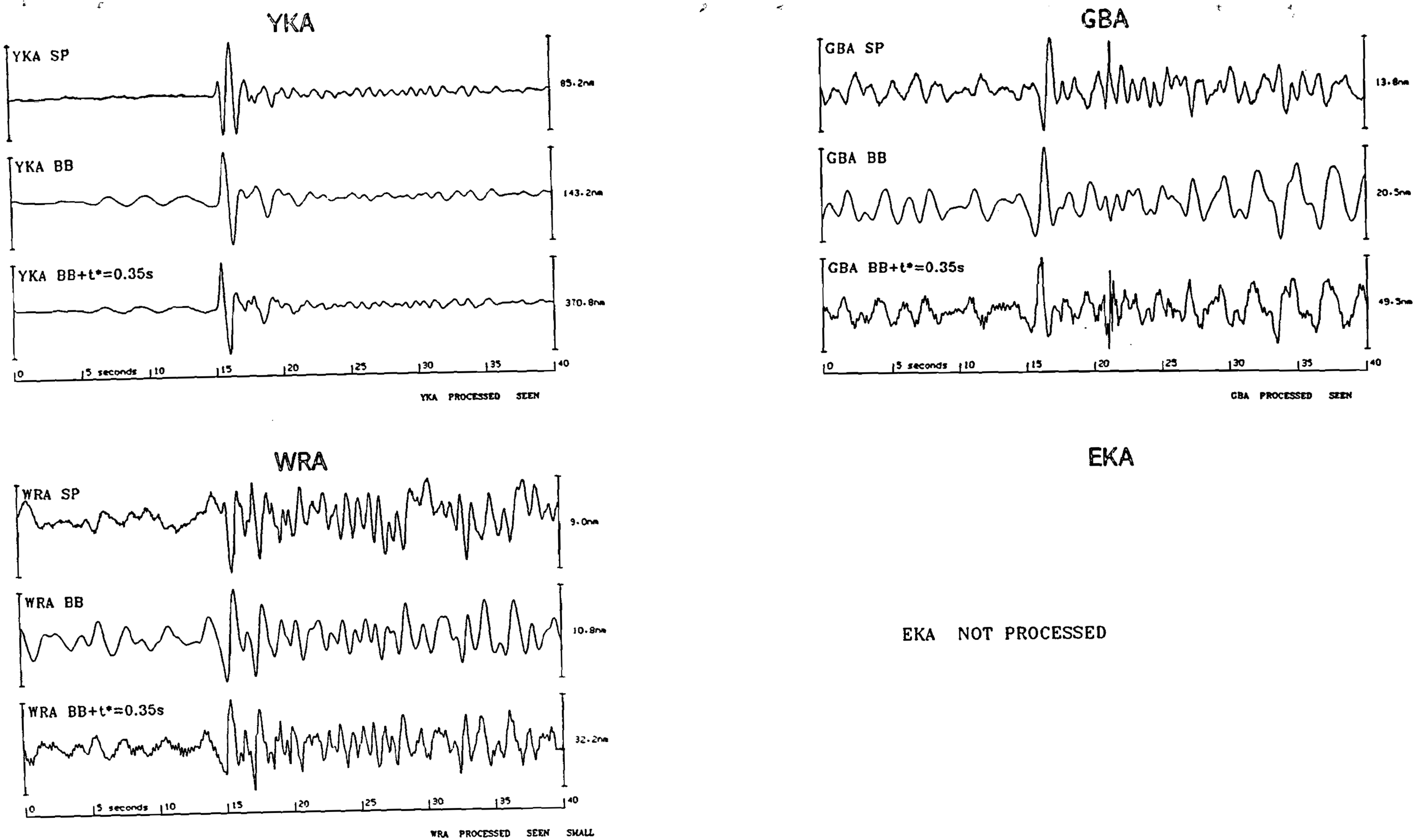

Figure A87 Short period, broad band and deconvolved P seismograms from the Mururoa explosion of 21 June 1987.

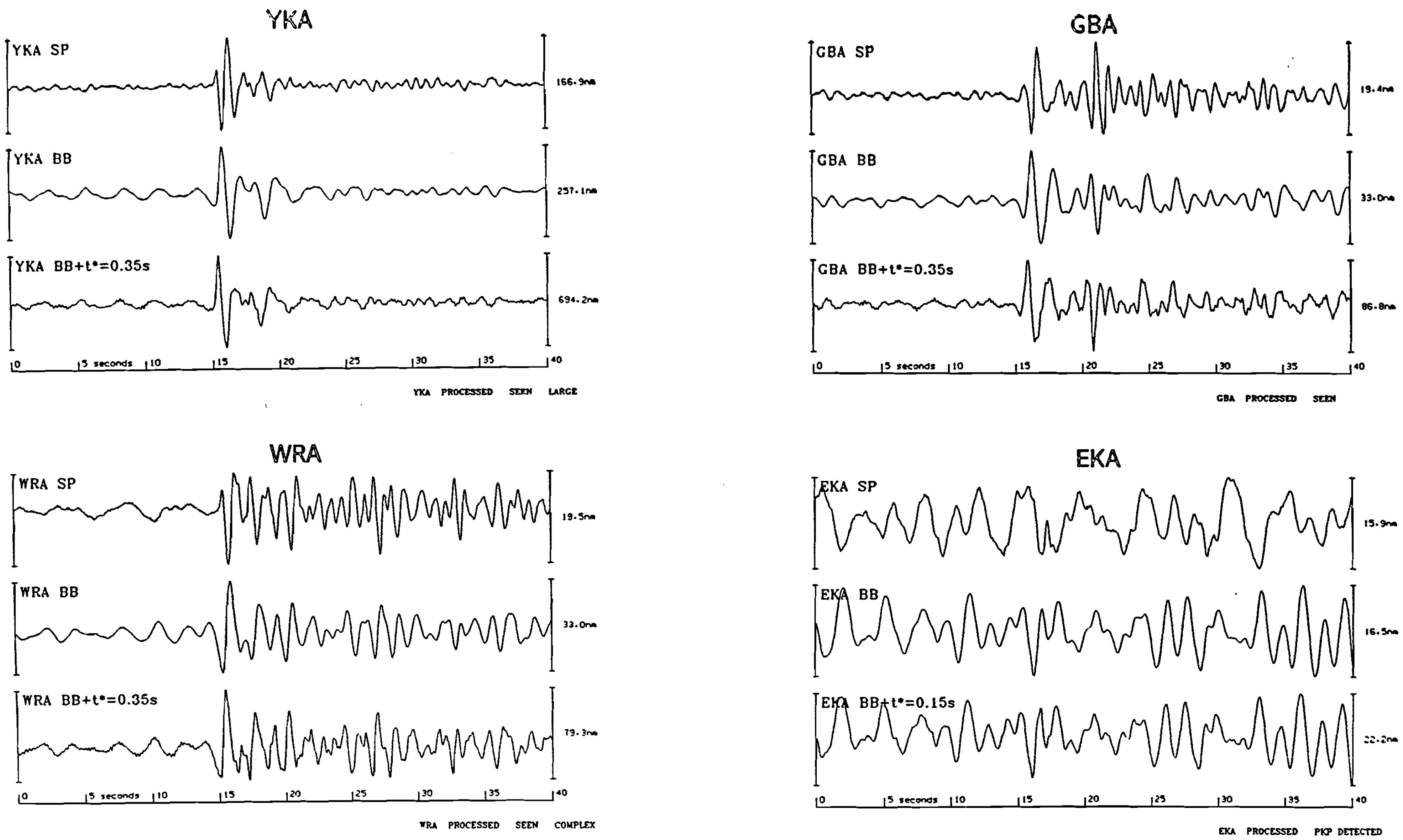

Figure A88 Short period, broad band and deconvolved P seismograms from the Mururoa explosion of 23 October 1987.

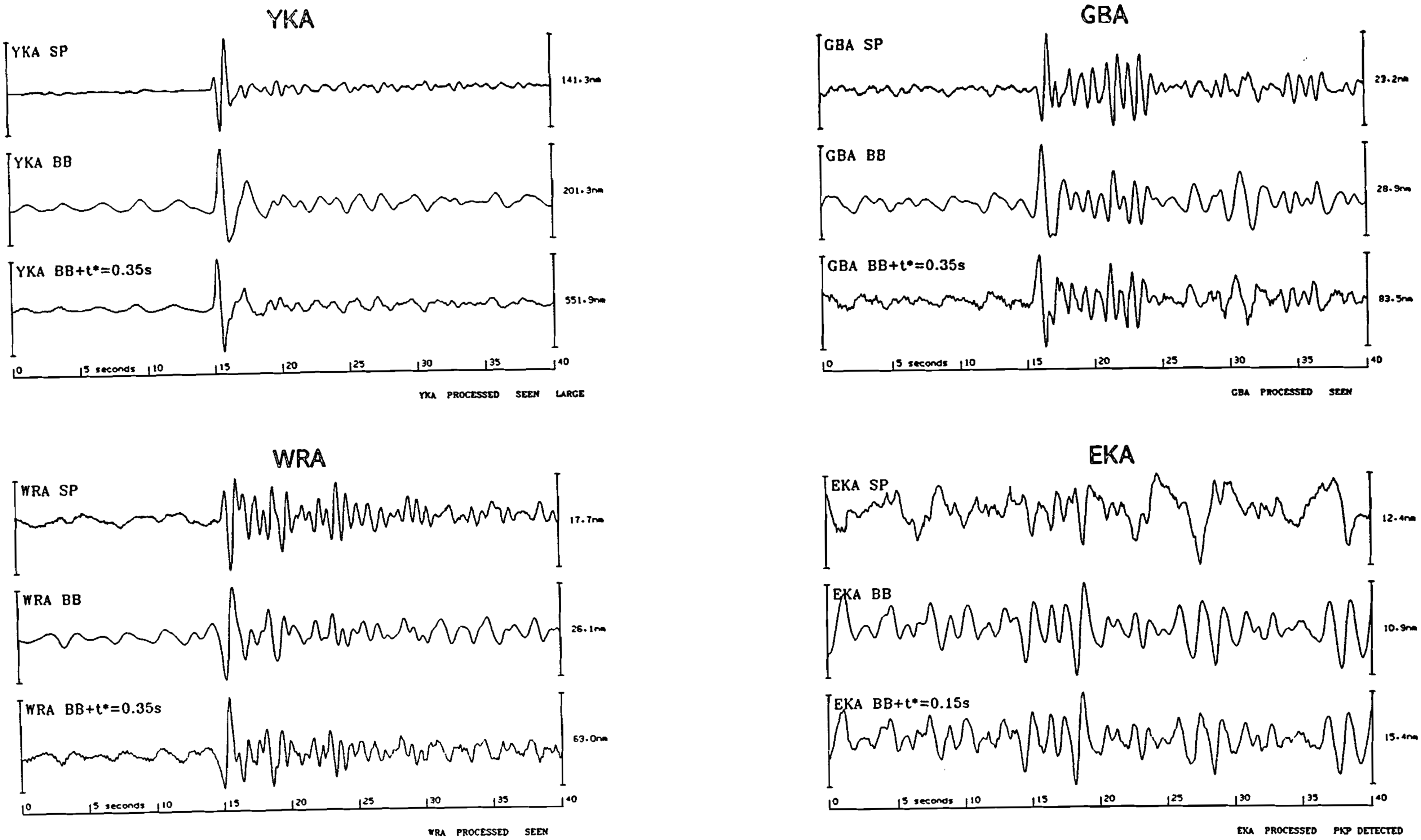

Figure A89 Short period, broad band and deconvolved P seismograms from the Mururoa explosion of 5 November 1987.

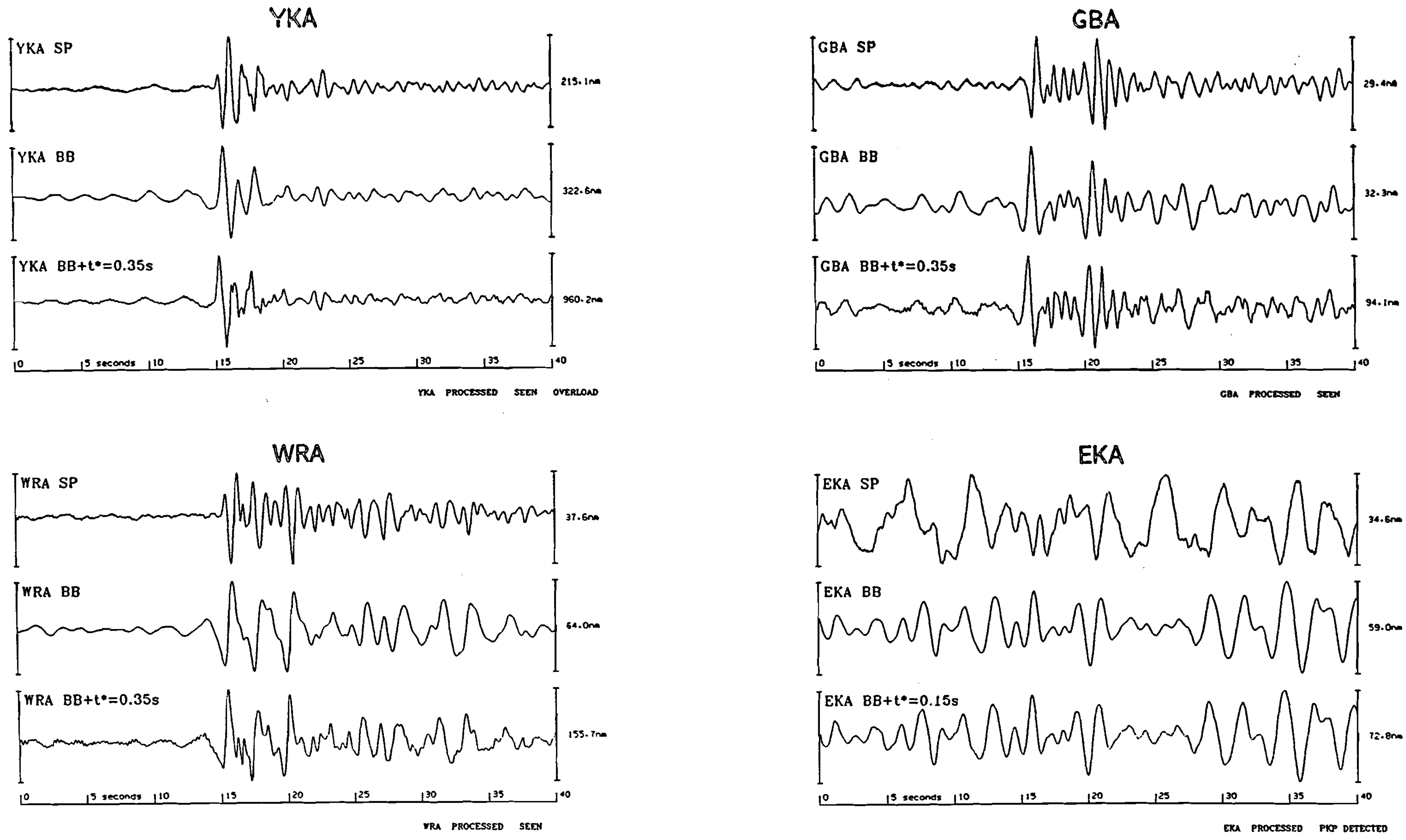

Figure A90 Short period, broad band and deconvolved P seismograms from the Mururoa explosion of 19 November 1987.

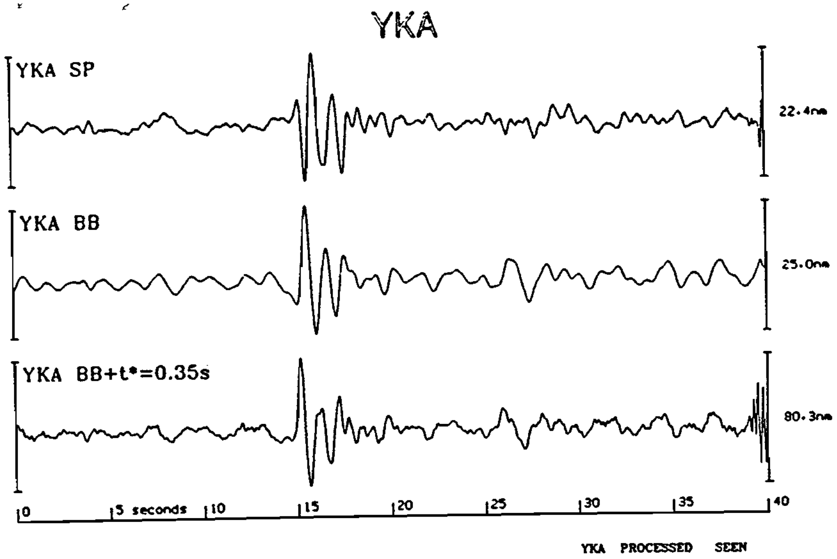

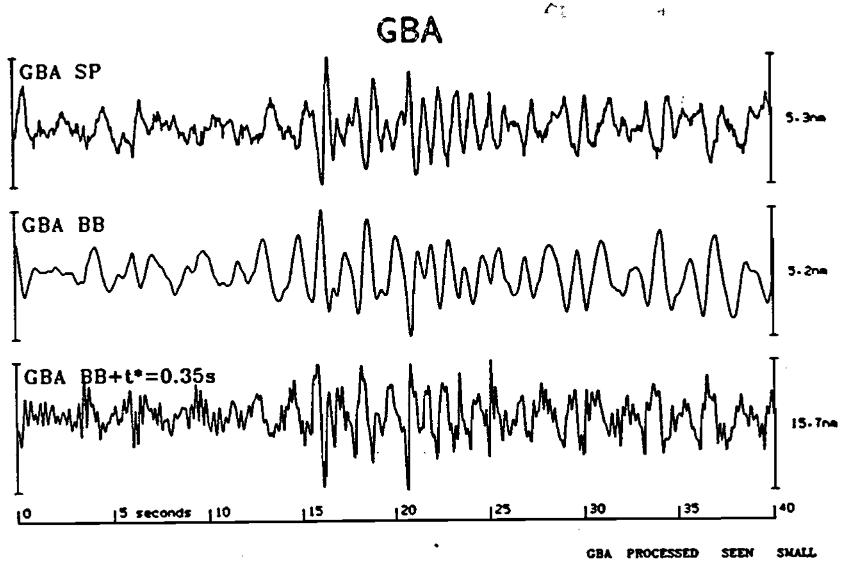

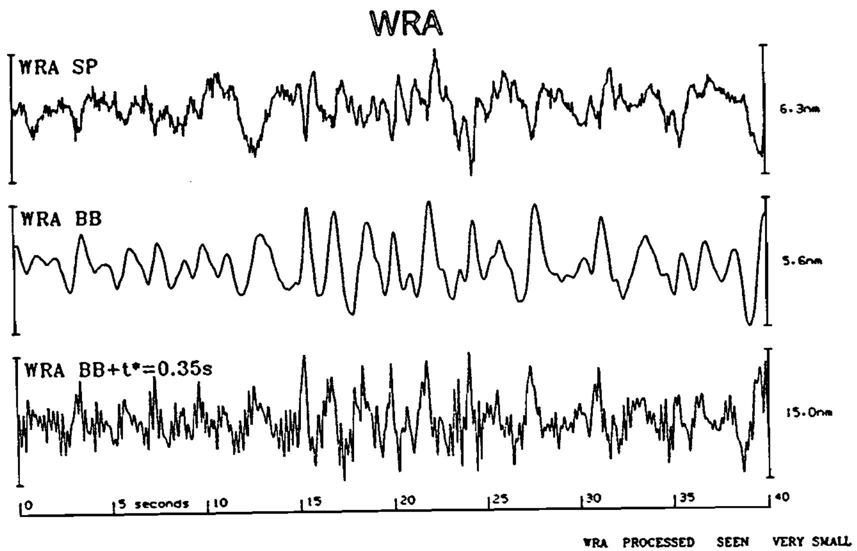

EKA

EKA NOT PROCESSED

Figure A91 Short period, broad band and deconvolved P seismograms from the Mururoa explosion of 29 November 1987.

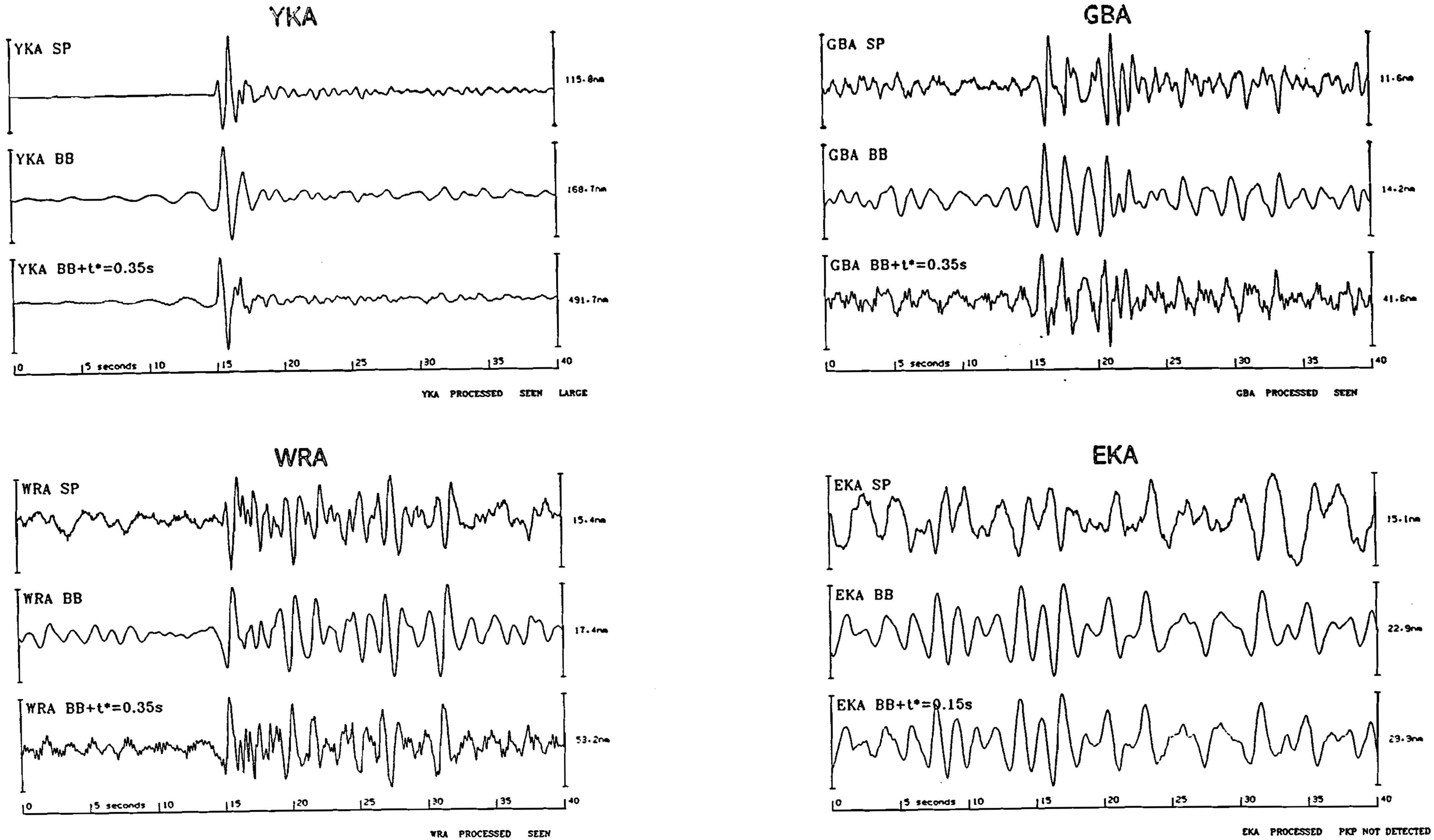

Figure A92 Short period, broad band and deconvolved P seismograms from the Mururoa explosion of 11 May 1988.

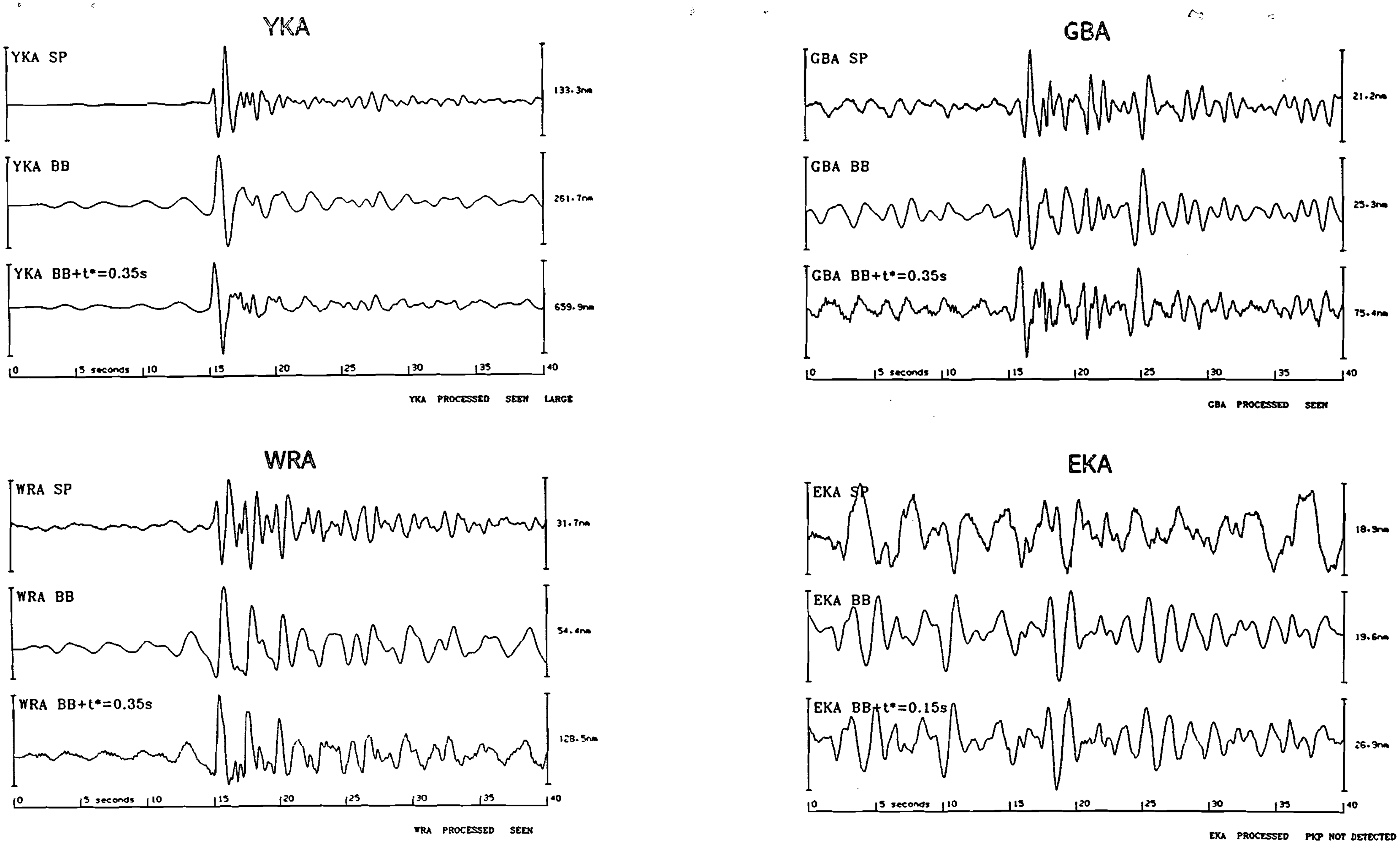

Figure A93 Short period, broad band and deconvolved P seismograms from the Mururoa explosion of 25 May 1988.

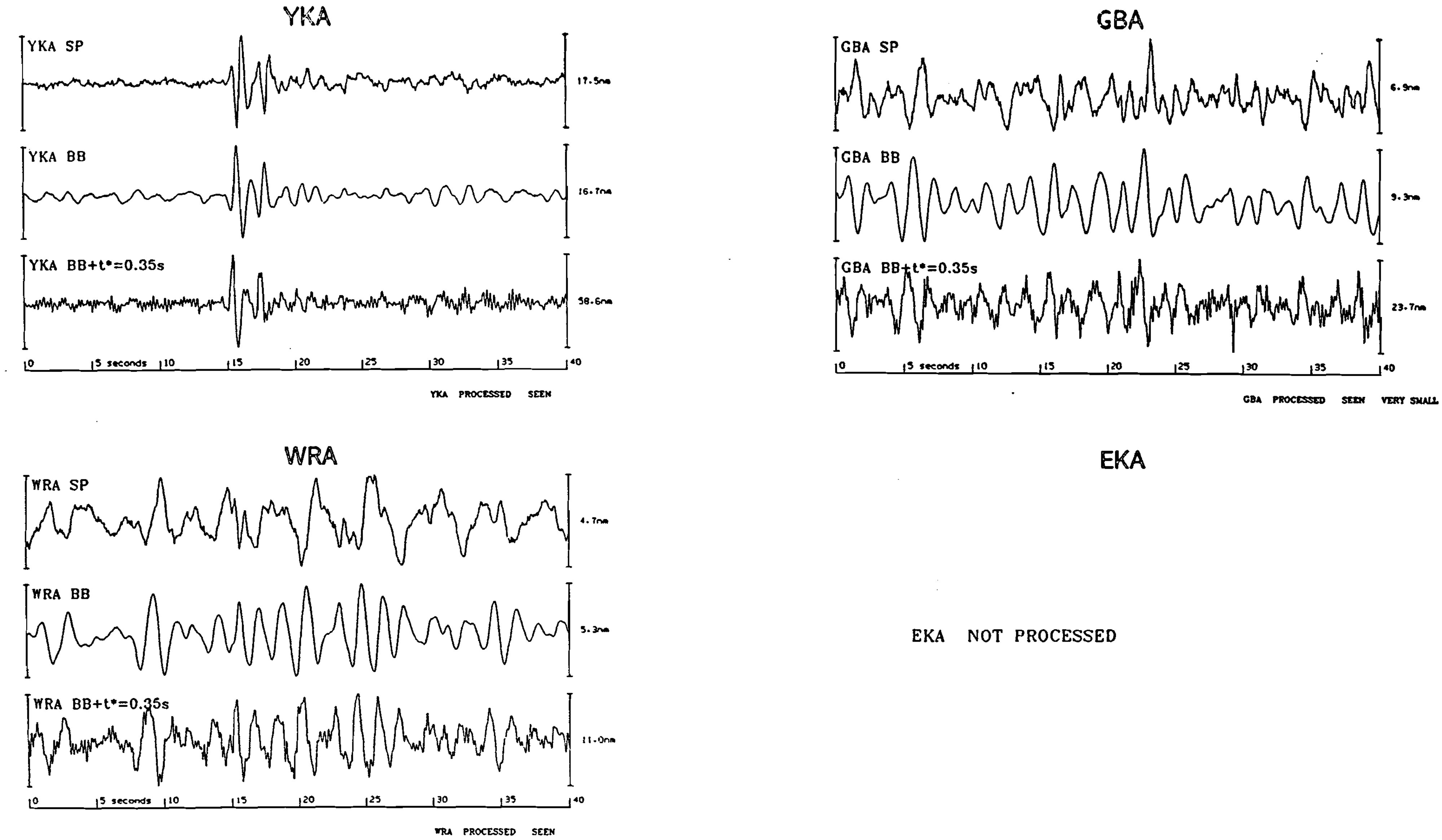

Figure A94 Short period, broad band and deconvolved P seismograms from the Mururoa explosion of 16 June 1988.

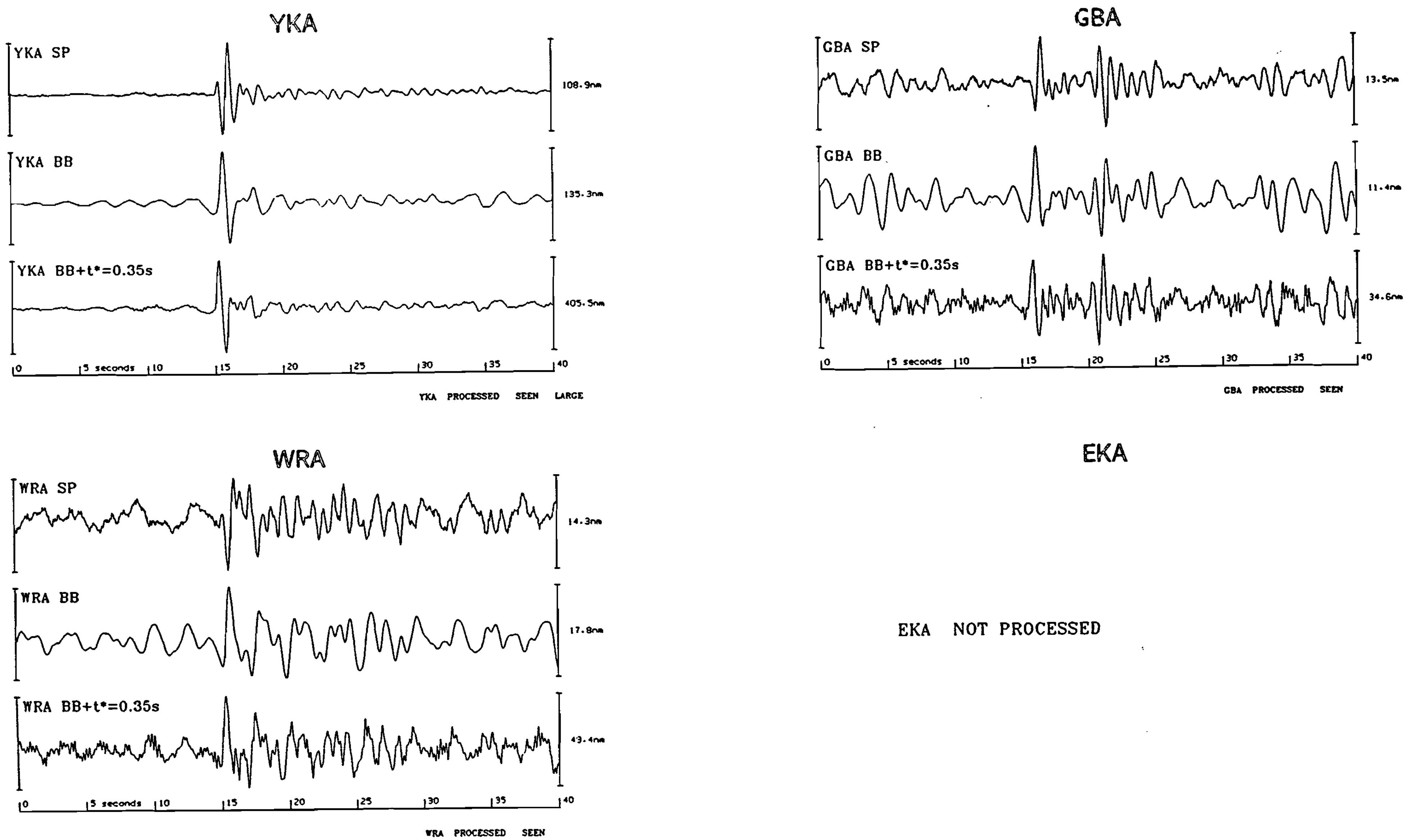

Figure A95 Short period, broad band and deconvolved P seismograms from the Mururoa explosion of 23 June 1988.

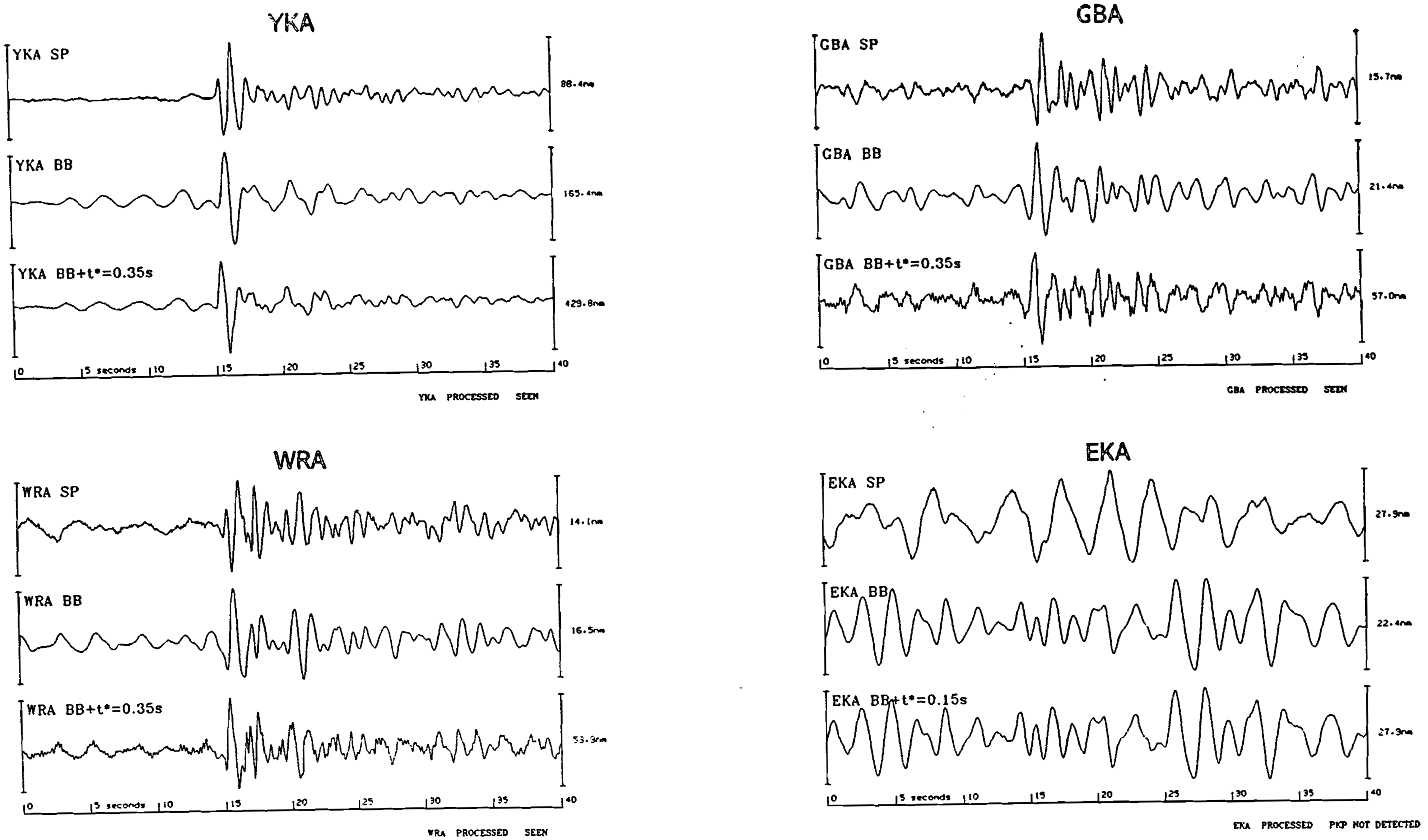

Figure A96 Short period, broad band and deconvolved P seismograms from the Mururoa explosion of 5 November 1988.

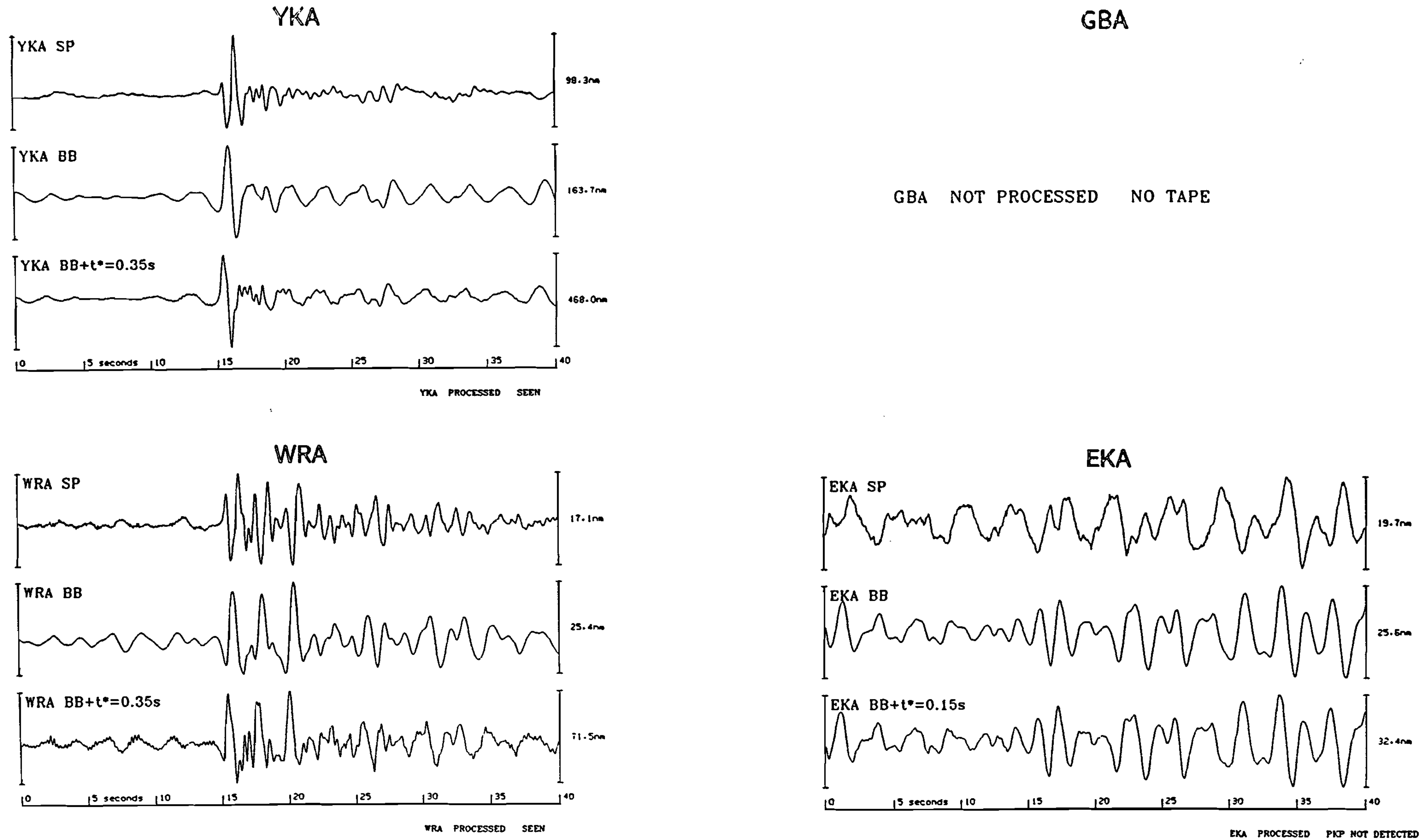

Figure A97 Short period, broad band and deconvolved P seismograms from the Mururoa explosion of 23 November 1988.

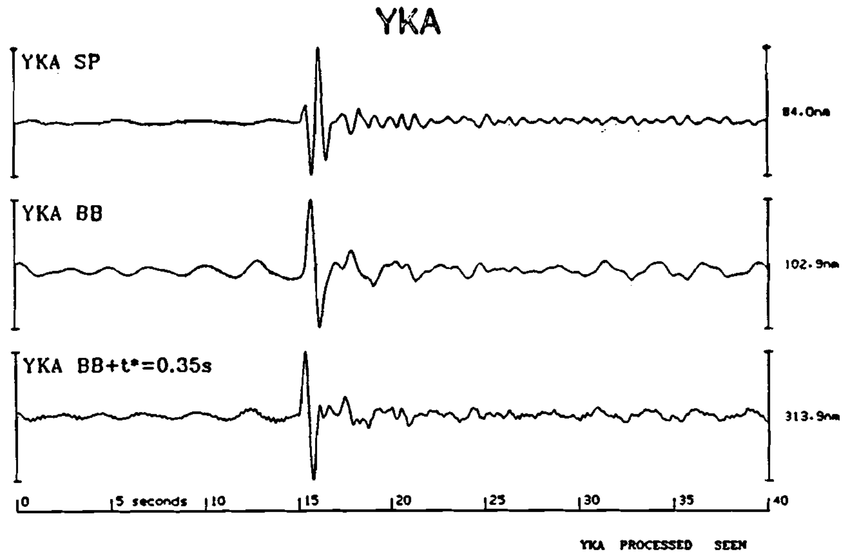

WRA

WRA NOT PROCESSED NOT AVAILABLE

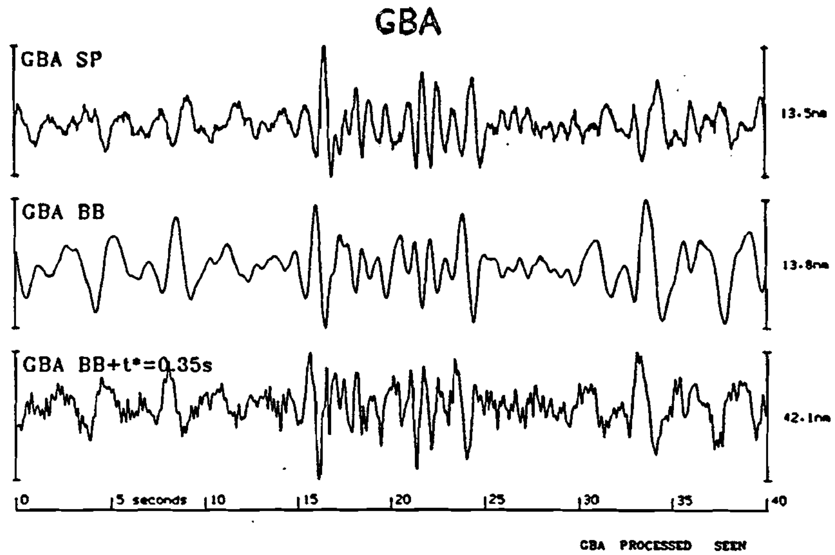

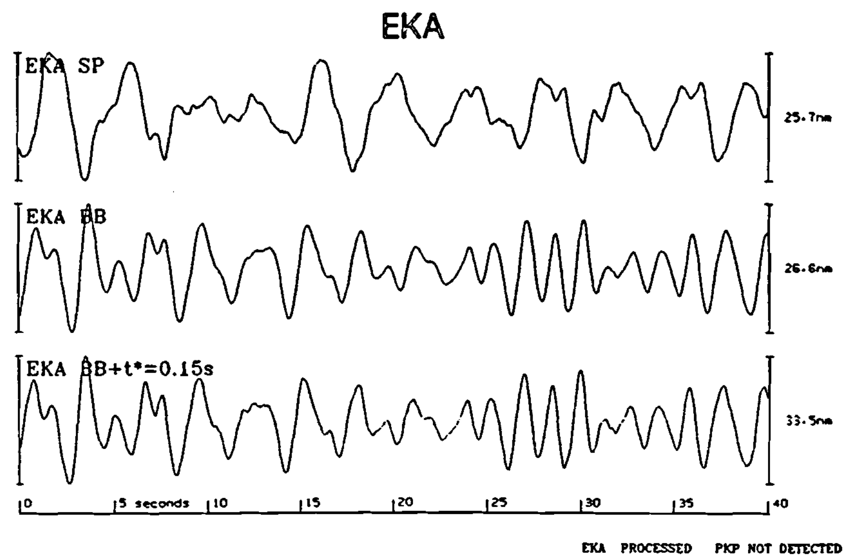

Figure A98 Short period, broad band and deconvolved P seismograms from the Mururoa explosion of 11 May 1989.

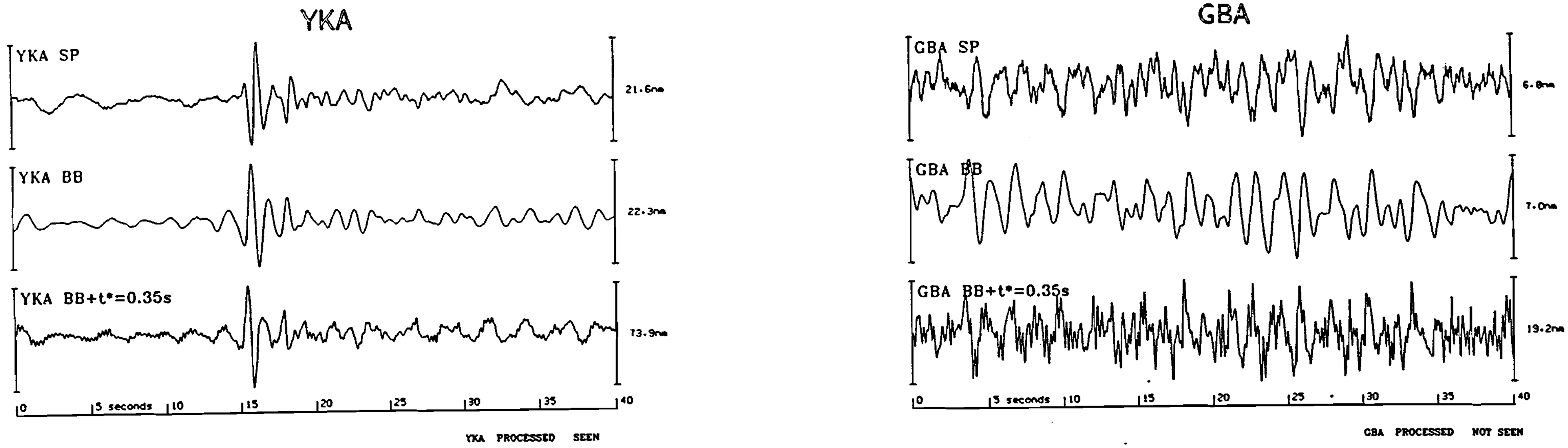

WRA

WRA NOT PROCESSED NOT AVAILABLE

EKA

EKA NOT PROCESSED

Figure A99 Short period, broad band and deconvolved P seismograms from the Mururoa explosion of 20 May 1989.

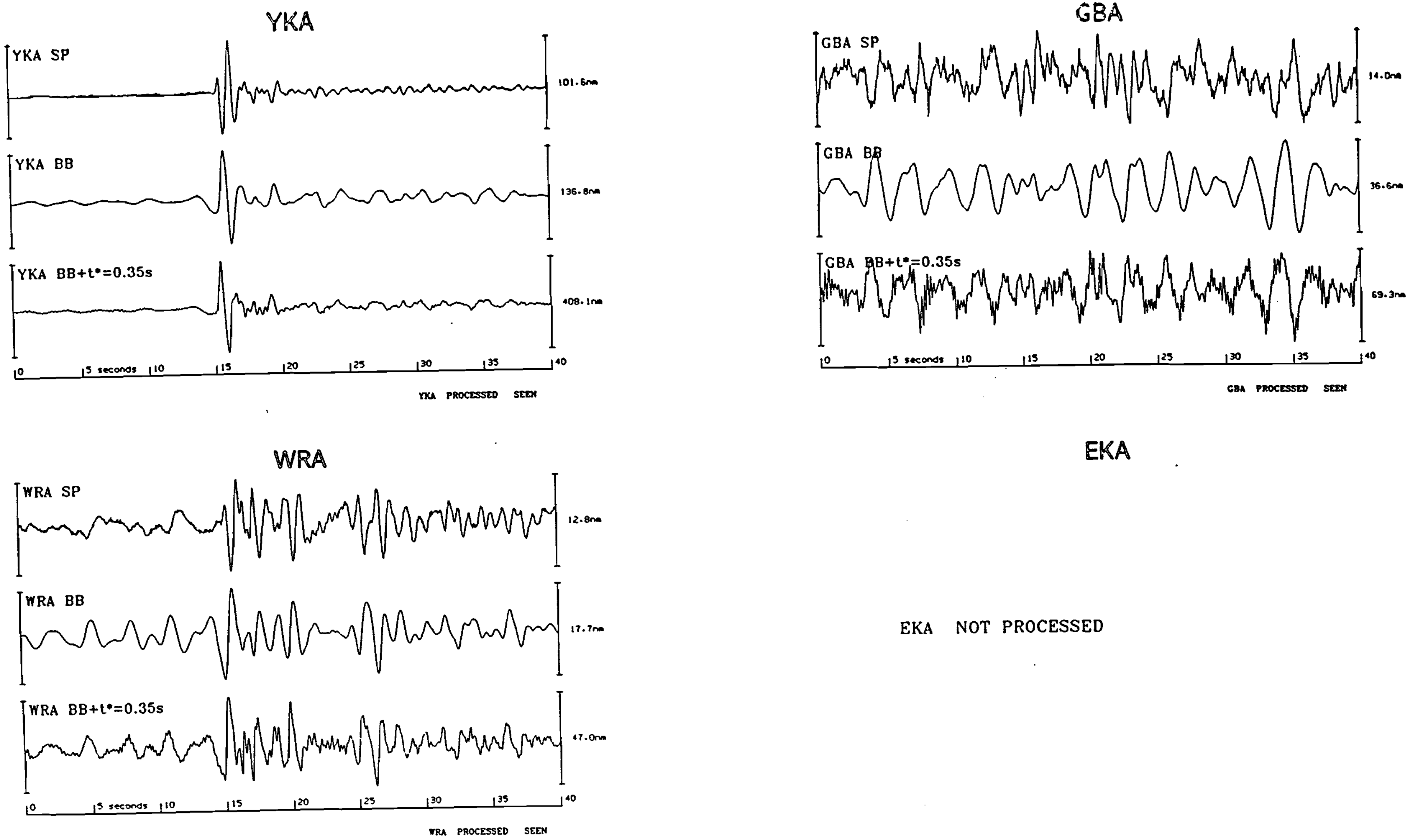

Figure A100 Short period, broad band and deconvolved P seismograms from the Mururoa explosion of 3 June 1989.

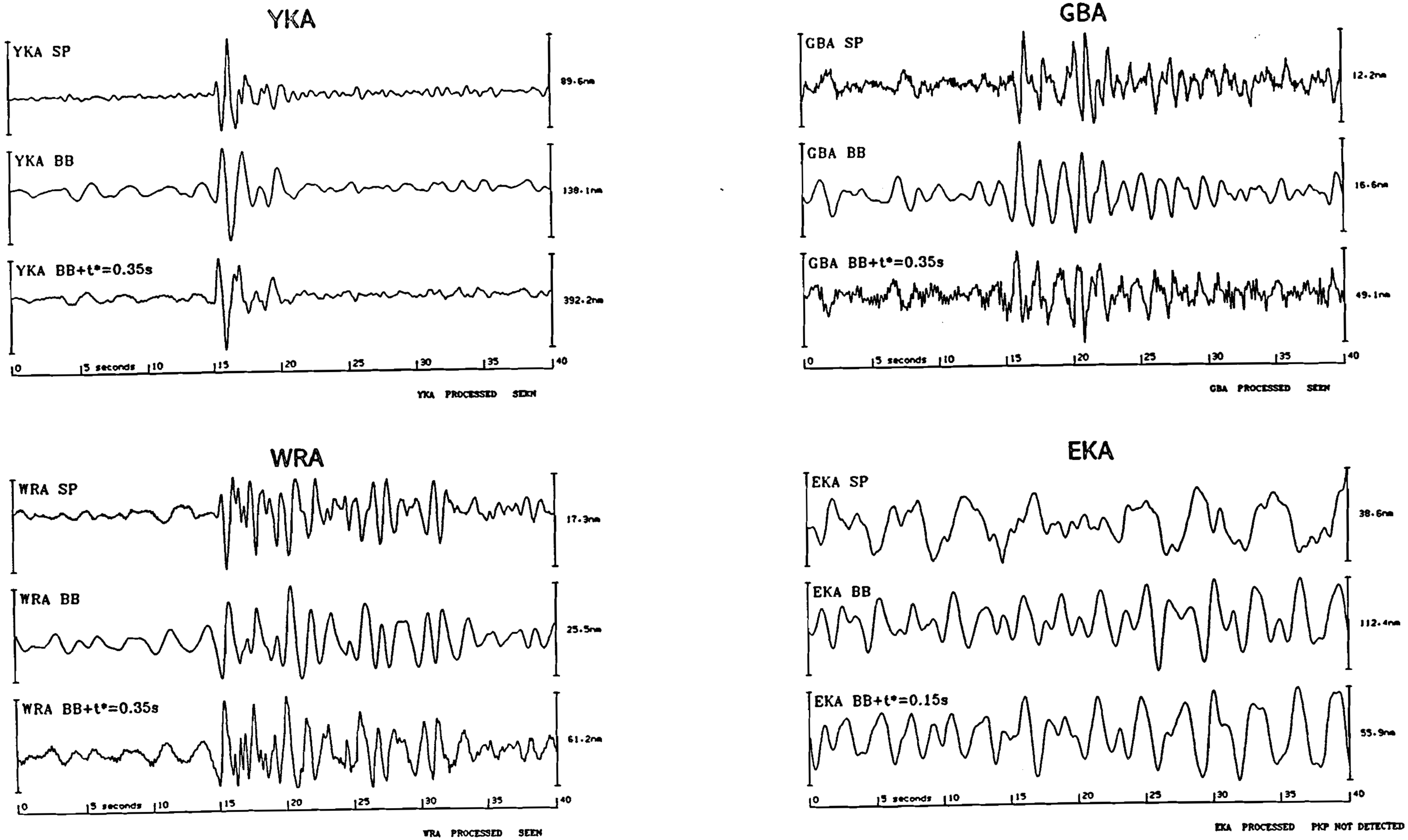

Figure A101 Short period, broad band and deconvolved P seismograms from the Mururoa explosion of 24 October 1989.

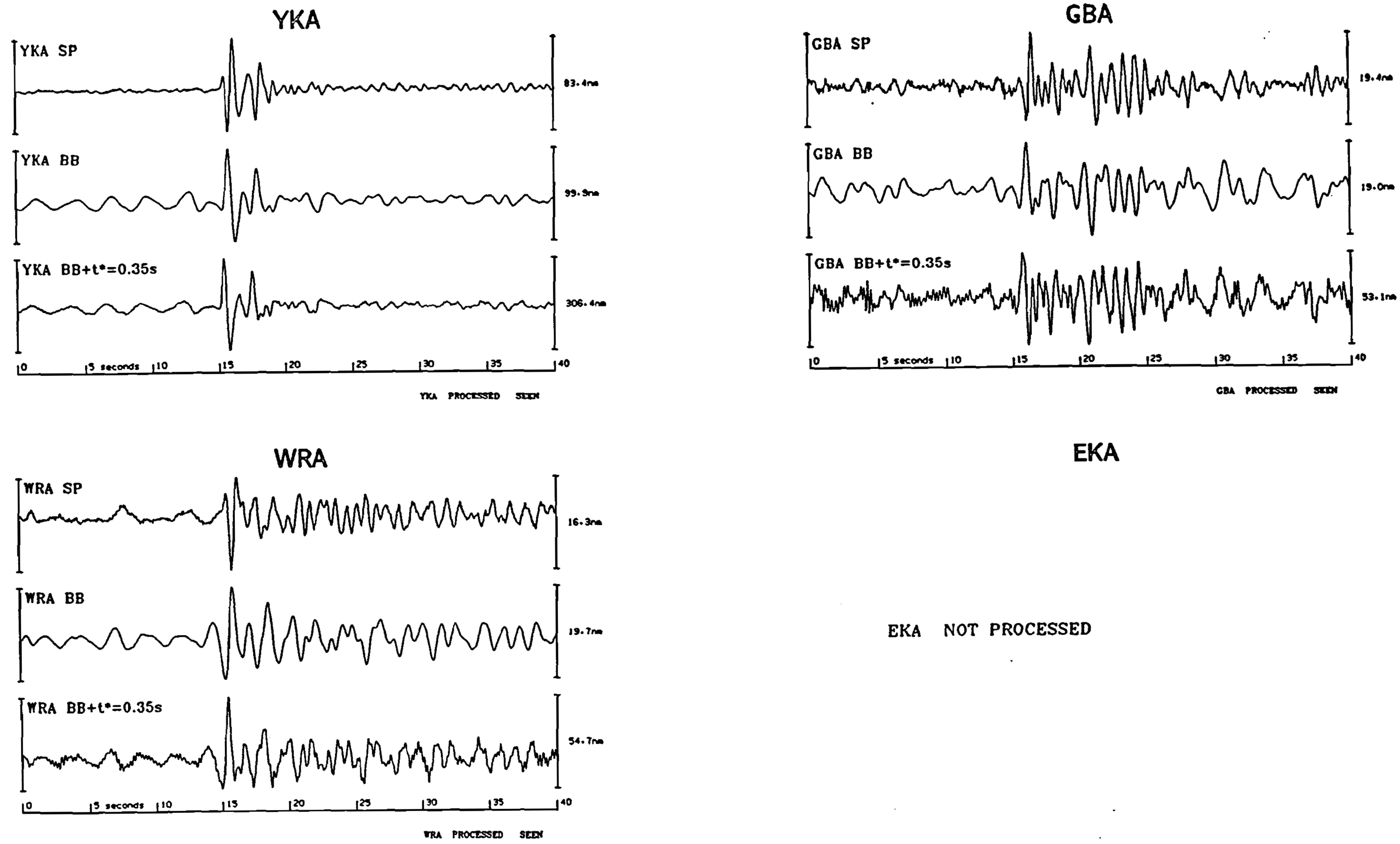

Figure A102 Short period, broad band and deconvolved P seismograms from the Mururoa explosion of 31 October 1989.

YKA

YKA NOT PROCESSED NO TAPE

GBA

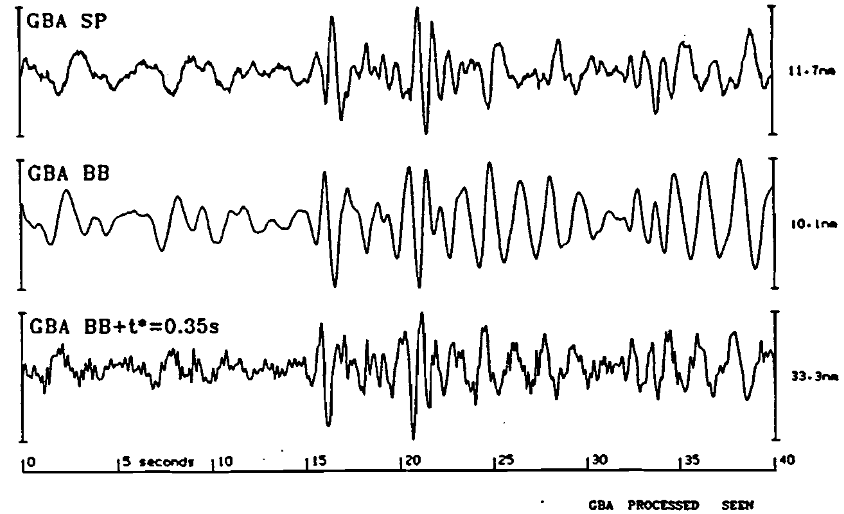

WRA

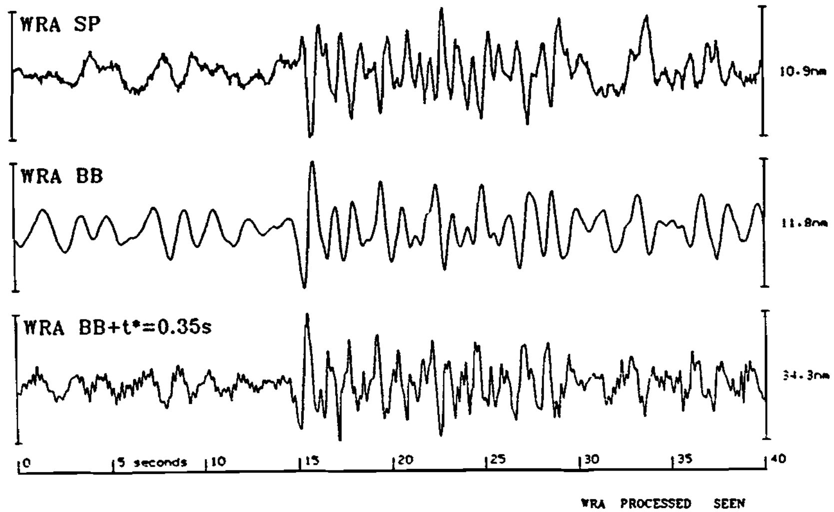

EKA

EKA NOT PROCESSED

Figure A103 Short period, broad band and deconvolved P seismograms from the Mururoa explosion of 20 November 1989.

APPENDIX B

SEISMOGRAMS FOR THE FANGATAUFA EXPLOSIONS

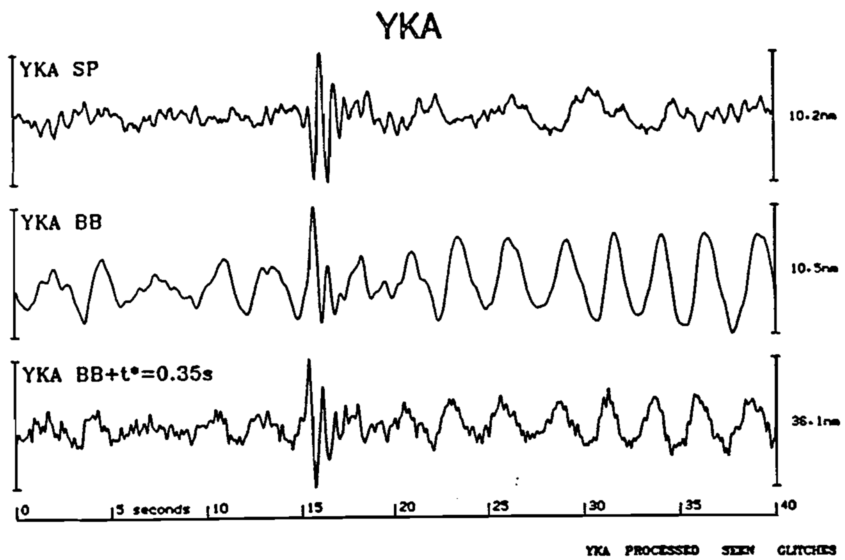

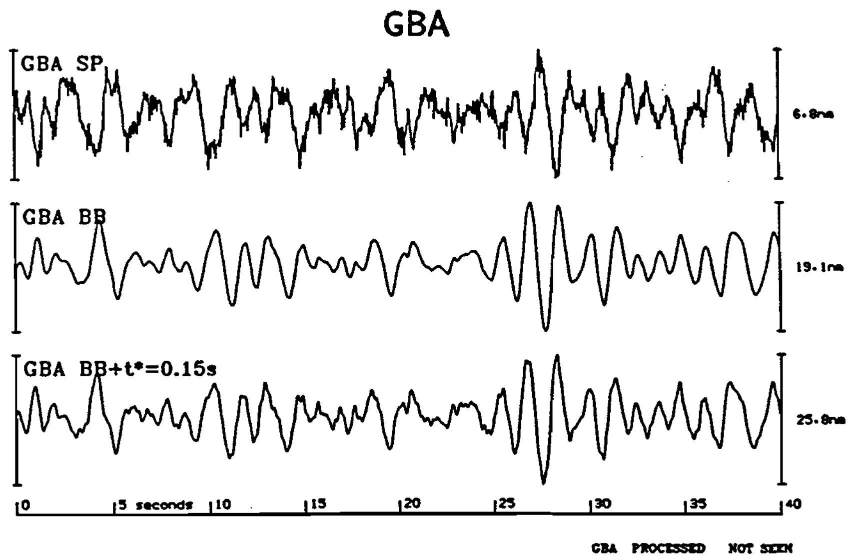

WRA

WRA NOT PROCESSED NO TAPE

EKA

EKA NOT PROCESSED

Figure B1 Short period, broad band and deconvolved P seismograms from the Fangataufa explosion of 5 June 1975.

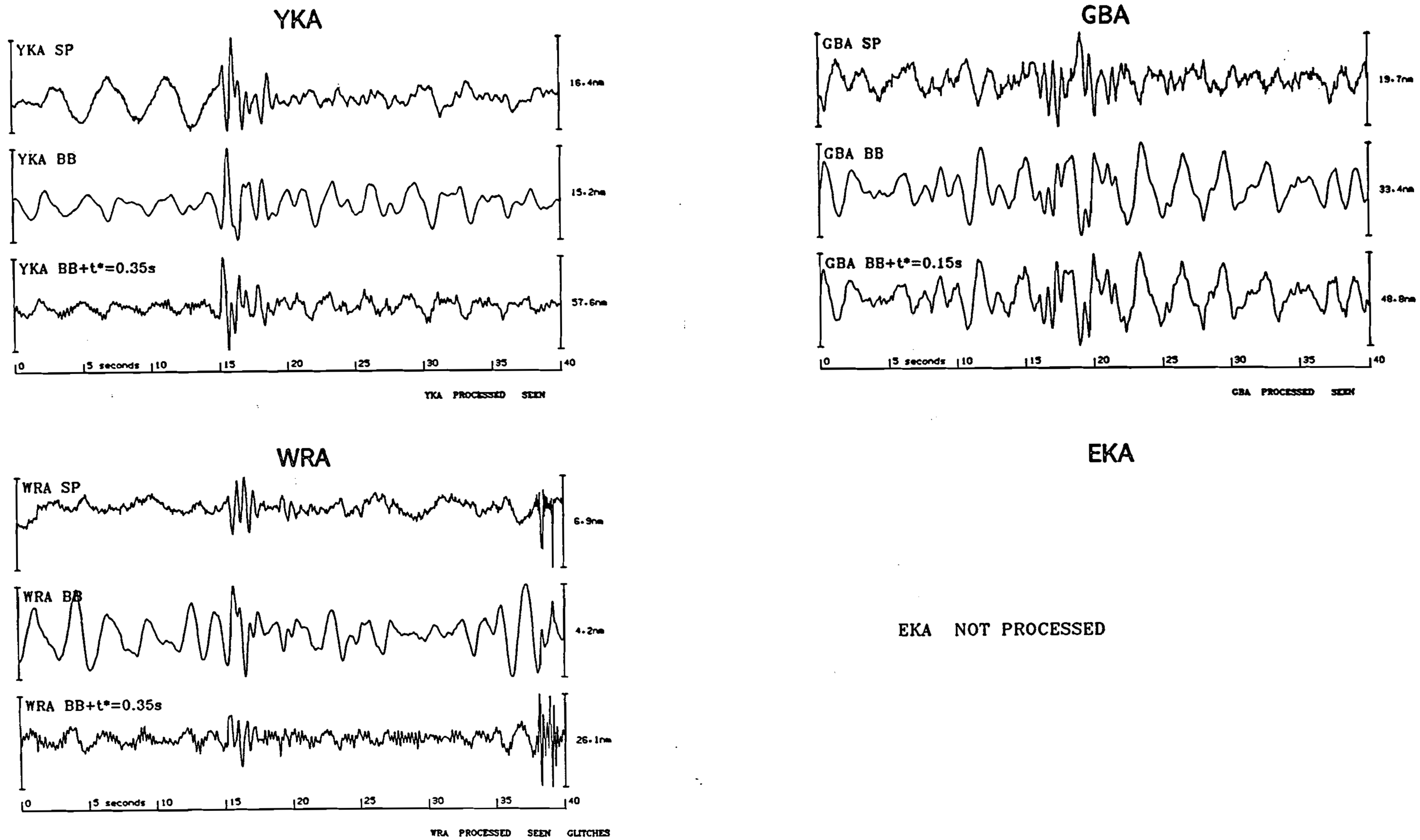

Figure B2 Short period, broad band and deconvolved P seismograms from the Fangataufa explosion of 26 November 1975.

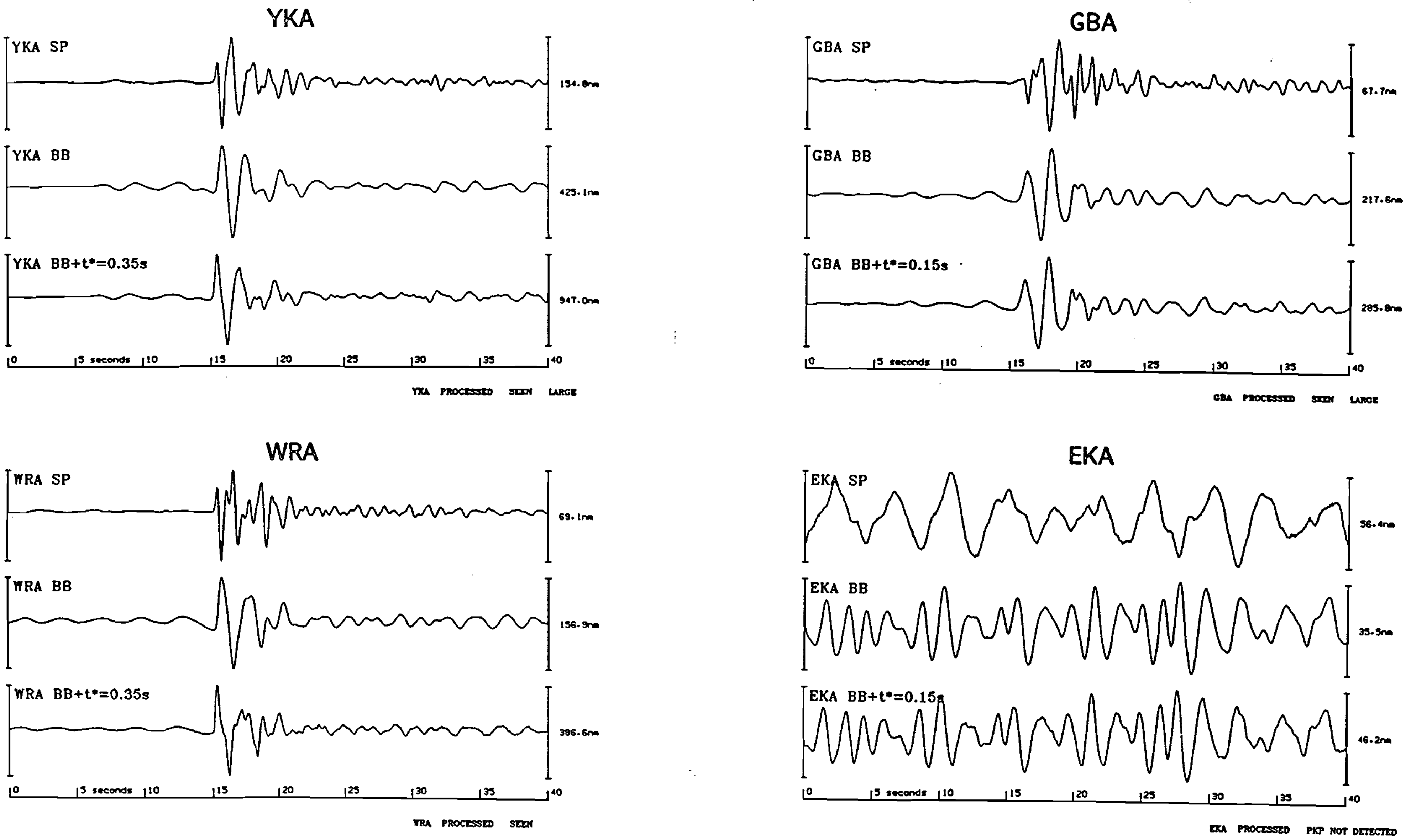

Figure B3 Short period, broad band and deconvolved P seismograms from the Fangataufa explosion of 30 November 1988.

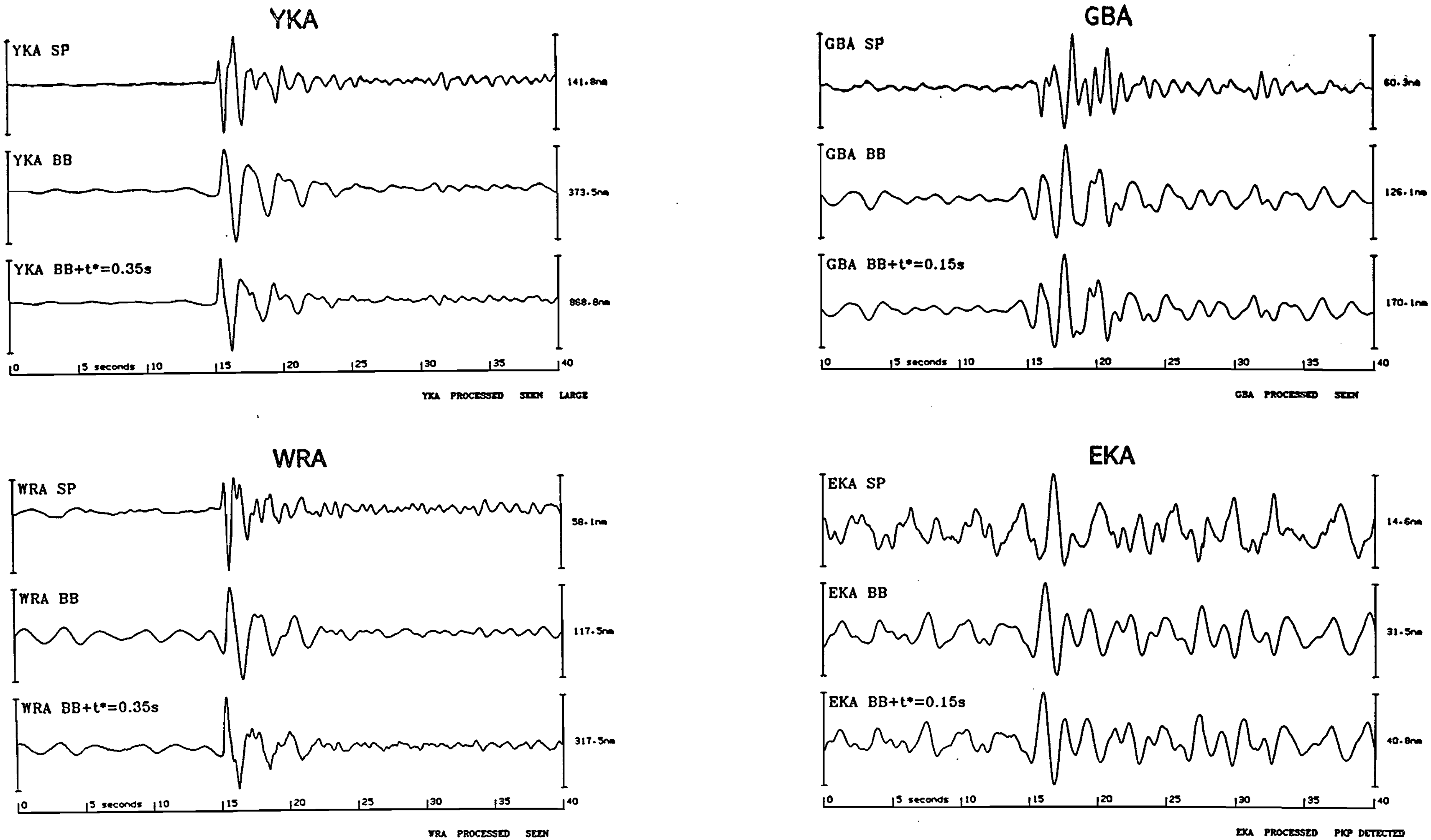

Figure B4 Short period, broad band and deconvolved P seismograms from the Fangataufa explosion of 10 June 1989.

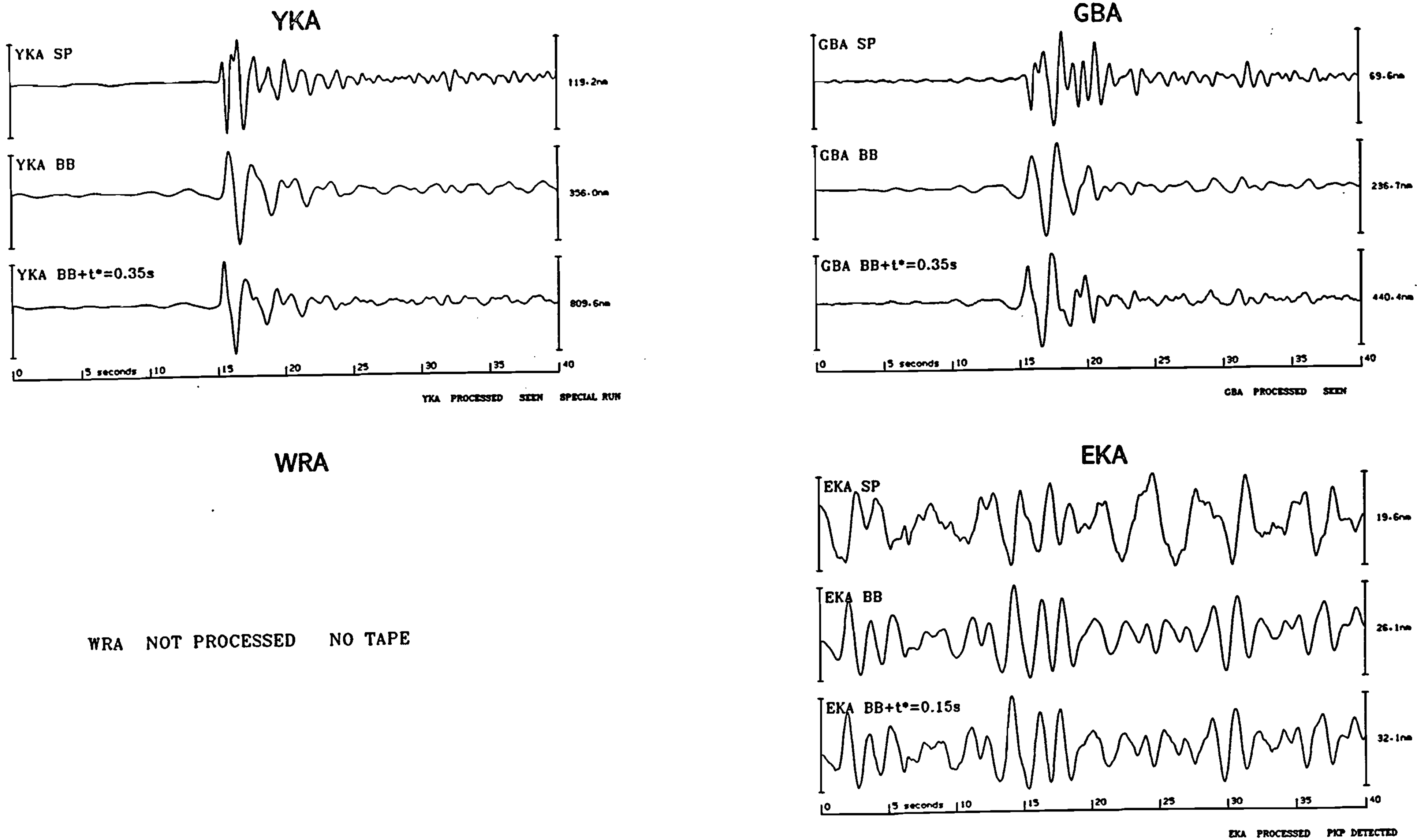

Figure B5 Short period, broad band and deconvolved P seismograms from the Fangataufa explosion of 27 November 1989.

APPENDIX C

TABLES OF MURUROA OBSERVATIONS

All the observations given in the tables are as measured except for ψ_∞, moment M_o, and magnitude m_b. ψ_∞ is calculated from the measured area H using the relation

$$\psi_\infty = \{2KG(\Delta)\}^{-1} H$$

where $K = [\rho_1 v_1/\rho_o v_o]^{1/2}$. ρ_1 & v_1 are the density and P wave speed respectively for the material in which the explosion was fired and ρ_o & v_o are the corresponding quantities for the material on which the recording station is sited. $G(\Delta)$ is the geometrical spreading effect and is listed by Carpenter [11]. M_o is calculated from ψ_∞ using the relation:

$$M_o = 4\pi\rho_1 v_1^2 \psi_\infty$$

All amplitudes listed are as measured and are for a system of unit gain at 1 Hz. Magnitude m_b, is thus given by

$$m_b = \log(A/T) + B(\Delta)$$

where A is the ½ peak-to-peak amplitude divided by the gain at period T, T is the period and $B(\Delta)$ is the distance correction term given by the table of Lilwall [9].

The values of $B(\Delta)$, $G(\Delta)$, ρ_o, v_o, ρ_1 & v_1 used are given in this appendix and in Appendix D.

Table 1A Yellowknife array - Broad band and short period observations

Date	ψ_∞ (m^3)	Moment (N m)	Duration (s)	Rise time (s)	Fall time (s)	pP-P time (s)	1/2 Pk-Pk (nm)	Period (s)	Frequency (Hz)	Gain	m_b	
760711	2493.46	0.9746E+15	0.68	0.28	0.12	0.47	20.02	0.82	1.21	1.40	5.16	23
770219	3331.19	0.1302E+16	0.61	0.22	0.13	0.39	24.94	0.68	1.48	1.83	5.22	23
770706	2276.35	0.8897E+15	0.57	0.26	0.13	0.46	19.24	0.82	1.21	1.40	5.14	23
771112	739.70	0.2891E+15	0.45	0.14	0.08	0.43	11.01	0.77	1.29	1.53	4.89	23
780227	82.17	0.3212E+14	0.41	0.11	0.06	0.34	1.53	0.60	1.67	2.09	4.00	23
780322	1146.95	0.4483E+15	0.44	0.16	0.08	0.36	15.45	0.70	1.43	1.75	5.02	23
780719	1296.07	0.5066E+15	0.71	0.13	0.10	0.45	4.99	1.00	1.00	1.00	4.62	23
780726	293.21	0.1146E+15	0.46	0.13	0.08	0.44	3.21	0.68	1.48	1.83	4.33	23
781102	791.13	0.3092E+15	0.47	0.19	0.10	0.31	8.94	0.60	1.67	2.09	4.77	23
781130	0.00	0.0000E+00	0.00	0.00	0.00	0.00	0.00	0.00	0.00	0.00	0.00	23
781217	1865.16	0.7290E+15	0.63	0.23	0.12	0.38	14.95	0.75	1.33	1.61	5.01	23
781219	3400.27	0.1329E+16	0.66	0.27	0.13	0.46	25.17	0.82	1.21	1.40	5.26	23
790301	2032.93	0.7946E+15	0.56	0.19	0.16	0.45	14.56	0.75	1.33	1.61	5.00	23
790309	1904.63	0.7445E+15	0.69	0.22	0.12	0.44	15.60	0.80	1.25	1.47	5.04	23
790324	2685.35	0.1050E+16	0.56	0.18	0.16	0.50	22.82	0.85	1.18	1.34	5.22	23
790404	2890.40	0.1130E+16	0.66	0.20	0.13	0.40	19.20	0.73	1.38	1.68	5.12	23
790618	1866.26	0.7295E+15	0.54	0.20	0.13	0.38	15.25	0.70	1.43	1.75	5.01	23
790629	4297.21	0.1680E+16	0.56	0.19	0.20	0.52	34.42	0.98	1.03	1.05	5.45	23
790725	0.00	0.0000E+00	0.00	0.00	0.00	0.00	0.00	0.00	0.00	0.00	0.00	33
790728	1100.89	0.4303E+15	0.44	0.17	0.10	0.39	13.09	0.73	1.38	1.68	4.95	23
791122	773.92	0.3025E+15	0.49	0.24	0.12	0.39	8.73	0.80	1.25	1.47	4.79	23
800223	408.89	0.1598E+15	0.45	0.21	0.09	0.39	5.35	0.63	1.60	2.00	4.55	23
800303	571.28	0.2233E+15	0.43	0.16	0.10	0.41	6.18	0.80	1.25	1.47	4.64	23
800323	13136.17	0.5134E+16	0.69	0.23	0.19	0.64	66.15	1.17	0.85	0.70	5.83	23
800401	3321.32	0.1298E+16	0.50	0.22	0.11	0.43	35.90	0.77	1.29	1.53	5.40	23
800404	725.45	0.2836E+15	0.51	0.17	0.15	0.45	7.73	0.90	1.11	1.22	4.77	23
800616	5666.75	0.2215E+16	0.47	0.17	0.15	0.55	47.56	0.98	1.03	1.05	5.59	23
800621	985.21	0.3851E+15	0.46	0.18	0.10	0.38	11.82	0.73	1.38	1.68	4.91	23
800706	1523.05	0.5953E+15	0.55	0.20	0.18	0.51	10.49	0.88	1.14	1.28	4.89	23
810227	568.76	0.2223E+15	0.50	0.19	0.15	0.39	6.12	0.73	1.38	1.68	4.62	23
810306	605.71	0.2368E+15	0.45	0.20	0.12	0.44	7.33	0.77	1.29	1.53	4.71	23
810328	1719.32	0.6720E+15	0.47	0.16	0.13	0.46	15.99	0.77	1.29	1.53	5.05	23
810410	1756.61	0.6866E+15	0.51	0.17	0.18	0.55	16.44	0.95	1.05	1.10	5.12	23
810708	3792.82	0.1482E+16	0.59	0.16	0.19	0.65	25.72	1.10	0.91	0.82	5.38	23
810711	230.05	0.8992E+14	0.43	0.11	0.09	0.38	3.25	0.60	1.67	2.09	4.33	23
810718	523.69	0.2047E+15	0.52	0.24	0.11	0.38	6.30	0.65	1.54	1.91	4.62	23
810803	3390.40	0.1325E+16	0.49	0.17	0.16	0.57	28.85	1.08	0.93	0.86	5.41	23
811111	1450.68	0.5670E+15	0.49	0.19	0.10	0.38	17.87	0.75	1.33	1.61	5.09	23
811205	1271.95	0.4972E+15	0.45	0.16	0.14	0.47	12.22	0.85	1.18	1.34	4.95	23
811208	2961.67	0.1158E+16	0.50	0.25	0.14	0.41	25.50	0.80	1.25	1.47	5.26	23
820220	0.00	0.0000E+00	0.00	0.00	0.00	0.00	1.84	0.68	1.48	1.83	4.09	23
820224	0.00	0.0000E+00	0.00	0.00	0.00	0.00	1.83	0.70	1.43	1.75	4.09	23
820320	3063.64	0.1197E+16	0.51	0.16	0.15	0.51	23.52	0.98	1.03	1.05	5.28	23
820627	309.43	0.1209E+15	0.54	0.23	0.10	0.34	2.49	0.75	1.33	1.61	4.24	23
820701	3598.74	0.1407E+16	0.55	0.22	0.14	0.52	29.42	1.02	0.98	0.95	5.40	23
820725	13059.41	0.5104E+16	0.55	0.20	0.17	0.52	84.63	0.90	1.11	1.22	5.81	23
830419	13070.38	0.5109E+16	0.57	0.23	0.14	0.49	96.19	0.85	1.18	1.34	5.85	23
830425	0.00	0.0000E+00	0.00	0.00	0.00	0.00	0.86	0.77	1.29	1.53	3.78	23
830618	446.61	0.1746E+15	0.61	0.18	0.11	0.41	3.22	0.73	1.38	1.68	4.34	23
830628	6182.11	0.2416E+16	0.55	0.21	0.14	0.47	56.87	0.85	1.18	1.34	5.62	23
830720	999.03	0.3905E+15	0.51	0.15	0.17	0.50	9.07	0.88	1.14	1.28	4.83	23
830804	4305.99	0.1683E+16	0.60	0.20	0.13	0.51	29.69	0.93	1.08	1.16	5.36	23
831203	501.76	0.1961E+15	0.56	0.15	0.17	0.52	4.68	0.85	1.18	1.34	4.53	23
831207	1720.42	0.6725E+15	0.46	0.18	0.15	0.55	18.57	0.98	1.03	1.05	5.18	23
840508	1308.13	0.5113E+15	0.61	0.23	0.16	0.41	10.94	0.77	1.29	1.53	4.88	23
840512	13816.00	0.5400E+16	0.57	0.21	0.18	0.57	85.48	0.95	1.05	1.10	5.83	23
840612	904.84	0.3537E+15	0.51	0.21	0.12	0.38	11.84	0.75	1.33	1.61	4.91	23
840616	6336.72	0.2477E+16	0.60	0.25	0.17	0.57	40.00	1.05	0.95	0.90	5.54	23
841027	987.95	0.3862E+15	0.54	0.20	0.18	0.41	9.32	0.77	1.29	1.53	4.81	23
841102	10405.86	0.4067E+16	0.65	0.20	0.22	0.59	64.46	1.00	1.00	1.00	5.73	23

Table 1A (cont'd) Yellowknife array - Broad band and short period observations

Date	ψ_{∞} (m^3)	Moment (N m)	Duration (s)	Rise time (s)	Fall time (s)	pP-P time (s)	1/2 Pk-Pk (nm)	Period (s)	Frequency (Hz)	Gain	m_b	
841201	0.00	0.0000E+00	0.00	0.00	0.00	0.00	1.66	0.82	1.21	1.40	4.08	23
841206	10195.33	0.3985E+16	0.52	0.19	0.18	0.52	83.65	0.90	1.11	1.22	5.80	23
850430	1538.40	0.6013E+15	0.64	0.21	0.14	0.51	11.24	0.85	1.18	1.34	4.91	23
850508	17708.61	0.6922E+16	0.73	0.24	0.17	0.59	79.58	0.95	1.05	1.10	5.80	23
850603	1679.85	0.6566E+15	0.54	0.16	0.15	0.54	16.39	0.85	1.18	1.34	5.08	23
850607	853.30	0.3335E+15	0.45	0.16	0.12	0.41	9.67	0.75	1.33	1.61	4.83	23
851024	484.44	0.1893E+15	0.47	0.12	0.12	0.40	6.39	0.88	1.14	1.28	4.68	23
851026	7269.85	0.2842E+16	0.61	0.25	0.17	0.57	45.14	1.00	1.00	1.00	5.57	23
851124	1629.41	0.6369E+15	0.55	0.22	0.17	0.51	13.22	0.93	1.08	1.16	5.01	23
851126	0.00	0.0000E+00	0.00	0.00	0.00	0.00	0.00	0.00	0.00	0.00	0.00	23
860426	1089.60	0.4259E+15	0.54	0.20	0.16	0.47	8.36	0.95	1.05	1.10	4.82	23
860506	1248.92	0.4882E+15	0.51	0.25	0.15	0.39	10.31	0.70	1.43	1.75	4.84	23
860527	1298.27	0.5074E+15	0.54	0.22	0.11	0.47	13.29	0.85	1.18	1.34	4.99	23
860530	12544.05	0.4903E+16	0.68	0.20	0.22	0.57	78.59	1.02	0.98	0.95	5.83	23
861206	1582.26	0.6184E+15	0.49	0.15	0.15	0.43	15.19	0.77	1.29	1.53	5.03	23
861210	6545.06	0.2558E+16	0.66	0.24	0.20	0.56	36.85	1.00	1.00	1.00	5.49	23
870505	1233.57	0.4822E+15	0.51	0.17	0.15	0.43	9.64	0.82	1.21	1.40	4.84	23
870520	8571.40	0.3350E+16	0.46	0.16	0.17	0.50	77.77	0.90	1.11	1.22	5.77	23
870606	2062.53	0.8062E+15	0.60	0.19	0.12	0.39	13.40	0.80	1.25	1.47	4.98	23
870621	5689.78	0.2224E+16	0.57	0.20	0.18	0.59	42.57	1.05	0.95	0.90	5.57	23
871023	11612.02	0.4539E+16	0.52	0.19	0.19	0.60	83.53	1.02	0.98	0.95	5.85	23
871105	9887.21	0.3865E+16	0.57	0.21	0.14	0.46	70.67	0.77	1.29	1.53	5.69	23
871119	0.00	0.0000E+00	0.00	0.00	0.00	0.00	0.00	0.00	0.00	0.00	0.00	23
871129	1371.73	0.5362E+15	0.49	0.18	0.14	0.47	11.27	0.88	1.14	1.28	4.92	23
880511	8432.15	0.3296E+16	0.60	0.18	0.21	0.54	58.02	0.95	1.05	1.10	5.66	23
880525	12182.20	0.4762E+16	0.66	0.19	0.20	0.61	66.98	1.15	0.87	0.74	5.82	23
880616	1128.31	0.4410E+15	0.52	0.21	0.11	0.39	8.80	0.82	1.21	1.40	4.80	23
880623	6849.89	0.2677E+16	0.54	0.20	0.18	0.50	55.16	0.88	1.14	1.28	5.61	23
881105	8899.26	0.3478E+16	0.69	0.20	0.17	0.60	44.39	1.10	0.91	0.82	5.61	23
881123	8132.80	0.3179E+16	0.66	0.18	0.18	0.60	49.62	1.10	0.91	0.82	5.66	23
890511	4179.89	0.1634E+16	0.49	0.20	0.14	0.44	42.40	0.82	1.21	1.40	5.48	23
890520	1603.09	0.6266E+15	0.60	0.24	0.12	0.40	10.85	0.75	1.33	1.61	4.87	23
890603	6478.17	0.2532E+16	0.52	0.18	0.20	0.52	50.93	0.98	1.03	1.05	5.62	23
891024	6582.34	0.2573E+16	0.59	0.19	0.22	0.55	44.94	0.98	1.03	1.06	5.56	37
891031	5309.29	0.2075E+16	0.54	0.20	0.14	0.43	42.09	0.77	1.29	1.63	5.44	37

*

$B(\Delta)=3.92$ $G(\Delta)=$ $0.6020E-11 s\ m^{-2}$ $\rho_0=2670.0 kg\ m^{-3}$ $v_0=5640.0 km\ s^{-1}$
$\rho_1=2400.0 kg\ m^{-3}$ $v_1=3600.0 km\ s^{-1}$ $K=0.76$

Table 2A Yellowknife array - Observations in the 0.5-4.0Hz band

Date	1/2 Pk-Pk (nm)	Period (s)	Frequency (Hz)	Gain	m_b	r.m.s. 0-3s (nm)	r.m.s. 0-6s (nm)	r.m.s. 0-9s (nm)	r.m.s. 0-15s (nm)	r.m.s. 3-9s (nm)	r.m.s. 3-15s (nm)	r.m.s. 9-18s (nm)	r.m.s. noise (nm)
760711	18.64	0.82	1.21	1.40	5.13	9.00	7.51	6.26	4.88	4.26	3.08	0.93	0.24
770219	25.13	0.70	1.43	1.75	5.23	9.65	7.31	6.07	4.77	2.94	2.27	1.12	0.29
770706	17.57	0.82	1.21	1.40	5.10	8.26	6.47	5.38	4.25	3.06	2.36	1.27	0.31
771112	10.35	0.77	1.29	1.53	4.86	4.88	3.90	3.20	2.67	1.87	1.73	1.50	1.41
780227	1.67	0.70	1.43	1.75	4.05	0.73	0.60	0.52	0.44	0.37	0.33	0.30	0.27
780322	15.57	0.73	1.38	1.68	5.03	6.69	4.82	3.95	3.10	0.98	0.91	0.81	0.30
780719	5.17	1.17	0.85	0.70	4.72	2.69	2.05	1.72	1.40	0.89	0.80	0.63	0.37
780726	3.29	0.73	1.38	1.68	4.35	1.38	1.02	0.87	0.72	0.44	0.41	0.34	0.27
781102	9.73	0.63	1.60	2.00	4.81	3.78	2.87	2.50	2.00	1.50	1.19	0.85	1.10
781130	0.00	0.00	0.00	0.00	0.00	0.00	0.00	0.00	0.00	0.00	0.00	0.00	0.00
781217	15.18	0.75	1.33	1.61	5.02	6.34	4.57	3.76	2.96	1.05	0.94	0.87	0.26
781219	23.26	0.77	1.29	1.53	5.21	10.58	8.48	7.14	5.61	4.53	3.36	1.40	0.26
790301	13.16	0.75	1.33	1.61	4.96	5.70	4.20	3.52	2.77	1.52	1.22	0.95	0.24
790309	15.07	0.77	1.29	1.53	5.02	6.82	5.29	4.43	3.51	2.47	1.95	1.17	0.23
790324	23.83	0.77	1.29	1.53	5.22	10.98	8.00	6.60	5.14	2.26	1.71	0.94	0.22
790404	18.95	0.70	1.43	1.75	5.11	7.45	5.43	4.53	3.60	1.76	1.54	1.12	0.28
790618	15.15	0.73	1.38	1.68	5.02	6.07	4.41	3.64	2.87	1.22	1.05	0.86	0.25
790629	36.45	0.90	1.11	1.22	5.44	17.43	12.81	10.59	8.30	4.05	3.17	2.23	0.78
790725	0.00	0.00	0.00	0.00	0.00	0.00	0.00	0.00	0.00	0.00	0.00	0.00	0.00
790728	12.95	0.73	1.38	1.68	4.95	5.43	3.91	3.27	2.63	1.12	1.11	1.07	0.43
791122	7.38	0.75	1.33	1.61	4.71	3.31	2.50	2.14	1.78	1.18	1.10	1.11	0.83
800223	5.89	0.68	1.48	1.83	4.60	2.40	1.75	1.45	1.16	0.51	0.48	0.41	0.25
800303	5.88	0.80	1.25	1.47	4.62	2.61	1.94	1.62	1.30	0.72	0.64	0.53	0.24
800323	67.26	1.13	0.89	0.77	5.81	33.33	25.45	20.93	16.46	10.07	7.80	3.81	0.26
800401	35.48	0.77	1.29	1.53	5.39	15.20	10.97	9.01	7.10	2.47	2.30	2.03	0.27
800404	7.64	0.82	1.21	1.40	4.74	3.66	2.77	2.31	1.80	1.14	0.85	0.38	0.28
800616	47.68	0.98	1.03	1.05	5.59	23.82	17.20	14.12	10.99	3.93	3.03	1.68	0.25
800621	12.09	0.73	1.38	1.68	4.92	5.19	4.02	3.37	2.66	1.89	1.45	0.92	0.31
800706	9.69	0.82	1.21	1.40	4.84	4.15	3.13	2.63	2.09	1.33	1.08	0.84	0.33
810227	6.30	0.77	1.29	1.53	4.64	2.82	2.06	1.72	1.35	0.68	0.53	0.39	0.29
810306	7.11	0.68	1.48	1.83	4.68	3.06	2.30	1.94	1.52	0.97	0.75	0.41	0.28
810328	14.84	0.75	1.33	1.61	5.01	6.15	4.52	3.76	3.00	1.52	1.34	1.09	0.32
810410	15.49	0.95	1.05	1.10	5.09	7.01	5.11	4.22	3.30	1.46	1.16	0.76	0.30
810708	26.82	1.00	1.00	1.00	5.35	12.66	9.81	8.10	6.36	4.29	3.24	1.43	0.74
810711	3.12	0.75	1.33	1.61	4.33	1.36	1.03	0.87	0.71	0.46	0.42	0.40	0.29
810718	6.59	0.70	1.43	1.75	4.65	2.80	2.07	1.76	1.44	0.86	0.79	0.66	0.60
810803	33.47	0.82	1.21	1.40	5.38	15.61	11.40	9.34	7.29	3.02	2.33	1.31	0.99
811111	18.16	0.75	1.33	1.61	5.10	7.89	5.73	4.80	3.80	1.85	1.60	1.28	1.16
811205	11.96	0.77	1.29	1.53	4.92	5.03	3.67	3.05	2.44	1.13	1.07	0.99	0.51
811208	24.40	0.85	1.18	1.34	5.25	12.77	9.50	7.80	6.09	3.09	2.37	1.21	0.35
820220	1.95	0.70	1.43	1.75	4.12	0.96	0.72	0.65	0.56	0.41	0.41	0.39	0.39
820224	2.03	0.90	1.11	1.22	4.19	0.89	0.67	0.59	0.54	0.34	0.41	0.45	0.33
820320	21.32	0.93	1.08	1.16	5.22	9.91	7.12	5.85	4.59	1.47	1.32	1.15	0.28
820627	2.60	0.70	1.43	1.75	4.25	1.09	0.82	0.68	0.56	0.31	0.30	0.32	0.26
820701	31.69	0.90	1.11	1.22	5.38	15.82	11.67	9.60	7.50	3.60	2.79	1.49	0.46
820725	73.78	0.98	1.03	1.05	5.78	37.34	26.97	22.25	17.44	6.74	5.63	3.88	0.43
830419	89.84	0.82	1.21	1.40	5.81	44.45	34.73	28.72	22.35	15.78	11.43	3.45	0.44
830425	0.76	0.73	1.38	1.68	3.71	0.41	0.36	0.33	0.29	0.27	0.25	0.22	0.25
830618	3.50	0.82	1.21	1.40	4.40	1.53	1.14	0.96	0.77	0.47	0.39	0.31	0.32
830628	56.64	0.77	1.29	1.53	5.60	25.43	18.69	15.36	12.07	5.54	4.51	2.94	0.20
830720	8.52	0.80	1.25	1.47	4.78	4.14	3.04	2.52	1.99	0.97	0.81	0.65	0.24
830804	29.80	0.93	1.08	1.16	5.36	15.21	11.25	9.32	7.29	3.85	2.94	1.60	0.86
831203	5.40	0.80	1.25	1.47	4.58	2.33	1.73	1.47	1.17	0.71	0.59	0.45	0.38
831207	17.08	0.90	1.11	1.22	5.11	8.07	5.89	4.83	3.83	1.58	1.45	1.36	0.77
840508	11.23	0.73	1.38	1.68	4.89	4.95	3.62	2.99	2.37	1.09	0.94	0.81	0.20
840512	77.10	0.98	1.03	1.05	5.80	37.24	27.50	22.73	17.84	9.04	7.16	4.58	0.20
840612	12.66	0.75	1.33	1.61	4.94	5.86	4.24	3.52	2.75	1.18	0.92	0.61	0.28
840616	40.03	0.95	1.05	1.10	5.50	19.86	15.37	12.81	10.12	6.99	5.42	2.65	0.18
841027	9.21	0.70	1.43	1.75	4.80	4.16	3.10	2.60	2.29	1.21	1.49	1.76	1.12
841102	57.02	0.77	1.29	1.53	5.60	27.74	21.09	17.37	13.69	8.24	6.48	3.69	1.21

Table 2A (cont'd) Yellowknife array - Observations in the 0.5-4.0Hz band

Date	1/2 Pk-Pk (nm)	Period (s)	Frequency (Hz)	Gain	m_b	r.m.s. 0-3s (nm)	r.m.s. 0-6s (nm)	r.m.s. 0-9s (nm)	r.m.s. 0-15s (nm)	r.m.s. 3-9s (nm)	r.m.s. 3-15s (nm)	r.m.s. 9-18s (nm)	r.m.s. noise (nm)
841201	1.04	1.02	0.98	0.95	3.95	0.47	0.37	0.32	0.30	0.20	0.24	0.26	0.27
841206	79.26	0.88	1.14	1.28	5.77	35.74	26.39	21.74	16.94	8.39	6.26	3.13	0.39
850430	10.90	0.88	1.14	1.28	4.91	5.24	3.87	3.20	2.53	1.29	1.06	0.67	0.15
850508	72.24	0.80	1.25	1.47	5.71	36.78	26.56	22.14	17.65	7.70	7.17	6.49	0.21
850603	17.26	0.88	1.14	1.28	5.11	7.59	5.52	4.54	3.55	1.45	1.15	0.71	0.20
850607	9.19	0.68	1.48	1.83	4.79	3.73	2.83	2.35	1.89	1.16	0.99	0.67	0.30
851024	5.93	0.65	1.54	1.91	4.60	2.54	1.95	1.63	1.33	0.86	0.77	0.58	0.67
851026	45.57	0.98	1.03	1.05	5.57	22.97	17.65	14.88	11.63	8.28	6.11	2.34	0.82
851124	11.73	0.93	1.08	1.16	4.96	5.38	3.97	3.27	2.58	1.26	1.05	0.79	0.26
851126	0.00	0.00	0.00	0.00	0.00	0.00	0.00	0.00	0.00	0.00	0.00	0.00	0.00
860426	7.28	0.85	1.18	1.34	4.73	3.51	2.68	2.27	1.78	1.24	0.94	0.50	0.17
860506	9.73	0.68	1.48	1.83	4.82	4.20	3.20	2.65	2.08	1.29	0.99	0.50	0.21
860527	14.60	0.85	1.18	1.34	5.03	6.79	4.92	4.05	3.19	1.23	1.10	0.83	0.23
860530	71.07	1.02	0.98	0.95	5.78	34.31	25.33	20.85	16.86	7.99	7.83	6.54	0.21
861206	14.70	0.75	1.33	1.61	5.01	6.37	4.71	3.87	3.03	1.47	1.16	0.63	0.32
861210	34.89	1.02	0.98	0.95	5.47	17.46	13.10	10.85	8.62	4.94	4.09	2.65	0.19
870505	8.90	0.90	1.11	1.22	4.83	4.65	3.47	2.88	2.28	1.26	1.03	0.68	0.27
870520	69.99	0.82	1.21	1.40	5.70	32.53	23.80	19.68	15.45	7.21	5.80	3.71	0.18
870606	13.18	0.77	1.29	1.53	4.96	5.75	4.43	3.70	2.93	2.00	1.58	0.88	0.38
870621	41.28	0.93	1.08	1.16	5.51	20.32	14.79	12.17	9.53	3.98	3.21	2.38	0.30
871023	76.44	1.00	1.00	1.00	5.80	37.81	28.31	23.18	18.23	9.57	7.63	5.24	2.03
871105	65.97	0.77	1.29	1.53	5.66	27.92	20.20	16.64	13.11	5.07	4.46	3.45	0.73
871119	0.00	0.00	0.00	0.00	0.00	0.00	0.00	0.00	0.00	0.00	0.00	0.00	0.00
871129	10.68	0.90	1.11	1.22	4.91	5.54	4.11	3.38	2.67	1.35	1.10	0.75	0.37
880511	52.08	1.00	1.00	1.00	5.64	24.90	18.31	15.10	11.84	5.66	4.49	2.62	0.25
880525	60.43	1.13	0.89	0.77	5.76	29.61	22.36	18.37	14.70	8.22	7.13	5.16	0.29
880616	8.10	0.82	1.21	1.40	4.77	3.81	3.02	2.52	1.98	1.49	1.12	0.52	0.28
880623	51.85	0.85	1.18	1.34	5.58	23.24	16.86	13.89	10.90	4.40	3.68	2.67	0.54
881105	38.86	0.73	1.38	1.68	5.42	21.01	15.20	12.95	10.26	5.55	4.61	3.06	0.48
881123	47.09	1.10	0.91	0.82	5.64	21.67	16.08	13.19	10.53	5.12	4.60	3.39	0.52
890511	40.97	0.80	1.25	1.47	5.46	17.39	12.60	10.37	8.10	3.18	2.53	1.53	0.28
890520	10.85	0.77	1.29	1.53	4.88	4.64	3.58	2.98	2.36	1.61	1.26	0.70	0.25
890603	46.33	0.88	1.14	1.28	5.54	22.07	16.16	13.29	10.37	4.62	3.55	2.01	0.28
891024	43.66	1.08	0.93	0.85	5.60	19.90	15.23	12.54	9.82	6.14	4.64	2.34	1.17
891031	39.76	0.77	1.29	1.63	5.42	18.29	14.64	12.04	9.38	7.08	5.14	1.51	0.59

Table 3A Yellowknife array - Observations in the 1.0-4.0Hz band

Date	1/2 Pk-Pk (nm)	Period (s)	Frequency (Hz)	Gain	m_b	r.m.s. 0-3s (nm)	r.m.s. 0-6s (nm)	r.m.s. 0-9s (nm)	r.m.s. 0-15s (nm)	r.m.s. 3-9s (nm)	r.m.s. 3-15s (nm)	r.m.s. 9-18s (nm)	r.m.s. noise (nm)
760711	12.60	0.75	1.33	1.61	4.94	5.31	4.14	3.46	2.72	1.97	1.47	0.63	0.15
770219	19.84	0.65	1.54	1.91	5.12	7.73	5.84	4.82	3.77	2.23	1.68	0.73	0.12
770706	12.35	0.75	1.33	1.61	4.93	5.39	4.05	3.37	2.64	1.56	1.21	0.72	0.22
771112	7.73	0.70	1.43	1.75	4.72	3.61	2.85	2.35	1.98	1.33	1.29	1.28	1.06
780227	1.37	0.63	1.60	2.00	3.96	0.55	0.43	0.38	0.31	0.25	0.21	0.16	0.15
780322	12.40	0.70	1.43	1.75	4.92	5.37	3.88	3.18	2.49	0.88	0.76	0.58	0.17
780719	2.87	1.08	0.93	0.86	4.41	1.48	1.18	1.00	0.86	0.65	0.61	0.52	0.28
780726	2.54	0.73	1.38	1.68	4.24	1.04	0.76	0.65	0.53	0.31	0.28	0.24	0.18
781102	8.54	0.63	1.60	2.00	4.75	3.37	2.50	2.17	1.72	1.17	0.92	0.66	0.80
781130	0.00	0.00	0.00	0.00	0.00	0.00	0.00	0.00	0.00	0.00	0.00	0.00	0.00
781217	11.48	0.70	1.43	1.75	4.89	4.84	3.52	2.89	2.26	0.91	0.73	0.50	0.13
781219	16.31	0.73	1.38	1.68	5.05	6.68	5.15	4.35	3.43	2.47	1.88	0.91	0.16
790301	9.46	0.68	1.48	1.83	4.80	4.08	3.02	2.50	1.97	1.01	0.82	0.67	0.13
790309	11.39	0.73	1.38	1.68	4.89	5.09	3.91	3.25	2.56	1.69	1.32	0.76	0.11
790324	17.53	0.73	1.38	1.68	5.08	7.72	5.71	4.71	3.66	1.85	1.36	0.66	0.11
790404	15.23	0.65	1.54	1.91	5.01	6.17	4.48	3.70	2.90	1.23	1.01	0.63	0.15
790618	12.38	0.68	1.48	1.83	4.92	5.09	3.67	3.03	2.38	0.91	0.77	0.64	0.19
790629	23.07	0.82	1.21	1.40	5.22	11.02	8.15	6.73	5.27	2.70	2.10	1.53	0.63
790725	0.00	0.00	0.00	0.00	0.00	0.00	0.00	0.00	0.00	0.00	0.00	0.00	0.00
790728	9.77	0.70	1.43	1.75	4.82	4.05	2.97	2.47	1.96	0.99	0.83	0.63	0.31
791122	5.55	0.65	1.54	1.91	4.57	2.42	1.86	1.57	1.32	0.89	0.84	0.85	0.60
800223	5.10	0.65	1.54	1.91	4.53	2.07	1.48	1.22	0.96	0.33	0.30	0.24	0.10
800303	4.09	0.75	1.33	1.61	4.45	1.82	1.34	1.13	0.89	0.50	0.39	0.23	0.11
800323	31.36	1.05	0.95	0.90	5.44	16.40	12.84	10.73	8.56	6.18	4.95	2.77	0.09
800401	26.59	0.70	1.43	1.75	5.26	11.39	8.33	6.84	5.34	2.28	1.81	1.20	0.11
800404	6.13	0.68	1.48	1.83	4.61	2.57	2.03	1.67	1.31	0.95	0.70	0.28	0.12
800616	29.20	0.93	1.08	1.16	5.35	15.55	11.38	9.34	7.28	3.15	2.42	1.20	0.16
800621	9.28	0.73	1.38	1.68	4.80	3.98	3.04	2.52	1.98	1.25	0.97	0.60	0.20
800706	6.96	0.68	1.48	1.83	4.67	2.97	2.24	1.87	1.49	0.92	0.75	0.64	0.21
810227	4.87	0.77	1.29	1.53	4.53	2.12	1.58	1.32	1.03	0.60	0.46	0.28	0.18
810306	5.75	0.65	1.54	1.91	4.58	2.26	1.73	1.45	1.14	0.77	0.59	0.29	0.15
810328	11.30	0.68	1.48	1.83	4.88	4.62	3.36	2.81	2.23	1.09	0.95	0.82	0.19
810410	11.59	0.60	1.67	2.09	4.89	5.02	3.63	3.00	2.35	0.95	0.77	0.52	0.18
810708	15.04	0.85	1.18	1.34	5.04	7.30	5.78	4.81	3.82	2.85	2.22	1.20	0.60
810711	2.36	0.77	1.29	1.53	4.22	0.99	0.75	0.63	0.51	0.32	0.29	0.28	0.19
810718	5.61	0.68	1.48	1.83	4.58	2.35	1.72	1.45	1.17	0.62	0.58	0.51	0.49
810803	22.09	0.75	1.33	1.61	5.18	10.23	7.56	6.21	4.84	2.34	1.78	0.98	0.75
811111	13.74	0.73	1.38	1.68	4.97	5.91	4.33	3.62	2.88	1.48	1.26	1.02	0.96
811205	9.08	0.65	1.54	1.91	4.78	3.74	2.73	2.26	1.83	0.82	0.83	0.73	0.36
811208	16.37	0.77	1.29	1.53	5.06	8.03	6.31	5.17	4.05	2.81	2.10	0.85	0.23
820220	1.53	0.88	1.14	1.28	4.06	0.69	0.52	0.44	0.38	0.23	0.24	0.25	0.20
820224	1.40	0.85	1.18	1.34	4.01	0.65	0.48	0.41	0.35	0.21	0.22	0.23	0.22
820320	14.18	0.75	1.33	1.61	4.99	7.04	5.08	4.18	3.28	1.20	1.01	0.81	0.20
820627	2.07	0.68	1.48	1.83	4.14	0.83	0.63	0.52	0.41	0.23	0.19	0.14	0.12
820701	18.67	0.77	1.29	1.53	5.12	9.43	7.12	5.93	4.65	2.88	2.20	1.14	0.35
820725	49.64	0.73	1.38	1.68	5.53	24.61	17.81	14.75	11.61	4.84	4.12	3.05	0.32
830419	61.61	0.75	1.33	1.61	5.63	28.66	23.03	18.91	14.74	11.21	8.14	2.52	0.29
830425	0.62	0.75	1.33	1.61	3.63	0.33	0.28	0.25	0.21	0.20	0.17	0.14	0.11
830618	2.65	0.68	1.48	1.83	4.25	1.18	0.89	0.75	0.61	0.39	0.33	0.25	0.21
830628	43.37	0.73	1.38	1.68	5.47	19.88	14.44	11.86	9.31	3.64	3.10	2.30	0.10
830720	6.22	0.75	1.33	1.61	4.63	2.75	2.02	1.67	1.32	0.65	0.54	0.49	0.17
830804	18.04	0.95	1.05	1.10	5.16	8.98	6.53	5.40	4.24	1.85	1.52	1.16	0.74
831203	4.07	0.70	1.43	1.75	4.44	1.82	1.34	1.14	0.90	0.54	0.45	0.33	0.27
831207	11.22	0.88	1.14	1.28	4.92	5.56	4.07	3.34	2.66	1.14	1.05	0.91	0.52
840508	8.45	0.70	1.43	1.75	4.76	3.82	2.82	2.33	1.86	0.94	0.81	0.61	0.11
840512	47.32	0.70	1.43	1.75	5.51	22.81	16.83	13.93	11.00	5.56	4.61	3.22	0.10
840612	10.14	0.70	1.43	1.75	4.84	4.37	3.19	2.64	2.06	0.96	0.73	0.46	0.20
840616	22.41	0.88	1.14	1.28	5.22	11.46	9.37	7.76	6.10	4.95	3.70	1.50	0.11
841027	7.31	0.65	1.54	1.91	4.69	3.24	2.44	2.03	1.72	0.96	1.03	1.06	0.68
841102	39.65	0.60	1.67	2.09	5.42	16.67	12.53	10.35	8.22	4.66	3.87	2.66	0.88

Table 3A (cont'd) Yellowknife array - Observations in the 1.0-4.0Hz band

Date	1/2 Pk-Pk (nm)	Period (s)	Frequency (Hz)	Gain	m_b	r.m.s. 0-3s (nm)	r.m.s. 0-6s (nm)	r.m.s. 0-9s (nm)	r.m.s. 0-15s (nm)	r.m.s. 3-9s (nm)	r.m.s. 3-15s (nm)	r.m.s. 9-18s (nm)	r.m.s. noise (nm)
841201	0.90	0.75	1.33	1.61	3.80	0.36	0.28	0.23	0.19	0.13	0.12	0.11	0.11
841206	55.89	0.68	1.48	1.83	5.57	25.50	19.01	15.68	12.25	6.62	4.99	2.34	0.17
850430	7.56	0.75	1.33	1.61	4.72	3.42	2.56	2.16	1.70	1.08	0.82	0.40	0.07
850508	45.32	0.75	1.33	1.61	5.50	20.46	15.21	12.84	10.30	6.15	5.28	3.79	0.09
850603	12.97	0.68	1.48	1.83	4.94	5.66	4.10	3.38	2.65	1.03	0.86	0.61	0.15
850607	7.72	0.63	1.60	2.00	4.71	3.12	2.35	1.95	1.54	0.90	0.72	0.42	0.23
851024	4.62	0.68	1.48	1.83	4.49	1.97	1.45	1.21	0.97	0.50	0.47	0.38	0.51
851026	25.02	0.82	1.21	1.40	5.26	12.79	10.20	8.48	6.66	5.09	3.81	1.72	0.56
851124	8.18	0.73	1.38	1.68	4.75	3.76	2.74	2.26	1.79	0.76	0.67	0.55	0.11
851126	0.00	0.00	0.00	0.00	0.00	0.00	0.00	0.00	0.00	0.00	0.00	0.00	0.00
860426	4.98	0.73	1.38	1.68	4.53	2.40	1.87	1.55	1.22	0.85	0.65	0.35	0.07
860506	7.53	0.68	1.48	1.83	4.70	3.13	2.35	1.94	1.52	0.87	0.67	0.34	0.13
860527	9.80	0.77	1.29	1.53	4.84	4.62	3.36	2.75	2.15	0.83	0.69	0.48	0.15
860530	49.45	0.68	1.48	1.83	5.52	21.68	15.89	13.14	10.58	4.92	4.74	3.95	0.13
861206	11.08	0.70	1.43	1.75	4.88	4.70	3.50	2.87	2.25	1.16	0.89	0.47	0.16
861210	18.79	0.93	1.08	1.16	5.16	10.19	7.58	6.25	4.97	2.60	2.22	1.53	0.10
870505	5.95	0.85	1.18	1.34	4.64	3.02	2.27	1.88	1.49	0.86	0.72	0.49	0.19
870520	47.97	0.70	1.43	1.75	5.51	22.20	16.32	13.47	10.58	5.09	4.09	2.43	0.12
870606	9.57	0.73	1.38	1.68	4.82	3.96	3.01	2.50	2.00	1.24	1.02	0.70	0.29
870621	24.50	0.80	1.25	1.47	5.24	12.41	8.96	7.38	5.81	2.19	1.94	1.81	0.19
871023	45.70	0.98	1.03	1.05	5.57	23.21	16.85	13.90	10.99	4.51	4.02	3.97	1.38
871105	47.21	0.73	1.38	1.68	5.51	19.67	14.34	11.77	9.22	3.78	3.07	2.07	0.37
871119	0.00	0.00	0.00	0.00	0.00	0.00	0.00	0.00	0.00	0.00	0.00	0.00	0.00
871129	7.16	0.77	1.29	1.53	4.70	3.50	2.75	2.26	1.78	1.23	0.96	0.55	0.26
880511	36.00	0.68	1.48	1.83	5.38	16.64	11.96	9.89	7.80	2.84	2.62	2.11	0.15
880525	36.39	0.65	1.54	1.91	5.39	16.88	13.16	10.90	8.73	5.97	4.89	3.13	0.12
880616	6.02	0.77	1.29	1.53	4.62	2.73	2.18	1.81	1.43	1.08	0.82	0.39	0.22
880623	37.06	0.70	1.43	1.75	5.40	16.76	12.10	9.96	7.80	2.89	2.40	1.72	0.41
881105	25.04	0.68	1.48	1.83	5.23	11.31	8.43	7.27	5.89	3.91	3.37	2.31	0.32
881123	30.46	0.60	1.67	2.09	5.31	13.16	9.96	8.23	6.54	3.86	3.19	2.00	0.34
890511	31.00	0.70	1.43	1.75	5.32	13.02	9.45	7.80	6.09	2.54	2.00	1.13	0.17
890520	7.47	0.75	1.33	1.61	4.71	3.22	2.49	2.06	1.63	1.08	0.85	0.51	0.15
890603	31.12	0.73	1.38	1.68	5.33	14.78	10.78	8.88	6.96	3.04	2.44	1.59	0.20
891024	28.08	0.60	1.67	2.38	5.21	13.13	9.60	7.97	6.28	3.01	2.48	1.90	0.93
891031	28.56	0.73	1.38	1.82	5.26	12.45	10.17	8.36	6.51	5.23	3.78	1.03	0.41

Table 4A Warramunga array - Broad band and short period observations

Date	ψ_∞ (m^3)	Moment (N m)	Duration (s)	Rise time (s)	Fall time (s)	pP-P time (s)	1/2 Pk-Pk (nm)	Period (s)	Frequency (Hz)	Gain	m_b	
770706	726.10	0.2838E+15	0.75	0.28	0.23	0.75	3.64	1.40	0.71	0.45	4.64	36
780227	0.00	0.0000E+00	0.00	0.00	0.00	0.00	0.00	0.00	0.00	0.00	0.00	36
780322	417.33	0.1631E+15	0.52	0.20	0.17	0.36	3.68	0.75	1.33	1.61	4.35	26
780719	197.84	0.7733E+14	0.52	0.15	0.15	0.64	0.88	0.50	2.00	2.51	3.71	36
780726	0.00	0.0000E+00	0.00	0.00	0.00	0.00	0.00	0.00	0.00	0.00	0.00	36
781130	13230.43	0.5171E+16	1.02	0.29	0.37	0.00	31.76	1.33	0.75	0.52	5.54	36
781219	775.99	0.3033E+15	0.84	0.28	0.24	0.00	3.08	0.80	1.25	1.47	4.29	36
790301	436.69	0.1707E+15	0.60	0.15	0.15	0.00	2.57	0.68	1.48	1.83	4.19	36
790309	752.71	0.2942E+15	0.81	0.24	0.21	0.00	3.42	0.77	1.29	1.53	4.33	36
790324	526.83	0.2059E+15	0.75	0.35	0.20	0.41	3.19	0.75	1.33	1.60	4.29	36
790618	803.46	0.3140E+15	0.75	0.22	0.20	0.00	3.25	0.75	1.33	1.60	4.30	36
790629	961.52	0.3758E+15	0.84	0.18	0.23	0.00	4.07	0.95	1.05	1.10	4.46	36
790725	29618.24	0.1158E+17	1.16	0.32	0.41	0.00	52.27	1.35	0.74	0.49	5.77	36
790728	612.59	0.2394E+15	0.73	0.27	0.24	0.00	3.26	0.82	1.21	1.40	4.32	36
791122	53.53	0.2092E+14	0.25	0.09	0.07	0.00	1.13	0.65	1.54	1.91	3.83	36
800223	280.73	0.1097E+15	0.76	0.22	0.27	0.00	1.44	0.85	1.18	1.34	3.97	36
800303	229.51	0.8971E+14	0.60	0.23	0.17	0.00	1.29	0.77	1.29	1.53	3.91	36
800323	3568.50	0.1395E+16	0.76	0.26	0.27	0.70	14.99	1.08	0.93	0.86	5.08	36
800401	1617.79	0.6323E+15	0.73	0.23	0.20	0.00	9.10	0.85	1.18	1.34	4.77	36
800404	0.00	0.0000E+00	0.00	0.00	0.00	0.00	0.00	0.00	0.00	0.00	0.00	26
800616	1082.66	0.4232E+15	0.65	0.23	0.19	0.00	6.25	1.05	0.95	0.90	4.69	36
800621	129.16	0.5048E+14	0.35	0.11	0.10	0.00	2.04	0.57	1.74	2.19	4.08	36
800706	524.45	0.2050E+15	0.82	0.24	0.23	0.00	2.09	0.75	1.33	1.60	4.11	36
800719	6279.45	0.2454E+16	0.88	0.25	0.34	0.00	19.87	1.17	0.85	0.70	5.25	36
801203	5289.31	0.2067E+16	0.96	0.22	0.32	0.00	14.34	1.15	0.87	0.74	5.10	36
810227	346.55	0.1355E+15	0.71	0.20	0.24	0.45	2.60	0.90	1.11	1.22	4.25	36
810306	0.00	0.0000E+00	0.00	0.00	0.00	0.00	1.01	0.80	1.25	1.47	3.80	36
810328	655.42	0.2562E+15	0.76	0.21	0.21	0.00	3.18	0.80	1.25	1.47	4.30	36
810410	812.62	0.3176E+15	0.90	0.24	0.26	0.00	2.76	1.08	0.93	0.86	4.35	36
810708	697.39	0.2726E+15	0.59	0.17	0.14	0.00	4.91	1.17	0.85	0.70	4.64	36
810718	87.61	0.3425E+14	0.46	0.18	0.09	0.00	1.77	0.82	1.21	1.40	4.06	36
810803	1728.45	0.6756E+15	0.86	0.22	0.25	0.00	4.81	1.05	0.95	0.90	4.57	36
811111	384.61	0.1503E+15	0.73	0.21	0.19	0.00	1.97	0.80	1.25	1.47	4.10	36
811205	536.09	0.2095E+15	0.81	0.29	0.22	0.00	2.68	0.73	1.38	1.68	4.21	36
811208	1313.50	0.5134E+15	0.66	0.23	0.22	0.00	7.32	0.85	1.18	1.34	4.68	36
820220	0.00	0.0000E+00	0.00	0.00	0.00	0.00	0.00	0.00	0.00	0.00	0.00	36
820224	82.51	0.3225E+14	0.49	0.11	0.19	0.00	0.64	0.82	1.21	1.40	3.61	36
820320	0.00	0.0000E+00	0.00	0.00	0.00	0.00	1.74	0.98	1.03	1.05	4.10	36
820627	0.00	0.0000E+00	0.00	0.00	0.00	0.00	0.00	0.00	0.00	0.00	0.00	36
820701	784.38	0.3066E+15	0.80	0.28	0.21	0.00	3.66	1.08	0.93	0.86	4.47	36
830419	5087.09	0.1988E+16	0.86	0.26	0.27	0.00	21.63	0.88	1.14	1.27	5.16	36
830425	0.00	0.0000E+00	0.00	0.00	0.00	0.00	0.00	0.00	0.00	0.00	0.00	36
830525	8285.48	0.3238E+16	0.99	0.28	0.35	0.00	22.39	1.02	0.98	0.95	5.23	36
830618	0.00	0.0000E+00	0.00	0.00	0.00	0.00	0.00	0.00	0.00	0.00	0.00	36
830628	1326.86	0.5186E+15	0.68	0.19	0.20	0.52	7.91	0.95	1.05	1.10	4.75	36
830720	0.00	0.0000E+00	0.00	0.00	0.00	0.00	1.97	0.90	1.11	1.22	4.13	36
830804	931.00	0.3639E+15	0.71	0.19	0.19	0.00	4.62	0.95	1.05	1.10	4.51	36
831203	83.82	0.3276E+14	0.45	0.14	0.12	0.00	1.02	0.82	1.21	1.40	3.82	36
831207	680.22	0.2659E+15	0.77	0.14	0.24	0.00	2.96	1.00	1.00	1.00	4.34	36
840512	3827.95	0.1496E+16	0.99	0.26	0.40	0.00	9.54	0.93	1.08	1.16	4.82	36
840612	0.00	0.0000E+00	0.00	0.00	0.00	0.00	0.00	0.00	0.00	0.00	0.00	36
840616	2220.65	0.8680E+15	1.04	0.22	0.26	0.00	6.06	1.38	0.73	0.47	4.84	36
841027	0.00	0.0000E+00	0.00	0.00	0.00	0.00	1.39	0.88	1.14	1.27	3.96	36
841102	4560.54	0.1783E+16	1.00	0.22	0.27	0.00	15.15	0.93	1.08	1.16	5.02	36
841201	0.00	0.0000E+00	0.00	0.00	0.00	0.00	0.00	0.00	0.00	0.00	0.00	36
841206	4157.05	0.1625E+16	1.00	0.23	0.29	0.00	12.43	0.98	1.03	1.05	4.95	36
850430	228.36	0.8926E+14	0.68	0.19	0.15	0.46	1.67	0.95	1.05	1.10	4.07	36
850508	7788.50	0.3044E+16	0.89	0.26	0.25	0.00	23.80	1.10	0.91	0.82	5.29	36
850603	314.12	0.1228E+15	0.50	0.11	0.09	0.47	2.69	0.95	1.05	1.10	4.28	36
850607	0.00	0.0000E+00	0.00	0.00	0.00	0.00	1.80	0.90	1.11	1.22	4.09	36

Table 4A (cont'd) Warramunga array - Broad band and short period observations

Date	ψ_∞ (m^3)	Moment (N m)	Duration (s)	Rise time (s)	Fall time (s)	pP-P time (s)	1/2 Pk-Pk (nm)	Period (s)	Frequency (Hz)	Gain	m_b	
851024	0.00	0.0000E+00	0.00	0.00	0.00	0.00	0.00	0.00	0.00	0.00	0.00	36
851026	2265.49	0.8855E+15	1.09	0.31	0.36	0.00	5.14	1.52	0.66	0.35	4.85	36
851124	624.51	0.2441E+15	0.89	0.21	0.20	0.00	2.92	1.10	0.91	0.82	4.38	36
851126	6587.55	0.2575E+16	0.98	0.30	0.33	0.00	15.77	1.00	1.00	1.00	5.07	36
860426	86.86	0.3395E+14	0.39	0.12	0.14	0.39	1.79	0.75	1.33	1.60	4.04	36
860506	216.44	0.8460E+14	0.47	0.13	0.08	0.00	1.89	0.75	1.33	1.60	4.07	36
860527	199.08	0.7781E+14	0.56	0.11	0.12	0.00	1.82	0.82	1.21	1.40	4.07	36
860530	4350.69	0.1701E+16	0.89	0.24	0.35	0.00	13.58	0.98	1.03	1.05	4.99	36
861112	1209.53	0.4728E+15	0.80	0.26	0.28	0.00	6.27	0.90	1.11	1.22	4.63	36
861206	213.10	0.8329E+14	0.56	0.17	0.11	0.00	1.76	0.70	1.43	1.75	4.03	36
861210	1706.51	0.6670E+15	1.15	0.31	0.34	0.00	4.80	1.35	0.74	0.49	4.73	36
870505	151.86	0.5936E+14	0.45	0.17	0.10	0.00	1.57	0.77	1.29	1.53	3.99	36
870520	3002.84	0.1174E+16	0.95	0.21	0.30	0.00	9.98	1.05	0.95	0.90	4.89	36
870606	0.00	0.0000E+00	0.00	0.00	0.00	0.00	0.99	0.75	1.33	1.60	3.78	36
870621	1182.82	0.4623E+15	0.85	0.21	0.22	0.00	4.10	0.95	1.05	1.10	4.46	36
871023	3325.26	0.1300E+16	0.96	0.28	0.28	0.00	9.75	0.93	1.08	1.16	4.83	36
871105	2357.06	0.9213E+15	0.88	0.26	0.25	0.00	8.93	0.88	1.14	1.27	4.77	36
871119	5868.32	0.2294E+16	1.00	0.26	0.33	0.00	18.73	0.98	1.03	1.05	5.13	36
871129	363.53	0.1421E+15	0.63	0.27	0.13	0.00	1.64	0.95	1.05	1.10	4.06	36
880511	1995.53	0.7800E+15	0.93	0.17	0.24	0.00	7.70	0.98	1.03	1.05	4.75	36
880525	6059.10	0.2368E+16	0.98	0.25	0.23	0.00	15.16	1.17	0.85	0.70	5.13	36
880616	202.61	0.7919E+14	0.52	0.16	0.11	0.00	1.02	0.80	1.25	1.47	3.81	36
880623	1193.31	0.4664E+15	0.69	0.26	0.17	0.00	7.30	0.85	1.18	1.34	4.68	36
881105	1782.82	0.6968E+15	0.80	0.24	0.20	0.00	7.02	1.13	0.89	0.78	4.78	36
881123	2320.81	0.9071E+15	0.81	0.23	0.18	0.00	8.15	1.15	0.87	0.74	4.85	36
890603	1735.12	0.6782E+15	0.81	0.24	0.20	0.00	6.30	0.98	1.03	1.05	4.66	36
891024	2413.34	0.9433E+15	0.94	0.18	0.28	0.00	8.69	1.05	0.95	0.90	4.83	36
891031	1862.94	0.7282E+15	0.80	0.25	0.22	0.00	8.19	0.82	1.21	1.40	4.72	36
891120	1100.79	0.4303E+15	0.73	0.23	0.21	0.00	4.64	0.95	1.05	1.10	4.52	36

*

$B(\Delta)=3.87$ $G(\Delta)=$ $0.6804E-11 s\ m^{-2}$ $\rho_0=2600.0 kg\ m^{-3}$ $v_0=5600.0 km\ s^{-1}$

$\rho_1=2400.0 kg\ m^{-3}$ $v_1=3600.0 km\ s^{-1}$ $K=0.77$

Table 5A Warramunga array - Observations in the 0.5-4.0Hz band

Date	1/2 Pk-Pk (nm)	Period (s)	Frequency (Hz)	Gain	m_b	r.m.s. 0-3s (nm)	r.m.s. 0-6s (nm)	r.m.s. 0-9s (nm)	r.m.s. 0-15s (nm)	r.m.s. 3-9s (nm)	r.m.s. 3-15s (nm)	r.m.s. 9-18s (nm)	r.m.s. noise (nm)
770706	3.48	1.48	0.68	0.39	4.66	1.60	1.71	1.63	1.39	1.64	1.33	0.80	0.47
780227	0.00	0.00	0.00	0.00	0.00	0.00	0.00	0.00	0.00	0.00	0.00	0.00	0.00
780322	3.74	0.77	1.29	1.54	4.37	1.64	1.43	1.28	1.11	1.06	0.92	0.71	0.29
780719	1.94	0.82	1.21	1.40	4.10	0.91	0.80	0.76	0.65	0.67	0.57	0.42	0.34
780726	0.00	0.00	0.00	0.00	0.00	0.00	0.00	0.00	0.00	0.00	0.00	0.00	0.00
781130	27.24	0.85	1.18	1.34	5.25	15.01	14.33	13.13	10.58	12.07	9.15	4.59	0.29
781219	2.46	0.73	1.38	1.68	4.18	1.44	1.26	1.20	1.22	1.06	1.16	1.10	0.21
790301	2.77	0.73	1.38	1.68	4.23	1.17	1.21	1.06	0.92	1.00	0.85	0.62	0.40
790309	3.17	0.77	1.29	1.53	4.30	1.49	1.31	1.26	1.09	1.13	0.97	0.73	0.42
790324	2.92	0.70	1.43	1.75	4.25	1.35	1.20	1.15	1.08	1.03	1.00	0.87	0.23
790618	3.40	0.77	1.29	1.53	4.33	1.43	1.20	1.07	0.90	0.84	0.71	0.51	0.27
790629	5.61	0.88	1.14	1.27	4.57	2.27	2.13	1.98	1.82	1.82	1.68	1.36	0.35
790725	44.62	1.27	0.78	0.57	5.66	24.58	22.84	21.24	17.09	19.36	14.63	6.91	0.27
790728	3.24	0.85	1.18	1.34	4.33	1.40	1.36	1.24	1.09	1.15	1.00	0.79	0.46
791122	1.53	0.85	1.18	1.34	4.00	0.73	0.76	0.66	0.59	0.62	0.55	0.48	0.29
800223	1.36	0.80	1.25	1.47	3.93	0.57	0.50	0.51	0.51	0.48	0.50	0.44	0.36
800303	1.28	1.42	0.70	0.43	4.20	0.64	0.60	0.65	0.58	0.66	0.56	0.50	0.40
800323	12.60	1.33	0.75	0.52	5.13	7.62	7.07	6.41	5.43	5.70	4.73	3.39	0.36
800401	8.07	0.80	1.25	1.47	4.71	3.45	2.92	2.81	2.45	2.42	2.13	1.59	0.23
800404	0.00	0.00	0.00	0.00	0.00	0.00	0.00	0.00	0.00	0.00	0.00	0.00	0.00
800616	5.59	0.75	1.33	1.60	4.54	3.07	2.96	2.63	2.32	2.37	2.09	1.60	0.34
800621	2.43	0.75	1.33	1.60	4.18	1.13	1.29	1.30	1.11	1.38	1.11	0.77	0.61
800706	2.35	0.75	1.33	1.60	4.16	0.90	1.00	0.89	0.76	0.89	0.72	0.49	0.35
800719	16.37	1.45	0.69	0.41	5.31	9.58	8.65	8.06	6.99	7.18	6.18	5.12	0.39
801203	12.49	1.48	0.68	0.39	5.21	7.10	6.59	6.03	5.21	5.41	4.62	3.99	0.27
810227	1.94	0.88	1.14	1.27	4.11	0.82	0.71	0.64	0.56	0.52	0.48	0.44	0.40
810306	1.13	0.73	1.38	1.68	3.84	0.63	0.59	0.51	0.45	0.44	0.39	0.35	0.38
810328	2.85	0.75	1.33	1.60	4.24	1.18	1.08	1.00	0.84	0.90	0.73	0.49	0.30
810410	2.33	1.85	0.54	0.20	4.67	1.20	0.96	0.85	0.73	0.61	0.55	0.47	0.24
810708	3.93	1.52	0.66	0.35	4.73	2.17	2.06	1.91	1.67	1.77	1.51	1.38	0.32
810718	1.13	0.73	1.38	1.68	3.84	0.59	0.52	0.50	0.44	0.44	0.39	0.36	0.34
810803	4.22	0.75	1.33	1.60	4.41	2.39	1.99	1.83	1.68	1.47	1.45	1.25	0.29
811111	1.83	0.68	1.48	1.83	4.04	0.89	0.75	0.70	0.71	0.58	0.66	0.69	0.24
811205	2.19	0.75	1.33	1.60	4.13	0.96	0.93	0.86	0.75	0.80	0.69	0.53	0.42
811208	6.88	0.80	1.25	1.47	4.64	2.88	2.40	2.35	2.02	2.03	1.75	1.37	0.26
820220	0.00	0.00	0.00	0.00	0.00	0.00	0.00	0.00	0.00	0.00	0.00	0.00	0.00
820224	0.93	1.00	1.00	1.00	3.84	0.48	0.51	0.51	0.42	0.52	0.41	0.34	0.29
820320	2.61	1.30	0.77	0.54	4.44	1.32	1.21	1.08	0.95	0.94	0.83	0.64	0.75
820627	0.00	0.00	0.00	0.00	0.00	0.00	0.00	0.00	0.00	0.00	0.00	0.00	0.00
820701	3.70	0.82	1.21	1.40	4.38	2.14	1.95	1.69	1.48	1.42	1.26	1.01	0.30
830419	19.56	0.80	1.25	1.47	5.09	8.38	7.07	6.14	5.80	4.64	4.95	4.83	0.28
830425	0.00	0.00	0.00	0.00	0.00	0.00	0.00	0.00	0.00	0.00	0.00	0.00	0.00
830525	18.68	0.95	1.05	1.10	5.12	9.70	9.92	8.95	8.57	8.55	8.26	7.53	0.10
830618	0.00	0.00	0.00	0.00	0.00	0.00	0.00	0.00	0.00	0.00	0.00	0.00	0.00
830628	7.40	0.82	1.21	1.40	4.68	3.38	3.10	2.84	2.36	2.52	2.02	1.22	0.47
830720	1.63	1.58	0.63	0.32	4.38	0.92	0.70	0.62	0.56	0.38	0.42	0.41	0.47
830804	3.66	1.30	0.77	0.54	4.58	2.22	2.11	1.86	1.68	1.64	1.52	1.22	0.43
831203	1.41	0.60	1.67	2.09	3.92	0.65	0.64	0.65	0.58	0.65	0.56	0.50	0.36
831207	2.18	1.80	0.56	0.22	4.62	1.29	1.15	1.05	1.08	0.91	1.01	0.97	0.60
840512	9.25	0.73	1.38	1.68	4.75	5.20	5.10	4.42	4.15	3.97	3.85	3.27	0.25
840612	0.00	0.00	0.00	0.00	0.00	0.00	0.00	0.00	0.00	0.00	0.00	0.00	0.00
840616	5.80	1.17	0.85	0.70	4.72	3.14	2.65	2.38	2.13	1.90	1.79	2.04	0.45
841027	1.38	0.60	1.67	2.09	3.91	0.69	0.65	0.62	0.54	0.58	0.49	0.36	0.26
841102	14.14	0.85	1.18	1.34	4.96	7.25	6.76	6.21	5.41	5.61	4.84	4.35	0.26
841201	0.00	0.00	0.00	0.00	0.00	0.00	0.00	0.00	0.00	0.00	0.00	0.00	0.00
841206	10.37	0.80	1.25	1.47	4.82	5.30	4.80	4.65	4.35	4.29	4.07	3.33	0.25
850430	1.41	1.73	0.58	0.25	4.39	0.80	0.70	0.61	0.56	0.48	0.48	0.49	0.27
850508	22.39	0.77	1.29	1.53	5.14	11.45	10.53	9.28	7.68	7.98	6.40	3.76	0.32
850603	2.65	1.83	0.55	0.21	4.71	1.42	1.19	1.04	0.94	0.78	0.77	0.73	0.32
850607	1.97	1.00	1.00	1.00	4.16	0.96	0.84	0.86	0.74	0.81	0.67	0.48	0.61

Table 5A (cont'd) Warramunga array - Observations in the 0.5-4.0Hz band

Date	1/2 Pk-Pk (nm)	Period (s)	Frequency (Hz)	Gain	m_b	r.m.s. 0-3s (nm)	r.m.s. 0-6s (nm)	r.m.s. 0-9s (nm)	r.m.s. 0-15s (nm)	r.m.s. 3-9s (nm)	r.m.s. 3-15s (nm)	r.m.s. 9-18s (nm)	r.m.s. noise (nm)
851024	0.00	0.00	0.00	0.00	0.00	0.00	0.00	0.00	0.00	0.00	0.00	0.00	0.00
851026	5.65	0.85	1.18	1.34	4.57	3.07	2.58	2.52	2.33	2.20	2.11	2.01	0.27
851124	2.39	0.95	1.05	1.10	4.23	1.13	1.13	0.98	0.80	0.89	0.69	0.38	0.28
851126	13.78	1.48	0.68	0.39	5.25	8.11	7.51	6.54	6.05	5.60	5.41	4.41	0.30
860426	1.45	0.85	1.18	1.34	3.98	0.82	0.83	0.72	0.64	0.66	0.59	0.48	0.37
860506	1.49	0.82	1.21	1.40	3.98	0.76	0.67	0.63	0.53	0.55	0.46	0.36	0.29
860527	1.32	1.77	0.56	0.23	4.39	0.67	0.57	0.65	0.62	0.64	0.60	0.53	0.37
860530	12.06	0.82	1.21	1.40	4.89	6.17	5.80	5.51	4.71	5.14	4.27	3.16	0.28
861112	5.87	0.82	1.21	1.40	4.58	2.78	2.68	2.48	2.08	2.32	1.86	1.22	0.27
861206	1.74	1.02	0.98	0.95	4.12	0.93	0.85	0.74	0.69	0.63	0.61	0.65	0.28
861210	3.88	1.10	0.91	0.82	4.51	2.28	2.02	1.87	1.88	1.62	1.77	1.69	0.36
870505	1.45	0.80	1.25	1.47	3.96	0.60	0.55	0.57	0.57	0.55	0.57	0.55	0.43
870520	8.57	0.93	1.08	1.16	4.77	4.78	4.56	3.95	3.77	3.45	3.46	2.95	0.26
870606	1.34	0.85	1.18	1.34	3.94	0.63	0.61	0.59	0.55	0.57	0.53	0.50	0.31
870621	3.26	0.77	1.29	1.53	4.31	1.90	1.70	1.52	1.47	1.28	1.34	1.26	0.27
871023	8.01	0.85	1.18	1.34	4.72	4.67	4.31	3.88	3.75	3.42	3.48	3.13	0.27
871105	8.06	0.75	1.33	1.60	4.70	3.92	3.52	3.12	2.71	2.63	2.31	1.68	0.24
871119	16.96	0.85	1.18	1.34	5.04	8.19	8.03	7.14	6.20	6.56	5.60	4.01	0.37
871129	1.60	0.85	1.18	1.34	4.02	0.73	0.68	0.68	0.65	0.66	0.63	0.56	0.33
880511	6.02	0.90	1.11	1.22	4.61	2.92	2.82	2.65	2.64	2.51	2.57	2.55	0.45
880525	11.56	1.00	1.00	1.00	4.93	6.95	6.66	5.99	5.04	5.45	4.43	2.79	0.37
880616	1.13	0.80	1.25	1.47	3.85	0.57	0.46	0.50	0.49	0.47	0.47	0.43	0.32
880623	5.65	0.77	1.29	1.53	4.55	2.67	2.44	2.23	2.07	1.97	1.89	1.54	0.46
881105	6.20	0.65	1.54	1.91	4.57	3.32	2.71	2.53	2.08	2.02	1.62	1.02	0.23
881123	6.66	1.02	0.98	0.95	4.70	4.01	3.78	3.48	2.93	3.17	2.59	1.73	0.23
890603	5.39	0.75	1.33	1.60	4.52	2.82	2.59	2.30	2.19	1.99	2.00	1.74	0.37
891024	6.82	0.95	1.05	1.10	4.68	3.75	3.66	3.48	3.18	3.34	3.03	2.76	0.32
891031	7.26	0.80	1.25	1.47	4.66	3.36	2.62	2.41	2.11	1.76	1.65	1.53	0.24
891120	4.40	0.75	1.33	1.60	4.43	2.36	2.06	2.01	1.89	1.81	1.75	1.43	0.42

Table 6A Warramunga array - Observations in the 1.0-4.0Hz band

Date	1/2 Pk-Pk (nm)	Period (s)	Frequency (Hz)	Gain	m_b	r.m.s. 0-3s (nm)	r.m.s. 0-6s (nm)	r.m.s. 0-9s (nm)	r.m.s. 0-15s (nm)	r.m.s. 3-9s (nm)	r.m.s. 3-15s (nm)	r.m.s. 9-18s (nm)	r.m.s. noise (nm)
770706	1.89	0.65	1.54	1.91	4.05	0.90	0.87	0.88	0.74	0.87	0.69	0.41	0.25
780227	0.00	0.00	0.00	0.00	0.00	0.00	0.00	0.00	0.00	0.00	0.00	0.00	0.00
780322	2.73	0.75	1.33	1.61	4.22	1.37	1.18	1.08	0.92	0.90	0.77	0.57	0.10
780719	1.33	0.65	1.54	1.91	3.90	0.53	0.54	0.47	0.40	0.44	0.36	0.25	0.13
780726	0.00	0.00	0.00	0.00	0.00	0.00	0.00	0.00	0.00	0.00	0.00	0.00	0.00
781130	16.13	0.95	1.05	1.10	5.06	7.71	8.25	7.36	5.97	7.17	5.45	2.84	0.12
781219	1.88	0.70	1.43	1.75	4.05	0.89	0.85	0.79	0.80	0.73	0.78	0.73	0.09
790301	2.09	0.75	1.33	1.60	4.11	0.86	0.81	0.74	0.64	0.67	0.57	0.41	0.16
790309	2.12	0.70	1.43	1.75	4.11	1.01	0.85	0.90	0.79	0.85	0.72	0.54	0.13
790324	2.03	0.70	1.43	1.75	4.09	0.87	0.80	0.79	0.78	0.75	0.75	0.69	0.08
790618	2.31	0.68	1.48	1.83	4.14	0.93	0.84	0.76	0.64	0.66	0.54	0.39	0.14
790629	3.78	0.77	1.29	1.53	4.37	1.38	1.40	1.30	1.24	1.26	1.21	1.00	0.13
790725	23.77	0.82	1.21	1.40	5.18	11.60	11.80	10.83	8.74	10.42	7.87	3.85	0.12
790728	2.04	0.77	1.29	1.53	4.10	0.94	0.93	0.92	0.78	0.90	0.73	0.47	0.22
791122	1.25	0.73	1.38	1.68	3.88	0.49	0.53	0.49	0.42	0.48	0.39	0.28	0.12
800223	1.02	0.77	1.29	1.53	3.80	0.39	0.34	0.32	0.28	0.27	0.25	0.20	0.14
800303	0.82	0.63	1.60	2.00	3.69	0.41	0.35	0.35	0.32	0.31	0.29	0.30	0.15
800323	8.53	0.73	1.38	1.68	4.72	4.16	4.08	3.76	3.24	3.55	2.96	2.15	0.11
800401	5.81	0.73	1.38	1.68	4.55	2.63	2.28	2.23	1.91	1.99	1.68	1.14	0.09
800404	0.00	0.00	0.00	0.00	0.00	0.00	0.00	0.00	0.00	0.00	0.00	0.00	0.00
800616	3.90	0.68	1.48	1.83	4.37	1.82	1.88	1.68	1.48	1.61	1.38	1.04	0.13
800621	1.77	0.65	1.54	1.91	4.02	0.78	0.88	0.88	0.73	0.93	0.72	0.46	0.38
800706	1.41	0.80	1.25	1.47	3.95	0.60	0.61	0.59	0.51	0.59	0.48	0.32	0.20
800719	10.76	0.68	1.48	1.83	4.81	5.34	4.93	4.69	4.13	4.32	3.77	3.11	0.17
801203	8.23	0.65	1.54	1.91	4.69	3.93	3.78	3.53	3.10	3.32	2.85	2.41	0.11
810227	1.33	0.80	1.25	1.47	3.92	0.59	0.47	0.44	0.37	0.34	0.29	0.21	0.16
810306	0.75	0.80	1.25	1.47	3.67	0.36	0.35	0.33	0.29	0.31	0.27	0.22	0.16
810328	2.03	0.73	1.38	1.68	4.09	0.79	0.74	0.69	0.58	0.63	0.52	0.36	0.13
810410	1.42	0.63	1.60	2.00	3.93	0.61	0.56	0.50	0.45	0.43	0.39	0.31	0.12
810708	3.07	0.65	1.54	1.91	4.26	1.40	1.38	1.19	1.04	1.07	0.93	0.89	0.16
810718	0.97	0.68	1.48	1.83	3.77	0.39	0.34	0.31	0.28	0.25	0.24	0.24	0.15
810803	3.00	0.68	1.48	1.83	4.26	1.20	1.17	1.10	1.01	1.05	0.96	0.75	0.15
811111	1.54	0.73	1.38	1.68	3.97	0.71	0.59	0.53	0.55	0.41	0.50	0.53	0.10
811205	1.65	0.73	1.38	1.68	4.00	0.69	0.64	0.62	0.52	0.58	0.47	0.31	0.14
811208	5.07	0.65	1.54	1.91	4.48	2.16	1.87	1.78	1.58	1.55	1.39	1.10	0.10
820220	0.00	0.00	0.00	0.00	0.00	0.00	0.00	0.00	0.00	0.00	0.00	0.00	0.00
820224	0.48	1.08	0.93	0.86	3.59	0.22	0.23	0.23	0.19	0.23	0.19	0.16	0.10
820320	1.22	1.30	0.77	0.54	4.11	0.62	0.58	0.59	0.55	0.57	0.54	0.45	0.27
820627	0.00	0.00	0.00	0.00	0.00	0.00	0.00	0.00	0.00	0.00	0.00	0.00	0.00
820701	2.44	0.75	1.33	1.60	4.18	0.93	1.03	0.93	0.83	0.93	0.81	0.63	0.11
830419	13.72	0.70	1.43	1.75	4.92	5.89	4.91	4.46	4.43	3.53	3.98	3.99	0.15
830425	0.00	0.00	0.00	0.00	0.00	0.00	0.00	0.00	0.00	0.00	0.00	0.00	0.00
830525	11.48	0.80	1.25	1.47	4.86	5.18	5.63	5.35	5.14	5.43	5.12	4.28	0.10
830618	0.00	0.00	0.00	0.00	0.00	0.00	0.00	0.00	0.00	0.00	0.00	0.00	0.00
830628	5.01	0.75	1.33	1.60	4.49	2.22	1.99	2.06	1.71	1.97	1.56	0.89	0.28
830720	0.93	0.77	1.29	1.53	3.76	0.51	0.42	0.36	0.32	0.24	0.25	0.23	0.24
830804	2.21	0.88	1.14	1.27	4.17	1.13	1.11	0.96	0.95	0.86	0.91	0.81	0.24
831203	1.10	0.65	1.54	1.91	3.82	0.49	0.45	0.40	0.36	0.35	0.31	0.27	0.16
831207	1.38	0.90	1.11	1.22	3.97	0.73	0.63	0.60	0.67	0.52	0.65	0.63	0.23
840512	6.42	0.77	1.29	1.53	4.60	3.09	2.92	2.66	2.48	2.42	2.30	2.03	0.13
840612	0.00	0.00	0.00	0.00	0.00	0.00	0.00	0.00	0.00	0.00	0.00	0.00	0.00
840616	3.16	0.88	1.14	1.27	4.32	1.37	1.32	1.20	1.22	1.12	1.18	1.22	0.19
841027	0.96	0.63	1.60	2.00	3.76	0.51	0.44	0.40	0.36	0.34	0.31	0.28	0.11
841102	10.25	0.65	1.54	1.91	4.79	4.84	4.90	4.45	3.76	4.25	3.43	2.52	0.13
841201	0.00	0.00	0.00	0.00	0.00	0.00	0.00	0.00	0.00	0.00	0.00	0.00	0.00
841206	6.83	0.63	1.60	2.00	4.61	3.17	3.13	3.23	3.01	3.26	2.97	2.28	0.12
850430	1.03	0.70	1.43	1.75	3.80	0.39	0.42	0.37	0.34	0.36	0.33	0.26	0.14
850508	16.08	0.75	1.33	1.60	5.00	6.49	7.33	6.33	5.22	6.25	4.86	2.42	0.11
850603	1.79	0.63	1.60	2.00	4.03	0.82	0.76	0.70	0.65	0.63	0.61	0.52	0.16
850607	0.94	0.63	1.60	2.00	3.75	0.43	0.37	0.45	0.41	0.46	0.41	0.32	0.26

Table 6A (cont'd) Warramunga array - Observations in the 1.0-4.0Hz band

Date	1/2 Pk-Pk (nm)	Period (s)	Frequency (Hz)	Gain	m_b	r.m.s. 0-3s (nm)	r.m.s. 0-6s (nm)	r.m.s. 0-9s (nm)	r.m.s. 0-15s (nm)	r.m.s. 3-9s (nm)	r.m.s. 3-15s (nm)	r.m.s. 9-18s (nm)	r.m.s. noise (nm)
851024	0.00	0.00	0.00	0.00	0.00	0.00	0.00	0.00	0.00	0.00	0.00	0.00	0.00
851026	3.41	0.77	1.29	1.53	4.33	1.35	1.31	1.26	1.34	1.22	1.34	1.30	0.14
851124	1.40	0.93	1.08	1.16	3.99	0.69	0.65	0.59	0.50	0.54	0.44	0.30	0.14
851126	9.15	0.88	1.14	1.27	4.78	4.05	3.89	3.59	3.32	3.34	3.11	2.53	0.13
860426	1.17	0.80	1.25	1.47	3.87	0.50	0.45	0.42	0.36	0.37	0.32	0.27	0.14
860506	1.11	0.70	1.43	1.75	3.83	0.53	0.44	0.38	0.34	0.29	0.27	0.25	0.13
860527	0.92	0.57	1.74	2.19	3.74	0.42	0.37	0.37	0.42	0.35	0.42	0.42	0.13
860530	9.07	0.57	1.74	2.19	4.73	4.05	3.89	3.79	3.14	3.66	2.87	1.78	0.15
861112	4.86	0.63	1.60	2.00	4.46	2.09	1.93	1.82	1.50	1.67	1.31	0.81	0.18
861206	1.36	0.65	1.54	1.91	3.91	0.77	0.63	0.54	0.47	0.38	0.36	0.35	0.14
861210	1.94	0.85	1.18	1.34	4.10	1.11	1.07	1.02	1.02	0.96	0.99	0.88	0.14
870505	1.25	0.63	1.60	2.00	3.87	0.51	0.45	0.41	0.43	0.35	0.41	0.42	0.20
870520	5.84	0.60	1.67	2.09	4.54	2.93	2.87	2.57	2.43	2.37	2.29	1.90	0.12
870606	0.91	0.75	1.33	1.60	3.75	0.42	0.40	0.36	0.36	0.32	0.35	0.35	0.14
870621	2.10	0.95	1.05	1.10	4.17	1.05	0.98	0.91	1.00	0.84	0.99	0.96	0.13
871023	5.22	0.93	1.08	1.16	4.56	2.40	2.22	2.15	2.28	2.01	2.25	2.15	0.13
871105	5.82	0.80	1.25	1.47	4.57	2.65	2.47	2.24	2.04	2.01	1.85	1.45	0.11
871119	12.05	0.63	1.60	2.00	4.85	5.21	5.38	5.01	4.16	4.91	3.85	2.16	0.22
871129	1.13	0.60	1.67	2.09	3.83	0.52	0.49	0.50	0.47	0.49	0.46	0.41	0.20
880511	4.39	0.60	1.67	2.09	4.41	1.97	1.94	1.81	1.72	1.72	1.65	1.47	0.24
880525	7.32	0.77	1.29	1.53	4.66	3.76	4.21	3.77	3.12	3.78	2.94	1.56	0.14
880616	0.79	0.73	1.38	1.68	3.68	0.35	0.28	0.27	0.25	0.22	0.22	0.22	0.15
880623	4.09	0.63	1.60	2.00	4.38	1.77	1.63	1.53	1.41	1.40	1.30	1.03	0.30
881105	4.39	0.57	1.74	2.19	4.41	2.06	1.87	1.68	1.38	1.45	1.15	0.74	0.15
881123	4.59	0.70	1.43	1.75	4.44	2.35	2.46	2.24	1.87	2.19	1.73	1.00	0.12
890603	3.75	0.60	1.67	2.09	4.35	1.68	1.53	1.40	1.31	1.24	1.20	1.05	0.14
891024	5.32	0.60	1.67	2.09	4.50	2.33	2.51	2.24	1.99	2.20	1.90	1.56	0.13
891031	5.12	0.73	1.38	1.68	4.49	2.12	1.66	1.59	1.47	1.25	1.26	1.11	0.14
891120	3.01	0.63	1.60	2.00	4.25	1.44	1.32	1.40	1.34	1.37	1.31	1.04	0.18

Table 7A Gauribidanur array - Broad band and short period observations

Date	Ψ_{∞} (m^3)	Moment (N m)	Duration (s)	Rise time (s)	Fall time (s)	pP-P time (s)	1/2 Pk-Pk (nm)	Period (s)	Frequency (Hz)	Gain	m_b	
760711	0.00	0.0000E+00	0.00	0.00	0.00	0.00	3.62	0.73	1.38	1.69	4.18	26
770319	0.00	0.0000E+00	0.00	0.00	0.00	0.00	26.08	0.80	1.25	1.47	5.06	26
770706	0.00	0.0000E+00	0.00	0.00	0.00	0.00	5.97	0.85	1.18	1.34	4.43	26
771112	0.00	0.0000E+00	0.00	0.00	0.00	0.00	5.08	1.05	0.95	0.90	4.44	26
771124	0.00	0.0000E+00	0.00	0.00	0.00	0.00	26.40	0.80	1.25	1.47	5.06	26
771217	0.00	0.0000E+00	0.00	0.00	0.00	0.00	4.37	0.85	1.18	1.34	4.29	26
780227	0.00	0.0000E+00	0.00	0.00	0.00	0.00	0.00	0.00	0.00	0.00	0.00	26
780322	0.00	0.0000E+00	0.00	0.00	0.00	0.00	2.48	0.90	1.11	1.22	4.07	26
780719	0.00	0.0000E+00	0.00	0.00	0.00	0.00	0.00	0.00	0.00	0.00	0.00	26
780726	0.00	0.0000E+00	0.00	0.00	0.00	0.00	0.00	0.00	0.00	0.00	0.00	26
781102	0.00	0.0000E+00	0.00	0.00	0.00	0.00	3.95	0.88	1.14	1.28	4.26	26
781130	0.00	0.0000E+00	0.00	0.00	0.00	0.00	24.73	0.80	1.25	1.47	5.03	26
781217	0.00	0.0000E+00	0.00	0.00	0.00	0.00	3.74	0.70	1.43	1.76	4.19	26
781219	0.00	0.0000E+00	0.00	0.00	0.00	0.00	4.04	0.80	1.25	1.47	4.25	26
790301	0.00	0.0000E+00	0.00	0.00	0.00	0.00	3.80	0.90	1.11	1.22	4.25	26
790309	0.00	0.0000E+00	0.00	0.00	0.00	0.00	2.26	0.93	1.08	1.16	4.03	34
790324	0.00	0.0000E+00	0.00	0.00	0.00	0.00	2.74	0.73	1.38	1.66	4.07	34
790404	0.00	0.0000E+00	0.00	0.00	0.00	0.00	0.00	0.00	0.00	0.00	0.00	26
790618	0.00	0.0000E+00	0.00	0.00	0.00	0.00	4.43	0.88	1.14	1.28	4.31	26
790629	0.00	0.0000E+00	0.00	0.00	0.00	0.00	5.25	0.77	1.29	1.54	4.35	26
790725	0.00	0.0000E+00	0.00	0.00	0.00	0.00	34.41	0.90	1.11	1.21	5.21	34
790728	0.00	0.0000E+00	0.00	0.00	0.00	0.00	3.19	0.88	1.14	1.27	4.17	34
791122	0.00	0.0000E+00	0.00	0.00	0.00	0.00	0.00	0.00	0.00	0.00	0.00	26
800223	0.00	0.0000E+00	0.00	0.00	0.00	0.00	1.22	0.75	1.33	1.59	3.72	34
800303	0.00	0.0000E+00	0.00	0.00	0.00	0.00	0.92	0.75	1.33	1.59	3.60	34
800323	0.00	0.0000E+00	0.00	0.00	0.00	0.00	11.55	0.85	1.18	1.33	4.72	34
800401	0.00	0.0000E+00	0.00	0.00	0.00	0.00	6.95	0.85	1.18	1.33	4.50	34
800404	0.00	0.0000E+00	0.00	0.00	0.00	0.00	1.26	0.82	1.21	1.39	3.75	34
800621	0.00	0.0000E+00	0.00	0.00	0.00	0.00	4.48	0.77	1.29	1.54	4.28	26
800706	0.00	0.0000E+00	0.00	0.00	0.00	0.00	0.00	0.00	0.00	0.00	0.00	26
800719	0.00	0.0000E+00	0.00	0.00	0.00	0.00	15.73	0.82	1.21	1.39	4.85	34
801203	0.00	0.0000E+00	0.00	0.00	0.00	0.00	9.64	0.73	1.38	1.66	4.61	34
810227	0.00	0.0000E+00	0.00	0.00	0.00	0.00	1.05	0.68	1.48	1.81	3.65	34
810306	0.00	0.0000E+00	0.00	0.00	0.00	0.00	1.11	0.85	1.18	1.33	3.70	34
810328	0.00	0.0000E+00	0.00	0.00	0.00	0.00	3.19	0.82	1.21	1.39	4.15	34
810410	0.00	0.0000E+00	0.00	0.00	0.00	0.00	1.60	0.77	1.29	1.52	3.84	34
810708	0.00	0.0000E+00	0.00	0.00	0.00	0.00	2.26	0.63	1.60	1.96	3.97	34
810711	0.00	0.0000E+00	0.00	0.00	0.00	0.00	0.00	0.00	0.00	0.00	0.00	34
810718	0.00	0.0000E+00	0.00	0.00	0.00	0.00	0.00	0.00	0.00	0.00	0.00	34
810803	0.00	0.0000E+00	0.00	0.00	0.00	0.00	0.00	0.00	0.00	0.00	0.00	34
811111	0.00	0.0000E+00	0.00	0.00	0.00	0.00	2.16	0.68	1.48	1.81	3.96	34
811205	0.00	0.0000E+00	0.00	0.00	0.00	0.00	2.62	0.93	1.08	1.16	4.10	34
811208	0.00	0.0000E+00	0.00	0.00	0.00	0.00	7.97	0.73	1.38	1.66	4.53	34
820220	0.00	0.0000E+00	0.00	0.00	0.00	0.00	0.00	0.00	0.00	0.00	0.00	34
820224	0.00	0.0000E+00	0.00	0.00	0.00	0.00	0.00	0.00	0.00	0.00	0.00	34
820320	0.00	0.0000E+00	0.00	0.00	0.00	0.00	2.42	0.68	1.48	1.81	4.01	34
820627	0.00	0.0000E+00	0.00	0.00	0.00	0.00	0.00	0.00	0.00	0.00	0.00	34
820701	0.00	0.0000E+00	0.00	0.00	0.00	0.00	0.00	0.00	0.00	0.00	0.00	34
820725	0.00	0.0000E+00	0.00	0.00	0.00	0.00	9.88	0.77	1.29	1.52	4.63	34
830419	0.00	0.0000E+00	0.00	0.00	0.00	0.00	22.25	0.77	1.29	1.52	4.99	34
830425	0.00	0.0000E+00	0.00	0.00	0.00	0.00	0.00	0.00	0.00	0.00	0.00	34
830525	0.00	0.0000E+00	0.00	0.00	0.00	0.00	19.12	0.82	1.21	1.39	4.93	34
830618	0.00	0.0000E+00	0.00	0.00	0.00	0.00	0.00	0.00	0.00	0.00	0.00	34
830628	0.00	0.0000E+00	0.00	0.00	0.00	0.00	7.98	0.85	1.18	1.33	4.56	34
830720	0.00	0.0000E+00	0.00	0.00	0.00	0.00	0.00	0.00	0.00	0.00	0.00	34
830804	0.00	0.0000E+00	0.00	0.00	0.00	0.00	3.18	0.60	1.67	2.05	4.12	34
831203	0.00	0.0000E+00	0.00	0.00	0.00	0.00	0.00	0.00	0.00	0.00	0.00	34
831207	0.00	0.0000E+00	0.00	0.00	0.00	0.00	2.23	0.90	1.11	1.21	4.02	34
840508	0.00	0.0000E+00	0.00	0.00	0.00	0.00	1.54	0.65	1.54	1.88	3.81	34
840512	0.00	0.0000E+00	0.00	0.00	0.00	0.00	12.23	0.77	1.29	1.52	4.73	34

Table 7A (cont'd) Gauribidanur array - Broad band and short period observations

Date	Ψ_∞ (m^3)	Moment (N m)	Duration (s)	Rise time (s)	Fall time (s)	pP-P time (s)	1/2 Pk-Pk (nm)	Period (s)	Frequency (Hz)	Gain	m_b	
840612	0.00	0.0000E+00	0.00	0.00	0.00	0.00	1.61	0.65	1.54	1.88	3.83	34
840616	0.00	0.0000E+00	0.00	0.00	0.00	0.00	5.37	0.88	1.14	1.27	4.39	34
841027	0.00	0.0000E+00	0.00	0.00	0.00	0.00	0.00	0.00	0.00	0.00	0.00	34
841102	0.00	0.0000E+00	0.00	0.00	0.00	0.00	9.86	0.77	1.29	1.52	4.63	34
841201	0.00	0.0000E+00	0.00	0.00	0.00	0.00	0.00	0.00	0.00	0.00	0.00	34
841206	0.00	0.0000E+00	0.00	0.00	0.00	0.00	11.90	0.85	1.18	1.33	4.73	34
850430	0.00	0.0000E+00	0.00	0.00	0.00	0.00	0.00	0.00	0.00	0.00	0.00	34
850508	0.00	0.0000E+00	0.00	0.00	0.00	0.00	14.25	0.93	1.08	1.16	4.83	34
850603	0.00	0.0000E+00	0.00	0.00	0.00	0.00	2.11	0.68	1.48	1.81	3.95	34
850607	0.00	0.0000E+00	0.00	0.00	0.00	0.00	0.00	0.00	0.00	0.00	0.00	34
851024	0.00	0.0000E+00	0.00	0.00	0.00	0.00	0.00	0.00	0.00	0.00	0.00	34
851026	0.00	0.0000E+00	0.00	0.00	0.00	0.00	5.46	0.88	1.14	1.27	4.40	34
851124	0.00	0.0000E+00	0.00	0.00	0.00	0.00	1.96	0.80	1.25	1.46	3.93	34
851126	0.00	0.0000E+00	0.00	0.00	0.00	0.00	16.27	0.90	1.11	1.21	4.88	34
860527	0.00	0.0000E+00	0.00	0.00	0.00	0.00	0.00	0.00	0.00	0.00	0.00	34
860530	0.00	0.0000E+00	0.00	0.00	0.00	0.00	9.36	0.85	1.18	1.33	4.63	34
861112	0.00	0.0000E+00	0.00	0.00	0.00	0.00	4.09	0.73	1.38	1.66	4.24	34
861206	0.00	0.0000E+00	0.00	0.00	0.00	0.00	0.75	0.55	1.82	2.23	3.50	34
861210	0.00	0.0000E+00	0.00	0.00	0.00	0.00	4.10	0.85	1.18	1.33	4.27	34
870505	0.00	0.0000E+00	0.00	0.00	0.00	0.00	2.13	0.82	1.21	1.39	3.98	34
870520	0.00	0.0000E+00	0.00	0.00	0.00	0.00	7.30	0.82	1.21	1.39	4.51	34
870606	0.00	0.0000E+00	0.00	0.00	0.00	0.00	1.78	0.63	1.60	1.96	3.87	34
870621	0.00	0.0000E+00	0.00	0.00	0.00	0.00	7.07	0.98	1.03	1.05	4.55	34
871023	0.00	0.0000E+00	0.00	0.00	0.00	0.00	9.03	0.85	1.18	1.33	4.61	34
871105	0.00	0.0000E+00	0.00	0.00	0.00	0.00	10.77	0.75	1.33	1.59	4.67	34
871119	0.00	0.0000E+00	0.00	0.00	0.00	0.00	12.75	0.85	1.18	1.33	4.76	34
871129	0.00	0.0000E+00	0.00	0.00	0.00	0.00	2.64	0.73	1.38	1.66	4.05	34
880511	0.00	0.0000E+00	0.00	0.00	0.00	0.00	5.74	0.75	1.33	1.59	4.39	34
880525	0.00	0.0000E+00	0.00	0.00	0.00	0.00	10.40	0.82	1.21	1.39	4.67	34
880616	0.00	0.0000E+00	0.00	0.00	0.00	0.00	2.06	0.93	1.08	1.16	3.99	34
880623	0.00	0.0000E+00	0.00	0.00	0.00	0.00	5.48	0.88	1.14	1.27	4.40	34
881105	0.00	0.0000E+00	0.00	0.00	0.00	0.00	7.83	0.82	1.21	1.39	4.54	34
890511	0.00	0.0000E+00	0.00	0.00	0.00	0.00	5.42	0.80	1.25	1.46	4.38	34
890520	0.00	0.0000E+00	0.00	0.00	0.00	0.00	0.00	0.00	0.00	0.00	0.00	34
890603	0.00	0.0000E+00	0.00	0.00	0.00	0.00	3.46	0.80	1.25	1.46	4.18	34
891024	0.00	0.0000E+00	0.00	0.00	0.00	0.00	6.08	0.73	1.38	1.66	4.41	34
891031	0.00	0.0000E+00	0.00	0.00	0.00	0.00	9.19	0.75	1.33	1.59	4.60	34
891120	0.00	0.0000E+00	0.00	0.00	0.00	0.00	4.21	0.70	1.43	1.73	4.25	34

*

$B(\Delta)=3.71$ $G(\Delta)=$ $0.0000E+00 s\ m^{-2}$ $\rho_0=2700.0 kg\ m^{-3}$ $v_0=5670.0 km\ s^{-1}$

$\rho_1=2400.0 kg\ m^{-3}$ $v_1=3600.0 km\ s^{-1}$ $K=0.00$

Table 8A Gauribidanur array - Observations in the 0.5-4.0Hz band

Date	1/2 Pk-Pk (nm)	Period (s)	Frequency (Hz)	Gain	m_b	r.m.s. 0-3s (nm)	r.m.s. 0-6s (nm)	r.m.s. 0-9s (nm)	r.m.s. 0-15s (nm)	r.m.s. 3-9s (nm)	r.m.s. 3-15s (nm)	r.m.s. 9-18s (nm)	r.m.s. noise (nm)
760711	3.17	0.63	1.60	2.02	4.11	1.51	1.35	1.36	1.32	1.29	1.26	1.19	1.04
770319	24.56	0.68	1.48	1.85	5.00	10.40	9.15	9.85	8.41	9.57	7.84	5.34	0.94
770706	5.19	0.85	1.18	1.34	4.37	2.65	2.50	2.42	2.04	2.30	1.86	1.28	0.73
771112	5.10	0.93	1.08	1.16	4.39	2.46	1.95	1.76	1.52	1.28	1.17	1.00	1.07
771124	23.61	0.73	1.38	1.69	5.00	10.44	8.95	10.04	8.08	9.83	7.37	3.72	0.71
771217	3.87	0.77	1.29	1.54	4.22	1.73	1.55	1.39	1.20	1.19	1.03	0.74	0.76
780227	0.00	0.00	0.00	0.00	0.00	0.00	0.00	0.00	0.00	0.00	0.00	0.00	0.00
780322	4.03	0.88	1.14	1.28	4.27	1.51	1.36	1.37	1.14	1.29	1.03	0.66	0.68
780719	0.00	0.00	0.00	0.00	0.00	0.00	0.00	0.00	0.00	0.00	0.00	0.00	0.00
780726	0.00	0.00	0.00	0.00	0.00	0.00	0.00	0.00	0.00	0.00	0.00	0.00	0.00
781102	3.13	0.70	1.43	1.76	4.11	1.35	1.19	1.12	0.98	0.99	0.87	0.84	0.80
781130	22.46	1.35	0.74	0.50	5.23	10.55	8.89	10.62	9.30	10.65	8.97	6.97	0.70
781217	4.19	0.77	1.29	1.54	4.26	1.94	1.69	1.61	1.34	1.41	1.14	0.74	0.59
781219	4.38	0.73	1.38	1.69	4.26	1.83	1.56	1.50	1.35	1.31	1.20	1.02	0.80
790301	3.29	0.75	1.33	1.61	4.14	1.47	1.36	1.23	1.12	1.10	1.02	0.95	0.93
790309	2.09	0.73	1.38	1.66	3.95	1.01	0.97	0.88	0.74	0.82	0.66	0.51	0.48
790324	2.63	1.10	0.91	0.82	4.18	1.35	1.18	1.17	1.04	1.06	0.95	0.76	0.53
790404	0.00	0.00	0.00	0.00	0.00	0.00	0.00	0.00	0.00	0.00	0.00	0.00	0.00
790618	4.03	0.90	1.11	1.22	4.28	1.97	1.74	1.63	1.54	1.43	1.41	1.44	1.25
790629	4.02	0.70	1.43	1.76	4.22	2.14	2.03	2.02	1.90	1.95	1.84	1.76	1.46
790725	29.52	0.85	1.18	1.33	5.13	13.89	12.44	13.75	11.69	13.67	11.07	7.68	0.49
790728	3.29	1.10	0.91	0.82	4.27	1.57	1.48	1.34	1.25	1.20	1.16	1.03	0.79
791122	0.00	0.00	0.00	0.00	0.00	0.00	0.00	0.00	0.00	0.00	0.00	0.00	0.00
800223	1.00	0.57	1.74	2.13	3.62	0.51	0.43	0.43	0.40	0.37	0.36	0.39	0.31
800303	0.94	0.63	1.60	1.96	3.60	0.42	0.42	0.39	0.37	0.37	0.36	0.29	0.21
800323	11.09	0.77	1.29	1.52	4.68	4.82	4.14	4.77	3.98	4.74	3.74	2.54	0.23
800401	6.62	0.82	1.21	1.39	4.47	3.05	2.78	2.71	2.29	2.53	2.06	1.30	0.39
800404	1.18	1.02	0.98	0.95	3.79	0.59	0.49	0.47	0.44	0.40	0.39	0.38	0.25
800621	4.07	0.75	1.33	1.61	4.24	1.83	1.76	1.59	1.74	1.45	1.72	1.64	1.14
800706	0.00	0.00	0.00	0.00	0.00	0.00	0.00	0.00	0.00	0.00	0.00	0.00	0.00
800719	14.02	0.77	1.29	1.52	4.78	5.99	4.95	5.01	4.37	4.44	3.86	2.90	0.59
801203	9.41	0.73	1.38	1.66	4.60	3.79	3.23	3.35	2.96	3.11	2.71	2.14	0.71
810227	1.00	0.75	1.33	1.59	3.63	0.52	0.52	0.49	0.42	0.48	0.39	0.27	0.26
810306	1.17	0.80	1.25	1.46	3.71	0.58	0.53	0.51	0.47	0.48	0.43	0.36	0.36
810328	3.03	0.80	1.25	1.46	4.12	1.32	1.08	0.99	0.79	0.77	0.59	0.56	0.29
810410	1.52	0.82	1.21	1.39	3.83	0.64	0.67	0.73	0.64	0.77	0.64	0.45	0.27
810708	3.31	0.63	1.60	1.96	4.14	1.75	1.68	1.63	1.53	1.56	1.47	1.37	1.02
810711	0.00	0.00	0.00	0.00	0.00	0.00	0.00	0.00	0.00	0.00	0.00	0.00	0.00
810718	0.00	0.00	0.00	0.00	0.00	0.00	0.00	0.00	0.00	0.00	0.00	0.00	0.00
810803	0.00	0.00	0.00	0.00	0.00	0.00	0.00	0.00	0.00	0.00	0.00	0.00	0.00
811111	2.09	0.70	1.43	1.73	3.95	0.88	0.79	0.78	0.67	0.72	0.60	0.40	0.39
811205	2.26	0.75	1.33	1.59	3.99	1.04	0.93	0.90	0.78	0.82	0.70	0.62	0.47
811208	7.68	0.70	1.43	1.73	4.51	2.87	2.65	2.68	2.29	2.57	2.12	1.44	0.43
820220	0.00	0.00	0.00	0.00	0.00	0.00	0.00	0.00	0.00	0.00	0.00	0.00	0.00
820224	0.00	0.00	0.00	0.00	0.00	0.00	0.00	0.00	0.00	0.00	0.00	0.00	0.00
820320	2.08	1.55	0.65	0.33	4.31	1.00	0.91	0.93	0.81	0.89	0.75	0.52	0.34
820627	0.00	0.00	0.00	0.00	0.00	0.00	0.00	0.00	0.00	0.00	0.00	0.00	0.00
820701	0.00	0.00	0.00	0.00	0.00	0.00	0.00	0.00	0.00	0.00	0.00	0.00	0.00
820725	8.84	1.63	0.62	0.29	4.98	4.01	3.60	3.69	3.08	3.52	2.80	1.85	0.87
830419	22.41	0.73	1.38	1.66	4.98	9.31	7.46	7.56	6.74	6.52	5.92	4.52	0.33
830425	0.00	0.00	0.00	0.00	0.00	0.00	0.00	0.00	0.00	0.00	0.00	0.00	0.00
830525	16.51	0.73	1.38	1.66	4.85	7.50	7.11	7.69	6.35	7.78	6.03	3.34	0.58
830618	0.00	0.00	0.00	0.00	0.00	0.00	0.00	0.00	0.00	0.00	0.00	0.00	0.00
830628	8.70	0.85	1.18	1.33	4.60	4.01	3.37	3.82	3.29	3.72	3.08	2.32	1.05
830720	0.00	0.00	0.00	0.00	0.00	0.00	0.00	0.00	0.00	0.00	0.00	0.00	0.00
830804	3.50	1.25	0.80	0.60	4.38	1.74	1.89	1.68	1.42	1.65	1.33	0.89	0.67
831203	0.00	0.00	0.00	0.00	0.00	0.00	0.00	0.00	0.00	0.00	0.00	0.00	0.00
831207	2.29	0.98	1.03	1.05	4.06	1.07	0.95	0.93	0.79	0.85	0.71	0.51	0.63
840508	1.81	0.68	1.48	1.81	3.88	0.91	0.79	0.76	0.67	0.68	0.59	0.45	0.37
840512	10.70	0.73	1.38	1.66	4.66	4.65	4.28	4.00	3.42	3.63	3.04	2.14	0.69

Table 8A (cont'd) Gauribidanur array - Observations in the 0.5-4.0Hz band

Date	1/2 Pk-Pk (nm)	Period (s)	Frequency (Hz)	Gain	m_b	r.m.s. 0-3s (nm)	r.m.s. 0-6s (nm)	r.m.s. 0-9s (nm)	r.m.s. 0-15s (nm)	r.m.s. 3-9s (nm)	r.m.s. 3-15s (nm)	r.m.s. 9-18s (nm)	r.m.s. noise (nm)
840612	2.20	1.15	0.87	0.74	4.12	1.27	1.05	1.14	1.01	1.07	0.93	0.70	0.97
840616	4.95	1.35	0.74	0.49	4.58	2.63	2.47	2.29	1.85	2.09	1.60	0.92	0.92
841027	0.00	0.00	0.00	0.00	0.00	0.00	0.00	0.00	0.00	0.00	0.00	0.00	0.00
841102	9.40	0.73	1.38	1.66	4.60	4.14	3.81	3.71	3.19	3.47	2.91	2.01	0.39
841201	0.00	0.00	0.00	0.00	0.00	0.00	0.00	0.00	0.00	0.00	0.00	0.00	0.00
841206	10.77	0.77	1.29	1.52	4.67	4.60	4.13	4.58	3.83	4.57	3.61	2.11	0.41
850430	0.00	0.00	0.00	0.00	0.00	0.00	0.00	0.00	0.00	0.00	0.00	0.00	0.00
850508	12.70	0.88	1.14	1.27	4.77	6.08	6.20	6.14	5.26	6.16	5.04	3.31	0.27
850603	2.48	2.03	0.49	0.15	4.62	1.16	1.06	1.04	0.94	0.98	0.88	0.84	0.91
850607	0.00	0.00	0.00	0.00	0.00	0.00	0.00	0.00	0.00	0.00	0.00	0.00	0.00
851024	0.00	0.00	0.00	0.00	0.00	0.00	0.00	0.00	0.00	0.00	0.00	0.00	0.00
851026	4.33	0.82	1.21	1.39	4.29	2.32	1.93	1.85	1.57	1.56	1.31	0.94	0.44
851124	1.91	0.80	1.25	1.46	3.92	0.90	0.85	0.81	0.65	0.75	0.57	0.46	0.39
851126	14.29	0.82	1.21	1.39	4.80	6.59	6.12	6.42	5.35	6.33	4.99	2.73	0.40
860527	0.00	0.00	0.00	0.00	0.00	0.00	0.00	0.00	0.00	0.00	0.00	0.00	0.00
860530	8.90	0.73	1.38	1.66	4.58	4.12	3.39	3.39	3.00	2.95	2.65	2.12	0.43
861112	4.32	0.73	1.38	1.66	4.27	1.84	1.65	1.58	1.31	1.44	1.14	0.75	0.28
861206	1.21	0.65	1.54	1.88	3.71	0.52	0.65	0.60	0.59	0.64	0.60	0.62	0.44
861210	3.69	1.42	0.70	0.42	4.50	1.80	1.44	1.33	1.13	1.01	0.88	0.66	0.37
870505	2.10	0.68	1.48	1.81	3.95	0.90	0.86	0.85	0.73	0.82	0.68	0.58	0.49
870520	6.12	1.25	0.80	0.60	4.62	2.97	2.86	3.27	2.66	3.40	2.58	1.32	0.68
870606	2.48	0.77	1.29	1.52	4.03	0.95	1.09	1.15	1.10	1.24	1.14	1.05	0.75
870621	5.71	1.02	0.98	0.95	4.48	2.82	2.28	2.10	1.81	1.62	1.45	1.22	0.80
871023	7.74	0.95	1.05	1.10	4.58	3.71	3.39	3.72	3.19	3.73	3.05	1.91	0.37
871105	10.09	0.75	1.33	1.59	4.64	4.13	3.65	4.31	3.50	4.39	3.33	1.63	0.50
871119	11.80	0.82	1.21	1.39	4.72	5.38	5.13	5.59	4.52	5.69	4.27	1.88	0.63
871129	2.88	0.70	1.43	1.73	4.09	1.08	1.02	1.04	0.88	1.02	0.82	0.55	0.31
880511	5.49	0.73	1.38	1.66	4.37	2.35	2.21	2.27	1.86	2.23	1.72	0.98	0.51
880525	9.56	0.75	1.33	1.59	4.61	4.43	3.74	3.53	3.22	2.98	2.84	2.45	0.72
880616	1.87	0.75	1.33	1.59	3.90	0.88	0.75	0.93	0.83	0.95	0.81	0.64	0.71
880623	5.09	0.82	1.21	1.39	4.36	2.10	1.73	2.08	1.71	2.07	1.60	0.81	0.69
881105	7.20	0.93	1.08	1.16	4.54	3.32	2.92	2.76	2.34	2.43	2.02	1.36	0.60
890511	6.15	0.80	1.25	1.46	4.43	2.86	2.35	2.45	2.12	2.22	1.89	1.29	0.79
890520	0.00	0.00	0.00	0.00	0.00	0.00	0.00	0.00	0.00	0.00	0.00	0.00	0.00
890603	4.25	0.85	1.18	1.33	4.28	2.49	1.90	2.33	2.12	2.24	2.01	1.61	1.40
891024	5.47	0.68	1.48	1.81	4.36	2.38	2.35	2.33	2.01	2.31	1.91	1.29	0.49
891031	9.29	0.70	1.43	1.73	4.59	3.59	3.27	3.58	3.11	3.58	2.97	2.00	0.62
891120	4.17	0.80	1.25	1.46	4.26	1.97	1.74	2.00	1.70	2.02	1.63	1.01	0.45

Table 9A Gauribidanur array - Observations in the 1.0-4.0Hz band

Date	1/2 Pk-Pk (nm)	Period (s)	Frequency (Hz)	Gain	m_b	r.m.s. 0-3s (nm)	r.m.s. 0-6s (nm)	r.m.s. 0-9s (nm)	r.m.s. 0-15s (nm)	r.m.s. 3-9s (nm)	r.m.s. 3-15s (nm)	r.m.s. 9-18s (nm)	r.m.s. noise (nm)
760711	2.91	0.55	1.82	2.32	4.07	1.32	1.18	1.14	1.04	1.04	0.95	0.81	0.64
770319	16.11	0.57	1.74	2.21	4.81	6.54	6.07	6.79	5.82	6.91	5.62	3.80	0.81
770706	3.41	0.77	1.29	1.54	4.17	1.49	1.42	1.45	1.27	1.43	1.20	0.84	0.48
771112	2.71	0.65	1.54	1.93	4.04	1.10	0.99	0.88	0.74	0.74	0.61	0.44	0.49
771124	15.71	0.63	1.60	2.02	4.80	6.09	5.09	6.30	5.11	6.40	4.84	2.63	0.44
771217	2.66	0.73	1.38	1.69	4.05	1.08	0.99	0.93	0.82	0.84	0.74	0.54	0.33
780227	0.00	0.00	0.00	0.00	0.00	0.00	0.00	0.00	0.00	0.00	0.00	0.00	0.00
780322	2.59	0.52	1.90	2.43	4.02	1.13	0.96	1.01	0.85	0.94	0.76	0.51	0.47
780719	0.00	0.00	0.00	0.00	0.00	0.00	0.00	0.00	0.00	0.00	0.00	0.00	0.00
780726	0.00	0.00	0.00	0.00	0.00	0.00	0.00	0.00	0.00	0.00	0.00	0.00	0.00
781102	2.33	0.57	1.74	2.21	3.97	1.04	0.86	0.82	0.70	0.69	0.58	0.49	0.41
781130	13.82	0.73	1.38	1.69	4.76	5.83	5.59	7.08	6.17	7.63	6.26	4.40	0.52
781217	3.25	0.70	1.43	1.76	4.13	1.32	1.17	1.18	0.98	1.11	0.87	0.55	0.40
781219	3.25	0.68	1.48	1.85	4.13	1.32	1.15	1.08	0.98	0.94	0.88	0.75	0.54
790301	2.33	0.70	1.43	1.76	3.99	1.00	0.88	0.87	0.76	0.80	0.68	0.62	0.49
790309	1.59	0.65	1.54	1.88	3.82	0.67	0.71	0.64	0.53	0.62	0.48	0.35	0.23
790324	2.23	0.68	1.48	1.81	3.97	1.00	0.83	0.86	0.74	0.78	0.66	0.48	0.25
790404	0.00	0.00	0.00	0.00	0.00	0.00	0.00	0.00	0.00	0.00	0.00	0.00	0.00
790618	2.45	0.80	1.25	1.47	4.03	1.03	0.94	0.96	0.86	0.93	0.82	0.70	0.63
790629	2.91	0.63	1.60	2.02	4.07	1.33	1.34	1.37	1.28	1.39	1.27	1.16	0.77
790725	17.26	0.75	1.33	1.59	4.87	7.33	7.19	8.44	7.11	8.94	7.05	4.49	0.28
790728	2.11	0.73	1.38	1.66	3.95	0.87	0.78	0.75	0.73	0.68	0.69	0.59	0.33
791122	0.00	0.00	0.00	0.00	0.00	0.00	0.00	0.00	0.00	0.00	0.00	0.00	0.00
800223	0.91	0.70	1.43	1.73	3.58	0.38	0.33	0.33	0.29	0.31	0.26	0.22	0.17
800303	0.84	0.57	1.74	2.13	3.55	0.36	0.33	0.29	0.27	0.26	0.24	0.18	0.14
800323	7.97	0.70	1.43	1.73	4.53	3.18	2.92	3.31	2.73	3.38	2.61	1.54	0.12
800401	4.87	0.73	1.38	1.66	4.32	2.06	1.82	1.81	1.59	1.67	1.45	1.03	0.17
800404	0.97	0.63	1.60	1.96	3.61	0.43	0.36	0.34	0.30	0.29	0.26	0.24	0.14
800621	2.48	0.63	1.60	2.02	4.00	1.05	1.02	1.00	0.97	0.98	0.95	0.81	0.51
800706	0.00	0.00	0.00	0.00	0.00	0.00	0.00	0.00	0.00	0.00	0.00	0.00	0.00
800719	9.26	0.65	1.54	1.88	4.59	3.67	2.91	2.97	2.51	2.54	2.12	1.50	0.23
801203	7.02	0.65	1.54	1.88	4.47	2.75	2.25	2.19	1.88	1.85	1.60	1.21	0.28
810227	0.84	0.77	1.29	1.52	3.56	0.41	0.39	0.37	0.32	0.34	0.29	0.20	0.14
810306	0.80	0.73	1.38	1.66	3.53	0.32	0.34	0.35	0.30	0.36	0.29	0.20	0.16
810328	2.05	0.75	1.33	1.59	3.95	0.85	0.68	0.65	0.52	0.53	0.41	0.42	0.19
810410	1.02	0.75	1.33	1.59	3.64	0.44	0.41	0.49	0.42	0.51	0.42	0.27	0.16
810708	2.74	0.63	1.60	1.96	4.06	1.46	1.26	1.11	0.95	0.89	0.77	0.66	0.40
810711	0.00	0.00	0.00	0.00	0.00	0.00	0.00	0.00	0.00	0.00	0.00	0.00	0.00
810718	0.00	0.00	0.00	0.00	0.00	0.00	0.00	0.00	0.00	0.00	0.00	0.00	0.00
810803	0.00	0.00	0.00	0.00	0.00	0.00	0.00	0.00	0.00	0.00	0.00	0.00	0.00
811111	1.76	0.70	1.43	1.73	3.87	0.70	0.58	0.58	0.49	0.51	0.42	0.29	0.17
811205	1.69	0.73	1.38	1.66	3.86	0.72	0.63	0.62	0.53	0.57	0.47	0.43	0.22
811208	5.89	0.60	1.67	2.05	4.39	2.21	2.02	2.06	1.78	1.99	1.66	1.13	0.18
820220	0.00	0.00	0.00	0.00	0.00	0.00	0.00	0.00	0.00	0.00	0.00	0.00	0.00
820224	0.00	0.00	0.00	0.00	0.00	0.00	0.00	0.00	0.00	0.00	0.00	0.00	0.00
820320	1.53	0.77	1.29	1.52	3.82	0.64	0.53	0.64	0.56	0.65	0.54	0.36	0.21
820627	0.00	0.00	0.00	0.00	0.00	0.00	0.00	0.00	0.00	0.00	0.00	0.00	0.00
820701	0.00	0.00	0.00	0.00	0.00	0.00	0.00	0.00	0.00	0.00	0.00	0.00	0.00
820725	5.97	0.65	1.54	1.88	4.40	2.70	2.39	2.55	2.09	2.47	1.91	1.09	0.31
830419	17.25	0.70	1.43	1.73	4.86	6.92	5.51	5.71	5.05	4.99	4.46	3.27	0.18
830425	0.00	0.00	0.00	0.00	0.00	0.00	0.00	0.00	0.00	0.00	0.00	0.00	0.00
830525	11.18	0.65	1.54	1.88	4.67	4.49	3.66	5.09	4.22	5.36	4.15	2.39	0.25
830618	0.00	0.00	0.00	0.00	0.00	0.00	0.00	0.00	0.00	0.00	0.00	0.00	0.00
830628	6.00	0.80	1.25	1.46	4.42	2.61	2.13	2.65	2.30	2.67	2.22	1.50	0.44
830720	0.00	0.00	0.00	0.00	0.00	0.00	0.00	0.00	0.00	0.00	0.00	0.00	0.00
830804	2.75	0.55	1.82	2.23	4.06	1.23	1.12	1.14	0.91	1.09	0.81	0.42	0.24
831203	0.00	0.00	0.00	0.00	0.00	0.00	0.00	0.00	0.00	0.00	0.00	0.00	0.00
831207	1.28	0.80	1.25	1.46	3.75	0.63	0.56	0.61	0.52	0.60	0.49	0.33	0.26
840508	1.75	0.60	1.67	2.05	3.86	0.82	0.64	0.61	0.52	0.47	0.41	0.32	0.20
840512	7.27	0.65	1.54	1.88	4.48	2.77	2.32	2.56	2.22	2.44	2.06	1.52	0.47

Table 9A (cont'd) Gauribidanur array - Observations in the 1.0-4.0Hz band

Date	1/2 Pk-Pk (nm)	Period (s)	Frequency (Hz)	Gain	m_b	r.m.s. 0-3s (nm)	r.m.s. 0-6s (nm)	r.m.s. 0-9s (nm)	r.m.s. 0-15s (nm)	r.m.s. 3-9s (nm)	r.m.s. 3-15s (nm)	r.m.s. 9-18s (nm)	r.m.s. noise (nm)
840612	1.58	0.70	1.43	1.73	3.83	0.81	0.68	0.63	0.54	0.53	0.45	0.36	0.36
840616	2.69	0.70	1.43	1.73	4.06	1.21	1.14	1.14	0.94	1.11	0.86	0.50	0.31
841027	0.00	0.00	0.00	0.00	0.00	0.00	0.00	0.00	0.00	0.00	0.00	0.00	0.00
841102	7.04	0.68	1.48	1.81	4.47	2.94	2.44	2.56	2.18	2.35	1.95	1.37	0.18
841201	0.00	0.00	0.00	0.00	0.00	0.00	0.00	0.00	0.00	0.00	0.00	0.00	0.00
841206	7.32	0.75	1.33	1.59	4.50	3.07	2.89	3.42	2.85	3.59	2.80	1.56	0.19
850430	0.00	0.00	0.00	0.00	0.00	0.00	0.00	0.00	0.00	0.00	0.00	0.00	0.00
850508	8.35	0.77	1.29	1.52	4.56	3.84	4.39	4.52	3.77	4.83	3.76	2.11	0.16
850603	1.57	0.60	1.67	2.05	3.82	0.80	0.69	0.71	0.60	0.67	0.53	0.36	0.42
850607	0.00	0.00	0.00	0.00	0.00	0.00	0.00	0.00	0.00	0.00	0.00	0.00	0.00
851024	0.00	0.00	0.00	0.00	0.00	0.00	0.00	0.00	0.00	0.00	0.00	0.00	0.00
851026	2.49	0.68	1.48	1.81	4.02	1.11	0.92	1.01	0.89	0.96	0.83	0.61	0.22
851124	1.29	0.63	1.60	1.96	3.73	0.58	0.50	0.50	0.41	0.45	0.35	0.26	0.21
851126	9.02	0.80	1.25	1.46	4.60	3.81	3.15	4.38	3.62	4.63	3.57	1.75	0.21
860527	0.00	0.00	0.00	0.00	0.00	0.00	0.00	0.00	0.00	0.00	0.00	0.00	0.00
860530	7.00	0.65	1.54	1.88	4.47	3.13	2.48	2.56	2.20	2.23	1.90	1.52	0.22
861112	3.08	0.70	1.43	1.73	4.12	1.37	1.21	1.18	0.98	1.08	0.85	0.57	0.17
861206	1.05	0.93	1.08	1.16	3.70	0.43	0.42	0.44	0.39	0.45	0.37	0.30	0.25
861210	2.02	0.60	1.67	2.05	3.93	0.95	0.75	0.74	0.64	0.61	0.54	0.40	0.21
870505	1.68	0.55	1.82	2.23	3.85	0.66	0.58	0.58	0.51	0.54	0.46	0.34	0.23
870520	3.71	0.73	1.38	1.66	4.20	1.72	1.64	2.13	1.72	2.31	1.72	0.80	0.26
870606	1.56	0.60	1.67	2.05	3.81	0.59	0.70	0.67	0.65	0.70	0.66	0.57	0.27
870621	2.98	0.98	1.03	1.05	4.17	1.45	1.12	1.28	1.12	1.19	1.03	0.77	0.29
871023	4.65	0.93	1.08	1.16	4.35	2.05	1.78	2.42	2.10	2.59	2.11	1.26	0.22
871105	7.66	0.73	1.38	1.66	4.51	3.08	2.61	3.28	2.68	3.37	2.57	1.20	0.30
871119	7.39	0.75	1.33	1.59	4.50	3.30	3.17	3.89	3.10	4.15	3.05	1.17	0.28
871129	2.24	0.63	1.60	1.96	3.97	0.82	0.74	0.77	0.65	0.74	0.60	0.40	0.20
880511	3.73	0.65	1.54	1.88	4.19	1.59	1.42	1.62	1.33	1.63	1.25	0.65	0.30
880525	6.69	0.65	1.54	1.88	4.45	2.90	2.41	2.44	2.08	2.18	1.82	1.31	0.31
880616	1.40	0.70	1.43	1.73	3.77	0.56	0.46	0.56	0.51	0.56	0.50	0.43	0.31
880623	3.46	0.73	1.38	1.66	4.17	1.50	1.24	1.60	1.29	1.64	1.23	0.52	0.31
881105	4.45	0.82	1.21	1.39	4.30	1.95	1.77	1.80	1.51	1.73	1.38	0.82	0.31
890511	4.99	0.75	1.33	1.59	4.33	1.97	1.70	1.88	1.59	1.84	1.48	0.86	0.38
890520	0.00	0.00	0.00	0.00	0.00	0.00	0.00	0.00	0.00	0.00	0.00	0.00	0.00
890603	3.13	0.75	1.33	1.59	4.13	1.70	1.31	1.60	1.44	1.54	1.37	1.09	0.79
891024	3.85	0.60	1.67	2.05	4.21	1.66	1.55	1.63	1.40	1.61	1.33	0.86	0.27
891031	7.50	0.65	1.54	1.88	4.50	2.94	2.51	2.71	2.43	2.58	2.29	1.67	0.38
891120	3.15	0.82	1.21	1.39	4.15	1.35	1.18	1.48	1.20	1.54	1.16	0.54	0.21

APPENDIX D

TABLES OF FANGATAUFA OBSERVATIONS

The title page to Appendix C gives a description of how ψ_{∞} and moment is calculated and describes how magnitude is calculated from the observations listed.

Table 1A Yellowknife array - Broad band and short period observations

Date	ψ_∞ (m^3)	Moment (N m)	Duration (s)	Rise time (s)	Fall time (s)	pP-P time (s)	1/2 Pk-Pk (nm)	Period (s)	Frequency (Hz)	Gain	m_b	
750605	454.50	0.1776E+15	0.46	0.18	0.13	0.36	5.00	0.75	1.33	1.61	4.55	23
751126	1327.93	0.5190E+15	0.55	0.17	0.16	0.86	8.37	0.65	1.54	1.91	4.76	23
881130	18383.31	0.7185E+16	0.77	0.20	0.27	0.79	59.11	0.90	1.11	1.22	5.66	23
890610	15709.78	0.6140E+16	0.71	0.19	0.27	0.80	52.23	0.90	1.11	1.22	5.61	23
891127	14373.01	0.5618E+16	0.77	0.21	0.24	0.81	50.96	0.73	1.38	1.82	5.52	37

*

$B(\Delta)=3.93$ $G(\Delta)=$ $0.5975E-11 s\ m^{-2}$ $\rho_0=2670.0 kg\ m^{-3}$ $v_0=5640.0 km\ s^{-1}$
$\rho_1=2400.0 kg\ m^{-3}$ $v_1=3600.0 km\ s^{-1}$ $K=0.76$

Table 2A Yellowknife array - Observations in the 0.5-4.0Hz band

Date	1/2 Pk-Pk (nm)	Period (s)	Frequency (Hz)	Gain	m_b	r.m.s. 0-3s (nm)	r.m.s. 0-6s (nm)	r.m.s. 0-9s (nm)	r.m.s. 0-15s (nm)	r.m.s. 3-9s (nm)	r.m.s. 3-15s (nm)	r.m.s. 9-18s (nm)	r.m.s. noise (nm)
750605	5.22	0.75	1.33	1.61	4.57	2.35	1.71	1.42	1.11	0.51	0.41	0.31	0.37
751126	8.21	0.60	1.67	2.09	4.75	3.38	2.68	2.22	1.77	1.29	1.02	0.65	0.36
881130	63.05	1.42	0.70	0.42	5.95	33.86	27.42	23.32	18.18	15.57	11.24	4.06	0.40
890610	60.14	1.10	0.91	0.82	5.76	33.00	25.73	21.54	16.87	12.30	9.14	4.51	0.41
891127	51.74	1.58	0.63	0.29	5.98	28.55	23.63	20.09	15.81	14.07	10.43	4.91	0.21

Table 3A Yellowknife array - Observations in the 1.0-4.0Hz band

Date	1/2 Pk-Pk (nm)	Period (s)	Frequency (Hz)	Gain	m_b	r.m.s. 0-3s (nm)	r.m.s. 0-6s (nm)	r.m.s. 0-9s (nm)	r.m.s. 0-15s (nm)	r.m.s. 3-9s (nm)	r.m.s. 3-15s (nm)	r.m.s. 9-18s (nm)	r.m.s. noise (nm)
750605	4.21	0.73	1.38	1.68	4.47	2.02	1.47	1.21	0.95	0.40	0.32	0.20	0.31
751126	6.72	0.60	1.67	2.09	4.66	2.77	2.15	1.77	1.40	0.93	0.73	0.44	0.17
881130	39.49	0.65	1.54	1.91	5.43	17.06	12.96	11.12	8.71	6.32	4.70	2.82	0.16
890610	39.98	0.65	1.54	1.91	5.44	17.74	13.49	11.16	8.79	5.43	4.24	3.01	0.32
891127	39.56	0.63	1.60	2.25	5.38	16.98	12.94	10.77	8.53	5.46	4.34	3.24	0.09

Table 4A Warramunga array - Broad band and short period observations

Date	ψ_∞ (m^3)	Moment (N m)	Duration (s)	Rise time (s)	Fall time (s)	pP-P time (s)	1/2 Pk-Pk (nm)	Period (s)	Frequency (Hz)	Gain	m_b	
751126	304.67	0.1191E+15	0.56	0.13	0.12	0.84	2.11	0.65	1.54	1.93	4.10	26
881130	6490.26	0.2537E+16	0.75	0.17	0.20	0.88	26.93	0.73	1.38	1.68	5.22	36
830610	7399.58	0.2892E+16	0.77	0.18	0.23	0.86	29.04	0.82	1.21	1.40	5.27	36

*

$B(\Delta)=3.87$ $G(\Delta)=$ $0.6802E-11 s\ m^{-2}$ $\rho_0=2600.0 kg\ m^{-3}$ $v_0=5600.0 km\ s^{-1}$
$\rho_1=2400.0 kg\ m^{-3}$ $v_1=3600.0 km\ s^{-1}$ $K=0.77$

Table 5A Warramunga array - Observations in the 0.5-4.0Hz band

Date	1/2 Pk-Pk (nm)	Period (s)	Frequency (Hz)	Gain	m_b	r.m.s. 0-3s (nm)	r.m.s. 0-6s (nm)	r.m.s. 0-9s (nm)	r.m.s. 0-15s (nm)	r.m.s. 3-9s (nm)	r.m.s. 3-15s (nm)	r.m.s. 9-18s (nm)	r.m.s. noise (nm)
751126	2.02	0.65	1.54	1.93	4.08	1.04	0.78	0.64	0.53	0.28	0.27	0.23	0.17
881130	27.47	0.65	1.54	1.91	5.21	14.38	12.98	10.87	8.52	8.60	6.25	2.31	0.18
890610	26.50	0.70	1.43	1.75	5.20	12.59	9.72	8.11	6.37	4.39	3.34	1.63	0.43

Table 6A Warramunga array - Observations in the 1.0-4.0Hz band

Date	1/2 Pk-Pk (nm)	Period (s)	Frequency (Hz)	Gain	m_b	r.m.s. 0-3s (nm)	r.m.s. 0-6s (nm)	r.m.s. 0-9s (nm)	r.m.s. 0-15s (nm)	r.m.s. 3-9s (nm)	r.m.s. 3-15s (nm)	r.m.s. 9-18s (nm)	r.m.s. noise (nm)
751126	1.88	0.55	1.82	2.32	4.04	0.94	0.70	0.58	0.47	0.26	0.23	0.17	0.11
881130	22.43	0.65	1.54	1.91	5.13	10.32	8.79	7.34	5.75	5.25	3.83	1.41	0.11
890610	21.47	0.73	1.38	1.68	5.12	8.65	6.42	5.34	4.23	2.32	1.92	1.31	0.23

Table 7A Gauribidanur array - Broad band and short period observations

Date	ψ_{∞} (m^3)	Moment (N m)	Duration (s)	Rise time (s)	Fall time (s)	pP-P time (s)	1/2 Pk-Pk (nm)	Period (s)	Frequency (Hz)	Gain	m_b	
750605	0.00	0.0000E+00	0.00	0.00	0.00	0.00	0.00	0.00	0.00	0.00	0.00	26
751126	0.00	0.0000E+00	0.00	0.00	0.00	0.00	3.88	0.63	1.60	2.02	4.20	26
881130	0.00	0.0000E+00	0.00	0.00	0.00	0.00	12.94	0.73	1.38	1.66	4.74	34
890610	0.00	0.0000E+00	0.00	0.00	0.00	0.00	12.74	0.70	1.43	1.73	4.73	34
891127	0.00	0.0000E+00	0.00	0.00	0.00	0.00	17.80	0.73	1.38	1.66	4.88	34

*

$B(\Delta)=3.71$ $G(\Delta)=$ 0.0000E+00s m^{-2} $\rho_0=2700.0$kg m^{-3} $v_0=5670.0$km s^{-1}
$\rho_1=2400.0$kg m^{-3} $v_1=3600.0$km s^{-1} K=0.00

Table 8A Gauribidanur array - Observations in the 0.5-4.0Hz band

Date	1/2 Pk-Pk (nm)	Period (s)	Frequency (Hz)	Gain	m_b	r.m.s. 0-3s (nm)	r.m.s. 0-6s (nm)	r.m.s. 0-9s (nm)	r.m.s. 0-15s (nm)	r.m.s. 3-9s (nm)	r.m.s. 3-15s (nm)	r.m.s. 9-18s (nm)	r.m.s. noise (nm)
750605	0.00	0.00	0.00	0.00	0.00	0.00	0.00	0.00	0.00	0.00	0.00	0.00	0.00
751126	6.82	0.70	1.43	1.76	4.45	3.07	3.20	2.75	2.25	2.58	1.99	1.10	1.29
881130	29.23	1.27	0.78	0.57	5.31	9.51	12.79	10.98	8.81	11.65	8.62	3.38	0.32
890610	26.55	1.13	0.89	0.78	5.19	8.19	11.40	10.27	8.16	11.17	8.16	3.28	0.89
891127	29.72	1.27	0.78	0.57	5.32	10.19	13.44	11.97	9.47	12.76	9.28	3.65	0.54

Table 9A Gauribidanur array - Observations in the 1.0-4.0Hz band

Date	1/2 Pk-Pk (nm)	Period (s)	Frequency (Hz)	Gain	m_b	r.m.s. 0-3s (nm)	r.m.s. 0-6s (nm)	r.m.s. 0-9s (nm)	r.m.s. 0-15s (nm)	r.m.s. 3-9s (nm)	r.m.s. 3-15s (nm)	r.m.s. 9-18s (nm)	r.m.s. noise (nm)
750605	0.00	0.00	0.00	0.00	0.00	0.00	0.00	0.00	0.00	0.00	0.00	0.00	0.00
751126	5.82	0.65	1.54	1.93	4.38	2.86	2.73	2.32	1.88	1.99	1.53	0.78	0.57
881130	17.92	0.65	1.54	1.88	4.88	4.14	7.12	6.60	5.21	7.53	5.45	1.78	0.19
890610	13.76	0.77	1.29	1.52	4.78	3.82	6.59	6.18	4.88	7.07	5.12	1.89	0.39
891127	14.83	0.77	1.29	1.52	4.81	5.27	7.99	7.14	5.68	7.91	5.78	2.28	0.25